Effects of heme oxygenase system on inflammation, oxidative stress, insulin signaling and tissue injury in liver, heart, kidney and pancreas in obese, diabetic and hypertensive rats

A Thesis

Submitted to the College of

Graduate and Postdoctoral Studies

In Partial Fulfillment of the Requirements

For the Degree of Doctor of Philosophy

In the Department of Physiology

University of Saskatchewan

Canada

By

MANISH MISHRA

PERMISSION TO USE

In presenting this thesis in partial fulfillment of the requirements for a Postgraduate degree from the University of Saskatchewan, I agree that the Libraries of this University may make it freely available for inspection. I further agree that permission for copying of this thesis/dissertation in any manner, in whole or in part, for scholarly purposes may be granted by the professor or professors who supervised my thesis work or, in their absence, by the Head of the Department or the Dean of the College in which my thesis work was done. It is understood that any copying or publication or use of this thesis or parts thereof for financial gain shall not be allowed without my written permission. It is also understood that due recognition shall be given to me and to the University of Saskatchewan in any scholarly use which may be made of any material in my thesis. Requests for permission to copy or to make other uses of materials in this thesis/dissertation in whole or part should be addressed to:

Head of the Department of Physiology

University of Saskatchewan

Saskatoon, Saskatchewan S7N 5E5

Canada

ABSTRACT

Tissue injury and metabolic dysfunction are salient features of obesity, diabetes, and hypertension. Inflammation and oxidative stress are considered key players behind this altered tissue homeostasis that drastically affect several vital organs including liver, heart, kidney and pancreas resulting in the development of hepatic steatosis, cardiomyopathy, nephropathy, pancreatic insulitis and abnormal glucose metabolism. Despite significant advancement in pharmaceutical interventions, the desired efficacy to manage these conditions is still lacking. In these situations, cytoprotective and functional attributes of the heme oxygenase (HO) system can be used as an alternative management tool. Although, the HO system is cytoprotective, its role in tissue injury and dysfunction in obesity, diabetes, and hypertension is not completely clear. To explore the importance of upregulating HO in these conditions, HO is induced through hemin in the rat models of obesity, diabetes and hypertension. My thesis work show that HO upregulation reduced the inflammation and oxidative stress-induced tissue injury in liver, heart, kidney, and pancreas through reduction of proinflammatory M1 macrophage marker (ED1) expression, cytokines (TNF-α, IL-1β, IL-6), oxidative-markers (8-isoprostane, ET-1) and profibrotic/extracellular matrix proteins (TGF-β, collagen-IV, fibronectin) and enhancement of the anti-inflammatory M2-macrophage markers (ED2, CD206, CD36, CD14), adiponectin and total-antioxidant capacity. HO upregulation improved glucose metabolism through potentiation of insulin signalling components (IRS-1, IRS-2, PI3K, GLUT4), reduced hyperglycemia, and enhanced several markers implicated in pancreatic repair and/or regeneration (c-Kit, Sca-1, Oct3/4, Pax2, β-catenin, Islet-1, Nkx6.1 and GLUT2). Collectively, the data from my thesis suggested the multifaceted cytoprotective mechanisms of the HO system against increasing tissue injury and metabolic dysfunction during obesity, diabetes and hypertension. Thus, HO upregulation through hemin may be part of therapeutic management strategies against tissue injury and metabolic dysfunction in obesity, diabetes and hypertension in the future.

ACKNOWLEDGEMENTS

Foremost, I would like to express my deepest gratitude and respect to my supervisor Dr. Joseph Ndisang for all the scientific support and guidance for my research work. I am thankful to him for valuable ideas, constructive criticism, scientific knowledge and training that enriched my growth and enabled me to become an independent researcher.

I would like to express my profound gratitude to my advisory committee members, Dr. Linda Hiebert, Dr. Kailash Prasad, Dr. Paul Lee, Dr. Michel Desautels, Dr. Veronica Campanucci, Dr. Nigel West and Dr. Sean Mulligan for their valuable insights, guidance, and constructive criticism at several occasions of my research study. I would like to acknowledge Dr. Thomas Fisher, Head, Department of Physiology who is always willing to help and being generous with his time, resources and advice.

I am grateful to Dr. Martha Smith-Norris, Acting Associate Dean (College of Graduate and Postdoctoral Studies) for providing me moral support, during my graduate studies.

I express my heartfelt and sincere thanks to Dr. Linda Hiebert, Dr. Kailash Prasad for their valuable advice, excellent guidance and painstaking efforts throughout the thesis. I am grateful to them for being helpful and supportive all throughout my journey.

My sincere thanks to my course instructors Dr. Venkat Gopalakrishnan, Dr. Linda Hiebert and Dr. William H. Laverty for nourishing my scientific understanding and skills. I would like to thank the administrative and animal staff, University of Saskatchewan for their assistance during my graduate program. My sincere and heartfelt thanks go to our technician Dilip Singh for his helping hand whenever needed.

I would like to give my special thanks to College of Medicine, University of Saskatchewan for providing the financial support in terms of James Regan Cardiology Scholarship and Graduate Teaching Assistantship during my PhD Program.

I would also like to acknowledge Dr. Satish Kumar, Scientist, CCMB, India, Dr. Sandeep Goel, Scientist, CCMB, India, and Dr. P.C. Pandey, Prof. Emeritus, India for their valuable guidance and moral support.

During this long journey, there are many people in my life without them it was not possible for me to complete my PhD. This thesis is dedicated to my loving parents Mr. Jagdish Prasad Mishra & Late Mrs. Leela Mishra and my family members for their endless love, patience, constant support and strength all these years and pushing me to do my best at every endeavor.

I would like to express my heart-felt thanks to my brother Sourabh for extending his moral support and special thanks to Satyendra Mandela, Kailash Mandela, Puneet Mandela, Hemlata Mandela for their unconditional, love, support and encouragement.

Especially, I would like to thank my in-laws Mr. A.P. Tiwari, Mrs. Urmila Tiwari and Anoop Tiwari for their constant help, care, support and motivation. Most importantly, I would like to express my heartfelt thanks to my life partner Shuchita Tiwari for her love, care, encouragement and moral support during several challenging occasions of my professional and personal life. Thank you for being my steady, constant partner and supporting me throughout my journey.

Finally, I would like to give my sincere thanks to the Almighty for his blessings and friends and families from Saskatoon for making my stay memorable in Canada.

DEDICATION

This thesis is dedicated to my loving parents

Mr. Jagdish prasad Mishra

Late Mrs. Leela Mishra

For their unconditional love, care, support and encouragement

TABLE OF CONTENTS

LIST OF FIGURES

LIST OF TABLES

ABBREVIATIONS

α-cell	Alpha cell
AMPK	Adenosine monophosphate-activated protein kinase
ANOVA	Analysis of variance
ANP	Artrial natriuretic peptide
Akt	Protein kinase B
β-cell	Beta-cell
BR	Bilirubin
BV	Biliverdin
CD	Cluster of differentiation
cGMP	Cyclic guanosine monophosphate
CO	Carbon monoxide
CoPP	Cobalt protoporphyrin
CXCR4	C-X-C chemokine receptor type-4
c-Kit	Tyrosine kinase protein c-Kit
CrMP	Chromium mesoporphyrin
δ-cell	Delta-cells
ELISA	Enzyme-linked immunosorbent assay
eNOS	Endothelial nitric oxide synthase
ESRD	End-stage-renal-disease
Erk	Extracellular signal-regulated kinase
ET-1	Endothelin-1
Fas/FasL	First apoptosis signal protein/first apoptosis signal ligand

Fe	Iron
FHC	Heavy chain ferritin
G6PDH	Glucose-6-phosphate dehydrogenase
GLUT2	Glucose transporter-2
GLUT4	Glucose transporter-4
GSH-px	Glutathione peroxidase
HO	Heme oxygenase
Hmox1	Heme oxygenase-1 gene
Hmox2	Heme oxygenase-2 gene
HOMA	Homeostatic model assessment
IgG	Immunoglobin G
IFNγ	Interferon gamma
IL-1β	Interleukin-1 beta
IL-6	Interleukin-6
IL-10	Interleukin-10
iNOS	Inducible nitric oxide synthase
IGF-1	Insulin like growth factor-1
IPGTT	Intraperitoneal glucose tolerance test
IRS-1	Insulin receptor substrate-1
IRS-2	Insulin receptor substrate-2
Islet-1	Insulin gene enhancer protein-1
JNK	c-Jun–N terminal kinase
Keap1	Kelch-like ECH-associated protein 1

Ldb1	Lim-domain-binding protein-1
LPS	Lipopolysaccharide
LV	Left ventricular
Maf-A	Musculoaponeurotic fibrosarcoma oncogene homologue-A
MAPK	Mitogen-activated protein kinase
mL	Milliliter
mmol	Millimolar
NADPH	Nicotinamide adenine dinucleotide phosphate
NAFLD	Non-alcoholic fatty-liver disease
NF-κB	Nuclear factor kappa B
Nkx6.1	Homeobox protein Nkx6.1
NOD	Non-obese diabetic
Nrf2	Nuclear factor-(erythroid-derived 2)-like 2
Oct3/4	Octamer-binding transcription factor-3/4
Pax2	Paired homeodomain transcription factor-2
Pax4	Paired homeodomain transcription factor-4
Pax6	Paired homeodomain transcription factor-6
Pdx1	Pancreatic duodenal homeobox-1
PI3K	Phosphoinositide-3-kinase
PKA	Protein kinase A
POU	Pit-Oct-Unc transcription factor
RAAS	Renin angiotensin aldosterone system
ROS	Reactive oxygen species

RNS	Reactive nitrogen species
SD	Sprague Dawley
Sca-1	Stem cell antigen-1
sGC	Soluble guanylate cyclase
SHRs	Spontaneous hypertensive rats
SnMP	Stannous-mesoporphyrin
SOD	Superoxide dismutase
STAT	Signal transducer and activator of transcription factor
STZ	Streptozotocin
T-cell	T-lymphocyte
T1D	Type-1 diabetes mellitus
T2D	Type-2 diabetes mellitus
TACE	Tumor necrosis factor-alpha converting enzyme
TGF-β	Transforming growth factor beta
TNF-α	Tumor necrosis factor-alpha
TNFR	Tumor necrosis factor receptor
TEAC	Trolox equivalent antioxidant capacity
UV	Ultra violet rays
VSELs	Very small embryonic like stem cells
WKY	Wistar-Kyoto
ZDF	Zucker diabetic fatty
ZF	Zucker fatty
ZL	Zucker lean

PREFACE

This thesis is composed of six chapters. The first chapter of the presented thesis is the detailed view of the key effectors of obesity, diabetes (T1D and T2D), hypertension associated tissue injury and metabolic dysfunction in liver, heart, kidney and pancreas, including inflammation, macrophage infiltration, proinflammatory cytokines and chemokines, oxidative stress, and insulin resistance. The first chapter of the thesis also includes the literature regarding mechanisms of pancreatic regeneration and regenerative markers or transcriptional factors expressed in the injured pancreas. In addition, the multifaceted cytoprotective role of HO system and Nrf2 has been discussed.

In this thesis, my research work is presented as four manuscripts; (chapters 2, 3, 4 and 5) and unpublished chapter 6. In these chapters, the first page of the manuscript describes the scientific contribution of mine and others. Chapter-2 describes the effects of an upregulated HO system in inflammation-induced hepatic injury and glucose metabolism in the spontaneous hypertensive rats (SHR); a genetic model of essential hypertension characterized by high blood pressure and tissue injury. Chapter-3 describes the effects of an upregulated HO system on cardiac tissue injury and hemodynamic and metabolic functions in Zucker fatty rats (ZF), a genetic obese model characterized by insulin resistance, glucose intolerance and hyper-triglycerides. Chapters-4 and 5 describe the effects of upregulated HO on hepatic and renal injury and improvement of their functions in Zucker diabetic fatty rats (ZDF), a model of T2D, characterized by glucose intolerance, hyperlipidemia, and obesity.

Chapter-6 encompasses the unpublished study that describes the effects of an upregulated HO system on inflammation and oxidative stress-mediated pancreatic injury and repair and / or

regeneration in streptozotocin-(STZ)-induced diabetes. Moreover, the chapter also reports the effects of HO-induction on insulin signalling and glucose metabolism.

Chapter-7 consists of a general discussion and conclusions from all results and highlights the significance of my studies in terms of resolution of tissue injury and improvement of glucose metabolism during obesity, diabetes (T1D and T2D), and hypertension. As well it outlines potential therapeutic benefits of a hemin-induced HO system that may be explored as a novel alternative approach against metabolic tissue injury and dysfunction. In the presented thesis, primary literature is usually cited, however, to limit the citation numbers, appropriate reviews were citied occasionally to describe the background and basic mechanisms. In addition, for a more detailed description of the HO system and cross talk between different effectors involved in metabolic tissue injury and dysfunction, my first-authored published manuscript is included in appendix A.

CHAPTER 1

INTRODUCTION

The prevalence of metabolic syndrome associated conditions, such as obesity, type-2 diabetes (T2D) and hypertension, is increasing at a fast pace across the globe (1,2). Recent evidence equivocally confirms the presence of some conditions of metabolic syndrome in type-1 diabetes (T1D) that is classically known as an autoimmune disease (3,4). Metabolic and vascular abnormalities during these conditions are life threatening and associated with higher mortality rate and financial expenditures (1,2).

During obesity, increasing adiposity, dysregulated adipokine secretions and lipotoxicity are the major causative factors for tissue and metabolic dysfunction (5-7). Beyond that obesity is a risk factor for development of T2D with development of insulin resistance and insulin insufficiency in target organs such as liver and skeletal muscle (5-7). Similarly, increasing tissue injury and dysfunctional insulin signalling and altered glucose metabolism are distinctive features of T1D and hypertension (8-11) and hypertensive subjects are more prone to develop diabetes during their lifetime (12). Although, these conditions follow a distinct etiology, tissue injury and dysregulated glucose metabolism are a common feature of obesity, diabetes (T1D, T2D) and hypertension (5-11,13-17), and inflammation and oxidative stress are considered as the major destructive forces behind these comorbidities (5-11,13-17).

It is well known that macrophages, an innate immunity component, play a major role in inflammation and oxidative stress-induced tissue injury and metabolic dysfunction (5-7,10,14,15,18). An enhanced accumulation of macrophages was seen in injured and dysfunctional tissues during obesity, diabetes (T1D, T2D), and hypertension and suggested that these invading

macrophages were involved in tissue destruction and abnormal glucose metabolism (5,7,10,11,14,15,17,19). Thus, macrophages are the key regulators of metabolic tissue injury and dysfunction during obesity, diabetes and hypertension.

1.1 Macrophage infiltration, inflammation and tissue injury

1.1.1 Origin, phenotypes and functions of macrophages

Macrophages are highly adaptive cells and possess tremendous diversity in their physiological functions that range from development, host defense, immunity to tissue repair (20-22). Due to their intrinsic adaptive capability, macrophages play a deterministic role in progression and severity of several pathogenic conditions of infection, metabolism, cancer, allergies and autoimmune disease (20-22).

On basis of their location, macrophages exist in two distinct types (20-22). The first type of macrophages is circulatory in nature and ubiquitously distributed in body (20-22). In contrast, the other types of macrophages known as resident macrophages which are stationary and generally organ specific (20-22). Although, both types of macrophages are derived from a common progenitor in the bone marrow, they possess significant differences in their functions and activation mechanisms due to transcriptional regulation (20-22).

1.1.2 Macrophage phenotypic plasticity

During various unfavorable conditions, macrophages can leave their existing phenotype and switch to a functional distinct phenotype to maintain tissue homeostasis (22,23). The process of this phenotypic conversion is known as macrophage polarization (Fig. 1-1) (22,23). The classical example of macrophage polarization is the conversion of the classical M1-macrophages

to alternative-activated M2-macrophages (Fig.1-1) (22-24).

Both classical M1-macrophages and alternative-activated M2-macrophages represent a distinct activation and cytokine and chemokine expression profile (22-24). The classical M1-macrophages are mainly activated by pro-inflammatory T-helper-1 cytokines such as tumor necrosis factor alpha (TNF-α), lipopolysaccharide (LPS), interferons and toll like receptor-ligands (22-24). Upon activation, classical M1-macrophages secrete pro-inflammatory cytokines such as TNF-α, interleukin-6 (IL-6) and interleukin-1beta (IL-1β) and reactive nitrogen species (RNS) and reactive oxygen species (ROS) and participate in inflammation and oxidative stress-mediated tissue injury (Fig. 1-1) (22-24).

In contrast, alternative-activated M2-macrophages possess tremendous scavenging and phagocytic capabilities and are activated through anti-inflammatory T-helper-2 cytokines such as interleukin-13, interleukin-10 and interleukin-4 (22-24). Regarding functions, alternative-activated M2-macrophages are related to tissue remodeling and repair processes (Fig. 1-1) (22-24). The exact mechanism and determinants of this phenotypic conversion is still not fully understood. However, scientific evidence suggests that several inflammatory and oxidative signaling molecules such as nuclear factor kappa B (NF-κB), signal transducer and activator of transcription (STAT), peroxisome proliferator-activated receptor, and cellular factors such as krupple like factor, interferon-regulatory factor and hypoxia inducing factor and pathogen-induced toxins are associated with this phenotypic conversion (23,25). Growing scientific evidence further suggests that several epigenetic components (histone modification, transcriptional activation or suppression of macrophage genes) and pathogenic stimuli and the local microenvironment surrounding macrophages, regulate this phenotypic interconversion (23,25,26).

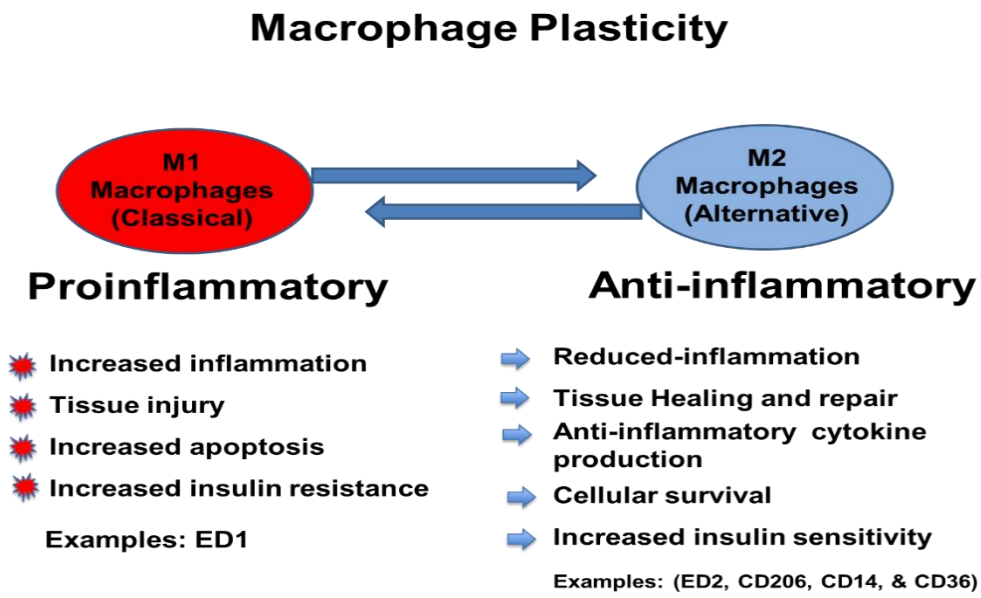

Fig.1-1: Macrophage polarization process and functional roles of classical and alternative macrophages. **Abbreviations used**; Classical M1-macrophages; Alternative-activated M2-macrophages; Cluster of differentiation-68 (ED1) macrophages; Cluster of differentiation-163 (ED2) macrophages; Cluster of differentiation-206 (CD206) macrophages; Cluster of differentiation-14 (CD14) macrophages; Cluster of differentiation-36 (CD36) macrophages.

1.1.3 Classical macrophages (M1-macrophages)

1.1.3.1 ED1 macrophages

The ED1 expressing macrophages are the pro-inflammatory classical M1-phenotype of macrophages (27,28). These macrophages are recognized by their surface expression of cluster of differentiation-(CD)-68 molecules (27,28). During various conditions of tissue inflammation and injury such as obesity, diabetes (T1D and T2D), and hypertension, an increased accumulation of ED1 macrophages in several tissues was reported (5,7,10,11,13,17,29,30). In all these pathological conditions, ED1 macrophages constitute a major part of the tissue infiltrate and participated in

inflammation initiation and tissue injury mechanisms (Fig.1-1) (5,7,10,11,13,17,29,30). Thus, during obesity, diabetes and hypertension, strategies targeted to reduce number and detrimental functions of ED1 macrophages will be advantageous to improve tissue health and functions.

1.1.4 Alternative-activated macrophage (M2-macrophages)

1.1.4.1 ED2 macrophages

ED2 macrophages are the anti-inflammatory alternative-activated M2-phenotype of macrophages that express a glucocorticoid regulated surface protein CD163 and possess tremendous potential for scavenging the haptaglobin-hemoglobin complex (31,32).

The occurrence of ED2 macrophages is documented in both rodent tissue and human tissues where the expression of ED2 macrophages is stimulated by a number of cellular factors (31,32). Heme proteins, glucocorticoids, IL-6 and IL-10 are known to stimulate ED2 expression while the pro-inflammatory TNF-family of cytokines, IFN-γ, IL-4 and LPS were shown to reduce ED2 expression (31-33). In normal physiology, ED2 macrophages are mainly associated with resolution of inflammation (10,11,13-15,17,31-33).

During various conditions of obesity, diabetes (T1D, T2D) and hypertension, a significant depressed expression of ED2 was shown to be associated with increasing tissue injury in several tissues (liver, heart, kidney and pancreas) (10,11,13-15,17,28,33). In contrast, pharmaceutically enhanced expression of ED2 macrophages was shown to be associated with the attenuation of tissue injury and an improvement of glucose metabolism (10,11,13-15,17,33). Collectively this evidence suggests the significant role of ED2 macrophages in the regulation of tissue injury and metabolism during metabolic diseases.

1.1.4.2 CD206 macrophages

CD206 macrophages belong to the class of anti-inflammatory alternative-activated M2-phenotype of macrophages that express mannose receptor protein on their surface (34). CD206 is expressed by several cells (resident macrophages, dendritic cells, lymphatic and non-vascular endothelial cells) and are mainly associated with clearance of excessive mannose-linked glycoproteins (34). Recently, it is reported that the expression of CD206 is highly elevated during inflammation and tissue injury conditions and a soluble form of CD206 is confirmed in humans (35). Moreover, a number of studies documented the anti-inflammatory role of CD206 during several inflammatory conditions of obesity, diabetes, and hypertension in maintenance of tissue homeostasis and repair (Fig. 1-1) (11,13,14,17,33). For example, in obese, diabetic and hypertensive animals, increased CD206 expression was associated with reduction of inflammation and tissue injury (11,13,14,17,33).

In addition, in diet-induced obese animals, increasing proinflammatory M1-macrophages and increasing M1/M2 macrophage ratio was closely associated with the development of insulin resistance while IL-10-induced accumulation of M2-macrophages (CD206, CD163, CD209a) decreases this ratio and improved insulin sensitivity (33).

In a diabetic nephropathy model, pentraxin-3-induced renoprotective effects were associated with the shift of inflammatory M1-macrophages ($iNOS^+$ and $CD16/32^+$) towards M2-macrophages ($CD206^+$ and an $Arg1^+$) (36). Studies in rodents further reported that during diabetes, transition of pro-inflammatory classical M1-macrophages to an anti-inflammatory alternative-activated M2-phenotype is greatly altered and contributes towards impaired wound healing and increased inflammation (37). However, under non-diabetic conditions, CD206 and CD36 participated in maintenance of the anti-inflammatory conditions through secretion of anti-inflammatory cytokines

such as IL-10 (37). Increased expression of CD206 and ED2 macrophages induced anti-inflammatory cytokines IL-10 is shown to play an important role in protection against atherosclerosis through regulation of heme protein homeostasis in the situation of intraplaque hemorrhage (38,39). These studies collectively proposed the anti-inflammatory and regulatory functions of alternative CD206 macrophages during metabolic and vascular alterations.

1.1.4.3 CD36 macrophages

CD36 macrophages are alternative-activated M2-phenotype of macrophages that mainly participate in internalization of oxidized lipids (oxLDL) generated through various inflammatory and oxidative processes (11,13,37,40). CD36-deficient rodents are hyperlipidemic due to altered lipid metabolism (41). Recently, in adipose tissue macrophages specific lipoprotein lipase (LPL) inhibition and subsequent CD36 downregulation was shown to be associated with inhibition of atherogenic foam cells formation. However, the above reduction in LPL and CD36 significantly increased the circulatory fatty acid levels that participated in development of hepatic insulin resistance and systemic glucose intolerance (42). These observations collectively suggest that CD36 prevents the sequestering of fat into the circulation and inhibits the development of insulin resistance in liver of obese mice. Similarly, in diabetic patients, CD36-deficiency is closely associated with dysregulated lipid metabolism and enhanced atherosclerosis and cardiovascular mortality (43). CD36-deficient patients showed dysregulated lipid metabolism (hyperlipidemia, triglyceridemia), impaired glucose tolerance and insulin resistance (44,45).

CD36 also participates in clearance of necrotic and apoptotic cells and associated inflammation through efferocytosis (46). In diabetic rodents, along with other M2-macrophages CD206, CD36 participated in maintenance of the anti-inflammatory conditions through secretion

of anti-inflammatory cytokines such as interleukin-10 (37). Similarly, during obesity and hypertension pharmaceutically enhanced CD36 expression with other M2-macrophage markers was associated with reduction of hyperlipidemia, tissue injuries with improvement of glucose metabolism (11,13). Thus, CD36 is an important regulator of inflammation and dysregulated metabolism during obesity, diabetes and hypertension.

1.1.5 Proinflammatory cytokines and chemokines in tissue injury

1.1.5.1 Tumor necrosis factor-alpha (TNF-α) and mechanism of tissue injury

Enhanced levels of circulatory and tissue TNF-α are reported in several conditions of inflammation and metabolic dysfunction during obesity, diabetes and hypertension (5-7,47-50). Both, proinflammatory M1-macrophages and dysregulated adipose tissue are the major producers of TNF-α during inflammation (5-7,51). As major roles, TNF-α, participates in inflammation initiation and tissue injury in these altered metabolic conditions (5-7,51). TNF-α-associated inflammation initiation is executed through activation of chemotaxis related protein MCP-1 that facilitates the accumulation of proinflammatory M1-macrophages at the site of tissue injury (7,51-53). In addition, locally produced TNF-α is also known to activate downstream Iκκβ-NF-κB inflammatory signaling and the JNK-stress-kinase pathway (50,54-56). The TNF-α-mediated activation of these pathways further augments the production of TNF-α itself, and other proinflammatory cytokines such as IL-6 and IL-1β. The collective elevated levels of these cytokines initiate a vicious cycle of systemic inflammation that leads to tissue injury in various vital organs (50,54-56). The TNF-α-induced mechanism of tissue injury is reported by several studies during obesity, diabetes and hypertension (49-53,57-60).

In diet-induced or genetic obesity, Kupffer cells or adipose tissue-derived TNF-α enhanced macrophage infiltration in hepatic tissue via increased accumulation of triglycerides and chemotaxis proteins (interferon gamma-induced protein-10 and MCP-1) and participate in development of steatohepatitis (51). In addition, TNF-α-mediated enhanced macrophage infiltration and activation of oncogenic signalling mediators such as signal transducer and activator of transcription 3 (STAT3), extracellular signal-regulated kinase (Erk) and JNK participates in hepatocellular carcinoma development during obesity (57). In contrast, the blockage of TNF-α signalling through TNF-α knockdown or tumor necrosis receptor-1 (TNFR1) ablation was shown to be associated with amelioration of steatohepatitis and hepatocellular carcinoma development (51,57).

Recent studies in both humans and rodents further suggested that obesity-induced augmentation of TNF-α converting-enzyme (TACE) and downregulation of fibrosis regulating sirtuin-1/metalloproteinase-inhibitor-3 axis are the important causes of enhanced fibrotic responses in the liver that subsequently develop into steatohepatitis and hepatic fibrosis (58,59). Moreover, TACE-induced TNF-α, self stimulates the release of profibrogenic procollagen-α1 (I), alpha smooth muscle actin and transforming growth factor beta (TGF-β) and induce hepatic fibrosis during obesity (58). In this condition, pharmaceutical inhibition of TACE through marimastat is shown to attenuate established hepatic steatosis (59). (Refer to chapter-4 for more details on hepatic injuries; ***PLoS One. 2013;***8(11): e79270).

Similarly, renal tissue is very sensitive to TNF-α-induced cytotoxic injuries (52,53). Elevated TNF-α levels are associated with podocyte injury and development of renal histopathological lesions in obese and T2D rodents (52,53). The TNF-α-mediated enhanced renal deterioration is governed through NF-κB-induced activation of TNFR2-receptor and subsequent

MCP-1-induced macrophage accumulation in renal tissue (52,53). In this condition of renal injuries, TNF-α blockage ameliorated the characteristic features of renal pathologies such as albuminuria, increased creatinine and renal lesions (52,53). (Refer to chapter-5 for more details on renal injuries; (***PLoS One. 2014;***9(1): e87936).

Likewise, in liver and kidney, TNF-α overproduction also severely affect the health and functions of cardiac and vascular tissue (49,50,60). In obese rodents, increased lipotoxicity and elevated levels of TNF-α-induced Iκκβ-NF-κB-JNK-axis and IL-1β are shown to induce cardiac inflammation, fibrosis and cardiac hypertrophy through enhanced macrophage infiltration that resulted in reduced survival of cardiomyocytes (50). In both hypertensive and obese rodents, TNF-α greatly suppresses protein kinase B (Akt)/endothelial nitric oxide (eNOS) signalling while overproducing the nitric oxide stress and phosphatase-and-tension-homologue (49,60). The collective effect of this vascular-signalling disturbance results in development of reduced vasodilatory response and increased systolic pressure and vascular inflammation and insulin resistance in obese and hypertensive rodents (49,60). In contrast, pharmaceutical or genetic blockage of TNF-α not only reduces cardiac and vascular injuries but also improves blood pressure (49,60). (Refer to chapter-3 for more details on cardiac injuries; ***Oxid Med Cell Longev. 2013;*** 2013:253657). Thus, the versality in TNF-α-associated tissue destructive functions and close cross talk with inflammatory and stress mediators, makes it a potent stimulator of inflammation-induced tissues injuries during metabolic diseases.

1.1.5.2 Interleukin-1 beta (IL-1β) and mechanism of tissue injury

Proinflammatory IL-1β is a major regulator of tissue injury and metabolic dysfunction during obesity, diabetes and hypertension (5,61-73). Infiltrating macrophage are the major

producers of IL-1β during these conditions (5,61-73), however, some non-monocytic cells are also involved in IL-1β production (63).

As major functions, IL-1β participates in inflammation-induced injury in several tissue compartments including adipose tissue, liver, heart, kidney and pancreas during obesity and diabetes and hypertension (5,61-73). Studies reported that IL-1β induced activation of nacht-lpr-pyd domains-containing protein-3 (Nlrp3) inflammasome is the principle mechanism of tissue injury and metabolic dysfunction during obesity, diabetes and hypertension (63,69,70,74-76). Conversely, activated Nlrp3 also increased the both IL1-β production and activation in a caspase-1 dependent manner (63,69,70,74-76).

During obesity, IL-1β is associated with inflammation induced adipose tissue injuries (5,61,62) and elevated production of IL-1β is principally governed by activation of either toll like receptor-4/myeloid-differentiation-primary-response-gene-88 or Nlrp3/caspace-1 signalling (62). The elevated levels of IL-1β by the above mechanisms, further augment monocyte production in bone marrow via hematopoietic progenitor cells and their chemotaxis towards the inflamed sites of adipose tissue leads to inflammation and adipose tissue injury (62).

Nlrp3/caspace-1 associated elevated levels of IL-1β was also documented in both adipocytes and adipose tissue of obese and T2D patients where IL-1β further produces proinflammatory mediators like IL-6, IL-8, TNF-α and MCP-1 and enhance leukocyte infiltration in adipose tissue (75,76). Inhibition of caspace-1 or metformin therapy significantly reduced IL-1β expression and inflammation (75,76). Increasing adiposity is shown to be associated with enhanced Nlpr3-mediated elevation of IL-1β and enhanced adipose and hepatic injuries in obese and T2D models of rodents, while weight reduction was associated with suppression of the Nlpr3-mediated IL-1β elevation (77).

IL-1β is also involved in hepatic deterioration during metabolic diseases (63,64,77). It is reported that increasing adiposity is one of the major reasons of IL-1β activation in hepatic resident macrophages (Kupffer cells) in a Nlrp3-inflammasome/caspace-1 dependent manner (63,64). The activated IL-1β further executes its tissue destructive role by two distinct mechanisms. In the first mechanism, IL-1β increases hepatic lipogenesis through stimulation of fatty acid synthase enzyme. While in the second mechanism, IL1-β enhances the accumulation of triglycerides in the liver. Both actions of IL-1β lead to enhanced production of proinflammatory mediators like TNF-α and MCP-1 and profibrotic collagen in the liver and participate in development of hepatic steatosis (63,64). In contrast, IL-1β blockage or Kupffer cells depletion protected from development of obesity-induced steatosis (63,64). Similarly, in T2D rodents, adipose tissue derived IL-1β and other proinflammatory cytokines (TNF-α, IL-6) and chemokines (MCP-1 and MIP-1α) synergistically induce hepatic and pancreatic injuries via enhancement of monocyte and leukocyte infiltration (65). In contrast, IL-1β antagonism was associated with reduction of these injuries in both organs.

IL-1β is shown to be a major regulator of cardiovascular tissue inflammation and cardiac deterioration during metabolic syndrome-associated conditions (69-72). In diabetic rats, IL-1β-induced vascular NADPH-oxidase and NF-κB and was shown to be associated with development of endothelial dysfunction and cardiac-vasculopathy while the IL-1β antagonist anakinra reduces the vascular inflammation and restored endothelium-dependent vascular relaxation (72). In addition, in a rodent experimental model of cardiac failure, inflammasome-mediated IL-1β activation is shown to induce cardiac inflammation, hypertrophy, and ventricular alteration (69). In contrast, the blockage of IL-1β was shown to be associated with suppression of cardiac inflammation and structural alteration and restoration of systolic performance. In T2D rodents, it

has been observed that, Nlrp3-inflammasome activation is a major regulator of production of inflammatory NF-κB and oxidative thioredoxin-interacting protein in local and systemic surroundings. These mediators increase oxidative stress and activate the IL-1β in a caspase-1 dependent fashion. The increased IL-1β further induces the remodelling in myocardium and participates in development of diabetic cardiomyopathy (70).

Hypertensive conditions are also a potent cause of cardiac injury through overproduction of IL-1β and other proinflammatory mediators (71). In hypertensive rodents, IL-1β along with TNF-α, IL-6 and chemokines (MCP-1, MIP-1α,) is shown to be associated with cardiac tissue inflammation and injury through overexpression of fibrotic mediators (TGF-β, collagen-IV) and markers of cardiac failure (71).

Recently, in a comprehensive study, it is shown that during both diabetes (T1D and T2D) increasing inflammatory and oxidative stress are the major regulators of Nlrp3-inflammasome-mediated IL-1β activation and subsequent renal endothelial inflammation, podocyte injury, renal fibrosis and development of nephropathy. IL-1β was also shown to downregulate nephrin and increase proinflammatory cytokines in diabetic kidney, while Nlrp3 ablation or IL-1β antagonism prevented renal injuries and development of diabetic nephropathy (74). Thus, similar to TNF-α, IL-1β is also a key cytokine in tissue injury of hepatic, renal and cardiac tissue during obesity, diabetes and hypertension and IL-1β blockage by various means has cytoprotective benefits (62-65,72,74,77).

1.1.5.3 Interleukin 6 (IL-6) and mechanism of tissue injury

IL-6 is a pleotropic cytokine that participates in several conditions of tissue injury and metabolic regulation during obesity, diabetes, and hypertension (5,47,48,78,79). In healthy

conditions, approximately one third of circulatory IL-6 is secreted by adipose tissue (80), however, during obesity, the stromal vascular fraction of visceral adipose tissue consisting of macrophages and endothelial cells secrete a large amount of IL-6 (81). It is reported that during inflammatory conditions of obesity, diabetes, and hypertension, the IL-6 level is highly elevated in both the circulation and in inflamed tissues and is considered a predictive marker of inflammation, tissue injury and dysregulated metabolism (47,78,82,83). Interestingly, in obese patients, a close relation of increasing serum IL-6 and other adipokines (TNF-α and leptin) with enhancement of C-reactive proteins is documented that suggests an important role of IL-6 in inflammation initiation (48). Similarly, in experimental rodent models of obesity, diabetes (T1D, T2D) and hypertension, increasing IL-6 expression along with other proinflammatory cytokines such as TNF-α and IL1-β are associated with inflammation-induced deterioration of liver, kidney and heart and dysregulated glucose metabolism (5,10,14,15,17,47,79).

IL-6-induced lipotoxicity through enhanced production of hepatic triglycerides and activation of downstream IL-1β and TNF-α are the major mechanisms of IL-6-associated inflammation and tissue injury (57,84). In response to a high fat diet, IL-6 has been shown to promote inflammation through enhanced lipid accumulation in liver and activation of proinflammatory STAT3, Erk, and JNK molecules associated with steatohepatitis and liver cancer development (57), while IL-6 deficiency was shown to be associated with reduced inflammatory monocyte infiltration and reduced activation of proinflammatory mediators in the livers of high fat diet rodents. In the obese rodents, enhanced production of proinflammatory STAT3 and elevated levels of IL-6 has been shown to be associated with fibrotic liver injury through enhanced production of the destructive acute phase protein fibrinogen in the liver (85). IL-6 deficiency has

been shown to ameliorate this activation state of hepatic STAT3 and adipose tissue fibrinogen molecules.

Despite destructive proinflammatory roles, an increasing number of scientific reports suggested the anti-inflammatory and metabolism regulatory roles of IL-6 in various conditions of metabolic alteration (86-97). During obesity, IL-6 protects against endotoxin-induced inflammation through enhanced expression of the anti-inflammatory CD206 expression via STAT3-dependent activation of interleukin-4R expression in macrophages and secretion of the anti-inflammatory cytokine IL-10. In contrast, blockage of IL-6 signaling is shown to enhance inflammation through augmentation of proinflammatory M1 cytokines (TNF-α, IL-1β, IL-6, IL-12p35) and oxidative stress mediators (iNOS2 and JNK) in liver and skeletal muscle (88). Similarly, disruption of IL-6 signaling enhances the production of TNF-α, and phosphorylation of inhibitor of NF-κB (IκB-α) in the liver (89). In obese rodents, IL-6 deficiency is associated with development of obesity, hepatosteatosis, liver inflammation and insulin resistance due to suppression of mitochondrial metabolism through reduction of important metabolic enzymes in the liver (87). Interestingly, exercise-induced IL-6 in skeletal muscle was shown to plays an anti-inflammatory role during various conditions of metabolic diseases, reviewed by Pedersen et al. (97).

From all this evidence, it is suggested that the IL-6 cytokine can be both proinflammatory and anti-inflammatory and is associated with metabolic regulation. The mechanism of this dual behavior of IL-6 is not clearly understood and it is believed that intrinsic crosstalk of different factors in a given cellular environment determine the anti-inflammatory and proinflammatory role of IL-6 in metabolic disease (5,10,14,15,17,47,79,86-97).

1.1.6 Role of proinflammatory chemokines in tissue injury

1.1.6.1 Monocyte chemotactic protein-1 (MCP-1)

Monocyte-chemoattractant-protein-1 (MCP-1) is a member of the chemokine-β family of cytokines that plays a major role in chemotaxis and activation of inflammatory macrophages (98). In both obese, diabetic rodents and humans, MCP-1 is reported as an intermediate link of adipose tissue inflammation-induced injury and adipose tissue dysfunctions (5,7,99,100). During obesity, T2D and hypertension, the elevation of MCP-1 levels is the first step in inflammation initiation where MCP-1 is shown to enhance ED1 macrophages infiltration and TNF-α production in adipose tissue (30,99,101). In addition, MCP-1 is also considered as a significant regulator of liver and skeletal muscle inflammation-induced injury during obesity and T2D and hypertension (11,99,100,102).

In high fat diet-induced obesity and T2D, propagermanium-induced MCP-1 inhibition, supressed the lipotoxicity, monocyte accumulation and hepatic steatosis development (99,100). In skeletal muscle, palmitate-induced MCP-1 was shown to increase skeletal muscle injury through an enhancement of a proinflammatory environment (102). For example; enhanced accumulation of ED1 macrophage, proinflammatory cytokine production (TNF-α and IL-1β), reduction of anti-inflammatory chemokine (C-X3-C motif) ligand 1 (CX3CL1), CX3C chemokine receptor 1 (CX3CR1) and interleukin-10 (IL-10) (102).

Similarly, in T2D-induced nephropathy and hypertension, MCP-1 upregulation was associated with several features of renal deterioration and abnormal glucose metabolism, such as increased monocyte infiltration, podocyte apoptosis, renal atrophy, albuminuria and insulin resistance (30,101). However, pharmaceutical inhibition of MCP-1 significantly reduced the renal pathologies (30,101).

Elevated levels of MCP-1 were also shown to induce vascular inflammation and remodelling (aortic wall thickening and fibrosis, arterial scaring) and development of atheroma during hypertension (103,104). In contrast, MCP-1 deficiency was shown to blunt hypertension-induced vascular tissue injury (103).

Increasing levels of MCP-1 is strongly correlated with inflammation-induced insulin resistance and altered glucose metabolism during obesity, diabetes and hypertension in several tissues (adipose tissue, liver and skeletal muscle) (7,30,99,100,102) and suggested that MCP-1-induced development of insulin resistance is principally governed through increased gluconeogenesis, lipotoxicity and production of proinflammatory cytokines TNF-α, IL-6 and IL-1β (7,30,99,100,102). In contrast, MCP-1 inhibition by various means, supressed lipotoxicity, gluconeogenesis and hyperglycemia while it improved insulin sensitivity and glucose metabolism (7,30,99,100,102).

Recently in two clinical trials, pharmaceutical inhibition of MCP-1 was shown to be associated with improved tissue health and metabolic functions (105,106). In T2D patients, 5 mg once a day of a MCP-1 inhibitor (CCX140-B) significantly lowered albuminuria and proteinuria without any toxic side-effects (105). Furthermore, MCP-1 blockade through JNJ-41443532 is associated with improved β-cell function and improvement in glycemia in obese-T2D patients (106). Collectively, these studies suggested that, MCP-1 is not only a crucial regulator of inflammation-induced injury during metabolic syndrome but also severely alters the insulin sensitivity and glucose metabolism through development of insulin resistance. Thus, MCP-1 inhibition has a beneficial impact on both tissue injury and metabolism. However, some studies in transgenic high fat-fed MCP-1 knockouts failed to show the MCP-1 induced macrophage

infiltration in adipose tissue and suggested the presence of an alternative pathway and tissue specific roles of MCP-1 in rodents (107,108).

1.1.6.2 Macrophage-inflammatory-protein-1 alpha (MIP-1α)

Macrophage-inflammatory-protein-1 alpha (MIP-1α) is the other chemokine that is associated with metabolic syndrome-induced tissue injury (5,7). It is reported that similar to MCP-1, MIP-1α is also associated with chemotaxis and facilitates the accumulation of macrophages in injured tissue (5,7). An elevated level of MIP-1α is documented in obesity and T2D and hypertensive conditions (5,7,10,11,13,14,17,19,65,71). In addition, inflammatory cytokines such as TNF-α are also shown to induce MIP-1α during tissue injury (7).

During both genetic and diet-induced obesity, MIP-1α is produced with MCP-1 and participates in adipose tissue inflammation initiation and adipose tissue injury through production of proinflammatory cytokines (5,7). Similarly, in diabetes and hypertensive conditions, MIP-1α production was associated with inflammatory injuries in heart, liver and kidney through augmentation of monocyte infiltration (10,11,13,14,17,19,65,71). Thus, MIP-1α is an important mediator of inflammation-induced tissue injury in metabolic and vascular conditions. (Refer to chapter-2 and chapter-3; ***Am J Hypertens. 2013;*** 26(9):1123-31 and ***Oxid Med Cell Longev. 2013;*** 2013:253657 for more details on MCP-1 and MIP-1α).

1.2 Oxidative stress and tissue injury during obesity, diabetes and hypertension

1.2.1 Oxidative stress in obesity, diabetes and hypertension

Increasing oxidative stress is a major contributor of tissue injuries and metabolic dysfunction in obesity, diabetes, and hypertension (8,13,14,109-114). During obesity and diabetes,

elevated lipid and hyperglycemia are the two major contributors that are associated with the production of several reactive oxygen species during these conditions (8,13,14,109-114). Hypertension that is the condition of dysregulated blood pressure, renin angiotensin aldosterone system (RAAS) and dysregulated lipid metabolism are the major producers of oxidative stress and associated injuries (19,113,114). In addition, metabolic by-products of non-enzymatic glycation of carbohydrate and lipid-peroxidation also produce significance levels of oxidative stress (8,13,14,109-114).

It is observed that during obesity and diabetes, mitochondria overactivation and increasing NADPH-oxidase enzyme activity are the key mechanism through which these reactive species are elevated (109-112,115,116). In addition, tissue infiltrating monocytes and lymphocytes are the major ROS producing cellular entities (5,7,115-118). Both these mechanisms collectively alter the tissue architecture and metabolic functions.

During both obesity and T2D, increased lipotoxicity is one of the significant contributors of insulin resistance development through activation of oxidative JNK stress signalling pathways (56,91,111,115,119,120). Amelioration of oxidative stress through genetic ablation of JNK or overexpression of antioxidant genes in mitochondria such as catalase was shown to improve insulin sensitivity and glucose metabolism (56,91,111,115,119,120). It is also shown that during increasing adiposity, generation of reactive oxygen species (ROS) is the first event in inflammation initiation that is regulated through NADPH-oxidase activation (121). The increased NADPH-oxidase and elevated ROS further activate the inflammatory molecules MCP-1 and proinflammatory cytokines (TNF-α, IL-6) through activation of NF-kB and participate in development of insulin resistance (5,115,121,122). Thus, elevated levels of oxidative stress are the

other major regulator of tissue injury and metabolic dysfunction in liver, kidney, heart and pancreas (8,10,115,123-126).

1.2.2 Oxidative stress, tissue injuries and dysfunctional metabolism

1.2.2.1 Oxidative stress and liver injury

Lipogenic oxidative stress is a significant risk factor for development of hepatic non-alcoholic fatty liver disease in obese and diabetic subjects, that is characterised by enhanced hepatic accumulation of fat and presence of histopathological lesions (steatosis, ballooning, fibrosis) along with elevation of functional hepatic alanine transaminase, aspartate transaminase and alkaline phosphatase markers and inflammation (127). A similar trend of histopathological disturbance has been observed in both T2D patients and diet-induced obese and diabetic animals (128-130).

In addition, in T2D patients and animals it is shown that the presence of hyperglycemia acerbates the hepatic injury during non-alcoholic fatty liver disease through further stimulation of fibrotic mediators and a number of lipid associated parameters and production of inflammatory mediators (131,132). These observations collectively suggest that the combined conditions of obesity and T2D will have more potent effects on the severity and progression of hepatic injury (131,132). In this situation, dietary interventions such as restricted dietary fat and cholesterol intake were shown to be associated with amelioration of lipotoxicity-induced hepatic pathologies and improvement in insulin functions (133). (Refer to chapter-2 and chapter-4 for more details on hepatic injuries; ***PLoS One***. ***2013;*** 8(11): e79270 and ***Am J Hypertens***. ***2013;*** 26(9):1123-31).

1.2.2.2 Oxidative stress and cardiac injury

Oxidative stress is also detrimental for cardiac tissue during increasing adiposity since increasing levels of oxidative mediators such as malondialdehyde, protein carbonyl and decreased activity of glutathione S-transferase, glutathione peroxidase, and paraoxonase1 were observed in cardiac tissue (134). In addition, obesity-induced oxidative stress negatively regulates cardiac health and metabolism through enhancement of several pathological features of cardiac tissue injury such as cardiac hypertrophy, fibrotic injury, cardiac stiffness, while it increased systolic blood pressure, endothelial dysfunction and impaired repolarization in the left ventricle (135).

It is reported in diet induced obesity that increased caloric intake-induced oxidative stress is associated with mitochondrial dysfunction, cardiac apoptotic injuries and impaired contractibility (136). In addition, in these animals a significant decreased expression of antioxidant enzymes manganese superoxide dismutase (MnSOD) and glutathione peroxidase 1 (GPx1) is documented (136). High-fat diet is also a potent cause of mitochondrial dysfunction and this abnormality is closely associated with elevated production of oxidative mediators that severely distort cardiac morphology and produced left ventricular hypertrophy and diastolic dysfunction (137). In contrast, catalase overexpression was shown to ameliorate the oxidative stress-mediated effects in the heart (137). Even in pre-diabetic rodents, increasing cardiac oxidative stress was associated with enhanced cardiac lipid-accumulation, ventricular hypertrophy, and diastolic dysfunction suggestive of early cardiac injuries (138).

Clinical studies also confirmed that excessive lipid-accumulation in cardiac tissue is a potent cause of increasing oxidative stress and inflammation. These factors equally participate in development of cardiac steatosis, cardiac dysfunction and cardiac insulin resistance (139).

Similarly, in obese animals, lipid peroxidation-induced oxidative stress in the myocardium was shown to acerbate cardiac morphology and the antioxidant defence system (140). Interestingly, even in the metabolic healthy obese condition, obesity-induced oxidative and endoplasmic reticulum-induced stress significantly deteriorate the cardiac architecture through enhanced fibrosis while reducing the antioxidant defense and accelerating the development of cardiomyopathy (141). These results suggest that during metabolic healthy obese conditions, oxidative stress and endoplasmic reticulum-induced stress are the major players of cardiac tissue injury while inflammation has a minor role at this early condition of metabolic dysfunction. Collectively this evidence suggests that similar to inflammation, elevated oxidative stress is a major cause of increasing cardiac injury and dysfunction during obesity, diabetes and hypertension. (Refer to chapter-3 for more details on cardiac injuries; ***Oxid Med Cell Longev. 2013;*** 2013:253657).

1.2.2.3 Oxidative stress and renal injury

Obesity is predominantly associated with development of glomerulopathy characterised by enhanced renal pathological features such as glomerular volume, foot-process width and proteinuria with decreased podocyte density (142). The most acceptable cause for these renal injuries are the increasing lipotoxicity (142). During obesity, lipid-induced oxidative stress functions at earlier stages and is a major contributor to development of renal pathologies (143,144). In a normotensive and hyperlipidemic obese (fa/fa) model of rats it is observed that induction of oxidative stress at an earlier stage is associated with increased levels of triglycerides and cholesterol and elevated levels of lipid peroxidation components (thiobarbituric acid relative substance) in kidney. These kidneys showed a progressive focal segmentary glomerular

hyalinosis and associated renal pathologies such as tubular injury, interstitial fibrosis and proteinuria. This suggests that increasing lipid-induced oxidative stress is associated with renal tissue destruction in obesity (143). Similarly, in obese-hypertensive and diabetic animals, obesity-induced early oxidative stress is the major cause of renal injury while hypertensive conditions further acerbates the pre-existing renal injuries (144).

Furthermore, in diabetic patients, it is reported that altered triglyceride and cholesterol metabolism is an effect of dysregulated lipid metabolism and is associated with enhanced accumulation of lipid in renal tissue and development of severe glomerulosclerosis, podocyte dysfunction and inflammation. Studies in both human and mouse models suggest that abnormal lipid oxidation is also a major reason for enhanced lipid deposition and fibrotic responses in renal tissue (145). The similar trend of lipid abnormality and renal injuries is further reported in diabetic patients suggesting that during diabetes, the functions of triglyceride regulating effectors such as PPAR-alpha, carnitine palmitoyltransferase 1, acyl-CoA oxidase, renal lipoprotein lipase is drastically supressed (146). In contrast, the diabetic condition upregulates the expression of cholesterol uptake receptors, LDL receptors, oxidized LDL receptors, and acetylated LDL receptors (146). Thus, abnormal lipid regulation is the major mechanism responsible for enhanced renal injuries during diabetes.

In a non-obese spontaneous model of T2D, an increased expression of oxidative stress mediators (NADPH p22 phox, and NADPH p47) and nitrosative stress mediators (eNOS, nitrotyrosin, nitrate and nitric oxide metabolite) were associated with renal pathologies such as increasing glomerular hypertrophy and expansion of the mesangial proliferation, increased creatinine clearance and urinary albumin (147). Collectively, these observations suggest that, development of renal injuries in diabetes is a collective effect of both oxidative and nitrosative

stress that drastically affect the renal architecture and functions (147). (Refer to chapter-5 for more details on renal pathologies during obesity and diabetes; (***PLoS One***. ***2014;*** 9(1): e87936).

1.2.3 8-isoprostane

8-isoprostane is a marker of lipid peroxidation widely used to determine oxidative stress in metabolic studies. 8-isoprotane is a by-product of lipid peroxidation formed by arachidonic acid peroxidation by reactive oxygens species (8,71,148,149). Chemically, it is very stable and less reactive then other less stable by-products of lipid peroxidation such as aldehydes and lipoperoxides that makes it suitable to evaluate oxidative stress (8,71,148,149). To determine the oxidative state at a systemic level, 8-isoprostane is measured in biological fluids (urine and plasma) while to determine tissue specific oxidative stress, 8-isoprostane is measured in tissue extracts (8,71,148,149). An enhanced level of 8-isoprostane is observed in metabolic altered conditions like obesity, diabetes (T1D, T2D) and hypertension (8,16,17,19,144,150-153) and correlated with oxidative stress-mediated tissue injury and metabolic dysfunction in various tissues.

In new-onset T1D patients and STZ-rats, increased lipid peroxidation was shown to be associated with enhanced generation of 8-isoprostane levels as a predictor of an oxidative stress environment and deviated glucose metabolism (8,151). In essential hypertensive patients, increasing plasma 8-isoprostane is associated with oxidative stress-mediated increasing salt sensitivity in hypertension (150). Similarly, in rodents, combined conditions of genetic obesity, diabetes and hypertension, enhanced 8-isoprostane was associated with oxidative renal injury evident by enhanced collagen-IV and albuminuria (144). In our previously published reports, enhanced 8-isoprostane levels were associated with enhanced oxidative fibrotic renal injury and renal hypertrophy in both obese-T2D diabetic and hypertensive rats (16,17,19). In non-alcoholic fatty liver disease patients, elevated

levels of oxidative markers such as nitric oxide 2-derived peptide and 8-isoprostane are suggestive of enhanced oxidative hepatic deterioration (153). During obesity, elevated, 8-isoprostane along with other oxidative stress markers such as 4-hydroxy-2-nonenal and protein carbonyls was suggestive of oxidative skeletal muscle injury and skeletal muscle insulin resistance while exercise significantly reduced the levels of oxidative markers and improved insulin sensitivity (152). Elevated 8-isoprostane levels along with endothelin-1 (ET-1) were also documented in injured fibrotic cardiac and renal tissues of obese diabetic and hypertensive rats (13,15,17,71). In these metabolic altered conditions, antioxidant treatment was shown to counteract against oxidative stress and improved dysregulated parameters (154,155).

Thus, increasing oxidative stress is a crucial factor in tissue degeneration during the metabolic dysfunctional states of obesity, diabetes, and hypertension. In these conditions, early detection through measurement of 8-isoprostane and use of antioxidants will help to counteract oxidative stress and associated tissue injury and dysfunction.

1.2.4 Antioxidant capacity in T1D

In normal physiology, several antioxidant enzymes regulate the elevated levels of oxidative stress and constitutes the antioxidant capacity of a given organ system (156-159). It is well known that T1D is an altered condition of oxidative stress tissue injury and dysregulated metabolism (8,10). During T1D, hyperglycemia generates a significant amount of reactive oxygen species and severely affect the pancreas and other organs (8,10). However, the pancreas is primarily affected due to intrinsic lower antioxidant capacity (160,161) which makes it more vulnerable against elevated oxidative stress-induced injuries. Similarly, in T1D patients, an abnormal response of antioxidant genes such as those for catalase, copper/zinc superoxide dismutase (Cu/Zn SOD), and

glutathione peroxidase (GSH-px) mRNA was observed with increased hyperglycemia (156). In this condition, approaches to enhance defense against oxidative stress will be quite beneficial to reduce T1D-associated injuries in the pancreas and other organs.

In rodents, enhanced β-cell specific expression of Cu/Zn SOD enzymes prevented oxidative stress-induced diabetogenesis (162). Similarly, catalase and manganese/zinc superoxide dismutase (Mn-SOD) overexpressing rodents have shown improved β-cell survival and reduced NF-κB activation in chemically-induced diabetes (163). In cultured insulin producing cells, overexpression of glutathione peroxidase, Cu/Zn SOD and catalase protects synergistically against both oxidative and nitrosative stress (157). In addition, enhanced expression of these antioxidant enzymes were also subjected to confer protection against proinflammatory cytokines-induced cytotoxicity (157).

Treatment done using non-enzymatic antioxidants such as β-carotene, α-tocopherol and ascorbic acid were also shown to reduce oxidative stress and pro-inflammatory cytokines in T1D patients in a dose dependent manner. Moreover, these non-enzymatic antioxidants also enhanced the expression of antioxidant enzymes including SOD and catalase (158). In STZ-induced diabetic rats, treatment with vitamin K1 attenuated the oxidative-stress-induced injury in pancreatic islets through significant reduction of NF-κB activation and inducible nitric oxide synthase (iNOS) expression and reduction in aldose reductase while increasing antioxidant enzymes (159). Thus, enhancing antioxidant capacity of the pancreatic compartment has a lifesaving benefits in T1D.

1.3 Insulin signaling in obesity, diabetes, and hypertension

1.3.1 Insulin signal transduction pathway and components

In normal physiology, the insulin signaling pathway is the major pathway responsible for

the maintenance of glucose homeostasis. The regulatory insulin signaling cascade is composed of several factors and proteins that collectively orchestrate glucose homeostasis (164). Insulin is a major activator of the insulin signaling machinery that initiate the proximal phase of the insulin signaling process through its binding to surface anchored insulin receptors in metabolically active tissues such as liver and muscle (164). Based on structure and functions, insulin receptors belong to the tyrosine kinase subfamily of proteins and consist of two segments, the insulin like growth factor-1 (IGF-1) receptor and the insulin receptor-related receptor (164,165). Moreover, the insulin receptor is a heterotetrameric complex that is composed of two distinct α and two β subunits. Between these subunits, insulin binds to the extracellular domain of the α subunit and this binding results in activation of a tyrosine kinase site on the β subunit which is located at an intracellular location (164,165). The activation of the β subunit is a result of insulin-induced depression of the β-subunit tyrosine kinase domain and is governed by a series of trans-phosphorylation and conformational change events that finally lead to increased kinase activity (164,165).

Recent evidence suggested that, although, the insulin receptor is the major binding site for insulin in pancreatic β-cells during high glucose levels, insulin is also shown to bind and activate IGF-1 or insulin receptor-IGF-1 conjugated or hybrid receptors (165). The insulin-induced activation of insulin receptor, IGF-1 or insulin receptor-IGF-1-conjugated, further activates the adaptor family of proteins popularly known as the insulin receptor substrate (IRS) through a series of binding and tyrosine phosphorylation. IRS proteins, which exists in multiple forms (IRS-1 to IRS-6) function as a connective adaptor molecule between proximal insulin signaling initiation and activation of downstream effector signaling pathways such as phosphatidylinositide-3-kinases/ protein kinase B (PI3K/Akt) and mitogen-activated protein kinase (MAPK) pathways (164,165). Insulin-mediated activation of the PI3K/Akt pathway further initiates the glucose translocation

process via glucose transporter molecules such as glucose transporter 4 (GLUT4) (165,166).

1.3.2 Dysfunctional insulin signaling in obesity, diabetes, and hypertension

1.3.2.1 TNF-α and dysfunctional insulin signalling and glucose metabolism

Evidence suggested that TNF-α is actively involved in development of abnormal glucose homeostasis during obesity, diabetes, and hypertension (6,7,49,167-169). TNF-α-induced inflammation is a crucial factor for development of insulin resistance in insulin target organs like liver, skeletal muscle and heart (6,7,49,167-169), thus, TNF-α is considered as a link between inflammation and insulin resistance.

Reduction of the tyrosine kinase activity of the insulin receptor (IR) and abnormal serine phosphorylation of IRS-1 are the major mechanisms through which TNF-α participates in the development of insulin resistance (6,168,169). The abnormal phosphorylation at the serine residues of IRS-1 further inhibits their tyrosine-phosphorylation-induced activation through the insulin receptor (IR) and in this condition, the insulin-induced activation of insulin signaling cascade is interrupted (6,168,169). In addition, TNF-α also suppresses GLUT4 expression and associated glucose uptake in skeletal muscle (6,167-169).

Scientific reports further suggested that TNF-α-mediated activation of downstream Iκκβ-NF-κB and JNK-stress-kinase pathways play a major role in development of insulin resistance during obesity and T2D (54-56,91,120). TNF-α-associated increased expression of JNK1 and JNK2 and altered phosphorylation of IRS-1 at the Ser312 residue and subsequent reduction of GLUT4-induced glucose uptake was also documented in human visceral adipocytes. However, either, JNK1/2 silencing or liver-X-receptor agonists-mediated inhibition of TNF-α, completely reverse insulin resistance while enhancing GLUT4-induced glucose uptake (120). Thus, in this

condition of reduced insulin sensitivity, TNF-α inhibition improved insulin sensitivity and glucose uptake in both genetic and diet-induced obesity (6,57,167).

It has become increasingly clear that TNF-α induced lipolysis is the other mechanism of development of inflammation and subsequent development of insulin resistance during obesity (55,170-172). TNF-α is shown to stimulate lipolysis of excessive fat in adipose tissue and, as a result, this free fat enters into the systemic circulation and participates in inflammation and insulin resistance in liver and skeletal muscle (55,170-172). An in vitro experiment suggested that TNF-α-mediated lipolysis is dependent on mitogen-activated protein kinase (MAPK) and NF-κB activation, that collectively, downregulate the lipid droplet-associated protein perilipin and enhance lipolysis (170), while NF-κB inhibition via a cell permeable peptide, inhibit the TNF-α-induce lipolysis (170). In vitro and in vivo observations in rodents suggested that TNF-α and its receptor TNFR both are negative regulators of adenosine monophosphate-activated protein kinase (AMPK) in skeletal muscle and TNF-α-mediated reduction of AMPK is regulated via TNF-α induced protein phosphatase 2C in skeletal muscle. The suppression of AMPK signaling reduces the fat oxidation while increases its accumulation in skeletal muscle (172). Deficiency of TNFR1/TNFR2 or TNF-α neutralization were shown to improve AMPK signaling and ameliorate the lipid-induced insulin resistance (172). Moreover, TNF-α upregulates adipose triglyceride lipase, while silencing of adipose triglyceride lipase in adipocytes completely abolish the TNF-α-induced fatty acid release (171). Thus, TNF-α-induced lipolysis plays a significant role in insulin resistance development in metabolic tissues.

Although, the above evidence in rodents collectively proposed a straightforward application of TNF-α blockage to overcome insulin resistance and tissue injury, the beneficial effects of TNF-α neutralization in humans was not very successful (173-175). In healthy obese

male subjects with insulin resistance, chronic TNF-α blockage with infliximab therapy showed abating effects only on inflammatory biomarkers such as C-reactive protein and fibrinogen but failed to improve insulin sensitivity and endothelial or vascular functions (173). Similarly, administration of the TNF-α blocker etanercept in obese T2D patients and patients with metabolic syndrome showed similar improvement in systemic inflammatory events through reduction of inflammatory mediators (C-reactive protein, IL-6, and fibrinogen) and increased total adiponectin but etanercept did not improve insulin resistance and vascular functions (174,175). These clinical studies collectively suggested that TNF-α neutralization may be effective in overcoming inflammation and insulin resistance in experimental rodents, however, in humans, the regulation of insulin resistance might involve some other effectors.

1.3.2.2 IL-1β and dysfunctional insulin signalling and glucose metabolism

Despite its crucial role in metabolic tissue injury, IL-1β also negatively affects glucose homeostasis (5,61,68,73,75,77,176-178). Both adipose tissue derived and macrophage derived IL-1β negatively affect insulin sensitivity, glucose metabolism and participates in development of insulin resistance during obesity (5,61,73). IL-1β suppresses the insulin signalling mechanism through inhibited expression and activation of insulin signalling components such as IRS-1, PI3K, GLUT4 and protein kinase B (PKB) in obese rodents (73). Similar observations are also documented in both human and murine adipocytes in vitro, where IL-1β treatment decreases insulin sensitivity through marked suppression of IRS-1 and GLUT4-induced glucose uptake (73). IL-1β also inhibits the insulin-induced tyrosine phosphorylation-mediated activation of IRS-1 and insulin-induced activation of PKB and Erk1/2 (61,176). In contrast, IL-1β blockage is associated

with improvement in the insulin signalling mechanism (73). Thus, during conditions of adiposity, IL-1β negatively regulates the insulin signalling mechanism.

In obese rodents, it is further reported that, IL-1β associated suppression of insulin signalling and development of insulin resistance is principally governed through monocytic Nlrp3-inflammasome activation (177). During obesity, enhanced lipotoxicity is the major activator of Nlrp3-inflammasome and subsequent activation of autophagy, ROS, and AMPK signaling pathways. The lipotoxicity-induced activation of these pathways resulted in enhanced production of IL-1β and development of insulin resistance (177). It is further explained that insulin resistance development through activation of Nlrp3-IL-1β axis is executed by two distinct direct and indirect mechanisms. The first inhibitory mechanism involves the direct suppression of insulin signalling through alteration in serine phosphorylation of IRS-1 and devoid of TNF-α requirement. The other indirect mechanism is dependent on IL-1β-mediated TNF-α production and subsequent inhibition of IRS-1. Thus, in IL-1β-associated development of insulin resistance, Nlrp3 activation is a major requirement (177). These observations were further confirmed in obese animals where adipose tissue showed a higher expression of the inflammasome component caspase-1, that is known to participate in activation of mature IL-1β through cleavage of pro-IL-1β (75,77,178). Interestingly, in murine adipose tissue, elevated levels of caspase-1 itself had reasonable capabilities to selectively modulate adipocyte differentiation and forced them to acquire an insulin resistant phenotype. In contrast, ablation of caspace-1 or Nlrp3-deficiency is shown to be associated with more metabolically active and insulin sensitive fat cells that showed enhanced GLUT4, adiponectin and fat-oxidation levels (178).

In T2D diabetic rats, elevated IL-1β is shown to stimulate hepatic gluconeogenesis through activation of the gluconeogenetic enzyme phosphoenolpyruvate carboxykinase. IL-1β-induced

gluconeogenesis is one reason for altered glycemic levels in T2D (65). Like TNF-α, IL-1β also induces lipotoxicity through increased lipolysis and suppression of lipid regulatory peroxisome proliferating-activated receptor γ and CCAAT/enhancer-binding protein-α (61,68). IL-1β-induced abnormal lipid regulation and subsequent elevated lipids in the systemic circulation collectively participate in development of insulin resistance during obesity and diabetes (61,68). IL-1β antagonism reduced lipotoxicity associated parameters (free fatty acids, cholesterol and triglyceride) while protecting from the insulin resistance development and hyperglycemia (61,68). Thus, detrimental functions of IL-1β enhance both tissue injury and metabolic dysregulation during diabetes and obesity.

1.3.2.3 IL-6 and dysfunctional insulin signalling and glucose metabolism

IL-6 plays important roles in deterioration of insulin sensitivity in metabolic organs such as liver and skeletal muscle during obesity and T2D and is associated with development of obesity and diabetes (54,57,85,120,179-181). The IL-6 associated reduction of adiponectin and dysregulation of carbohydrate and fat metabolism is a major cause of insulin resistance development during T2D and obesity (181). In contrast, IL-6 deficiency reverses these conditions while improving the lipid and carbohydrate metabolism through enhanced adiponectin secretion (181). Interestingly, studies in obese and diabetic humans and rodents indicated that compared to TNF-α and other mediators (CRP and leptin), IL-6 is more closely associated with several parameters of insulin resistance and abnormal glucose metabolism (179). In contrast, weight loss or caloric restriction significantly reduce IL-6 levels and improve glucose metabolism at both tissue and systemic levels (179).

During obesity, elevated levels of hepatic fat also stimulate the production of IL-6 and other proinflammatory cytokines (TNF-α, IL-1β) through activation of the Ikkβ-NF-κB axis and subsequent development of low insulin sensitivity, glucose intolerance and insulin resistance in both liver and skeletal muscle (54). IL-6 associated STAT3, Erk, and JNK activation and subsequent abnormal phosphorylation of IRS-1 at Ser312 are the other mechanisms of insulin resistance and abnormal glucose metabolism in liver while IL-6 ablation was shown to improve insulin sensitivity (57,120). In vivo and in vitro experiments further suggested that IL-6 was also a major reason for enhanced hepatic glucose production and reduced insulin-dependent insulin receptor autophosphorylation and activation of Akt molecules resulting in development of insulin resistance (85). In addition, IL-6 also inhibit insulin-induced glucose lowering effects via inhibition of the IRS-PI3K axis. However, the above inhibiting effect of IL-6 on IRS-PI3K is differentially regulated and tissue specific. In liver IL-6 inhibits IRS-1 and PI3K while in skeletal muscle it is executed through IRS-2 and PI3K inhibition (180). Moreover, in skeletal muscle IL-6 stimulate fat accumulation through activation of lipid stimulatory fatty acyl-CoA enzyme. Thus, IL-6-induced lipotoxicity and altered insulin signalling are major reasons of skeletal muscle insulin insensitivity and glucose intolerance during inflammation (180). However, IL-6 inhibition ameliorates the negative consequence of abnormal or supressed insulin signalling (85). Collectively these observations suggested a close association of IL-6 in the development of insulin resistance during metabolic syndrome conditions.

Although, collectively the above evidence suggested a potent role of IL-6 in development of insulin resistance, many studies reported that IL-6-mediated positive modulation of insulin signalling and glucose metabolism during obesity and diabetes.

In obese liver IL-6 and STAT-3 are shown to inhibit gluconeogenesis through activation of hepatic glucose-6 phosphatase at transcriptional level (86,89). IL-6 inhibition resulted in gluconeogenesis and development of glucose intolerance and insulin resistance in liver, adipose tissue and skeletal muscle of obese animals (88). IL-6 was also shown to increase insulin secretion through stimulation of pancreatic α-cell and intestinal L cells and reduce hyperglycemia in obese diabetic animals while IL-6 blockage ameliorates these beneficial effects of IL-6 on hyperglycemia (96). Similarly, in human skeletal muscle, IL-6 improves insulin sensitivity through enhancement of glucose regulating processes (glucose transportation, glycogen conversion and glucose disposal) (92,93). The IL-6 associated reduction of muscle insulin resistance is governed by increased phosphorylation-mediated activation of STAT3, AMPK and p38 mitogen-activated protein kinase (92,93). It is further shown that IL-6-induced AMPK activation is regulated through increased cyclic adenosine monophosphate and adenosine monophosphate *vs* adenosine triphosphate ratio that results in increased skeletal muscle energy expenditure (94). Recently, in obese and diabetic mice, a glucose regulatory drug, protectin-DX was shown to act as an IL-6 secretagogue in skeletal muscle and ameliorates the hepatic glucose production via STAT3-mediated transcriptional suppression of gluconeogenesis. Thus, it is suggested that stimulation of skeletal muscle IL-6 and the liver glucose regulatory axis through protectin-DX will be highly valuable to reduce insulin resistance during obesity (95). Interestingly, in a comprehensive study, it is reported that depot specific expression of IL-6 is a critical factor in execution of its beneficial or destructive role during obesity and metabolic syndrome conditions (90,91). For example, during obesity, adipose derived IL-6 is mainly associated with development of insulin resistance through suppression of IRS-1. In contrast, in the hepatic compartment, Kupffer cells derived IL-6 causes improvement in insulin resistance through enhanced expression of IRS-2, which suggests the

tissue-specific dependence in IL-6 associated functions during obesity (90,91). Thus, the dual functionality of IL-6 is still not completely understood and is a matter of intensive research.

1.3.3 T1D and dysregulated glucose metabolism

Like obesity, T2D and hypertension, insulin insufficiency, increasing inflammation, oxidative stress and hyperglycemia severely alter the insulin signaling mechanism in T1D, as evident by suppressed expression and functions of insulin signaling components such as IRS-1, IRS-2, GLUT4, PI3K and PKB in metabolically active tissues (8,182-195). In experimental animal models, any alteration or absence of these components results in abnormal glucose homeostasis through dysfunctional insulin signaling (8,182-195). Thus, optimal function of insulin signaling components are the essential requirements for maintenance of glucose homeostasis.

1.4 Pancreatic tissue injury and Type-1 diabetes (T1D)

1.4.1 Prevalence of T1D

T1D is a chronic condition of inflammation and increasing β-cell death that is increasing at a very fast pace around the globe (1). Global health reports ranked it as one of the leading causes of mortality due to its close association with cardiovascular and renal disorders (1). The clinical management of diabetes mellitus is onerous and expensive (1). Despite, astonishing growth in the field of pharmaceutical research for anti-diabetic medications, only limited options are available for its treatment such as insulin therapy and oral medications, which are inadequate and produce the danger of unwanted side effects (196,197). In addition, in terminal T1D patients, islet transplantation is a lifesaving clinical intervention, however, there are numerous hurdles associated with islet transplantation procedures such as immune-mediated allograft rejection, low efficacy of

transplanted β-cells, inflammatory reactions, graft survival and less availability of cadaveric donors. These factors drastically decrease the efficacy and feasibility of islet transplantation process in T1D patients (198).

1.4.2 T1D and pancreatic tissue injury

Regarding the pancreatic injury mechanism, T1D is an autoimmune form of diabetes where T-lymphocyte-(T-cell)-mediated β-cell destruction, produces a condition of insulin inadequacy and hyperglycaemia (199,200). The T-cell-mediated autoimmune mechanism of T1D is unique and begins with the inflammatory process known as insulitis (199,200). During the insulitis process, many T-cells and macrophages invade pancreatic tissue and initiate the vicious cycle of inflammation and activation of several β-cell death pathways including granzymes or perforin-mediated β-cell death, Fas/FasL and TNF-α/TNF-R-induced β-cell killing, proinflammatory cytokine-induced β-cell death, and oxidative stress-induced β-cell death (201-204). Thus, during T1D, final β-cell death involves several different mechanisms and effector molecules that makes its pathogenesis quite difficult. In this abnormal condition, reduction of inflammatory and oxidative stress, replenishment and enhanced survival and functions of β-cells are the necessary requirement in T1D management.

A plethora of scientific studies suggested that the pancreas has a reasonable degree of plasticity through which pancreatic cells can regenerate and fulfill the required cell number or repair the injured (205-220) tissue. Observational studies in pancreatic injury models including pancreatectomy, partial duct-ligation and toxin-induced pancreatic injury documented the regeneration of both the endocrine and exocrine pancreas (205-220), however, the mechanism of pancreatic repair or regeneration was quit variable, which may be due to differences in animal

strains and experimental procedures and type of injury.

1.4.3 Mechanisms of pancreatic repair and /or regeneration

1.4.3.1 β-cell replication and pancreatic regeneration

There are two distinct mechanisms of pancreatic regeneration, replication (221,222) or neogenesis (223). Replication of β-cells is one of the physiological mechanisms in the pancreas that is responsible for increasing β-cell number and subsequent increase in β-cell mass. In the process of replication, a pre-existing β-cell generates a new daughter β-cell through cellular division. The newly generated nascent daughter β-cell further enters into a maturation phase and differentiates into a functional mature β-cell (221,222). The scientific literature suggested that the process of replication is differentially governed by several epigenetic factors and cell cycle regulators at both the neonatal and adult stages (221,222). In addition, various systemic regulators such as nutritional and growth components and hormones are the other essential factors that participate in regulation of β-cell generation and functional maturation (221,222). Thus, regulation of β-cell generation through replication is quite variable at both the neonatal and adult stage and involves several effector molecules reviewed in (221,222).

Studies utilizing genetic linage tracing experiments in pancreatic injury models suggested that β-cell replication is the only method of generation of new β-cells during the adult stage and almost all β-cells of the adult pancreas have replicative capabilities (205-208), thus, refuting the concept of neogenesis during the adult stage.

In contrast, observations in rodents contradicted this concept and suggested that during the post-natal stage or adult stage, the process of β-cell replication and production of new β-cells is very slow and cannot fulfill the requirement for β-cells (221,224,225). Additionally, aging was a

significant contributor towards the slower rate of β-cell turnover in adults (224,226). 5-bromo-2-deoxyuridine labelling experiments further confirmed these observations in mice and suggested that proliferation and replication of the β-cell is a very slow process and decreased with age (221,224,225). Similar observations have been documented in rodent and human pancreas (227,228) and suggested that β-cell regeneration from replication of pre-existing β-cells follows slow kinetics and mostly occurred at the post-natal stage and declined with time and age (227,228). Furthermore, studies in rodents explained that during the adult stage, the presence of a replication refractory period in pancreatic islets slowed down the replication of pre-existing β-cell**s** (207,229). Moreover, various metabolic stress conditions such as hyperglycemia, toxic injury and insulin resistance are also partially capable of activating β-cell replication and proliferation and insulin secretion (224,230-233), However, regardless of this partial activation, replication has less importance in replenishment of β-cells in the injured pancreas at the adult stage. Thus, in the adult, β-cell turnover through replication is a very slow process that declines with age and time and cannot sufficiently fulfill β-cell requirements.

1.4.3.2 β-cell neogenesis and pancreatic regeneration

Neogenesis is another mechanism of pancreatic regeneration by which the injured pancreas replenishes the cell number and regains essential functions. Pancreatic neogenesis is also known as process of *de novo* formation of both exocrine and endocrine pancreatic cells from either stem cell progenitors or from cells of different lineages (223). It is suggested that neogenesis is particularly important in T1D-induced pancreatic injury conditions, since it provides a starting population of pancreatic cells including β-cells. Neogenesis derived pancreatic cells further proliferate and replace the lost and injured pancreatic cells and participate in both tissue repair and

restoration of pancreatic functions, for example replenishment of β-cells and insulin production (223).

Studies in rodents revealed that pancreatic neogenesis frequently occurs at the neonatal stage and after this period the occurrence of this regenerative process progressively declines with age (234-238). However, at the neonatal stage, the percentage of neogenesis derived islets cells was lower than the number of cells derived from replication (234,235), suggesting that β-cells neogenesis and replication both participate in maintenance of β-cell mass during the neonatal period.

In contrast, at the post-natal stage, there was a significant decrease in frequency of replication of pancreatic cells through an apoptosis-mediated remodeling mechanism that shifts the regenerative process toward neogenesis (226), suggesting that the neogenesis-mediated pancreatic regeneration mechanism dominants over replication during the post-natal period. Moreover, experimental studies using carbonic anhydrase II as a marker of the post-gestation period suggested that at the post-natal stage both exocrine and endocrine pancreatic cells may be derived from the neogenesis process (235). Observations in rodents and autopsied donor human pancreas also documented neogenesis in the adult pancreas (209-220).

1.4.3.3 Pancreatic regeneration and controversies

Although, these observations strongly supported the occurrence of neogenesis during the adult life span, various other scientific reports suggested that there is either an absence of neogenesis or very restricted regeneration occurring in the adult pancreas (205,207,226,234-237,239-244).

In mice, Solar and colleagues reported that exocrine ductal precursor $Hnf1b^{+}$ cells participate in neogenesis and differentiate into β-cells. However, this neogenic conversion of ductal to β-cells only occur in the embryonic period after which these cells lose their ability to enter into the neogenic phase. These observations were further confirmed by ductal ligation and toxin-mediated ablation of ductal or β-cells, where no conversion of ductal to β-cells was observed (239). Lineage tracing studies also refuted the concept of injury-induced activation of pancreatic progenitors that participate in β-cell regeneration post injury. In adult rodents, pancreatic duct ligation studies failed to document the occurrence of a β-cell regenerating neogenic process and expansion of β-cell mass (242). A study using InsCremTmG transgenic mice suggested that even during pregnancy or after pancreatic tissue injury (partial pancreatectomy or partial ductal ligation) there was an absence of neogenic β-cell regeneration in adult rodents where β-cell regeneration through neogenesis is a rare event during adulthood (244). Similarly, in humans, the generation of β-cells after partial pancreatectomy was not observed, and suggested that this may be the reason for development of diabetes in patients after pancreatic resection surgery (240). Lineage tracing studies using mucin gene Muc1 in rodents also argued against neogenesis in the adult stage (241). This study showed that exocrine cells, such as ductal cells only give rise to islet cells during the developmental period but at adulthood they are confined to the exocrine pancreas and do not transdifferentiate into endocrine islet cells (241).

Similarly, after complete ablation of β-cells after a high dose of STZ followed by ductal ligation, only regeneration of exocrine acini cell was reported. There was a complete absence of β-cell regeneration from any exocrine source or progenitors (243). A study in rodents also failed to see neogenic conversion of acinar to β-cell, however, new acinar cells may develop from pre-existing acinar cells (245).

Using a DNA analog-based lineage-tracing technique, it is further reported that at the adult stage, slow replication is the only method for β-cell replenishment throughout life and there was no involvement of any kind of specific progenitors in β-cell growth and regeneration (207,224). Dor and colleagues also reported that during the adult stage, β-cells only arise from pre-existing β-cells and do not involve stem cell progenitors (205).

Collectively, this evidence refuted the existence of β-cell regeneration from progenitors or through transdifferentiation of exocrine cells. Despite the huge number of supporting and contradicting reports, pancreatic regeneration in adults is still a controversial issue. Moreover, differences in animal strain, and variability in experimental procedures also incorporated a significant heterogenicity in these studies and warrant further investigations.

1.5 Marker implicated in pancreatic repair and/or regeneration

1.5.1 Tyrosine-protein kinase protein (c-Kit)

c-Kit is an important transmembrane glycoprotein protein that defines pluripotency, differentiation and longevity of embryonic stem cells and hematopoietic cells (246). c-Kit is activated through its ligand stem cell factor that is necessary for its biological functions (246).
The expression of c-Kit is documented in both developing exocrine and endocrine pancreas (247). c-Kit expressing cells showed an enhanced Pdx1 and insulin gene, proliferation and survival and were shown to participated in both islet neogenesis and pancreatic development during the fetal stage (247). In the murine model, β-cell specific c-Kit expression was shown to enhance β-cell proliferation and functional maturity and insulin secretion and counteracted against high fat induced detrimental features (248). Studies in rodent injury models suggested that c-Kit is a characteristic marker of the resident progenitor population of the pancreas that participates in

pancreatic neogenesis (249-251). In the STZ-induced pancreatic injury model, a prolonged increased expression of c-Kit in response to endocrine injuries is suggestive of involvement of c-Kit in β-cell regeneration (249). Similarly, in a cerulein-induced pancreatic injury model of adult rats, presence of c-Kit expressing cells are considered as islet progenitors and are involved in islet repair and regeneration during injury (251). Furthermore, in the STZ-induced pancreatic injury model, bone marrow derived c-Kit expressing transplanted cells were shown to reduce hyperglycemia through proliferation and increased insulin content. The study further suggested that these c-Kit positive cells promote endogenous pancreatic regeneration and proliferation of preexisting β-cells (252). All these studies collectively suggested the involvement of c-Kit expressing cells in pancreatic regeneration. Thus, c-Kit is an important marker for the progenitor phenotype of pancreatic cells and can be a candidate molecule in isolation and characterization of pancreatic stem cells in regenerative cell based therapies for diabetes treatment in the future.

1.5.2 Stem cell antigen-1 (Sca-1)

Sca-1 is a glycosyl-phosphatidylinositol-anchored cell surface protein that is involved in cell differentiation, growth and renewal and maintenance of hematopoietic stem cells (253-259). Several studies documented the Sca-1 expression in rodent pancreas and suggested that Sca-1 participate in pancreatic regeneration, repair and maintenance (253-260). Sca-1 deficiency is shown to be associated with defective hematopoietic cells and progenitor development in Sca-1 null mutants (Sca-1/Ly-6A) that hamper the self-renewal and functions of hematopoietic cells and the development of specific progenitor populations (260).

Using Sca-1 expression as an identification marker, a number of pancreatic progenitors have been isolated and characterized in the murine pancreas at both the post-natal and adult stage

from peri-ductal, peri-islet, centroacinar, and terminal ductal region (253,254). These Sca-1 expressing progenitor cells are highly proliferative and able to develop into multiple lineages of pancreatic cells including endocrine and exocrine lineages upon pancreatic injury (253,254). Additionally, Sca-1 positive progenitors express several transcription factors associated with both endocrine and exocrine pancreas growth, differentiation and functions and are responsive towards glucose-induced insulin secretion (253,254).

Sca-1 is considered to be an important regulating factor in pancreatic growth, development and regeneration during various conditions of pancreatic tissue injury including diabetes (261-263). During STZ-induced pancreatic injury in adult NOD mice a large number of IgG-positive cells at the periductal region were observed which are capable of forming multiple layers of cells in the pancreas. Moreover, these cells expresses a number of markers of hematopoietic stem cells such as Sca-1, c-Kit, suggesting that these IgG positive cells originated from hematopoietic stem cells (261). Cellular analysis through flow cytometry in NOD mice and pre-diabetic mice revealed that during diabetes, Sca-1, c-Kit and CD31 expressing endothelial progenitor cells migrated from bone marrow to peripheral blood in response to pancreatic injury signals and participate in pancreatic repair (262). Similarly NOD mice derived Sca-1 and c-Kit expressing hematopoietic stem cells have been transduced with lentivirus encoding pro-insulin II and transplantation of these cells in NOD mice were shown to reduce pancreatic insulitis and diabetes progression (263). Collectively, this evidence suggested the role for Sca-1 expressing progenitors in pancreatic repair Furthermore, Sca-1 expressing pluripotent very small embryonic like stem cells (VSELs) were identified in experimental models of rodents and suggested that deviated functions of these cells with age is a major cause of development of diabetes and cancer (256-259).

During, STZ-induced pancreatic injury, Sca-1 expressing bone marrow derived VSELs

were shown to express several pancreatic differentiation markers (Nkx6.1, Pdx1, and pancreas tissue factor-1), and temporarily improved hyperglycemia in STZ-induced diabetes. The study further explains that in response to pancreatic damage, these VSELs cells migrated from bone marrow to peripheral blood and further entered into the injured pancreas and participated in pancreatic repair and regeneration (256). Similarly, Sca-1 and CXCR4 positive VSELs cells expressed Oct3/4 and stage specific embryonic antigen-1 and developed into multiple lineages of cells including β-cells. Upon administration into an STZ-diabetic mice, these VSELs migrated to the injured pancreas and reduced hyperglycemia (257). Moreover, in a pancreatectomy model of mice, Sca-1 expressing VSELs were present in the adult mouse pancreas and were capable of differentiating into Pdx1 and Oct3/4 expressing progenitors which possibly regenerate into both exocrine and endocrine cells (258). These results collectively suggested that Sca-1 expressing VSELs have an important role in pancreatic repair and regeneration and may be used as a cellular tool for pancreatic repair during pancreatic injury.

1.5.3 Insulin gene enhancer protein-1 (Islet-1)

Islet-1 is a transcriptional factor which plays an important role in pancreas development and regeneration (264,265). Islet-1 is a stimulating factor for several genes associated with insulin secretion, protein trafficking, metabolism and differentiation in the pancreas suggesting it plays an important regulatory role in β-cells growth, functions and maintenance of glucose homeostasis (264). These observations were further confirmed in STZ, Akita, Db/Db models, where Islet-1 overexpression was associated with enhanced β-cell proliferation and colony formation through activation of c-Myc and cyclinD1 growth regulating genes (265). It is reported that Isl-1 along with its co-activator Lim-domain-binding protein-1 (Ldb1) participates in both endocrine

development and insulin promoter activation. In contrast, Ldb1 deficiency resulted in massive reduction in number of α-cells, β-cells and δ-cells and development of hyperglycemia suggesting a crucial role of Ldb1/Islet-1 axis in pancreatic development and function. (266).

Moreover, Islet-1 is essential for endocrine growth-associated processes and functions in the pancreas (267,268). In contrast, Islet-1 deficiency altered endocrine development through reduced proliferation and survival of endocrine progenitors Pax6 positive cells and downregulation of transcriptional factor Maf-A resulting in supressed expression of both insulin and glucagon hormones and hyperglycemia and impaired glucose tolerance (267,268).

Studies in rodents further extended the important role of Islet-1 in exocrine pancreatic development at the embryonic stage (269). Studies in mice revealed that Islet-1 is required for the generation of both the exocrine and endocrine pancreas, which is differentially regulated in a site-specific manner Islet-1 expression in the dorsal mesenchyme is required for exocrine pancreas development while islet expression in endodermal cells regulates endocrine pancreatic development. Thus, Islet-1 regulates the development of both the endocrine and exocrine pancreas independently (269).

1.5.4 Beta-catenin (β-catenin)

β-catenin is a major component of the Wnt signaling pathway that governs the various stages of organogenesis of both the exocrine and endocrine pancreas (270-273). It is observed that at the embryonic stage β-catenin is highly expressed with other Wnt factors and then decreased with time and is undetectable during the adult stage due to regulation of its inhibitor adenomatous polyposis coli gene (272). In vitro and in vivo studies in rodents showed that Wnt/β-catenin signalling governs β-cell growth, proliferation and expansion via enhancement of cyclin D2, Pdx1,

GLUT2, and Nkx6.1 and improves insulin release and glucose disposal while reducing hyperglycemia (273). Interestingly, β-catenin activation participates in pancreatic regeneration in rodents through enhancement of both β-cell replication and neogenesis (270). In contrast, Wnt/β-catenin blockage was associated with decreased pancreatic β-cell proliferation and islet or β-cell mass and regeneration, insulin secretory functions and development of impaired glucose tolerance (270,273).

Although, the above studies acknowledged the potential role of β-catenin in regulation of endocrine development and functions, it is also required for exocrine pancreas development and functions (271,274,275). In mice, β-catenin is shown to be essential for exocrine acinar cell lineage growth and specification (271,274), and its deficiency is associated with abnormal pancreatic development (271,274). In contrast, β-catenin deletion did not affect the islet endocrine cell mass or functions (271,274). Studies further explained that β-catenin-mediated functions were essential prior to E16.5 days of development and loss of β-catenin prior to E16.5 resulted in a decrease in the number of recognizable nascent acini and the pancreatic cellular mass (274). The reason for this exocrine developmental specificity is explained in β-catenin stabilization studies in rodents (275). This study suggested that β-catenin stabilization has dual opposing roles in pancreatic function and development at different stages of life. At the early period β-catenin stabilization was associated with loss of Pdx1 expression in early pancreatic progenitor cells and prevents differentiation and expansion of early pancreatic progenitor cells. In contrast, at a later stage, β-catenin activation was associated with increased proliferation and enlargement of the exocrine pancreas (275). Collectively this evidence supported the important role of β-catenin in exocrine pancreatic development. Despite these controversial reports, a clear majority of published scientific reports supported a regulatory role for β-catenin in the endocrine pancreas, and suggested

that β-catenin signaling regulates several processes including β-cell growth, proliferation, and insulin secretion. Thus, activation of Wnt/β-catenin has a positive impact on β-cell growth and developmental functions in both the embryonic and adult stage.

1.5.5 Octamer-binding transcription factor-3/4 (Oct3/4)

The Oct3/4 is a member of the POU (Pit-Oct-Unc) domain transcription factor family that is involved in regulation of pluripotency and self-renewal of embryonic stem cells (276). Both in vitro and histological analysis in humans further suggested that Oct3/4 expressing pluripotent stem cells participate in regeneration of both the endocrine and exocrine pancreas (277,278). In the murine species, the pluripotent Oct3/4 expressing VSELs population is considered as a resident tissue progenitor and is shown to participate in tissue regeneration of the pancreas (258). Partial pancreatectomy studies (70%) studies in adult mice further reported that Oct3/4 expressing VESLs are involved in pancreatic regeneration during pancreatic injury (258). Interestingly, transplantation of human placenta derived Oct3/4 expressing multipotent progenitor cells restored the blood glucose levels through increased insulin production in diabetic animals (279) that is suggestive of their role in endocrine pancreas regeneration. Studies further suggested that the pancreatic transcriptional factor Maf-A is a regulator of differentiation of Oct3/4 positive multipotent stem cells into islet-like and insulin positive cells (280), since, Maf-A overexpression in these cells enhances a number of genes associated with pancreatic development and secretory functions. Furthermore, transplantation of these Maf-A overexpressing Oct3/4 cells in diabetic animals have been shown to restore blood glucose levels through increased insulin production (280). Thus, collectively the above evidence suggests an important role of Oct3/4 in regulation of endocrine pancreatic regeneration and differentiation processes in both humans and rodents.

However, since Oct3/4 is usually expressed with other pancreatic markers during regeneration, its individual role in pancreatic regeneration requires more specific studies.

1.5.6 Paired homeodomain transcription factor Pax2

Pax2 is a member of the paired homeodomain transcription factor family that is involved in embryonic development, differentiation and maintenance of pluripotency of stem cells (281). Among the several members of Pax-transcription factors, Pax4 and Pax6 actively participate in pancreatic development and functions (282,283). Pax4 is required for development of insulin producing cells while Pax6 plays a major role in pancreatic α-cell differentiation (282,283). However, a limited number of studies up until now have evaluated the functions of Pax2 in the pancreas. Pax2 expression is documented in both insulin and glucagon producing cell lines (284-286). However, RT-PCR analysis in rodents showed that Pax2 was only expressed during early embryonic pancreatic development and decreased with the time and determine the relative proportion of endocrine and exocrine tissues (284).

Although, in vitro studies showed the role of Pax2 in activation of pro-glucagon hormone promoter (285), studies in adult Pax2-deficient mice contradicted this observation and suggested that Pax2 is not an essential factor for the formation, growth and maturation of proglucagon producing islets, since Pax2-deficient mice were shown to have normal development of islet α-cells (285). Thus, short-term expression of Pax2 is required only at the early phase of pancreatic proglucagon promoter activity. Pax2 expression is also reported in both pancreatic insulin and glucagon producing cells and adult rodent islets (286). In rodent islets, two isoforms of Pax2 have been detected i.e., Pax2A and Pax2B, while in cell lines, in addition to Pax2A and Pax2B, a distinct third isoform, Pax2D2 is also detected (286). Functional assays suggested that both Pax2 isoforms

(Pax2A and Pax2B) are only involved in glucagon gene expression through their binding to the glucagon promoter at different sites while devoid of any effect on insulin gene expression (286). These observations collectively, suggested that Pax2 functions are more related to glucagon hormone transcription not the endocrine insulin transcription (286). Thus, it can be inferred that Pax2 only regulates the exocrine development at both embryonic and post-natal stages, however, its role in endocrine pancreatic development and function is not clear and requires further research.

1.5.7 Homeobox protein-Nkx6.1(Nkx6.1)

Nkx6.1 is a homeobox protein that was initially described by Rudnick et al., in rodent β-cells and α-cells in vitro (287). Immunostaining and expression analysis further confirm its expression during early pancreatic developmental stages, where it co-express with the important endocrine transcription factor Pdx1 and suggested that Nkx6.1 and Pdx1 co-express in early pancreatic development and are essential for pancreatic development and maturation of β-cells at the adult stage (288). Nkx6.1 is also shown to govern the survival and proliferation of transdifferentiating β-cell progenitors with other transcriptional factors and participates in the β-cell developmental process (289,290), since Nkx6.1 deletion in rodents was subjected to a dramatic loss of β-cell precursors and blockage of β-cell neogenesis (290).

Nkx6.1 expression is also documented in the adult pancreas (291-293). It is reported that, during the adult stage, it regulates the survival, maturation and insulin secreting functions of β-cells since Nkx6.1 ablation induces increasing β-cell death in rodents (290,291,293,294). During the adult stage, Nkx6.1 expression was shown to be restricted to insulin producing β-cells (291,294). and requires Pdx1 and GLUT-2 to execute its function (291,295). Conversely, Nkx6.1 also governs the GLUT2 and glucagon-1 like peptide expression that are essential for β-cell

functions. Studies further suggested that both Nkx6.1 and it paralog Nkx6.2 are important in endocrine β-cell fate determination (296). However, in Nkx6.1 null mutants it is reveled that Nkx6.2 has a limited capacity to compensate for Nkx6.1 functions (294). In addition, in vitro studies in modified primary human β-cells showed that Nkx6.1 co-express with several factors associated with β-cell growth and secretory function (Islet-1, Pdx1, Pax6, prohormone convertases 1/3 and 2, and secretory granule proteins) (292). These cells contain glucose-induced insulin secretory capacity and upon transplantation facilitated improved glucose regulation in diabetic mice. Thus, Nkx6.1 functions were dependent on other pancreatic transcriptional factors, which collectively orchestrate β-cell growth and function (292).

Nkx6.1 was also shown to regulate the glucagon producing α-cell (296) and control glucagon hormone production at the transcriptional level (293,297). This regulation is primary achieved by inhibition of glucagon gene transcription at transcriptional levels (293,297) In contrast, Nkx6.1 blockage resulted in a decrease in glucose stimulated insulin release while doubling of glucagon mRNA. Thus, Nkx6.1 plays an essential role in functional β-cell maturation and insulin secretory functions in the pancreas while it inhibits glucagon hormone transcription in β-cells (293).

1.5.8 Glucose transporter-2 (GLUT2)

GLUT2 is considered as a maturation marker for β-cells that are mainly responsible for initiation of the glucose-stimulated insulin release function (298,299). Analysis of GLUT2-deficient islets showed that GLUT2 deficiency negatively effects glucose utilization, insulin secretion and its biosynthesis. Moreover, in the absence of GLUT2, there is no compensatory expression of other glucose transporters such as GLUT1 or GLUT3, which collectively showed

the crucial requirement of GLUT2 in β-cell functions (298).

Comparative analysis of GLUT2 in neonatal and post-natal stages in mice, showed that at the neonatal stage, GLUT2 resides at a cytoplasmic location and confers limited glucose sensing capacity to β-cells while at the time of birth GLUT2 is expressed on the plasma-membrane and performs better glucose sensing. Thus, the cellular location of GLUT2 plays an important role in glucose sensing in the mature adult β-cells (299,300).

In rodents, GLUT2 deficiency was associated with hyperglycemia, hyperinsulinemia and reduced survival, and these rodents showed elevated levels of plasma free fatty acids, glucagon hormone and impaired glucose tolerance (301,302). Similarly, β-cell specific inhibition of GLUT2 through antisense RNA resulted in elevated levels of glucose as well as impaired levels of insulin secretion (303). In contrast, transgenic GLUT2 expression was associated with increased survival, and glucose-induced insulin secretion, suggesting the importance of GLUT2 transporter in both survival and glucose metabolism (301,302).

Experimental studies in rodents further revealed that during diabetes (T1D and T2D), GLUT2 expression is either absent or suppressed and absence of GLUT2 is considered as an important hallmark of β-cell dysfunction (302,304-306). In addition, GLUT2 deficiency or suppression was associated with development of diabetic symptoms and impaired pancreatic development (302-304). In contrast, GLUT2 overexpression facilitates normal glucose utilization and insulin secretory capacity of islets (298,305,307). Thus, GLUT2 is an important regulator of β-cell growth and maturation and insulin secretory functions during normal physiology. However, conditions like diabetes severely affect both the expression and function of GLUT2 that collectively results in aberrant β-cell growth and functions.

1.6 Heme oxygenase (HO) system

(This section is adapted and modified from my published article. Refer to the Appendix A for comprehensive details of heme oxygenase system and its regulation. **Mishra et al., *Curr Pharm Des. 2014*; *20(9):1370-91).***

1.6.1 Overview of the HO system

The heme oxygenase system (HO) is a group of microsomal enzymes which catabolize the oxidative breakdown of heme. (Fig. 1-2) (308). The increasing accumulation of heme is toxic for cells; thus, the HO system regulates its level through its breakdown into carbon monoxide (CO), iron (Fe^{+2}) and biliverdin (BV). The catabolic heme degradation through HO-enzymes is a multistep process and requires molecular oxygen and nicotinamide adenine dinucleotide phosphate (NADPH). The iron and biliverdin produced through heme degradation is further transformed to ferritin and bilirubin that function as antioxidants (Fig. 1-2)(308).

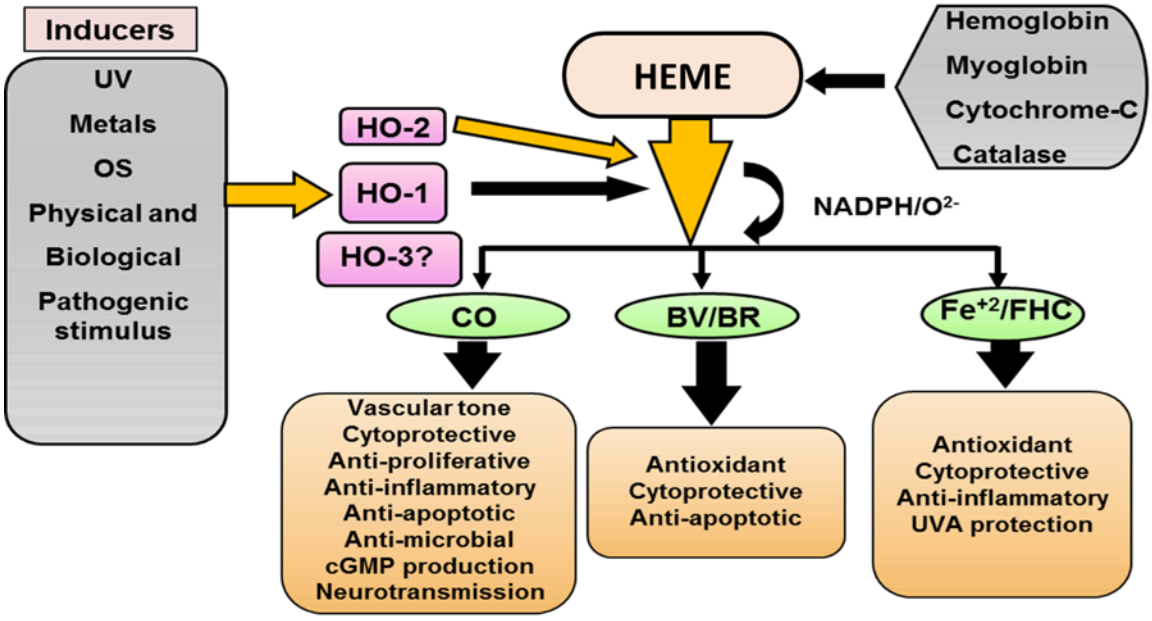

Figure 1-2: Cytoprotective role of the heme oxygenase system. HO-1 catalyzes oxidative degradation of cellular heme to produce carbon monoxide, iron and biliverdin. Adapted and modified from my published article, Ref. (308), **Mishra et al., *Curr Pharm Des. 2014***; 20(9):1370-91. Refer to Appendix A for more details.

Upregulation of HO-1 and its end-products by a variety of stimuli or by a pharmacological inducer exerts cellular protection against different pathological conditions via activation of distinct signaling pathways. (adapted and modified from ref. (308)). **Abbreviations used;** Carbon monoxide (CO), Biliverdin (BV); Bilirubin (BR); Iron (Fe^{+2}); Heavy chain ferritin (FHC); Cyclic guanosine monophosphate(cGMP); Soluble guanylate cyclase (sGC); Oxidative stress (OS); Ultra violet rays (UV); Nicotinamide adenine dinucleotide phosphate (NADPH); Oxygen (O^{2-})

1.6.2 Isoforms of the HO system

The HO system is composed of three different enzyme molecules HO-1, HO-2 and HO-3 (309-311). Among these three forms, the first isoform HO-1, is inducible and initially described as heat shock protein (310,311). In normal conditions, heme works as a substrate for HO-1 induction while a number of other factors and physiological situations are able to induce a significant level of HO-1, for example, ultra-violet rays and hydrogen peroxide, heavy metals, nitric oxide, hypoxia, heat shock, endotoxin and conditions of stress like oxidative stress (Fig. 1-2) (308). In addition, various biological, pharmaceutical and chemical compounds are able to induce and potentiate HO-1 expression in biological systems (308). Thus, safe induction of HO-1 through various pharmaceutical inducers is possible in the living system, which provides an opportunity to explore its functions in various cellular compartments.

The second isoform HO-2, is constitutively expressed in almost all organs and shares the major responsibility of heme metabolism with HO-1 in the mammalian system (Fig. 1-2) (308,310,311). The third HO-3 is a less studied isoform of the HO system and is thought to be a pseudogene which has no defined functions (Fig. 1-2) (309).

Genetically, the enzymes HO-1 and HO-2 are products of two different genes Homox-1 and Homox-2 and share a sequence homology of 43% (312). Interestingly, the HO-1 promoter contains various binding sites for NF-κB, activating protein-1 , activating protein-2 and IL-6 (313-315), while HO-2 shows a glucocorticoid response element in their promoter region (316). A striking difference between human HO-1 and HO-2 promoter is the presence of (GT)n dinucleotide length polymorphism and G(-1135)A and T(-413)A, single nucleotide polymorphisms, in the Hmox-1 gene of human which is completely absent from the Hmox-2 gene. Studies have further shown that the HO-1 promoter polymorphism is associated with susceptibility and outcome of various diseases, like pulmonary, cardiovascular, renal transplantation, neurological disease and diabetes (317-319).

1.6.3 Cytoprotective roles of HO system

HO system and its metabolites have a vast array of cytoprotective and regulating roles in several conditions of obesity, diabetes, and hypertension (Fig. 1-2)(308). The HO system has been shown to protect several tissues (heart, kidney, skeletal muscle, liver and pancreas) from oxidative and inflammatory tissue injury during metabolic diseases (308). In addition, pharmaceutical or genetic upregulation of the HO system was shown to be associated with improved metabolic regulation during obesity, diabetes, and hypertension (For a detailed view of HO system and its

cytoprotective roles in metabolic disease, refer to the Appendix A that is my first author publication. **Mishra et al.**, ***Curr Pharm Des***. ***2014;*** *20(9):1370-91)*

1.7 Nuclear factor-(erythroid-derived 2)-like 2 factor (Nrf2) and HO-1 regulation

Nrf2 is a member of the Cap 'n' collar transcription factors family that modulates several important cellular signaling processes related to human disease and metabolism (320,321). Nrf2 is regarded as a sensor for increasing oxidative stress that can induce a number of cytoprotective pathways to combat against increasing oxidative stress (320,321).

1.7.1 Nrf2-mediated transcriptional regulation of HO-1

The scientific literature suggests a close interaction between Nrf2 activation and the HO system during various conditions of stress in mammals. Moreover, it has been observed that HO-1 transcription initiation is executed in an Nrf2 dependent manner (320,321). Moreover, the HO-1 promoter contains a stress responsive element which activates HO-1 transcription in multiple conditions of stress, and confers cytoprotection against cellular stress (320,321). Studies have further shown that Nrf2 transcriptional factors respond to oxidative stress by binding to the antioxidant response element in the promoter of HO-1 genes coding for antioxidant enzymes which leads to coordinate enhanced expression of genes coding for cytoprotective proteins. Thus, during oxidative stress conditions, HO-1 upregulation is transcriptionally controlled by Nrf2 transcriptional factors (320,321). The Nrf2/HO-1 axis has been shown to confer protective effects in various conditions of inflammatory and oxidative tissue injury and in various conditions of abnormal tissue homeostasis associated with diabetes (322-332). (For further, details on Nrf2/HO axis please refer to recent published article from our lab (320). (**Ndisang et al.,*Curr Pharm Des.***

2017;23(10):1465-1470).

1.7.2 HO-1-mediated upregulation of Nrf2

Although, a large majority of evidence collectively proposed HO-1 regulation through Nrf2 signalling, HO-1 also regulates Nrf2 and its functions in cellular systems. A close modulating interaction between HO-1 and Nrf2 is observed in a number of studies that is shown to be cytoprotective (322-333).

Both *in vitro* and *in vivo* studies in rodents showed that during elevated oxidative stress, nuclear HO-1 actively participates in Nrf2 activation and stabilization and protects from proteolytic degradation (333). This HO-1-mediated increase in Nrf2 half-life further potentiates the antioxidant defence through augmentation of phase II oxidants and glucose regulating enzymes (333).

CO which is a metabolic by-product of HO-1 is also shown to activate Nrf2 (334-336). In endothelial cells, CO-associated cytoprotective effects against increasing endoplasmic reticulum stress was regulated through Nrf2 activation (334,335). In addition, in mice, the HO/CO axis is shown to regulate mitochondrial biogenesis through activation of the Nrf2 transcription factor and protect from inflammatory lethal sepsis (336).

A number of HO-inducers such as hemin, cobalt protoporphyrin (CoPP) are also shown to exert HO-mediated cytoprotective effects through activation of Nrf2 factor (337,338). HO-1 inducers such as hemin and CoPP both induce HO-1 via Nrf2 activation in a dose dependent manner in the glomerulus (337). This study further suggested a regulating mechanism of HO-1 through which HO-1 reduces it sustained expression and prevent the renal cells (337). Similarly, in the rodent lung transplantation model, hemin-mediated activation of HO-1 is governed through

Nrf2 activation and confers protection against lung injuries through potentiation of antioxidant defence while reducing inflammation. In contrast, hemin-induced effects were abrogated by an HO-1 inhibitor (338). Studies further showed that HO-induced Nrf2 activation and subsequent cytoprotection is governed through Erk1/2 and PI3K/Akt pathway activation (339,340). The involvement of Erk1/2 and PI3K/Akt pathway in HO-mediated regulation of metabolism and tissue protection was also confirmed in an in vivo model where HO-1 is induced by hemin (15,341). From this evidence, it is suggested that a close cross talk between HO system and Nrf2 is one reason for the modulatory roles of HO system in various conditions of dysregulated metabolism and tissue injury.

1.7.3 Cytoprotective role of Nrf2 in diabetes

A large number of studies have shown important cytoprotective advantages of Nrf2 transcriptional factor activation during the diabetic condition (322-332). Additionally, Nrf2 is considered as one of the regulating factors against increasing oxidative stress and disturbed antioxidant defenses during diabetes (322-327). In rodents, genetic activation of Nrf2 is also shown to associate with suppression of development and progression of diabetes through improvement of insulin secretion and insulin signaling mechanisms (327). Moreover, Nrf2-induced cytoprotective mechanisms also protected from development of high-caloric diet-induced hyperglycemia and diabetes in db/db mice (327). Moreover, Nrf2 activation was also shown to associate with increased expression of antioxidant enzymes such as NADPH: quinone-acceptor-oxidoreductase-1, Hmox1, glutathione peroxidase-2, and glutathione peroxidase-4, not only in pancreatic islets but also in liver, while Nrf2 null mutants have shown abrogated expression of these antioxidant enzymes. Similarly, genetic knockdown of Nrf2 has been shown to exacerbate the diabetic

condition as evident by elevated levels of hyperglycemia through increased gluconeogenesis and reduced glycolysis (331). In contrast, Nrf2 induction through its inducer, also mimicked diabetes counteracting effects in rodents (327), Similarly, in skeletal muscles and liver, Nrf2 activation participated in maintenance of physiological glucose levels through improved peripheral glucose consumption and increased insulin sensitivity (327,332). In addition, Nrf2 plays an important role in the diabetic cutaneous wound healing process (322,323). It is observed that during diabetes, hyperglycemia induced oxidative stress severely reduces the antioxidant defence through activation of Keap1 (a negative regulator of Nrf2) and suppression of nuclear translocation of Nrf2 and subsequent production of antioxidant enzymes (322). This reduction in antioxidant defense collectively results in impaired cutaneous wound healing. However, Keap1 inhibition through topical siKeap1 therapy or siRNA restored this weakened antioxidant system and improved wound healing through enhanced regeneration in diabetes animals (322). In addition, Nrf2 null mutants showed a reduced wound healing through reduced expression of antioxidant enzymes, TGF-β expression with higher expression of the matrix degrading enzyme matrix metalloproteinase 9, compared to $Nrf2^{+/+}$ mice (323). The similar mechanism of impaired wound healing is documented in human skin samples. In contrast sulforaphane and cinnamaldehyde (Nrf2 activator) ameliorates the above conditions of impaired wound healing (323). Thus, in diabetes, suppression of Nrf2-mediated enhancement of antioxidant defense is one of the major reasons for delayed wound healing and regeneration.

Nrf2 also participates in repair and/or regeneration of renal, skeletal and liver injuries (324-326). In the acute renal injury model, transplantation of Nrf2 overexpressing mesenchymal cells improved the renal functions and renal repair markers such as AQP1 and CK-18 (324). In contrast renal injury markers such as Kim-1 and cystatin-C were reduced (324). Similarly, studies in a

skeletal muscle injury model reported that Nrf2 deficiency is closely related to enhanced skeletal muscle injury and suppressed stem-cell associated muscle regeneration (325). Both in vivo and in vitro studies in rodents and human liver cells suggest that, the hepatic regeneration element is a major target of the Nrf2/antioxidant response element (ARE) and participates in hepatic repair. However, during Nrf2 deficiency or increasing oxidative stress the Nrf2/ ARE-mediated regulation of hepatic regeneration element is suppressed and results in exacerbation of hepatic injury and reduced the hepatic regeneration or repair (326). This evidence collectively proposed the functional requirement of Nrf2 in repair and regeneration of renal, skeletal muscle and liver.

Evidence further suggested that the Nrf2-induced cytoprotective effects were advantageous for β- cell survival and functions in the pancreas (328-330). Studies utilizing transgenic animals revealed that Nrf2 activation conferred protection against oxidative and nitrosative stress-induced β-cell death while it improved insulin secretory functions (328). Similarly, in human islets, Nrf2 activation through its synthetic-inducer (Dh404) increased the expression of NADPH-dehydrogenase-[quinone]-1, HO-1, glutamate cysteine ligase and phase II antioxidant genes. In addition, Nrf2 activation through Dh404 was shown to associate with significant reduction in oxidative/inflammatory damage of pancreatic islets through suppression of ROS and proinflammatory cytokines such as IL-1β, IL-6, IFN-γ and MCP-1 (329). Interestingly, Nrf2 has been shown to regulate the levels of unfolded and misfolded proteins in β-cells, through ubiquitin-proteasome-induced degradation and supressed their accumulation which may be cytotoxic for β-cell longevity (330). In contrast, genetic silencing of Nrf2 abolished the Nrf2-mediated cytoprotective advantages against increasing endoplasmic-reticulum-induced stress in β-cells (330). Thus, activation of Nrf2 has a cytoprotective benefit in the diabetic system not only in the

pancreatic compartment but also in other major organs of glucose homeostasis such as liver and skeletal muscle.

1.8 Summary

Enhanced tissue injury and dysfunctional metabolism are the characteristic features of obesity, diabetes, and hypertension that actively participate in development of tissue pathologies such as fatty liver disease, cardiomyopathy and nephropathy and pancreatic injuries.

As governing factors, elevated inflammation and oxidative stress are the major players behind these undesirable conditions of altered tissue homeostasis. In response to increasing adiposity during obesity and T2D, enhanced accumulation of inflammatory M1-macrophages in metabolic tissues (liver, heart, kidney) are the initial event during inflammation that are principally governed by the chemokine molecules (MCP-1 and MIP-1α). Tissue accumulated macrophages produce higher levels of proinflammatory cytokines (TNF-α, IL-1β, IL-6) and reactive oxygen species in the local tissue environment and activates the major inflammatory NF-κB and JNK-stress signalling pathways and initiates a vicious cycle of inflammatory and oxidative stress in metabolic tissues.

Activation of these pathways further augment the production of these proinflammatory cytokines and oxidative mediators that leads to development of systemic inflammatory/oxidative conditions and associated tissue injury and dysfunctional glucose metabolism. Additionally, these proinflammatory cytokines are also responsible for elevated levels of free fatty acid in both the local and systemic circulation due to lipolysis and induction of lipotoxicity-mediated tissue injuries in several vital organs such as liver, skeletal muscle and cardiac tissue.

Increasing levels of proinflammatory and oxidative mediators are also known to induce fibrotic tissue injury via activation profibrotic mediators such as TGF-β, collagen and fibronectin in hepatic, cardiac and renal tissues that collectively leads to development of pathological conditions of liver cirrhosis, cardiomyopathy and nephropathy and organ failure if not managed. Moreover, hypertension which is primarily a condition of dysregulated blood pressure is also shown to be associated with increased tissue injury and metabolic dysfunction both in vascular and metabolic tissue (heart kidney, liver and skeletal muscle) through lipid, RAAS-induced inflammation and oxidative stress.

Due to their tissue destructive role, inflammatory and oxidative mediators are responsible factors for development of metabolic dysfunctional states such as insulin resistance, glucose intolerance in liver, skeletal muscle and cardiac tissues. Elevated levels of proinflammatory cytokines and oxidative mediators negatively affect the insulin signaling mechanism via inhibiting the expression and activation of major insulin signalling components (IRS-1, IRS-2, PI3K, GLUT4) while reducing the insulin-induced glucose uptake in liver, heart and skeletal muscle.

Furthermore, T1D that is governed by autoimmunity-associated mechanisms also severely injure pancreatic tissue through T-cell-induced insulitis and subsequent enhanced β-cell apoptosis via various mechanisms which results in pancreatic injuries. In addition, during T1D, hyperglycemia-induced inflammation and oxidative stress further contributes to tissue injury and metabolic alteration in peripheral organs. Thus, obesity, diabetes (T1D, T2D), and hypertension are associated with increasing tissue injury and abnormal glucose metabolism and require an efficient management tool.

In these conditions, the cytoprotective and metabolism regulatory capabilities of the HO system and its metabolites (CO, BV and iron) can be used as an alternative tool. Moreover, a close

cross talk between the HO system and Nrf2 can regulate inflammatory and metabolic signalling at transcriptional levels, thus, exploration of the regulatory role of the Nrf2/HO axis may be advantageous during tissue injury and dysfunctional glucose metabolism. Due to inducible features, the HO system provides a great opportunity for safe induction by various pharmaceutical inducers in cellular systems that make it a reasonable choice for use as a therapeutic agent in several metabolic diseases. Although, HO is cytoprotective, its effect on hepatic, cardiac, renal and pancreatic injury and associated metabolic dysfunction is not well understood. Thus, the present study is designed to evaluate the role of the HO system on hepatic, cardiac, renal and pancreatic injury and dysfunction during obesity, diabetes (T1D, T2D) and hypertension.

1.9 Rationale

Increasing conditions of tissue injury and metabolic alteration in obesity, diabetes and hypertension present a great risk to human life and a daunting task to manage (1). During this metabolic dysfunctional state, elevated levels of proinflammatory cytokines (TNF-α, IL-1β, IL-6) chemokines (MCP-1, MIP-1α), oxidative mediators and increased macrophage accumulation in the tissue compartment are major reasons for enhanced tissue injury, dysfunctional metabolic responses and organ failure (8,16,71,342-344).

Locally produced inflammatory and oxidative responses are further augmented through activation of the central NF-κB-JNK inflammatory-oxidative axis and systemically injure almost every organ of the body (8,343,345). If these unfavourable conditions of tissue injury persist, it further progresses into fibrotic organ injury through activation of profibrotic and extracellular matrix deposition (TGF-β, fibronectin, collagen) (129) and development of pathological

conditions of hepatosteatosis, cardiomyopathy, nephropathy and pancreatic lesions (8,16,71,342-344).

Additionally, inflammatory and oxidative stress are considered as major destructive forces for the insulin signalling mechanism and glucose metabolism through development of insulin resistance and altered glucose tolerance. Thus, in these comorbid conditions of tissue injury and metabolic dysfunction, therapeutic approaches directed to reduce tissue injury and improvement of metabolic alteration is warranted.

An upregulated HO system through its pharmaceutical inducer hemin can be used as an alternative approach to counteract these tissue injuries and metabolic alterations. Although, reports from our lab and many others have shown the cytoprotective metabolic regulatory efficacy of the HO system in abnormal metabolic homeostasis in obesity, hypertension, diabetes (T1D and T2D) (8,10,15,19,341,346), the underlying mechanisms are not clearly understood. Thus, the present study is designed to understand the multifaceted mechanism of HO-mediated cytoprotective effects on tissue injury and metabolism.

1.10 General hypothesis

Based on the above scientific information, it is hypothesized that upregulation of the HO system by hemin would counterect the liver, heart, kidney and pancreatic tissue injury while improving insulin signaling in models of obese ZF, ZDF, SHR and STZ rats.

1.11 Thesis objectives

The major objectives of my thesis are as follows;

1) To determine the effect of hemin on HO-1 induction in the liver, heart, kidney and pancreas of SHR, ZDF, ZF and STZ rats.
2) To investigate the effects of hemin therapy on inflammatory cytokines and chemokines of liver, heart, kidney of SHR, ZDF, ZF rats
3) To investigate the effect of hemin therapy on proinflammatory M1 and anti-inflammatory M2 macrophage markers in liver, heart, kidney and pancreas of SHR, ZDF, ZF and STZ rats.
4) To assess whether hemin therapy suppresses oxidative stress in SHR, ZDF, ZF and STZ rats.
5) To assess the effect of hemin therapy on profibrotic and extracellular matrix mediators in the liver, heart and kidney of ZDF, ZF rats
6) To access the role of hemin therapy on major components of the insulin signal transduction pathway in SHR, ZDF, ZF and STZ rats
7) To investigate the effects of hemin therapy on glucose intolerance and insulin resistance in ZF rats.
8) To access the role of hemin treatment on ANP and adiponectin in heart and kidney of ZF and ZDF rats.
9) To assess the effects of hemin therapy on hepatic, cardiac, and renal lesions and functions in ZF and ZDF rats.
10) To study the effects of hemin therapy on markers of pancreatic repair and/or regeneration in STZ rats.

CHAPTER 2

The heme oxygenase system selectively suppresses the proinflammatory macrophage M1 phenotype and potentiates insulin signaling in spontaneously hypertensive rats

Joseph Fomusi Ndisang and Manish Mishra

This chapter has been published as a paper in

American Journal of Hypertension, September 2013; 26(9): 1123-31

Contribution: This article ***Am J Hypertens. 2013;*** *Sep;26(9):1123-31* was co-authored with my supervisor Joseph Fomusi Ndisang. This chapter reports the beneficial effects of the hemin-induced HO system on hepatic injuries and dysregulated glucose metabolism in a rat model of hypertension (SHR) and suggests that increasing inflammation and dysregulated insulin signalling mechanisms during hypertension is a major cause of hepatic injuries and impaired glucose metabolism. As co-author, I contributed to the western immunoblotting experiments, statistical analysis and data interpretation. My supervisor Joseph Fomusi Ndisang participated in research design, wrote the manuscript and performed data analysis. This study was financially supported by a grant from the Heart and Stroke Foundation of Saskatchewan, Canada to Dr. Ndisang.

2.1 Abstract

Background

The mechanisms by which heme oxygenase (HO) improves glucose metabolism in essential hypertension are not completely understood. Because dysfunctional insulin signaling is associated with elevated inflammation and high cholesterol and triglycerides, we investigated the effects of HO on the proinflammatory macrophage M1-phenotype and the anti-inflammatory macrophage M2-phenotype in spontaneously hypertensive rats (SHRs). SHRs are a model of human essential hypertension with features of metabolic syndrome, including impaired glucose metabolism.

Methods

Spectrophotometric analysis, enzyme immunoassay, enzyme-linked immunosorbent assay, and Western immunoblotting were used. HO was enhanced with hemin or inhibited with chromium-mesoporphyrin (CrMP).

Results

Hemin suppressed inflammation by abating proinflammatory macrophage M1-phenotype (ED1) and chemokines such as macrophage-chemoattractant-protein-1 (MCP-1) and macrophage-inflammatory-protein-1 alpha (MIP-1α) while enhancing anti-inflammatory macrophage M2-phenotype by potentiating ED2, CD206, and CD14. Similarly, hemin improved insulin signaling by enhancing insulin receptor substrate 1 (IRS-1), IRS-2, phosphatidylinositol 3 kinase (PI3K), and glucose transporter 4 (GLUT4) but reduced total cholesterol and triglycerides. These effects were accompanied by increased HO-1, HO activity, and cyclic guanosine monophosphate (cGMP), whereas the HO inhibitor CrMP nullified the hemin effects. Importantly, the effects of the HO system on ED1, ED2, CD206, and CD14 in SHRs are novel.

Conclusions

Hemin abated inflammation in SHRs by selectively enhancing the anti-inflammatory macrophage M2-phenotype that dampens inflammation while suppressing the proinflammatory macrophage M1-phenotype and related chemokines such as MCP-1 and MIP-1α. Importantly, the reduction of inflammation, total cholesterol, and triglycerides was accompanied by the enhancement of important proteins implicated in insulin signaling, including IRS-1, IRS-2, PI3K, and GLUT4. Thus, the concomitant reduction of inflammation, total cholesterol and triglycerides and the corresponding potentiation of insulin signaling are among the multifaceted mechanisms by which the HO system improves glucose metabolism in essential hypertension.

2.2 Introduction

Impaired glucose metabolism is linked to insulin resistance and considered the major contributor to the development of metabolic syndrome (1). Similarly, glucose metabolism is deregulated in patients with essential hypertension (2).

Many studies have underscored the role of inflammatory-insults in insulin resistance (3). Moreover, macrophage infiltration plays a major pathophysiological role in dysfunctional insulin signaling and impaired glucose metabolism (4, 5). Similarly, elevated inflammatory activity triggered by macrophage infiltration is a cardinal pathophysiological feature in spontaneously hypertensive rats (SHRs), a model of human essential hypertension (6, 7).

Generally, macrophages express distinct patterns of surface receptors when responding to different stimuli (3, 8). To date, two different polarization states of macrophages have been described. These include “classical,” or M1-phenotype, and “alternative,” or M2-phenotype (3, 8). The M1-phenotype triggers inflammation, whereas the M2-phenotype counteracts inflammation

(3, 8). Therefore, novel therapeutic modalities that selectively suppress the proinflammatory macrophage M1-phenotype and lower blood pressure but enhance the macrophage M2-phenotype that counteracts inflammation would be needed for patients comorbid with essential hypertension and impaired glucose metabolism. The heme oxygenase (HO) system may be explored in this regard. HO is a microsomal enzyme with inducible (HO-1) and constitutive (HO-2) isoforms (9) that break down the heme-moiety to yield cytoprotective products, including bilirubin, ferritin, and carbon monoxide (9). Bilirubin and ferritin suppress oxidative stress and inflammation, whereas carbon monoxide induces vasorelaxation, lowers blood pressure, and enhances insulin release (9, 10).

Although, we recently reported the antidiabetic effect of the HO system in different models, including SHRs (11), uninephrectomized deoxycorticosterone acetate hypertension (12), Zucker diabetic fatty rats (13) and Goto-Kakizaki rats (14, 15) to date, the effects of the HO system on macrophage polarization in SHRs have not been reported. Given that inflammation due to macrophage infiltration is a causative factor of impaired insulin signaling (4,16), this study was designed to investigate the effects of upregulating the HO system on the expressions of M1 and M2 macrophage phenotypes in SHRs, a model with impaired glucose metabolism (17, 18). In addition, the effect of the HO system on chemokines implicated in macrophage infiltration, such as macrophage-chemoattractant-protein-1 (MCP-1) (19) and macrophage-inflammatory-protein 1 alpha (MIP-1α) (20) were also assessed. Moreover, the effect of the HO system on MIP-1α has not been reported. Therefore, the major objective of this study was to investigate whether hemin therapy would selectively enhance the anti-inflammatory macrophage M2-phenotype that alleviates inflammation while concomitantly abating the proinflammatory M1-phenotype and chemokines that stimulate macrophage infiltration. Because elevated inflammation is known to

impair insulin signaling (4, 16, 21), we also investigated whether the suppression of inflammation by hemin would be accompanied by the potentiation of proteins of insulin signaling such as insulin receptor substrate 1 (IRS-1), IRS-2, phosphatidylinositol 3 kinase (PI3K), and glucose transporter 4 (GLUT4).

Given that macrophage infiltration is implicated in impaired insulin signaling (4, 16, 21), we hypothesized that hemin therapy would abate inflammation and potentiate insulin signaling by selectively enhancing the macrophage M2-phenotype that dampens inflammation while concomitantly suppressing the proinflammatory M1-phenotype in SHRs.

2.3 Methods

2.3.1 Animal treatment and biochemical assays

Our experimental protocol was approved by the University of Saskatchewan Standing Committee on Animal Care, which is in conformity with the Guide for Care and Use of Laboratory Animals stipulated by the Canadian Council on Animal Care and the National Institutes of Health. Eight-week-old male SHRs and age-matched Wistar-Kyoto (WKY) rats were purchased from Charles River Laboratories (Willington, MA), housed at 21°C with 12-hour light/dark cycles, fed with standard laboratory chow, and given access to drinking water *ad libitum*. Our study design included the following groups (n = 6 per group): (i) controls (WKY rats and SHRs), (ii) hemin-treated SHRs, (iii) hemin-treated WKY rats, and (iv) SHRs treated with hemin and the HO inhibitor chromium-mesoporphyrin (CrMP). Hemin was administered at a dose of 15 mg/kg by intra peritoneal injection, whereas CrMP was injected at a dose of 4 μmol/kg intraperitoneally, as previously described (22).

Systolic blood pressure was measured weekly in conscious animals by standard tail-cuff non-invasive method (Harvard Apparatus, Montreal, Canada), whereas fasting glucose was determined with a diagnostic autoanalyzer (BD, Franklin Lakes, NJ) after 6 hours of fasting, as previously reported (11, 14, 15, 22). At the end of the 4-week treatment, the animals were weighed, anesthetized with pentobarbital sodium (50 mg/kg intraperitoneally), and killed, and the liver, soleus muscle, and blood were collected. From the plasma, total cholesterol and triglycerides were routinely measured by Saskatoon Royal University Hospital in Canada, as previously reported (11). Other biochemical parameters including cyclic guanosine monophosphate (cGMP) were measured by enzyme immunoassay (Cayman Chemical, Ann Arbor, MI), whereas MCP-1 and MIP-1α were measured by enzyme-linked immunosorbent assay kits (OmniKine Assay; Biotechnology, Sunnyvale, CA) following the manufacturer's instructions.

2.3.2 Determination of HO-1 concentration and HO activity

HO activity in the liver and soleus muscle was measured as bilirubin production using our established method (22). The amount of bilirubin in each sample was quantified using extinction coefficient for bilirubin of 40 mM/cm, and expressed as nanomoles per milligram protein per hour. The protein content was measured using Bradford assay. As a positive control, spleen tissue was used. Liver and soleus muscle HO-1 concentration was determined by enzyme-linked immunosorbent assay (Stressgen-Assay Design, Ann Arbor, MI), as previously reported (22).

2.3.3 Western immunoblotting

The liver was homogenized and centrifuged as previously described (22). Primary antibodies (Santa Crutz Biotechnology, Santa Cruz, CA) targeting ED1 (CD68) (sc-59103), ED2

(CD163) (sc-58956), CD14 (sc-9150), CD206 (sc-48758)), PI3K (sc67306), IRS-1 (sc-559), IRS-2 (sc-8299), and GLUT4 (Abcam, Cambridge, MA) were used. Densitometric analysis was done with UN-SCAN-IT software (Silk Scientific, Orem, Utah). Beta-actin (Sigma, St. Louis, MO) was used as a control to ascertain equivalent loading.

2.3.4 Statistical analysis

All data were expressed as means SEM from at least 4 independent experiments unless otherwise stated. Statistical analyses were done using Student *t-test* and 2-way analysis of variance by means of Statistical Analysis System (SAS) software version 9.3 (SAS Institute, Cary, NC). Group differences at the level of $p<0.05$ were considered statistically significant.

2.4 Results

2.4.1 Hemin therapy enhanced HO-1, HO activity, and cGMP in the liver and soleus muscles

Our results indicate that SHRs had normal glucose levels. Although, SHRs were normoglycemic (Table 2-1), hemin administration slightly but significantly lowered glucose levels, whereas the HO inhibitor CrMP abolished the hemin-induced glucose-lowering effect. On the other hand, hemin and CrMP affected body weight. In hemin and CrMP-treated animals, a slight body-weight loss (<9%) was observed (Table 2-1). Although, loss of body weight can cause reduction of glycemia, this was not the case in our study because we observed a slight decrease of glycemia in hemin-treated animals but a slight increase in CrMP treated animals, suggesting that the HO system may have an intrinsic antidiabetic effect. Hemin also lowered blood pressure in SHRs and WKY rats, although, the hemin effect was greater in SHRs (Table 2-1).

To investigate the role of the HO system on insulin signaling, we determined the effects of hemin therapy on important components of the HO signal transduction pathway, including HO-1, HO activity, and cGMP in the liver and soleus muscle. The liver and skeletal muscles, including the soleus muscles, are important for glucose metabolism (15, 23). In liver tissue obtained from untreated SHRs (control), the basal levels of HO-1, HO activity, and cGMP, a secondary messenger through which endogenously produced carbon monoxide by the HO system acts (9), were significantly reduced by 2.7-, 1.8-, and 2.1-fold, respectively, as compared with age-matched WKY control rats. Interestingly, the administration of hemin greatly increased the depressed basal HO-1, HO activity and cGMP levels in SHRs by 8.5-, 9.8-, and 7.8-fold, respectively (Fig. 2-1a-c). On the other hand, co-administering the HO-inducer hemin and the HO inhibitor CrMP resulted in the annulment of the hemin-induced increase of HO-1, HO activity, and cGMP. Similarly, treatment with CrMP alone caused further depletion of the depressed basal levels of HO-1, HO activity, and cGMP in SHRs (Fig. 2-1a-c). Hemin therapy also enhanced HO-1 and HO activity in WKY rats, although, the magnitude was smaller than in hemin-treated SHRs.

Because glucose uptake by skeletal muscles is an important physiological process for glucose disposal and metabolism, we assessed the effects of hemin therapy on HO-1, HO activity, and cGMP in the soleus muscles (15). In control SHRs (untreated), the basal levels of HO-1 and HO activity were slightly higher than those in WKY rats. Treatment with hemin increased HO-1 and HO activity in SHRs by 3.2- and 3-fold, respectively (Fig. 2-1d, e). The enhanced HO activity would increase endogenous carbon monoxide, which would in turn stimulate cGMP (22). Both cGMP and carbon monoxide are known to enhance glucose metabolism (24, 25). Consistently, we detected a 3.2-fold increase of cGMP in hemin-treated SHRs (Fig. 2-1f). Contrarily, the co-administration of the HO inducer hemin and the HO blocker reversed the hemin-dependent

increase of HO-1 and HO activity, with annulment of the hemin-induced increase of cGMP. Although, the basal HO activity in SHRs was higher than the control, it did not cause an increase in cGMP (Fig. 2-1e, f), suggesting that the transient increase in HO activity might have occurred with a magnitude below the threshold necessary to trigger an increase in cGMP. A similar observation has been previously reported (11). Hemin therapy also enhanced HO-1, HO activity, and cGMP in normotensive WKY control rats, although a greater increment was observed in hemin-treated SHRs (Fig. 2-1).

2.4.2 Hemin therapy abated total cholesterol and triglycerides in SHRs

Given that elevated cholesterol and high triglycerides levels are common denominators of impaired insulin signaling and deregulated glucose metabolism (26), we determined the effect of hemin total cholesterol and triglycerides. In control SHRs, the levels of total cholesterol and triglycerides were significantly elevated by 1.96- and 1.92-fold, respectively, as compared with WKY control rats (Fig. 2-2a, b). However, the administration of hemin significantly abated the elevated levels of total cholesterol in SHRs by 49.8%, reinstating comparable levels as observed in WKY rats. Similarly, hemin therapy markedly reduced triglyceride levels in SHRs by 33.1%, suggesting that hemin therapy is more effective in abating total cholesterol than triglycerides (although, the levels in WKY control rats were not attained). On the other hand, the cotreatment with the HO inducer hemin and the HO inhibitor CrMP abolished the effects of hemin on total cholesterol and triglycerides, suggesting a role of the HO system in the regulation of total cholesterol and triglycerides. Hemin also lowered total cholesterol and triglycerides in WKY rats, although, the hemin effect was greater in SHRs (Fig. 2-2a, b).

2.4.3 Hemin therapy suppressed proinflammatory chemokines that stimulate macrophage infiltration in SHRs

Because MIP-1α and MCP-1 are chemokines that stimulate macrophage infiltration (19, 20), we investigated the effects of hemin on these chemokines. In control SHRs, the basal levels of plasma and liver MCP-1 were significantly elevated by 3.5- and 4.1-fold, respectively, as compared with WKY rats (Fig. 2-3a, b). Interestingly, the administration of hemin to SHRs greatly reduced the elevated levels of plasma MCP-1 to comparable levels as observed in WKY rats. Similarly, hemin therapy significantly abated the high liver levels of MCP-1 in SHRs by 2.6-fold, although, it did not reinstate similar levels as in the WKY control rats (Fig. 2-3b). On the other hand, the co-administration of the HO inducer hemin and the HO inhibitor CrMP abolished the hemin effects and reinstated the elevated levels of plasma and liver MCP-1 (Fig. 2-3a, b).

Because MIP-1α is a potent chemokine implicated in macrophage infiltration and the effect of the HO system on MIP-1α in SHRs has not been reported, we also evaluated control SHRs, the basal levels of MIP-1α in the liver were markedly elevated by 3.3-fold as compared with WKY rats (Fig. 2-3c). Interestingly, the application of hemin to SHRs greatly attenuated the elevated MIP-1α levels by 3.3-fold, whereas the co-application of hemin together with the HO inhibitor CrMP abolished the effects of hemin (Fig. 2-3c). Hemin therapy was also effective against MCP-1 and MIP-1α in WKY rats, although, the effect was less intense compared with the untreated and unhealthy SHR controls (Fig. 2-3a-c). In WKY rats, hemin treatment reduced plasma and liver MCP-1 by 37.2% and 32.2%, respectively, compared with reductions of 72.6% and 62.2% in SHRs. Similarly, hemin therapy attenuated liver MIP-1α in WKY rats by 37.3%, whereas a greater magnitude of 69.2% was observed in SHRs (Fig. 2-3a-c), suggesting that hemin therapy may have greater selectivity for SHRs with unhealthy status.

2.4.4 Hemin therapy selectively abated inflammatory proteins that deregulate insulin signalling

Given that macrophage infiltration is implicated in dysfunctional glucose metabolism (3,8), we used ED1 to quantify the expression of proinflammatory macrophage M1-phenotype (27-30). Our Western immunoblotting and relative densitometric analyses indicated that the basal protein expression of ED1 in SHRs was markedly elevated compared with that in WKY rats (Figure 4a). However, the administration of hemin significantly attenuated the elevated basal expression of the proinflammatory M1-phenotype marker ED1 in SHRs by 2.9-fold.

To examine whether the hemin-induced suppression of macrophage M1-phenotype will be accompanied by changes in the anti-inflammatory macrophage M2-phenotype, we also examined the effects of hemin therapy on the M2-phenotype using several selective markers for M2, including ED2, CD206, and CD14 (27-30). Our results indicate that the basal expressions of ED2, CD206, and CD14 in SHRs were markedly reduced by 4.6-, 2.5-, and 7.2-fold, respectively, compared with that in WKY rats (Fig. 2-4b-d). Interestingly, hemin therapy significantly enhanced the depressed basal expressions of ED2, CD206, and CD14 by 3.1-, 1.4-, and 3.7-fold, respectively, suggesting that hemin may selectively modulate the polarization of macrophages in SHRs toward the M2-phenotype that counteracts inflammatory insults. Importantly, the effects of the HO system on ED1, ED2, CD206, and CD14 in SHRs are novel finding that have not been previously reported.

2.4.5 Hemin therapy potentiated insulin signal transduction pathway

Because the suppression of macrophage infiltration is accompanied by the potentiation of insulin signaling (21) and we observed that hemin therapy abated the proinflammatory macrophage M1-phenotype, we investigated whether the attenuation of macrophage-induced

inflammation in SHRs will be accompanied by the corresponding potentiation of proteins of the insulin signal transduction pathway, such as IRS-1, IRS-2, PI3K, and GLUT4 (3).

Our Western immunoblotting and relative densitometric analyses of the expressed proteins revealed that the basal protein expressions of IRS-1, IRS-2, PI3K, and GLUT4 in SHRs were significantly lower by 3.5-, 8.8-, 10.9, and 8.6-fold, respectively, than that in WKY rats (Fig. 2-5a-d), suggesting reduced insulin signaling in SHRs. Interestingly, hemin therapy robustly enhanced the expressions of IRS-1, IRS-2, PI3K, and GLUT4 in SHRs by 1.7-, 3.9-, 9.3-, and 4.2-fold, respectively (Fig. 2-5a-d), suggesting that a novel mechanism by which hemin potentiates insulin signaling and improve glucose metabolism in SHRs is concomitantly abating the proinflammatory macrophage M1-phenotype while enhancing the anti-inflammatory M2-phenotype.

2.5 Discussion

Our study unveils novel mechanisms by which the HO system abates inflammation and potentiates insulin signaling to improve glucose metabolism in SHRs, a genetic rat model of essential hypertension with characteristics of the human metabolic syndrome, including insulin resistance and impaired glucose metabolism (17,18). In untreated SHRs, the levels of the proinflammatory macrophage M1-phenotype, total cholesterol, and triglycerides were markedly elevated. These factors may have contributed to impaired insulin signaling, given that macrophage infiltration, elevated cholesterol, and high triglycerides are known to deregulate glucose metabolism (3, 8, 26). Interestingly, hemin therapy abated inflammation due to macrophages, reduced cholesterol/triglycerides, and improved glucose metabolism in SHRs. Importantly, the selective enhancement of the anti-inflammatory macrophage M2-phenotype and corresponding

reduction of the proinflammatory M1-phenotype by hemin is a novel mechanism by which hemin therapy suppresses inflammation in essential hypertension. Moreover, this selective effect of hemin may be indicative of a modulatory role of the HO system that favors the polarization of macrophages toward the anti-inflammatory macrophage M2-phenotype. However, further investigations are needed to fully characterize the effects of upregulating the HO system on macrophage polarization. Importantly, the effects of the HO system on the pro inflammatory M1-phenotype marker ED1 and the anti-inflammatory M2-phenotype markers ED2, CD206, and CD14 in SHRs are novel findings that have not been previously reported. An important revelation from our study is that the hemin dependent suppression of the proinflammatory macrophage M1-phenotype was associated with a parallel reduction of chemokines such as MIP-1α and MCP-1, which stimulate macrophage infiltration (19,20), whereas the co-administration of the HO inducer hemin together with the HO inhibitor CrMP nullified the hemin effects, suggesting a role of the HO system in the regulation of these chemokines. Moreover, the effect of the HO system on MIP-1α in SHRs is a novel observation reported here for the first time.

Another interesting observation from our study is the potentiation of insulin signaling following the suppression of inflammation. In hemin-treated animals, important components of the insulin signal transduction pathway, including IRS-1, IRS-2, PI3K, and GLUT4, were significantly enhanced. Given that patients with essential hypertension eventually develop diabetes (31) and SHRs are a model of essential hypertension, this study suggest that although SHRs are normoglycemic, impaired insulin signaling may be a forerunner to overt hyperglycemia in essential hypertension. Therefore, the reduced levels of IRS-1, IRS-2, PI3K, and GLUT4 are a signature to the defective insulin signaling in SHRs, which interestingly was corrected by hemin. Because our study also indicates that hemin therapy lowers blood pressure in SHRs, it could be

argued that the improved insulin signaling is due to the blood pressure–lowering effect. However, we recently reported the antidiabetic effects of hemin therapy in different normotensive diabetic models, including Goto-Kakizaki rats, Zucker diabetic fatty rats, and streptozotocin-induced diabetes (13-15, 22). Consistently, other investigators have also reported the insulin-sensitizing effects of HO inducers in normotensive animals (32, 33). Therefore, evidence from this study and other reports strongly suggest that the HO system is also endowed with an intrinsic insulin-sensitizing effect. Hemin therapy also enhanced the HO system with reduction of total cholesterol and triglycerides, MCP-1, and MIP-1α in WKY rats, although, the magnitude was smaller than that in SHRs. The reasons for this selective effect of the HO system are not fully understood. Importantly, the selectivity of the HO system in diseased conditions such as essential hypertension and deregulated insulin signaling as observed in SHRs could be explored against the comorbidity of hypertension and impaired glucose metabolism.

Although, we previously reported the effects of the HO system in the gastrocnemius muscle of SHRs (11), tissue-specific response is a well-known phenomenon in the pathophysiology of impaired insulin signaling and deregulated glucose metabolism. Emerging evidence indicates that different tissues may respond distinctly to the same stimuli, indicating that a physiological response in one tissue may not necessarily be the same in another tissue (34, 35). Whether the reported effects were unique for the gastrocnemius muscle or universal for other tissues in SHRs is critical for understanding the role of hemin in insulin signaling and glucose metabolism in essential hypertension.

Collectively, these results suggest that the selective potentiation of the macrophage M2 phenotype that dampens inflammation, with the corresponding decline of the proinflammatory macrophage M1-phenotype and related chemokines such as MCP-1 and MIP-1α are responsible

for the suppression of inflammation in hemin-treated SHRs. Importantly, the concomitant reduction of inflammation and cholesterol/triglycerides and associated potentiation of insulin signaling are the multifaceted mechanisms by which the HO system improves glucose metabolism in essential hypertension.

Disclosure: The authors declared no conflict of interest.

Acknowledgement: This work was supported by the Heart & Stroke Foundation of Saskatchewan, Canada to Joseph Fomusi Ndisang.

Table 2-1: Effects of hemin and chromium mesoporphyrin (CrMP) on physiological and biochemical variables

Parameter	Animals and treatment groups				
	WKY control	SHR control	WKY + hemin	SHR + hemin	SHR + CrMP + hemin
Body weight (grams)	513 ± 10.3	409 ± 9.7	495 ± 12.6*	393 ± 8.4*	378 ± 9.1*
Fasting glucose (mmol/L)	7.0 ± 0.3	7.2±0.4	6.3 ± 0.3*	6.1 ± 0.2*	7.5 ± 0.5**
Systolic blood pressure (mm Hg)	120.8 ± 5.6	185.9 ± 12.3***	112.9 ± 4.8	123.6 ± 5.5****	191.9 ± 10.3***

*p<0.05 vs. respective control; **p<0.05 vs. SHR + hemin; ***p<0.01 vs. all groups; ****p<0.01 vs. SHR Control; n = 6 per group

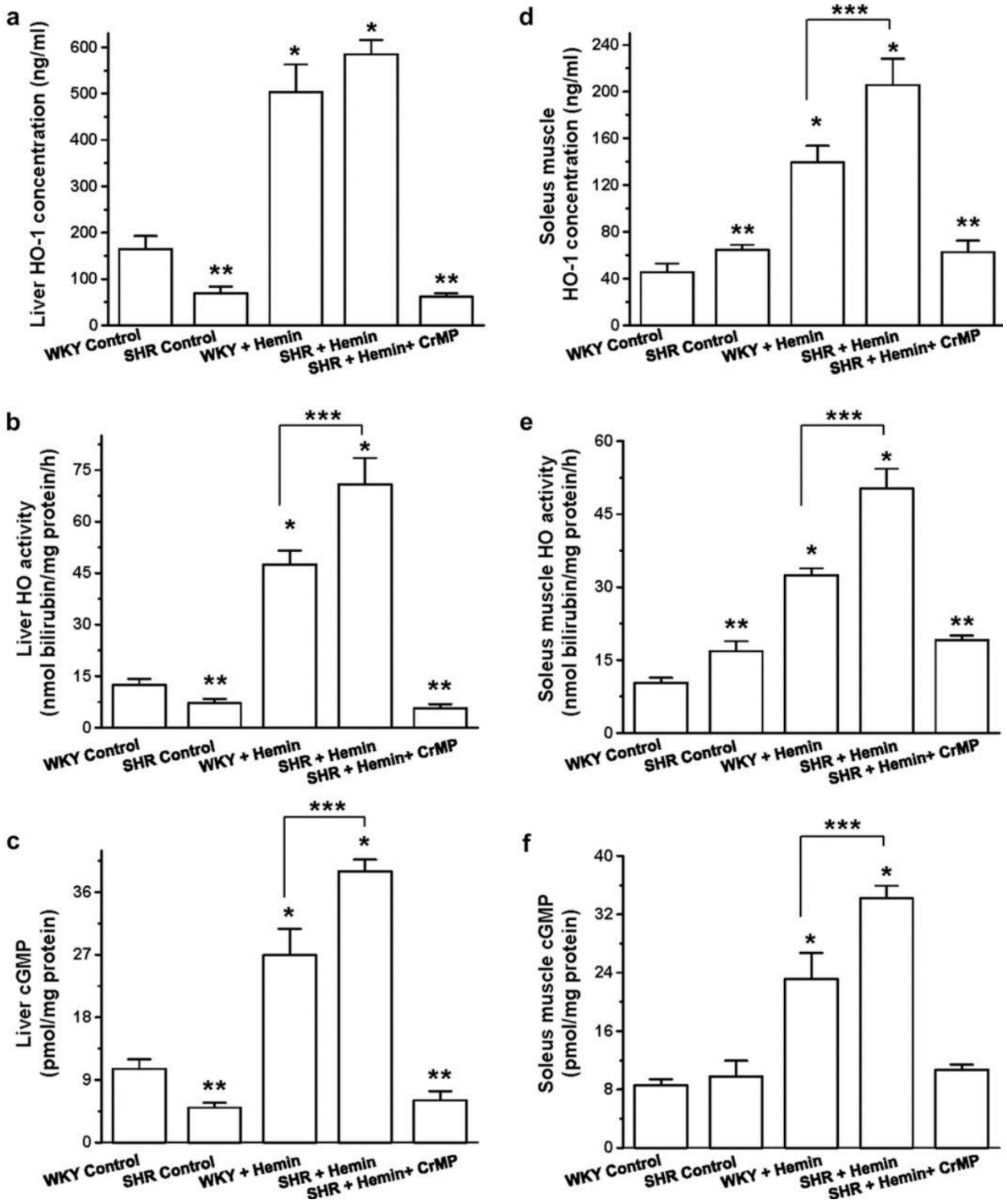

Figure 2-1: Effects of the heme oxygenase (HO) inducer hemin and the HO inhibitor chromium mesoporphyrin (CrMP) on liver and soleus muscle HO-1 concentration, HO activity, and cyclic guanosine monophosphate (cGMP) levels. The basal HO-1 (a), HO-activity (b), and cGMP (c)

levels in hepatic tissue from spontaneously hypertensive rats (SHRs) were reduced compared with the normotensive Wistar-Kyoto (WKY) control rats but were robustly increased by hemin therapy, whereas cotreating the SHRs with hemin and the HO blocker CrMP reversed the hemin effects, whereas treatment with CrMP alone resulted in further reduction of the basal HO-1, HO activity, and cGMP in the liver of SHRs. Hemin also increased HO-1 and HO activity in WKY rats, although, less intensely than in SHRs. (d) The basal HO-1 concentration in SHRs was slightly elevated compared with that in normotensive WKY control rats. Treatment with hemin enhanced HO-1 levels, whereas the co-administration of the HO inducer hemin and the HO blocker CrMP nullified the effects of hemin. Hemin also increased HO-1 levels in WKY rats, although, less intensely than in SHRs. (e) The basal HO activity in SHRs was slightly elevated compared with that in normotensive WKY control rats. The administration of hemin increased HO activity in SHRs, whereas the cotreatment with hemin and the HO blocker CrMP reversed the effects of hemin. Hemin therapy also enhanced HO activity in WKY rats but to a lesser magnitude than in SHRs. (f) Hemin treatment enhanced cGMP levels in SHRs, whereas cotreatment of hemin and CrMP abolished the hemin effect. Hemin therapy also enhanced cGMP levels in WKY rats. Bars represent means ± SEM. n = 6 rats per group. *$p<0.01$ vs. all groups; **$p<0.05$ vs. all groups; ***$p<0.05$ vs. SHRs + hemin.

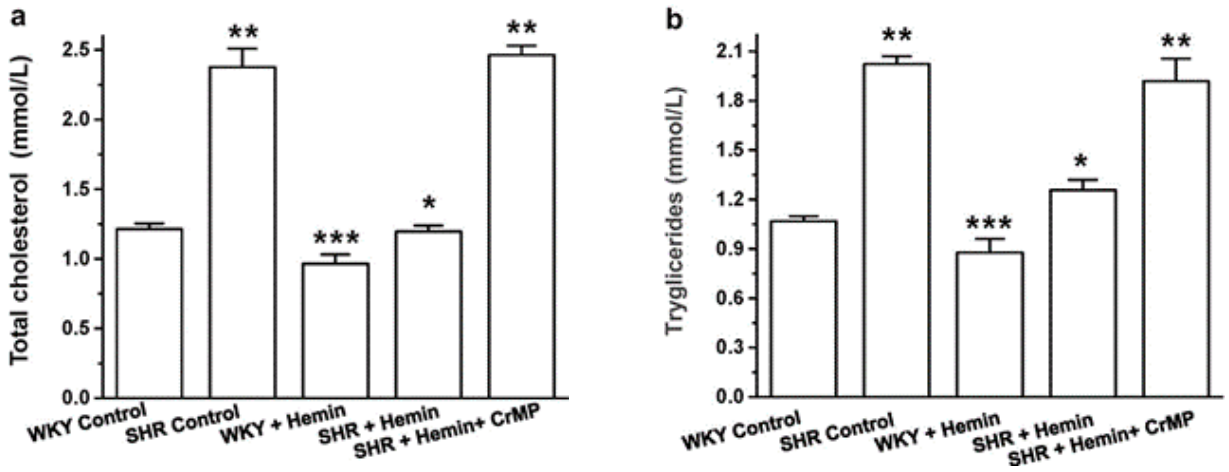

Figure 2-2: Effects of the heme oxygenase (HO) inducer hemin and the HO inhibitor chromium mesoporphyrin (CrMP) on total cholesterol and triglycerides. (a) The basal levels of total cholesterol in spontaneously hypertensive rats (SHRs) were markedly elevated compared with those in the Wistar-Kyoto (WKY) control rats. Treatment with hemin abated the elevated levels of total cholesterol, whereas the co-application of the HO inducer hemin and the HO blocker CrMP nullified the effects of hemin. Hemin also suppressed total cholesterol levels in WKY rats, although, less intensely than in SHR rats. (b) The basal levels of triglycerides in SHRs were greatly elevated compared with those in WKYs. Treatment with hemin reduced the levels of triglycerides in SHRs, whereas the co-administration of hemin and the HO blocker CrMP reversed the effects of hemin. Hemin therapy also attenuated triglycerides in WKYs but to a lesser magnitude than in SHRs. Bars represent means ± SEM. n = 6 rats per group. *$p<0.01$ vs. SHR controls or SHRs + hemin + CrMP; **$p<0.01$ vs. all groups; ***$p<0.05$ vs. WKY control rats.

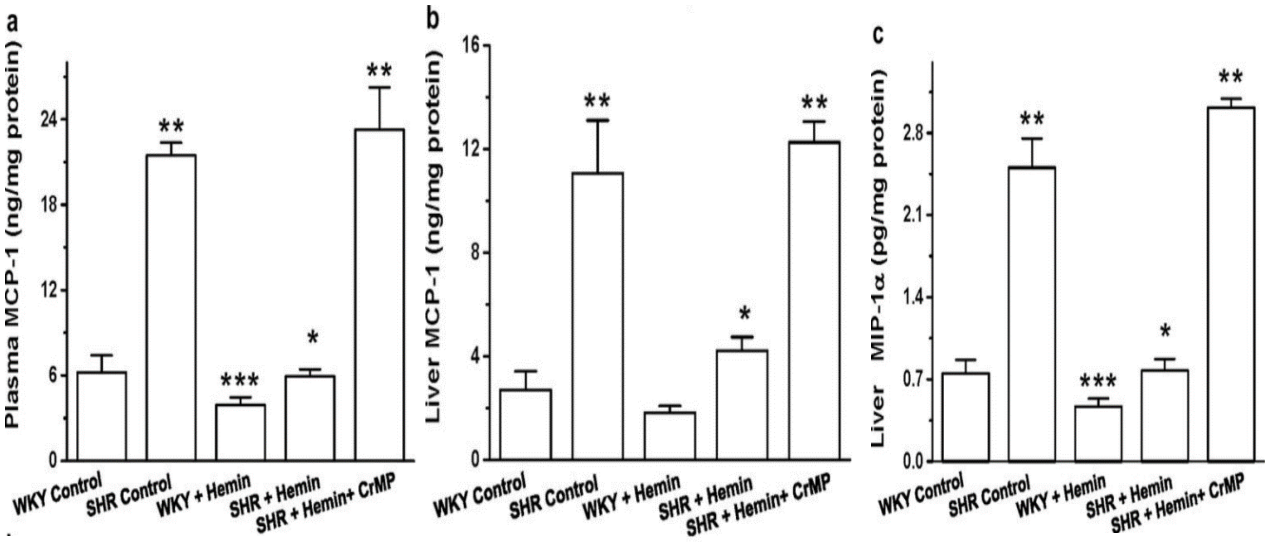

Figure 2-3: Effects of the heme oxygenase (HO) inducer hemin and the HO inhibitor chromium mesoporphyrin (CrMP) on plasma and liver macrophage-chemoattractant-protein-1 (MCP-1) and macrophage-inflammatory-protein-1 alpha (MIP-1α) in spontaneously hypertensive rats (SHRs) and Wistar-Kyoto (WKY) rats. The basal levels of plasma MCP-1 (a), liver MCP-1 (b), and liver MIP-1α (c) in SHRs were markedly elevated compared with the levels in WKY control rats, but hemin administration greatly reduced the elevated levels of MCP-1 and MIP-1α, whereas the HO inhibitor CrMP reversed the effects of hemin MCP-1 and MIP-1α. Hemin therapy also attenuated MCP-1 and MIP-1α in WKY rats but to a lesser magnitude than in SHRs. Bars represent means ± SEM. n = 6 rats per group. *$p<0.01$ vs. SHR controls or SHRs + hemin + CrMP; **$p<0.01$ vs. all groups; ***$p<0.05$ vs. WKY control rats.

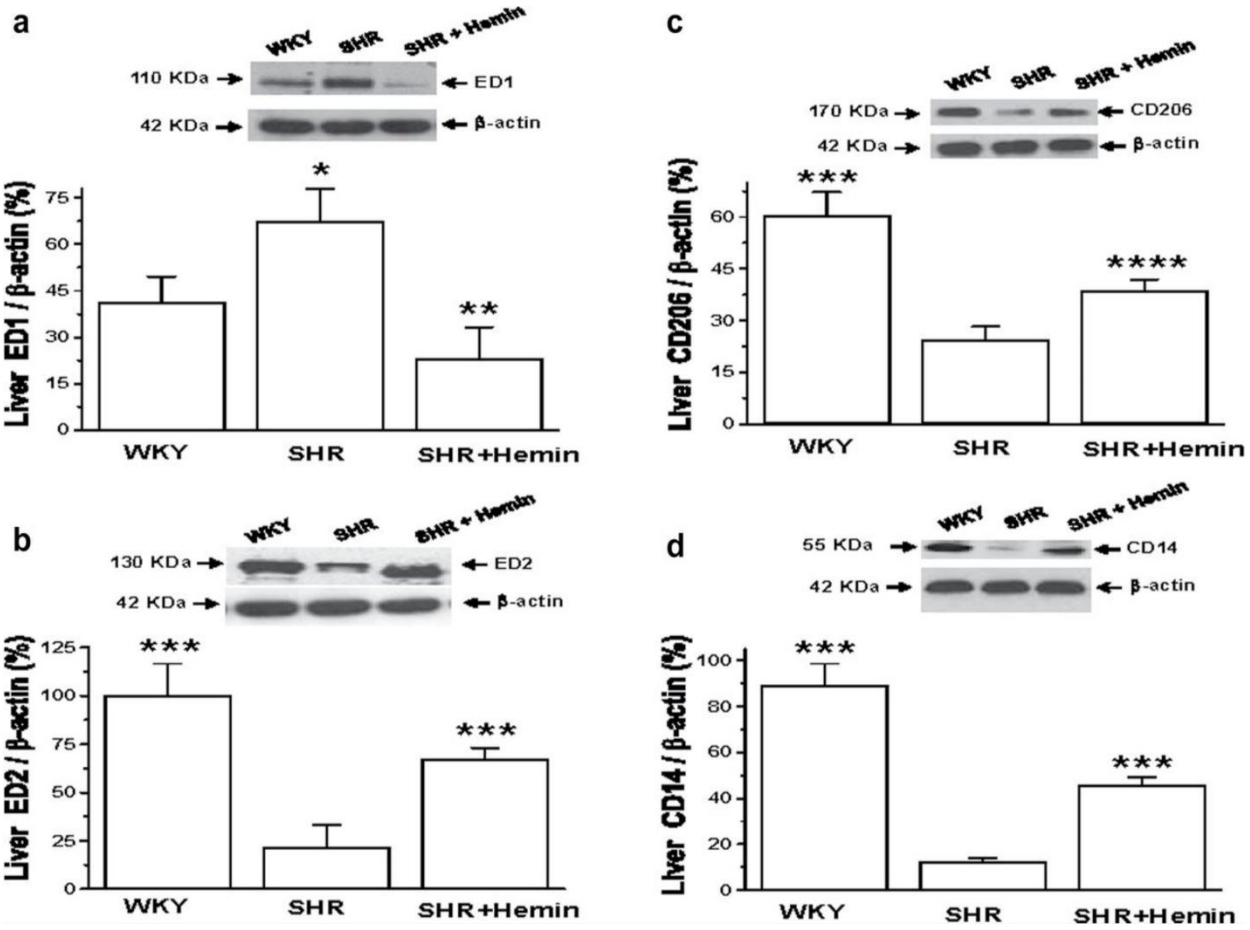

Figure 2-4: Effect of hemin therapy on the proinflammatory macrophage M1-phenotype marker ED1 and the anti-inflammatory macrophage M2-phenotype markers ED2, CD206, and CD14. Representative Western immunoblots and relative densitometric analyses revealed that treatment with hemin suppressed ED1 but enhanced ED2 (b), CD206 (c), and CD14 (d) in spontaneously hypertensive rats (SHRs). Bars represent means ± SEM, n = 4 rats per group. *p<0.05 vs. Wistar-Kyoto (WKY) rats; **p<0.05 vs. SHRs; ***p<0.01 vs. all groups; ****p<0.05 vs. all groups.

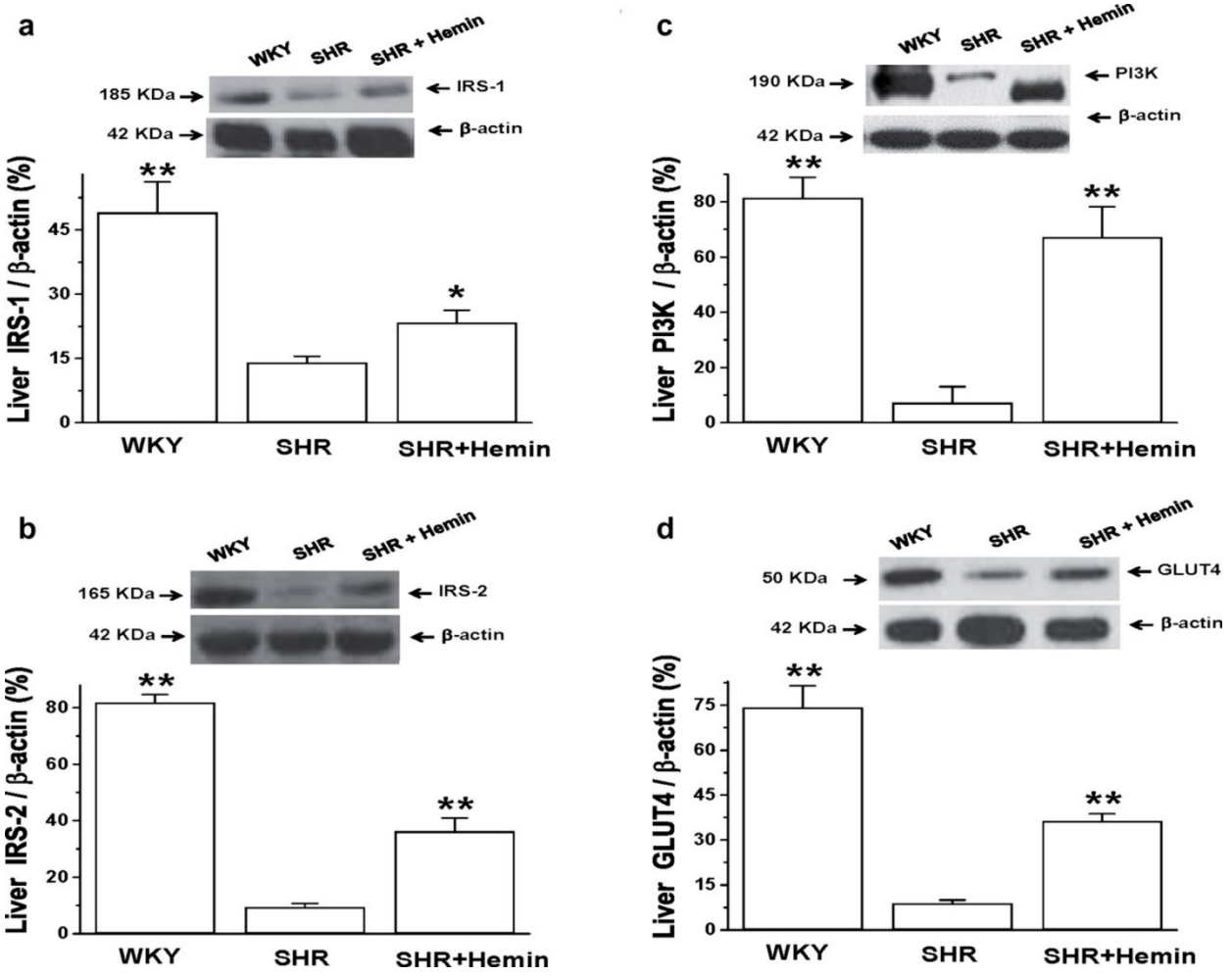

Figure 2-5: Effect of hemin on proteins of the insulin signal transduction pathway such as insulin receptor substrate 1 (IRS-1), IRS-2, phosphatidylinositol 3 kinase (PI3K), and glucose transporter 4 (GLUT4). Representative Western immunoblots and relative densitometry indicates that hemin therapy markedly increased the depressed expressions of IRS-1 (a), IRS-2 (b), PI3K (c), and GLUT4 (d) in spontaneously hypertensive rats (SHRs). Bars represent means ± SEM. n = 4 rats per group. *p<0.05 vs. all groups; **p<0.01 vs. all groups. Abbreviation: WKY, Wistar-Kyoto.

2.6 References

1. Grundy SM, Cleeman JI, Daniels SR, Donato KA, Eckel RH, Franklin BA, Gordon DJ, Krauss RM, Savage PJ, Smith SC Jr, Spertus JA, Costa F. Diagnosis and management of the metabolic syndrome: an American Heart Association/National Heart, Lung, and Blood Institute Scientific Statement. Circulation 2005; 112:2735-2752.

2. Garcia-Puig J, Ruilope LM, Luque M, Fernandez J, Ortega R, Dal-Re R. Glucose metabolism in patients with essential hypertension. Am J Med 2006; 119:318-326.

3. Ndisang JF. Role of heme oxygenase in inflammation, insulin-signalling, diabetes and obesity. Mediators Inflamm 2010; 2010:359732.

4. Sell H, Habich C, Eckel J. Adaptive immunity in obesity and insulin resistance. Nat Rev Endocrinol, 2012; 8:709-716.

5. Finucane OM, Reynolds CM, McGillicuddy FC, Roche HM. Insights into the role of macrophage migration inhibitory factor in obesity and insulin resistance. Proc Natur Soc, 2012; 71:622-633.

6. Ndisang JF, Wu L, Zhao W, Wang R. Induction of heme oxygenase-1 and stimulation of cGMP production by hemin in aortic tissues from hypertensive rats. Blood 2003; 101:3893-3900.

7. Sato S, Mukai Y, Yamate J, Kato J, Kurasaki M, Hatai A, Sagai M. Effect of polyphenol-containing azuki bean (Vigna angularis) extract on blood pressure elevation and macrophage infiltration in the heart and kidney of spontaneously hypertensive rats. Clin Exp Pharmacol Physiol 2008; 35:43-49.

8. Gordon S, Martinez FO. Alternative activation of macrophages: mechanism and functions. Immunity 2010; 32:593-604.

9. Ndisang JF, Tabien HE, Wang R. Carbon monoxide and hypertension. J Hypertens 2004; 22:1057-1074.

10. Henningsson R, Alm P, Ekstrom P, Lundquist I. Heme oxygenase and carbon monoxide: regulatory roles in islet hormone release: a biochemical, immunohistochemical, and confocal microscopic study. Diabetes 1999; 48:66-76.

11. Ndisang JF, Lane N, Syed N, Jadhav A. Up-regulating the heme oxygenase system with hemin improves insulin sensitivity and glucose metabolism in adult spontaneously hypertensive rats. Endocrinology 2010; 151:549-560.

12. Ndisang JF, Jadhav A. The heme oxygenase system attenuates pancreatic lesions and improves insulin sensitivity and glucose metabolism in deoxycorticosterone acetate hypertension. Am J Physiol Regul Integr Comp Physiol 2010; 298: R211-R223.

13. Ndisang JF, Lane N, Jadhav A. The heme oxygenase system abates hyperglycemia in Zucker diabetic fatty rats by potentiating insulin sensitizing pathways. Endocrinology 2009; 150:2098-2108.

14. Ndisang JF, Jadhav A. Up-regulating the heme oxygenase system enhances insulin sensitivity and improves glucose metabolism in insulin-resistant diabetes in Goto–Kakizaki rats. Endocrinology 2009; 150:2627-2636.

15. Ndisang JF, Lane N, Jadhav A. Upregulation of the heme oxygenase system ameliorates postprandial and fasting hyperglycemia in type 2 diabetes. Am J Physiol Endocrinol Metab 2009; 296: E1029–E1041.

16. Suganami T, Tanaka M, Ogawa Y. Adipose tissue inflammation and ectopic lipid accumulation. Endocr J, 2012;59:849-857.

17. Potenza MA, Marasciulo FL, Chieppa DM, Brigiani GS, Formoso G, Quon MJ, Montagnani M. Insulin resistance in spontaneously hypertensive rats is associated with endothelial dysfunction characterized by imbalance between NO and ET-1 production. Am J Physiol Heart Circ Physiol 2005; 289:H813-H822.

18. Aitman TJ, Glazier AM, Wallace CA, Cooper LD, Norsworthy PJ, Wahid FN, Al-Majali KM, Trembling PM, Mann CJ, Shoulders CC, Graf D, St Lezin E, Kurtz TW, Kren V, Pravenec M, Ibrahimi A, Abumrad NA, Stanton LW, Scott J. Identification of Cd36 (Fat) as an insulin-resistance gene causing defective fatty acid and glucose metabolism in hypertensive rats. Nat Genet 1999; 21:76-83.

19. Suresh MV, Yu B, Machado-Aranda D, Bender MD, Ochoa-Frongia L, Helinski JD, Davidson BA, Knight PR, Hogaboam CM, Moore BB, Raghavendran K. Role of macrophage chemoattractant protein-1 in acute inflammation after lung contusion. Am J Respir Cell Mol Biol 2012; 46:797-806.

20. Westerbacka J, Corner A, Kolak M, Makkonen J, Turpeinen U, Hamsten A, Fisher RM, Yki-Jarvinen H. Insulin regulation of MCP-1 in human adipose tissue of obese and lean women. Am J Physiol Endocrinol Metab 2008; 294: E841-E845.

21. Pan Y, Wang Y, Cai L, Cai Y, Hu J, Yu C, Li J, Feng Z, Yang S, Li X, Liang G. Inhibition of high glucose-induced inflammatory response and macrophage infiltration by a novel curcumin derivative prevents renal injury in diabetic rats. Br J Pharmacol 2012; 166:1169-1182.

22. Ndisang JF, Jadhav A. Heme oxygenase system enhances insulin sensitivity and glucose metabolism in streptozotocin-induced diabetes. Am J Physiol Endocrinol Metab 2009; 296: E829-E841.

23. Walter BF, Emile B. Medical Physiology, 2nd edn. Philadelphia: Saunders Elsevier, 2009.

24. Lira VA, Soltow QA, Long JH, Betters JL, Sellman JE, Criswell DS. Nitric oxide increases GLUT4 expression and regulates AMPK signaling in skeletal muscle. Am J Physiol Endocrinol Metab 2007; 293: E1062-E1068.

25. Mosen H, Salehi A, Alm P, Henningsson R, Jimenez-Feltstrom J, Ostenson CG, Efendic S, Lundquist I. Defective glucose-stimulated insulin release in the diabetic Goto–Kakizaki (GK) rat coincides with reduced activity of the islet carbon monoxide signaling pathway. Endocrinology 2005; 146:1553-1558.

26. Reaven GM. Insulin resistance, the insulin resistance syndrome, and cardiovascular disease. Panminerva Medica 2005; 47:201–210.

27. Aki K, Shimizu A, Masuda Y, Kuwahara N, Arai T, Ishikawa A, Fujita E, Mii A, Natori Y, Fukunaga Y, Fukuda Y. ANG II receptor blockade enhances anti-inflammatory macrophages in anti-glomerular basement membrane glomerulonephritis. Am J Physiol Renal Physiol 2010; 298: F870-F882.

28. Heusinkveld M, de Vos van Steenwijk PJ, Goedemans R, Ramwadhdoebe TH, Gorter A, Welters MJ, van Hall T, van der Burg SH. M2 macrophages induced by prostaglandin E2 and IL-6 from cervical carcinoma are switched to activated M1 macrophages by CD4+ Th1 cells. J Immunol 2011; 187:1157-1165.

29. Anzai A, Anzai T, Nagai S, Maekawa Y, Naito K, Kaneko H, Sugano Y, Takahashi T, Abe H, Mochizuki S, Sano M, Yoshikawa T, Okada Y, Koyasu S, Ogawa S, Fukuda K. Regulatory role of dendritic cells in postinfarction healing and left ventricular remodeling. Circulation 2012; 125:1234-1245.

30. El Hadri K, Mahmood DF, Couchie D, Jguirim-Souissi I, Genze F, Diderot V, Syrovets T, Lunov O, Simmet T, Rouis M. Thioredoxin-1 promotes anti-inflammatory macrophages of the M2 phenotype and antagonizes atherosclerosis. Arterioscler Thromb Vasc Biol 2012; 32:1445-1452.

31. Perticone F, Maio R, Sciacqua A, Andreozzi F, Iemma G, Perticone M, Zoccali C, Sesti G. Endothelial dysfunction and C-reactive protein are risk factors for diabetes in essential hypertension. Diabetes 2008; 57:167-171.

32. Li M, Kim DH, Tsenovoy PL, Peterson SJ, Rezzani R, Rodella LF, Aronow WS, Ikehara S, Abraham NG. Treatment of obese diabetic mice with a heme oxygenase inducer reduces visceral and subcutaneous adiposity, increases adiponectin levels, and improves insulin sensitivity and glucose tolerance. Diabetes 2008; 57:1526-1535.

33. Peterson SJ, Drummond G, Kim DH, Li M, Kruger AL, Ikehara S, Abraham NG. L-4F treatment reduces adiposity, increases adiponectin levels, and improves insulin sensitivity in obese mice. J Lipid Res 2008; 49:1658-1669.

34. Farret A, Filhol R, Linck N, Manteghetti M, Vignon J, Gross R, Petit P. P2Y receptor mediated modulation of insulin release by a novel generation of 2-substituted-5'-O-(1-boranotriphosphate)-adenosine analogues. Pharm Res 2006; 23:2665–2671.

35. Zhang X, Lam KS, Ye H, Chung SK, Zhou M, Wang Y, Xu A. Adipose tissue-specific inhibition of hypoxia-inducible factor 1α induces obesity and glucose intolerance by impeding energy expenditure in mice. J Biol Chem 2010; 285:32869-32877.

CHAPTER 3

The risk of heart failure and cardiometabolic complications in obesity may be masked by an apparent healthy status of normal blood glucose

Shuchita Tiwari, Manish Mishra, Ashok Jadhav, Courtney Gerger, Paul Lee, Lynn Weber and Joseph Fomusi Ndisang

This chapter has been published as a research paper in

Oxidative Medicine and Cellular Longevity Volume 2013, Article ID 253657, 16 pages

Contribution: The article, ***Oxid Med Cell Longev***. ***2013;*** *253657,* was co-authored with Shuchita Tiwari, Ashok Jadhav, Courtney Gerger, Paul Lee, Lynn Weber, and my supervisor Joseph Fomusi Ndisang. This chapter describes the role of an upregulated HO system on cardiac injuries in a rat model of obesity (ZF rats) and the mechanisms by which hemin therapy counteracts inflammation and oxidative stress while improving insulin signaling, glucose metabolism and cardiac functions. Moreover, this chapter suggests that altered insulin signaling and cardiac functions are the forerunners for development of overt hyperglycemia and heart failure in obesity. In this study, I participated in animal and biochemical experiments, collection of data, and statistical analyses and interpretation. The idea for the study was conceived by my supervisor Joseph Fomusi Ndisang and financial supported by the Heart and Stroke Foundation of Saskatchewan, Canada grant to Dr. Ndisang.

3.1 Abstract

Although many obese individuals are normoglycemic and asymptomatic of cardiometabolic complications, this apparent healthy state may be a misnomer. Since heart failure is a major cause of mortality in obesity, we investigated the effects of heme-oxygenase (HO) on heart failure and cardiometabolic complications in obese normoglycemic Zucker-fatty rats (ZFs). Treatment with the HO-inducer, hemin, reduced markers of heart failure, such as osteopontin and osteoprotegerin, abated left-ventricular (LV) hypertrophy/fibrosis, extracellular matrix/profibrotic proteins including collagen-IV, fibronectin, TGF-β1, and reduced cardiac lesions. Furthermore, hemin suppressed inflammation by abating macrophage-chemoattractant-protein-1, macrophage-inflammatory protein-1 alpha, TNF-α, IL-6, and IL-1β but enhanced adiponectin, atrial-natriuretic peptide (ANP), HO activity, insulin sensitivity, and glucose metabolism. Correspondingly, hemin improved several hemodynamic/echocardiographic parameters including LV diastolic wall thickness, LV-systolic wall thickness, mean-arterial pressure, arterial-systolic pressure, arterial-diastolic pressure, LV developed pressure, +dp/dt, and cardiac output. Contrarily, the HO-inhibitor, stannous mesoporphyrin nullified the hemin effect, exacerbating inflammatory/oxidative insults and aggravated insulin resistance (HOMA-index). We conclude that perturbations in insulin signaling and cardiac function may be forerunners to overt hyperglycemia and heart failure in obesity. Importantly, hemin improves cardiac function by suppressing markers of heart failure, LV hypertrophy, cardiac lesions, extracellular matrix/profibrotic proteins, and inflammatory/oxidative mediators, while concomitantly enhancing the HO-adiponectin-ANP axis.

3.2 Introduction

The recent escalation of obesity in every segment of the population including children, adolescences, and adults poses a great health challenge of considerable socioeconomic burden (1, 2). The impact on healthcare systems may become unsustainable given the numerous chronic diseases such as type-2 diabetes, dyslipidemia, hypertension, and other related cardiometabolic complications associated with obesity (1-3). Cardiac complications including heart failure are among the major causes of mortality in obese individuals. Obesity causes lipotoxicity and adipose tissue dysfunction with excessive production of adipokines like tumor necrosis factor-α (TNF-α) and interleukin 6 (IL-6) IL-1β, all of which are implicated in heart failure and related cardiometabolic complications (4, 5). However, obesity may not always translate into increased risk for these comorbidities (6). Some obese individuals dubbed "metabolically healthy" are protected against obesity related metabolic diseases. These "metabolically healthy" obese individuals are insulin sensitive with normal lipid metabolism and cardiac function similar to healthy lean individuals, which is in stark contrast to "metabolically unhealthy" obese individuals with high risk of developing cardiometabolic complications (6). However, the apparent state of good health in "metabolically healthy" obese sub-phenotype may be a misnomer because the development of several characteristics of metabolic syndrome is now being observed in many adults who previously manifested the healthy obese phenotype (7), suggesting that individuals with a healthy obese phenotype may not remain healthy for their entire lives. Several parameters including environmental and behavioral factors may modify obesity sub-phenotypes, and the transition from healthy to unhealthy. Whether healthy obese individuals can maintain insulin sensitivity during the entire life or whether healthy obesity simply represents delayed onset of obesity related cardiometabolic complications has to be clarified.

In obesity, excessive oxidative stress, intense inflammatory activity, insulin resistance, deregulated lipid metabolism, altered glucose metabolism, and impaired mitochondrial biogenesis are among the pathophysiological driving forces that precede the early stages of cardiac dysfunction. Many cardiac complications have the common denominator of elevated inflammation due to the infiltration of macrophage M1-phenotype (8). Generally, macrophages exhibit two different forms dubbed "classical" or M1-phenotype and "alternative" or M2-phenotype (8), and each phenotype expresses distinct patterns of surface receptors when responding to different stimuli. The M1-phenotype stimulates inflammation while the M2-phenotype blunts inflammation (8). During macrophage infiltration, the M1-phenotype is stimulated by different chemokines including macrophage-inflammatory-protein-1 alpha ((MIP-1α), chemokine (C-C motif) ligand-3 (CCL3)) and macrophage-chemoattractant-protein-1 ((MCP-1) (9), chemokine (C-C motif ligand-2 (CCL2)) (9). The activation of the macrophage M1-phenotype is generally associated with elevated levels of proinflammatory cytokines including TNF-α, IL-6, and IL-1β (10-12). Moreover, the levels of macrophage M1-phenotype, MCP-1, TNF-α, IL-6, and IL-1β are elevated in obesity and insulin resistance (9, 10, 13), and these factors play a major pathophysiological role in heart failure (4). In obesity, markers of heart failure such as osteopontin (14) and osteoprotegerin (15) are elevated (16, 17). Similarly, the levels of extracellular matrix/profibrotic proteins like transforming growth factor beta (TGF-β), collagen, and fibronectin are elevated in obesity (18). Therefore, in obesity elevated chemokines, cytokines and increased macrophage-M1 infiltration would act in concert with elevated extracellular matrix/profibrotic and heart-failure proteins to exacerbate cardiac tissue destruction and compromise heart function. Thus, novel strategies capable of selectively suppressing macrophages M1-phenotype, proinflammatory cytokines/chemokines, and extracellular matrix/profibrotic proteins are needed.

In many pathophysiological conditions, various stress response immune-regulatory proteins, including heme oxygenase (HO-1), are activated as an innate defense mechanism (19-22). However, the pathophysiological activation of HO-1 may only result in a transient or marginal increase of HO activity that falls below the threshold necessary to activate the downstream signaling components through which the HO system elicits its cytoprotective effects, so a robust and surmountable increase of HO activity with HO inducers like hemin may be needed for cardioprotection (23-27). Generally, HO is composed of two main isoforms (HO-1 or inducible) and (HO-2 or constitutive), which are largely responsible for the antioxidant and anti-inflammatory effects of HO (28). We recently reported the cardioprotective effects of the HO system in Zucker diabetic fatty rats (ZDFs) (13), a model characterized by obesity, insulin resistance, and overt hyperglycemia. However, because ZDFs are hyperglycemic, their pathophysiological profile is not reflective of individuals dubbed "metabolically healthy," a subtype of obesity characterized by normoglycemia (7). Given that the incidence of cardiometabolic complications is increasing in many adults who previously manifested the metabolically healthy obese phenotype (7), novel studies with animal models that closely mimic the pathophysiological profile of metabolically healthy obese subtype are needed. Therefore, this study will investigate the effects of the HO system on cardiometabolic complications in Zucker fatty rats (ZFs), an obese model with normoglycemia and cardiometabolic complications (29) that closely mimic the pathophysiological profile of metabolically healthy obese individuals with normoglycemia and an apparent state of good health. Although, the HO system is cytoprotective, its effects on cardiomyopathy in ZFs remain to be elucidated.

Since dysfunctional insulin signaling, obesity, elevated inflammation, and cardiac hypertrophy are forerunners to heart failure, this study will also investigate the multifaceted

mechanisms by which the HO system preserves cardiac function in ZFs. Whether an upregulated HO system by hemin is capable of modulating macrophage polarization towards the M2-phenotype that blunts inflammation, while suppressing the proinflammatory M1-phenotype, will be assessed. As macrophage infiltration is stimulated by chemokines like MIP-1α and MCP-1 (9), and the effects of the HO system on these chemokines in ZFs have not been reported, this study will also determine left-ventricular MIP-1α and MCP-1 and correlate changes of these chemokines to the expression of the proinflammatory macrophage M1-phenotype in the left ventricle of ZFs. Similarly, the effect of hemin therapy on important markers of heart failure such as osteopontin (13) and osteoprotegerin (14) will be investigated. Importantly, no study has reported the levels of expression of osteopontin and osteoprotegerin in myocardial tissue of ZFs. Therefore, this study will unveil the multifaceted mechanisms by which hemin therapy improves cardiac function and insulin signaling in obesity.

3.3 Materials and methods

3.3.1 Animals, treatment groups, and biochemical parameters

Our experimental protocol was in conformity with the Guide for Care and Use of Laboratory Animals stipulated by the Canadian Council on Animal Care and the National Institutes of Health (NIH Publication no. 85-23, revised 1996) and was approved by University of Saskatchewan Animal Ethics Committee. Male ZFs (12 weeks old) and sex/age matched Zucker lean (ZL) rats were purchased from Charles River Laboratories (Willington, MA, USA). The animals were housed at 21°C with 12-hour light/dark cycles, fed with standard laboratory chow, and had access to drinking water ad libitum. The HO-inducer, hemin (30 mg/kg i.p., Sigma, St Louis, MO, USA), and HO-blocker stannous-mesoporphyrin ((SnMP) 2 mg/100 g body weight i.p.) were purchased from Porphyrin Products (Logan, UT, USA), and prepared as we previously

reported and administered biweekly for 8 weeks (13, 30, 31). At 16 weeks of age, the animals were randomly assigned to the following experimental groups (n = 6 per group): (A) controls (ZF and ZL), (B) hemin-treated ZF and ZL, (C) ZF + hemin + SnMP, and (D) ZF + vehicle dissolving hemin and SnMP.

During the treatment period body weight and glucose were monitored on a weekly routine. Body weight was measured using a digital balance (Model Mettler PE1600, Mettler Instruments Corporation, Greifensee, Zurich, Switzerland). At the end of the 8-week treatment period, the animals were 24 weeks of age. A day prior to killing, the animals were fasted in metabolic cages for 24 hr urine collection and weighed. Systolic blood pressure was determined by non-invasive tail-cuff method (Model 29-SSP, Harvard Apparatus, Montreal, Canada), while a Millar Mikro-Tip ultraminiature tip sensor pressure transducer catheter (Model SPR-407, Harvard Apparatus, Montreal, Canada) for invasive hemodynamic parameters. In addition, a Vevo 660 high frequency ultrasound machine (Visual Sonics, Markham, ON, Canada) equipped with B-mode imaging was used for echocardiographic measurements as we previously reported (13). After anaesthetizing the animals with pentobarbital sodium (50 mg/kg i.p.), blood was collected by cardiac puncture, and the heart was cleaned and weighed with an analytical balance (Precisa Instruments Ltd., Dietikon, Switzerland) as we previously reported (32). The atria were removed from the heart and the right ventricle free wall separated from the left ventricle including the septum as we previously reported (32).

Left-ventricular HO activity was evaluated spectrophotometrically as we previously reported (30, 32). ELISA kits were used for HO-1 (Stressgen-Assay Design, Ann Arbor, MI, USA), adiponectin (Phenix Pharmaceuticals, Inc., Burlingame, CA, USA), TNF-α, IL-6, and IL-1β (Immuno-Biological Laboratories Co Ltd., Gunma, Japan), MIP-1α, and MCP-1 (OmniKine,

Assay Biotechnology Company Inc., Sunnyvale, CA, USA) (33, 34), while EIA kits for 8-isoprostane, ANP, ET-1, cGMP, and kits for cholesterol and triglyceride were purchased from Cayman (Cayman Chemical, Ann Arbor, MI, USA) following the manufacturers' instructions as we reported (13, 30, 32). Intraperitoneal glucose tolerance test (IPGTT) and homeostasis model assessment of insulin resistance (HOMA-IR) were done as we previously reported (30).

3.3.2 Histological, morphological, and immunohistochemical analyses of left ventricle

Histological and morphometric analyses were done as we previously described (35). Sections of 5 μm were cut and stained with hematoxylin and eosin for histological analysis. Masson's Trichrome staining detected left-ventricular collagen deposition. Morphometrical evaluation of left-ventricular longitudinal myocyte thickness was done by randomly measuring 30 cardiac muscle fibers from each experimental group by a blinded researcher using a microscope (Aperio Scan Scope Model CS, Aperio Technologies Inc., Vista, CA, USA) and analyzed using Aperio ImageScope V11.2.0.780 software (Aperio, e-Pathology Solution, Vista, CA, USA). Morphologic assessment of collagen deposition in left-ventricular sections was accessed using Aperio Image Scope (Aperio Technologies Inc., Vista, CA, USA). Each left-ventricular section was magnified at 200x, and 20 random snaps were taken per slide ($20 \times 6 = 120$ images per group) subsequently scored semi-quantitatively by a blinded researcher as we previously reported (13, 35).

Immunohistochemistry was done as we previously reported (36). Sections of 5 μm of left-ventricular tissue were treated with bovine serum albumin in phosphate buffered saline to block nonspecific staining and incubated overnight with ED1 (1: 500 dilutions; sc-59103, Santa Cruz Biotechnology, CA, USA). The sections were later treated with goat anti-mouse IgG for 30 min

(1: 200 dilutions; Jackson Immuno-Research Laboratories, Inc., ME, USA). Immunohistochemical staining was done using the standard avidin-biotin complex method with the chromagen 3,3′-diaminobenzidine (DAB) at the final detection step. Sections of heart tissue were scanned using virtual microscope (Aperio Scan Scope Model CS, Aperio Technology Inc., Vista, CA, USA). Quantitative assessment of ED1 was done by a blinded researcher who randomly examined 20-22 fields of each left ventricular section magnified at 200x. Macrophages which were positively stained with ED1 (brown from immune stained sections) were quantified by manually counting the ED1-stained cells around the blood vessels and interstitial spaces of myocardium.

3.3.3 Western immunoblotting

Left-ventricular tissue was homogenized as previously reported (13, 30-32, 35). Primary antibodies (Santa Cruz Biotechnology, Santa Cruz, CA, USA), ED1 (CD68) (sc-59103), ED2 (CD163) (sc-58956), CD14 (sc-9150), CD206 (sc-48758), CD36 (sc-9154), osteopontin (sc-21742), osteoprotegerin (sc-11383), PI3K (sc67306), IRS-1 (sc-559), collagen-IV (sc-11360), fibronectin (sc-18825), TGF-β1/2/3 (sc7892)) and GLUT4 (ab654, Abcam Inc., Cambridge, MA, USA) were used. Densitometric analysis was done with UN-SCAN-IT software (Silk Scientific Inc., Orem, UT, USA). G6PDH antibody (A9521, Sigma St. Louis, MO, USA) was used as a control to ascertain equivalent loading.

3.3.4 Statistical analysis

All data are expressed as means ± SEM from at least four independent experiments unless otherwise stated. Statistical analyses were done using two-way ANOVA, using Statistical Analysis

System (SAS), software Version 9.3 (SAS Institute Inc., Cary, NC, USA) and Student's *t-test*. Group differences at the level of $p<0.05$ were considered statistically significant.

3.4 Results

3.4.1 Hemin therapy upregulates the HO System to improve cardiac function

To investigate the mechanisms underlying the improvement of cardiac function in obese insulin resistant ZFs, we measured the concentration of HO-1 and HO activity. In ZF-control rats, the basal level of HO-1 concentration and HO activity was significantly lower than that of ZL control (Figures 3-1(a) and 3-1(b)). However, hemin administration increased HO-1 and HO activity in ZF by 8.4- and 11.3-fold, respectively. The enhanced HO activity would increase endogenous carbon monoxide that would in turn stimulate cGMP (30, 32). Both cGMP and carbon monoxide are known to enhance insulin signaling and glucose metabolism (37). Accordingly, we detected a 3.4-fold increase of cGMP in hemin-treated animals (Figure 3-1(c)). In contrast, the coadministration of the HO blocker, SnMP and the HO inducer, and hemin abolished the hemin-induced increase of HO-1 and HO activity, with corresponding reduction of cGMP levels (Figure 3-1(c)). Hemin therapy also enhanced HO-1, HO activity, and cGMP levels in ZL-control rats (Figures 3-1(a), 3-1(b), and 3-1(c)). In hemin-treated ZLs, HO-1, HO activity and cGMP were enhanced by 3.1-, 2.8-, and 2.4-fold, respectively, as compared to 8.4-, 11.3-, and 3.4-fold, respectively, in hemin-treated ZFs, suggesting greater selectivity of hemin to the HO system in unhealthy ZFs characterized obesity, insulin resistance, and cardiomyopathy (29).

Since cardiac hypertrophy is amongst the forerunners to heart failure, we investigated the effects of hemin on cardiac hypertrophy. Our results indicate that hemin therapy significantly reduced cardiac hypertrophy in ZF, whereas the coadministration of hemin and SnMP nullified the

effect (Table 3-1). Echocardiography was used to further assess left ventricular hypertrophy. Our hemodynamic data obtained during catheterization of the left side of hearts from ZFs showed association between elevated myocardial hypertrophic response and obesity. A significant 2-fold increase in left-ventricular free wall thickness, an important index of cardiac hypertrophy (38), was observed during diastole and systole, and interestingly these were abated by hemin by 33.3% and 15.6%, respectively (Table 3-2). Other hemodynamic deficiencies in ZFs including abnormalities in left-ventricular end-diastolic volume, left-ventricular end systolic volume, stroke volume, and cardiac output which were reduced by 17.5%, 16%, 8.3%, and 7.7%, respectively (Table 3-2), were increased by hemin therapy by 15.2%, 27.3%, 13.6% and 12.4%, respectively. Hemin therapy also improved cardiac hemodynamics by lowering arterial-systolic pressure, arterial-diastolic pressure, mean-arterial pressure, and total peripheral resistance by 12.4%, 11.4% and 12.2%, 17.6%, respectively, with corresponding reduction of +dp/dt (the maximal rate of increase in left-ventricular pressure), left ventricular developed pressure, and heart rate.

Treatment with hemin and SnMP caused loss of body weight in ZL controls and ZFs, which, however, did not exceed 9% (Table 3-1). The loss of weight may not be due to toxicity as we recently showed that several indices of toxicity including plasma gamma-glutamyl transferase, aspartate aminotransferase, and alanine aminotransferase were within normal range (30). Although, ZFs had normoglycemia, hemin and SnMP affected blood glucose. In hemin-treated animals, there was a slight but significant reduction of glycemia, whereas in SnMP-treated animals a slight increase was observed (Table 3-1). Similarly, hemin therapy slightly reduced glycemia in ZL controls. The vehicle dissolving hemin and SnMP had no effect on the measured parameters.

3.4.2 Hemin therapy abates MCP-1, MIP-1α, TNF-α, endothelin-1, and 8-isoprostane but enhanced ANP in ZFs

Since 8-isoprostane stimulates ET-1 (39), and both ET-1 and 8-isoprostane are involved in the oxidative destruction of tissue, we measured ET-1 and 8-isoprostane. ET-1 in untreated ZFs was markedly elevated as compared to ZL controls (Figure 3-2(a)) but was significantly abated by hemin. In contrast, the coadministration of hemin and the HO blocker, SnMP, annulled the effect of hemin (Figure 3-2(a)). Because elevated oxidative stress is linked to impaired insulin signaling and cardiac dysfunction, we measured urinary 8-isoprostane, an important marker of oxidative stress (40). In ZFs, the basal levels of 8-isoprostane were significantly elevated (Figure 3-2(b)) but were reduced by hemin, whereas cotreatment of hemin with SnMP nullified the effects. Given that ET-1 and ANP are known to interact reciprocally (41), we investigated whether the hemin-dependent suppression of ET-1 (Figure 3-2(a)) would be associated with a parallel potentiation of ANP. In ZFs, the basal ANP levels were markedly depressed by 1.7-fold (Figure 3-2(c)) but interestingly were robustly enhanced by hemin by 3.3-fold. In contrast, the coadministration of hemin with SnMP abolished the effects of hemin.

We also investigated the effects of hemin on MIP-1α and MCP-1 since these chemokines trigger macrophage infiltration (9). In ZFs, the basal MCP-1 levels were significantly increased by 4.6-fold (Figure 3-2(d)) but were attenuated by hemin by 2.8-fold, whereas the coadministration with SnMP nullified the effects of hemin (Figure 3-2(d)). Although, hemin therapy greatly attenuated MCP-1 by 64% in ZF, however comparable levels as observed in the ZL controls were not reinstated. Hemin therapy was also effective in suppressing MIP-1α (Figure 3-2(e)). In ZFs, the basal MIP-1α levels were significantly elevated by 4.9-fold but were reduced by hemin by 3.5-fold, whereas the cotreatment of hemin with SnMP nullified the effects (Figure 3-2(e)). Since

TNF-α is implicated in macrophage infiltration (9), we also assessed the effects of hemin on TNF-α. In ZFs, the basal levels of TNF-α were elevated by 3.5-fold but were significantly attenuated by hemin by 2.6-fold (Figure 3-2(f)), whereas cotreatment with SnMP abolished the effect of hemin. Hemin therapy also affected ET-1, 8-isoprostane, ANP, MCP-1, and MIP-1α in ZL controls although, the magnitude of effect was smaller than that in ZFs (Figure 3-2).

3.4.3 Hemin selectively abated the proinflammatory macrophage M1 phenotype but enhanced the anti-inflammatory M2 phenotype in the left ventricle of ZFs

After having observed the hemin-dependent reduction of cytokines/chemokines implicated in macrophage infiltration such as MIP-1α, MCP-1, and TNF-α, we investigated whether the suppression of these chemokines/cytokines in the left ventricle of ZFs would be accompanied by the selective attenuation of the proinflammatory macrophage M1-phenotype using a specific marker such as ED1 (42) to quantify the expression of the proinflammatory M1-phenotype in left-ventricular tissue and other markers for the assessment of anti-inflammatory M2-phenotype including ED2 (42), CD14 (43, 44), CD206 (8), and CD36 (45, 46).

Our Western immunoblotting and relative densitometry revealed that the basal expression of the proinflammatory macrophage M1-phenotype marker, ED1, in ZFs was markedly elevated by 4.8-fold as compared to ZL controls (Figure 3-3(a)) but was significantly reduced by hemin by 3.5-fold although control levels were not attained. On the other hand, the basal expression of several markers of the anti-inflammatory macrophage M2-phenotype including ED2, CD206, CD36, and CD14 was significantly depressed in ZFs by 2.1-, 5.7-, 3.6-, and 2.9-fold, respectively, (Figures 3-3(b), 3-3(c), 3-3(d), and 3-3(e)). Interestingly, hemin therapy greatly enhanced the depressed ED2, CD206, CD36, and CD14 in ZFs by 3.8-, 4.1-, 2.3-, and 2.6-fold, respectively,

suggesting that a novel mechanism by which hemin therapy blunts inflammation is by selectively modulating the polarization of macrophage toward the M2-phenotype that dampens inflammation.

3.4.4 Hemin therapy suppressed macrophage infiltration in the left ventricle of ZFs

Following the observation from our Western blot experiment that hemin therapy reduced left-ventricular ED-1, a marker of macrophage infiltration, we use the ED-1 antibody to further confirm macrophage infiltration in the left ventricle by immunohistochemistry (Figure 3-4(a)). Our results reveal that left-ventricular sections from ZL-control rats were almost devoid of the dark brown ED1 positive staining. However, in untreated ZF control rats, a greater number of ED1-positively stained dark brown cells were observed, indicating increased macrophage infiltration. Interestingly, in hemin-treated ZFs, there was a marked reduction in the number of dark brown-stained macrophages, suggesting reduction of macrophage infiltration. Correspondingly, hemin therapy significantly reduced the quantitative ED1 score (Figure 3-4(b)).

3.4.5 Hemin therapy enhanced insulin signaling but suppressed extracellular matrix and profibrotic proteins implicated in cardiac injury

Since visceral adiposity and elevated inflammation impair insulin signaling (47), we investigated the effects of hemin therapy on the expression of important components of the insulin signal transduction pathway including IRS-1, PI3K, and GLUT4. In in ZFs, the basal expression of IRS-1, PI3K, and GLUT4 was significantly reduced by 11.2-, 2.5-, and 2.3-fold as compared to the ZL control (Figures 3-5(a), 3-5(b), and 3-5(c)) but was enhanced by hemin by 5.7-, 4.01-, and 1.9-fold, respectively.

To further confirm the antihypertrophic effect of hemin therapy, we measured collagen-IV, an important protein implicated in cardiac hypertrophy and fibrosis (35). In ZFs, the basal

expression of left-ventricular collagen-IV was significantly elevated by 6.9-fold but was abated by hemin by 2.8-fold (Figure 3-5(d)). Given that excessive deposition of extracellular matrix/profibrotic proteins and inflammation due to macrophage infiltration are cardinal pathophysiological events implicated in cardiac insult (47, 48), while atrial natriuretic peptide (ANP) and adiponectin are known to suppress fibrosis caused by the deposition of extracellular matrix (49, 50), we investigated whether the concomitant potentiation of ANP, adiponectin, and the HO system by hemin would abate TGF-β. In ZFs, the basal expression of TGF-β was significantly elevated by 4.6-fold but was markedly attenuated by hemin by 3.4-fold (Figure 3-5(e)). Since TGF-β mobilizes the extracellular matrix by stimulating fibronectin and collagen to cause fibrosis and cardiac injury (49, 51), we also measured the expression of fibronectin. In ZF rats, the basal expression of fibronectin was increased by 7.5-fold but was markedly attenuated by hemin therapy by 4.5-fold (Figure 3-5(f)).

3.4.6 Hemin improved glucose tolerance, enhanced the insulin-sensitizing protein, adiponectin, but abated insulin resistance

After having observed the hemin-induced potentiation of insulin signalling, to further confirm the role of hemin therapy on glucose metabolism, we assessed the effects of hemin on glucose tolerance, insulin resistance, and the insulin-sensitizing protein, adiponectin in ZFs, an obese model with elevated inflammation. Since inflammation due to macrophage infiltration is implicated in insulin resistance and cardiomyopathy (47, 48), and ZFs are characterized by insulin resistance (29), we investigated whether the hemin dependent suppression of macrophage infiltration would be accompanied by improved glucose metabolism. In untreated ZFs, IPGTT analysis showed marked increase in glycemia as compared to ZL controls and hemin-treated ZFs at all time points tested (Figure 3-6(a)), suggesting improved glucose tolerance in hemin-treated

ZFs. Although, ZFs were hyperinsulinemic with elevated basal glycemia, when challenged with a bolus injection of glucose, only to a meagre glucose stimulated insulin release was observed (Figure 3-6(b)), suggesting glucose intolerance. On the other hand, glucose challenge to ZL controls and hemin-treated ZFs greatly stimulated insulin release (Figure 3-6(b)), suggesting improved glucose tolerance. Hemin also reduced the elevated insulin resistance HOMA-IR in ZFs (Figure 3-6(c)), whereas coadministration with SnMP reversed the effects of hemin (Figure 3-6(c)).

We also investigated the effects of hemin therapy on adiponectin, an anti-inflammatory, insulin sensitizing and cardioprotective protein (52, 53). Interestingly, hemin therapy significantly enhanced the depressed basal adiponectin levels in ZFs, whereas treatment with SnMP abolished and further reduced the depressed levels of adiponectin (Figure 3-6(d)). Hemin therapy also reduced HOMA-IR index in ZL controls and enhanced adiponectin although, the effect was less intense as compared to ZFs.

3.4.7 Hemin therapy suppressed left-ventricular fibrosis, cardiomyocyte hypertrophy, and longitudinal cardiac myofibril thickness in ZFs

Histological and morphometric analyses Using Masson's trichrome and hematoxylin and eosin staining were done to further confirm the cardioprotection by hemin. Cardiomyocytes appeared as dark reddish while extracellular matrix, such as collagen, stained blue (Figure 3-7(a)). Left ventricular sections from ZL controls appeared morphologically normal, with scanty interstitial collagen deposition. In contrast left-ventricular images from ZFs showed moderate to-severe fibrosis, with scarring of cardiomyocytes, and interstitial and perivascular collagen depositions (Figure 3-7(a)). Interestingly, hemin therapy attenuated the severity of scarring and

intestinal and perivascular collagen deposition, evidenced by reduced extracellular and perivascular blue staining (Figure 3-7(a)). Correspondingly, semi-quantitative analysis showed that hemin therapy significantly abated the elevated collagen deposition and perivascular fibrosis in ZFs, reinstating comparable levels to ZL control (Figure 3-7(b)). Hemin therapy was also effective against cardiomyocyte hypertrophy (Figure 3-7(c)). In ZFs, cardiomyocytes were enlarged with increscent nuclei and the inner myofibril spaces were decreased, as compared to normal cardiomyocytes in ZL controls (Figure 3-7(c)). In ZFs, the longitudinal cardiac myofibril thickness was 37% higher than that of ZL controls (Figure 3-7(d)) but was reduced by 27% in hemin-treated ZFs. Although, ZL-control values were not reinstated, hemin increased intermyofibril spaces in ZFs close to the levels observed in ZL controls (Figure 3-7).

3.4.8 Hemin therapy suppressed the elevated expression of markers of heart failure in the left ventricle of ZFs

To further confirm the cardioprotective effects of an upregulated HO system, we investigated the effects of hemin therapy on important markers of heart failure such as osteopontin (13) and osteoprotegerin (14). Since left-ventricular hypertrophy is associated with heart failure (54), we determined whether the hemin-dependent suppression of left-ventricular hypertrophy in ZFs would be accompanied by the reduction of markers of heart failure. Our results indicate that, in ZFs, the basal expression levels of osteopontin and osteoprotegerin were significantly elevated by 4.6- and 7.1-fold, respectively, as compared to ZL controls (Figures 3-8(a) and 3-8(b)). Interestingly, treatment with hemin attenuated the expressions of osteopontin and osteoprotegerin by 3.5- and 3.3-fold, respectively, (Figures 3-8(a) and 3-8(b)).

3.5 Discussion

The present study indicates that the multifaceted mechanisms by which hemin therapy improves cardiomyopathy in obesity include (i) the suppression of visceral adiposity, (ii) the reduction of macrophageM1 phenotype, (iii) the attenuation of markers of heart failure, (iv) the reduction of extracellular matrix/profibrotic proteins, and (v) the amelioration of insulin resistance, with corresponding enhancement of glucose metabolism. In ZFs, excessive visceral adiposity, increased macrophage infiltration and the elevated levels of 8-isoprostane, MIP-1α, MCP-1, TNF-α, IL-6, IL-1β, and ET-1 proteins of heart failure, and extracellular-matrix deposition are among the complex molecular processes that characterize the intricate relationship between inflammation, oxidative stress, cardiac fibrosis, and the progressive development of insulin resistance and cardiomyopathy (5, 47-49, 55-57). Importantly, the present study unveils that hemin therapy selectively enhances the anti-inflammatory macrophage M2-phenotype in left-ventricular tissue of ZFs while concomitantly abating the proinflammatory M1-phenotype, suggesting that a novel mechanism by which hemin therapy suppresses cardiac inflammation in obesity is by selectively favoring the polarization of macrophage towards the M2-phenotype that ablates inflammation. Correspondingly, hemin therapy abated several chemokines and cytokines that promote macrophage infiltration including MIP-1α, MCP-1, TNF-α, IL-6, and IL-1β (9-11). Interestingly, the suppression of visceral adiposity and inflammation in hemin-treated ZFs was accompanied by reduced insulin resistance and improved glucose intolerance, and the potentiation of important components of the insulin signal transduction pathway including IRS-1, PI3K, and GLUT4, which in addition to the hemin-dependent enhancement of adiponectin, an anti-inflammatory, insulin sensitizing, and cardioprotective protein (52, 53) may account for improved glucose metabolism in obese conditions.

Hemin therapy also reduced LV hypertrophy, cardiac fibrosis, and cardiomyocyte longitudinal muscle-fiber thickness, a pathophysiological feature of cardiomyocyte hypertrophy (35), with a corresponding suppression of markers of heart failure such as osteopontin and osteoprotegerin (14, 15), as well as the reduction of extracellular matrix protein like TGF-β, fibronectin, and collagen which are implicated in cardiac hypertrophy and fibrosis (49, 57). Since TGF-β mobilizes the extracellular matrix by stimulating fibronectin and collagen causing tissue damage and hypertrophy (49, 57), the concomitant reduction of TGF-β, fibronectin, and collagen-IV in ZFs may account for reduced cardiac lesions. Another mechanism by which the HO system suppresses extracellular matrix and profibrotic agents like TGF-β and ET-1 may be due to the HO-dependent potentiation of ANP, a substance known to suppress extracellular matrix (41, 58). Generally, ANP and ET-1 have opposing effects (59). For example, ANP reduces fibrosis by inhibiting TGF-β1 and fibronectin (41), while ET-1 acts in conjunction with TGF-β1 to stimulate the synthesis of fibronectin (58). Similarly, ANP suppresses inflammation to reduce insulin resistance (59), while ET-1 stimulates inflammatory/oxidative insults causing insulin resistance (60). On the other hand, ANP stimulates the production of adiponectin (61), a protein with insulin-sensitizing and anti-inflammatory effects (52). The effects of ANP are largely mediated by cGMP (62), and adiponectin is also known to enhance cGMP (63). Moreover, ANP and the HO system have mutual stimulatory effects. Accordingly, ANP enhances HO (64, 65), and similarly, the HO system has been shown to upregulate ANP and adiponectin (23, 66). Therefore, the synergistic potentiation of the HO-adiponectin-ANP axis and insulin signaling with corresponding ablation of extracellular matrix/heart failure proteins, the reduction of oxidative stress, and inflammation mediators such as macrophage M1-phenotype, MIP-1α and MCP-1, TNF-α, IL-6, IL-1β, ET-1, and 8-isoprostane are among the multifaceted mechanisms by which hemin therapy improved

cardiac function. Thus, novel strategies capable of potentiating the HO-adiponectin-ANP axis would improve cardiomyopathy and insulin signaling in obesity.

Cardiomyocyte hypertrophy and myocardial fibrosis are early microscopic changes in heart failure. Subsequently, macroscopic alterations including increased left-ventricular wall thickness, diastolic/systolic dysfunction, and impaired cardiac hemodynamics become evident. Interestingly, hemin therapy modulated several hemodynamic and echocardiographic parameters to improve cardiac function (67). These include the reduction of left-ventricular diastolic wall thickness, left-ventricular systolic wall thickness, mean-arterial pressure, arterial-systolic pressure, arterial-diastolic pressure, left-ventricular developed pressure, +dp/dt, and total peripheral resistance, with corresponding enhancement of stroke volume and cardiac out, and thus improved cardiac function in hemin-treated ZFs. Hemin therapy also enhanced the HO system, cGMP, adiponectin, and ANP, abated 8-isoprostane, MCP-1, MIP-1α, TNF-α, IL-6, IL-1β, and ET-1 and lowered HOMA-IR index in ZL-control rats although, the magnitude was smaller as compared to ZFs with depressed HO activity. The reasons for this selective effect of HO are not fully understood. However, it is possible that as ZL controls are healthy animals with normal/functional insulin-signalling, the HO system may be more stable as compared to ZFs which have deregulated HO system with depressed HO-1 and HO activity. Importantly, the selectivity of the HO system in diseased conditions could be explored against the comorbidity of insulin-resistant diabetes and obesity.

Although, we recently reported the cardioprotective effects of the HO system in ZDFs (13), a model characterized by obesity, insulin resistance, and overt hyperglycemia, pathophysiological profile of ZDF is not reflective of the metabolically healthy individuals who are characterized by obesity and normoglycemia (7). In contrast, ZFs closely mimic the pathophysiological profile of metabolically healthy obese individuals with normoglycemia, so our findings may be applicable

to this subtype of obese individuals. Moreover, with the rising incidence of cardiometabolic complications in many adults who previously manifested the metabolically healthy obese phenotype (7), novel studies with animal models that closely mimic the pathophysiological profile of metabolically healthy obese subtype are needed. Therefore, studying the effects of the HO system on ZFs may offer new perspective in the pathophysiology of cardiometabolic complications and especially the progressive deterioration of cardiac function which may eventually lead to heart failure given the elevated levels of proteins of heart failure detected in untreated ZFs.

Collectively, our study unveils the beneficial effect of upregulating the HO system in the comorbidity of obesity and insulin resistance and suggests that the suppression of oxidative mediators, macrophage M1-phenotype infiltration and extracellular matrix/remodeling proteins are among the multifaceted mechanisms by which the HO system maintains and enhances insulin signaling and counteract diabetic cardiomyopathy. These data suggest that although, ZFs are normoglycemic, perturbations of insulin signaling, and cardiac function may be forerunners to overt hyperglycemia and heart failure in obesity.

3.6 Conclusion

The novelty of our study includes: (i) the hemin-induced selective enhancement of the anti-inflammatory M2-phenotype in left-ventricular tissue of ZFs and parallel reduction of the proinflammatory macrophage M1-phenotype and MIP-1α, a chemokine implicated in macrophage infiltration; (ii) the hemin-dependent suppression of heart failure proteins such as osteopontin and osteoprotegerin; (iii) the suppression of inflammatory cytokines in ZFs; and (iv) the hemin-induced reduction of insulin resistance and improvement of cardiac function in ZFs. Since we

recently reported that the HO system suppressed pericardial adiposity in a model characterized by obesity, insulin resistance, and overt hyperglycemia (13), and the present study indicates that hemin therapy abates cardiac inflammation in obesity, an interorgan crosstalk of inflammatory mediators between the myocardium and pericardial adipose tissue can be envisaged in the pathophysiology of diabetic cardiomyopathy. Importantly, the concomitant modulation of macrophage polarization in left ventricles towards the anti-inflammatory M2 phenotype alongside the parallel reduction of proinflammatory cytokines and chemokines implicated in macrophage infiltration and tissue destruction may be indicative of a putative interorgan crosstalk and the movement of inflammatory mediators from the pericardial fat to the myocardium or vice versa, and this may be particularly important in the progressive development of cardiomyopathy, insulin resistance, and related cardiometabolic complications. Although, this linkage has to be established, this study would set the stage for further exploration of the putative interorgan communication between pericardial fat and the heart.

Conflict of interests: The authors have no conflict of interests that could be perceived as prejudicing the impartiality of the research reported.

Acknowledgement: This work was supported by a grant from the Heart & Stroke Foundation of Saskatchewan, Canada to Joseph Fomusi Ndisang.

Table 3-1: Effect of hemin and stannous mesoporphyrin (SnMP) on physiological and biochemical variables in Zucker fatty (ZF) and Zucker lean (ZL) rats

Parameters	Animal groups					
	ZL control	ZL + hemin	ZF control	ZF + hemin	ZF + hemin + SnMP	ZF + vehicle
Body weight (g)	472.9 ± 9.7	445.5 ± 11.6†	746.8 ± 21.5§	685.9 ± 14.7§	691.4 ± 15.2$^{\$}$	702.8 ± 24.6
Fasting glucose (mmol/L)	7.2 ± 0.6	6.5 ± 0.3*	8.2 ± 0.5§	6.9 ± 0.4*	8.5 ± 0.4*	8.1 ± 0.4
Heart weight (g)	1.5 ± 0.03	1.1 ± 0.02†	3.4 ± 0.06§	2.0 ± 0.04§	3.0 ± 0.03$^{\$}$	3.1 ± 0.04
Cardiac hypertrophy (g/kg body weight)	3.1 ± 0.07	2.5 ± 0.06*	4.6 ± 0.16§	2.9 ± 0.08*	4.4 ± 0.17*	4.4 ± 0.09

$^{\dagger}p<0.05$ versus ZL; $^{\$}p<0.05$ versus ZF; $^{\S}p<0.05$ versus ZL control; $^{*}p<0.05$ versus ZF-control or ZL-control.

Table 3-2: Effect of hemin therapy on hemodynamic and echocardiographic parameters

Parameters	Experimental groups			P-value		
	ZF	ZL	ZF + hemin	ZF versus ZL	ZF versus ZF + hemin	Effect of hemin on ZF
Arterial systolic pressure (mmHg)	153 ± 5.2	124 ± 3.4#	134 ± 6.3*	0.001	0.018	Reduced by 12.4%
Arterial diastolic pressure (mmHg)	109 ± 3.2	92 ± 2.5#	96 ± 4.7*	0.003	0.024	Reduced by 11.9%
Mean arterial pressure (mmHg)	123 ± 3.8	102 ± 2.7#	109 ± 5.2*	0.002	0.022	Reduced by 11.4%
Total peripheral resistances (mmHg·min/mL)	1.7 ± 0.1	1.4 ± 0.1	1.4 ± 0.1	0.060	0.080	Reduced by 17.6%
LV developed pressure (mmHg)	161 ± 4.1	136 ± 8.0#	140 ± 5.8*	0.012	0.030	Reduced by 13.0%
$+dp/dt_{(max)}$ (mmHg/sec)	3634 ± 127	3050 ± 200#	3050 ± 169*	0.027	0.027	Reduced by 16.1%
Heart rate (beats/min)	328 ± 9.2	331 ± 7.2	289 ± 14.2*	0.814	0.020	Reduced by 11.9%
LV diastolic wall thickness (mm)	2.7 ± 0.1	1.7 ± 0.1#	1.8 ± 0.1*	0.0001	0.0001	Reduced by 33.3%
LV systolic wall thickness (mm)	3.2 ± 0.1	2.1 ± 0.1#	2.7 ± 0.1*	0.0001	0.007	Reduced by 15.6%
LV end diastolic volume (mL)	0.33 ± 0.01	0.40 ± 0.04	0.38 ± 0.02	0.075	0.169	Increased by 15.2%
LV end systolic volume (mL)	0.11 ± 0.01	0.16 ± 0.01#	0.14 ± 0.01	0.001	0.089	Increased by 27.3%
Stroke volume (mL)	0.22 ± 0.01	0.24 ± 0.02	0.25 ± 0.02	0.564	0.311	Increased by 13.6%
Cardiac output (mL/min)	72.8 ± 3.6	78.9 ± 9.0	81.8 ± 9.8	0.519	0.412	Increased by 12.4%

Values for each echocardiography and hemodynamic endpoint were averaged for each rat and the mean values used in statistical analyses, with *n*: number of rats. Differences among treatment groups were compared using one-way ANOVA followed by Fisher's Least Square Difference

(LSD) posteriori tests. Differences of $p<0.05$ were considered statistically significant. Values are means ± SE; n = 6 per group. *$p<0.05$ versus control ZF rats, $^{\#}p<0.05$ versus control ZL rats. LV: left ventricle; $+dp/dt_{(max)}$, maximal rate of increase in left ventricular pressure.

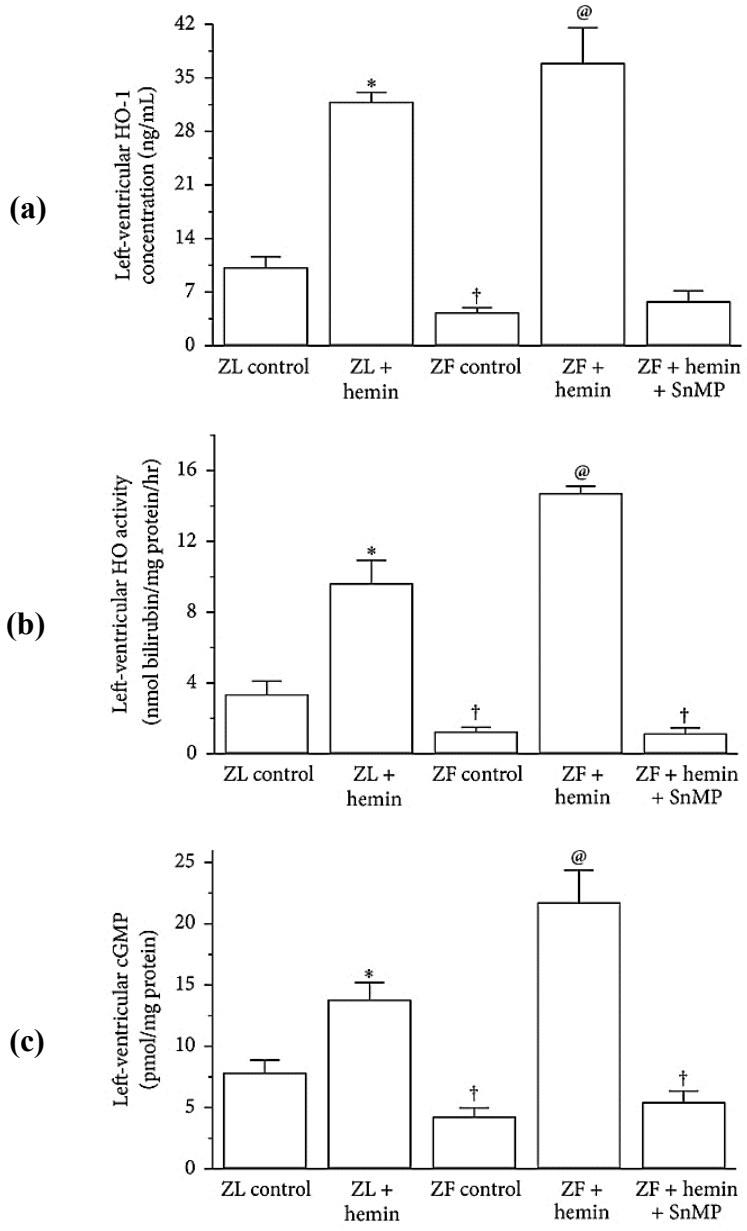

Figure 3-1: Effects of the HO inducer, hemin, and the HO inhibitor, SnMP on HO-1, HO activity and cGMP in the left ventricle of ZLs and ZFs. (a) Hemin enhanced HO-1, whereas SnMP nullified the effects of hemin. (b) Hemin increased HO activity, while SnMP abolished the hemin effect.

(c) Hemin enhanced cGMP, which, however, was abolished by SnMP. Bars represent means ± SEM; n = 6 rats per group (*p<0.01 versus ZL control; †p<0.05 versus ZL control; @p<0.01 versus ZF + hemin + SnMP or ZF control).

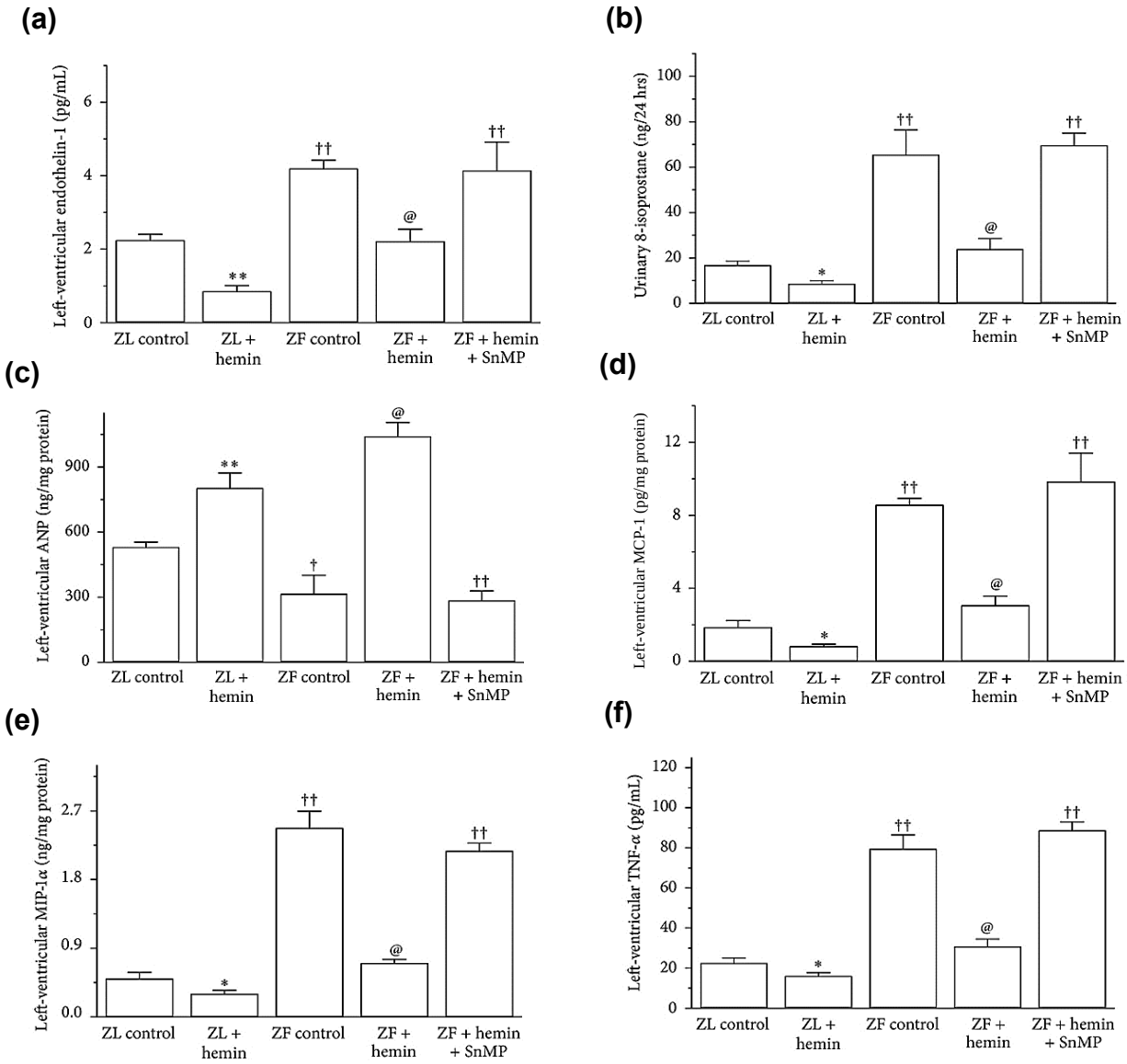

Figure 3-2: Effects of the HO inducer, hemin and the HO inhibitor, SnMP on endothelin-1, ANP, MCP-1, MIP-1α, and TNF-α in left-ventricular tissue from ZLs and ZFs. Hemin therapy: (a) reduced endothelin-1, (b) attenuated 8-isoprostane, (c) increased ANP, (d) suppressed MCP-1,

(e) abated MIP-1α, and (f) reduced TNF-α, whereas SnMP abolished the hemin effects. Bars represent means ± SEM; n = 6 rats per group (*p<0.05, **p<0.01 versus ZL control; †p<0.05, ††p<0.01 versus ZL control; @p<0.01 versus ZF + hemin + SnMP or ZF control).

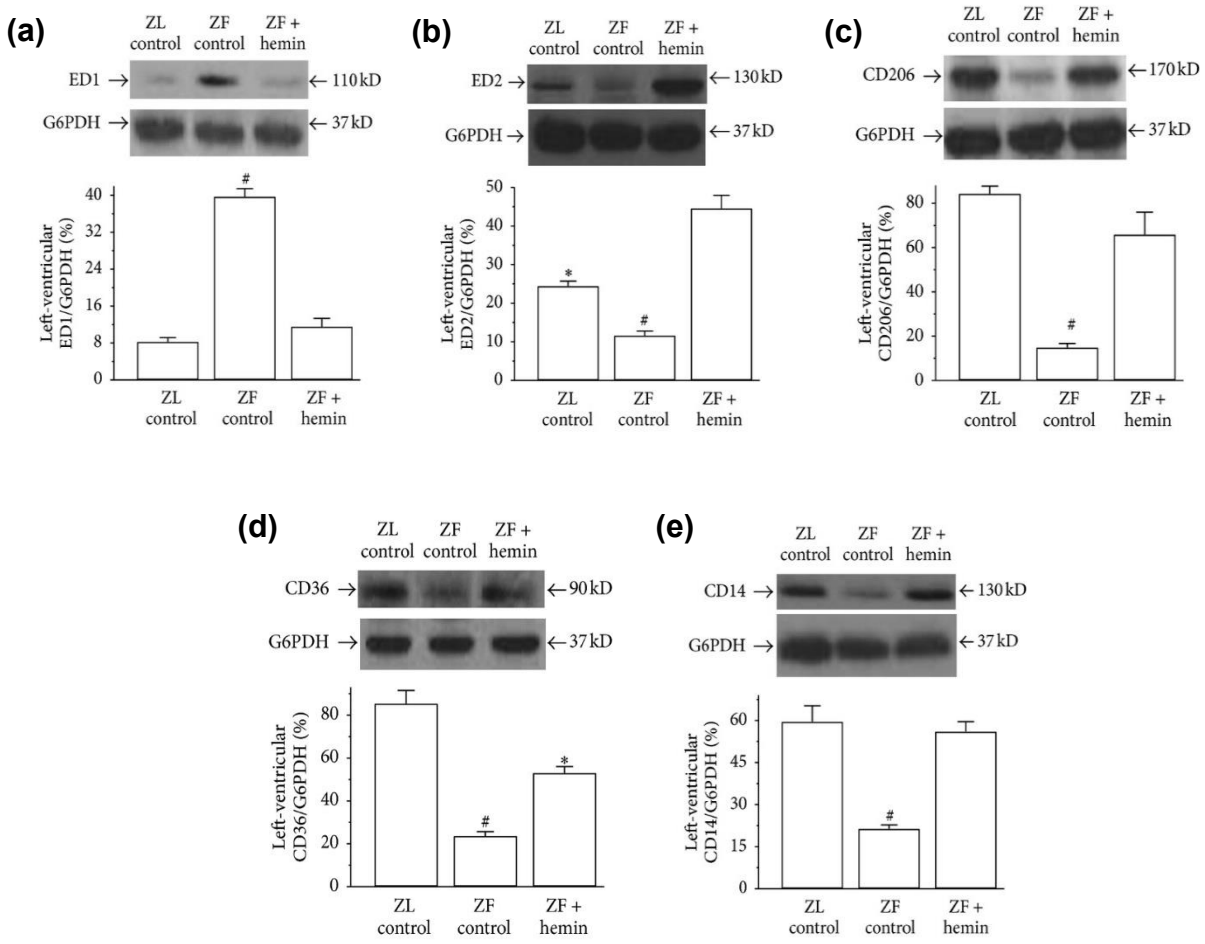

Figure 3-3: Effects of hemin on ED1, ED2, CD206, CD36, and CD14 in left-ventricular tissue from ZLs and ZFs. Hemin therapy (a) abated ED1, but (b) enhanced ED2, (c) increased CD206, (d) enhanced CD36, and (e) increased CD14 in ZFs. Bars represent means ± SEM; n = 4 rats per group (*p<0.01 versus all groups; #p<0.01 versus all groups).

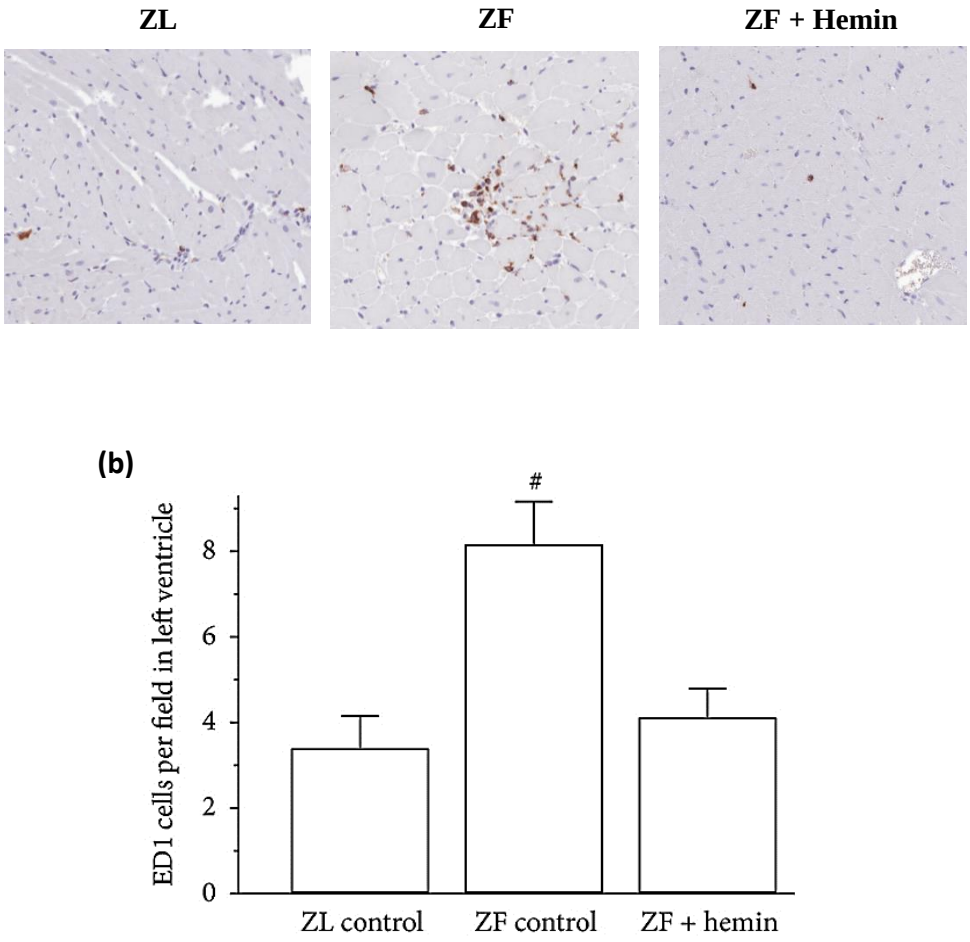

Figure 3-4: (a) Representative photomicrographs of cross-sections of the left-ventricle showing macrophage infiltration (ED1-positive cells stained dark brown) (magnification ×200). (b) Quantitative analyses of macrophage infiltration per field indicating that in ZFs the number of ED1-positive dark-brown cells (macrophage infiltration) was markedly elevated as compared to ZL control but interestingly was significantly attenuated by hemin therapy. Bars represent means ± SEM; n = 6 rats per group ($^{\#}p<0.01$ versus all groups).

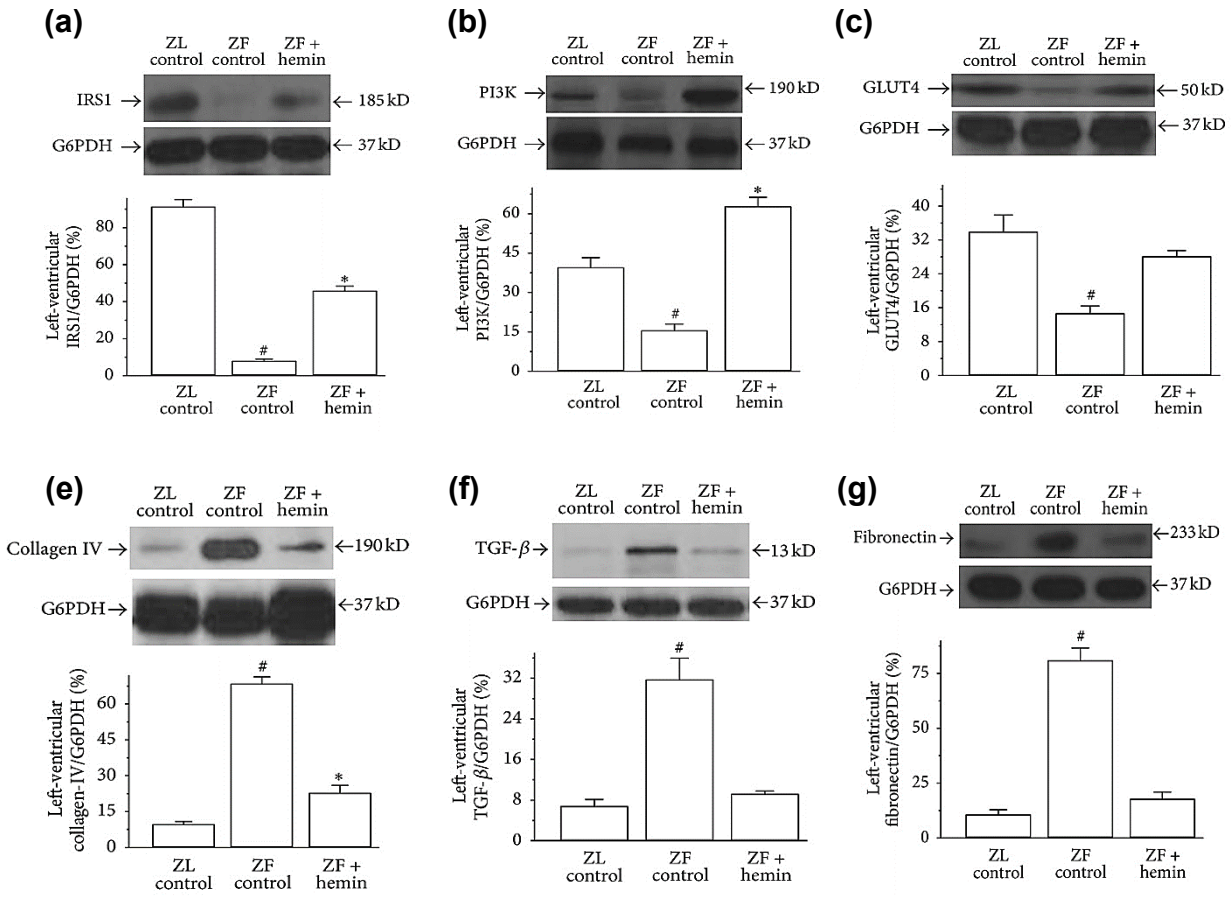

Figure 3-5: Effects of hemin on the expression of important proteins of the insulin signal transduction pathway such as IRS-1, PI3K, GLUT4, and the expression of profibrotic/extracellular matrix proteins including collagen-IV, TGF-β, and fibronectin in left-ventricular tissue from ZLs and ZFs. Representative Western immunoblotting and relative densitometry of the expressed proteins normalized by G6PDH indicates that hemin therapy significantly (a) enhanced IRS-1, (b) increased PI3K, (c) upregulated GLUT4, but (d) abated collagen-IV, (e) reduced TGF-β, and (f) suppressed fibronectin in ZFs. Bars represent means ± SEM; n = 4 rats per group (*$p<0.01$ versus all groups; $^{\#}p<0.01$ versus all groups).

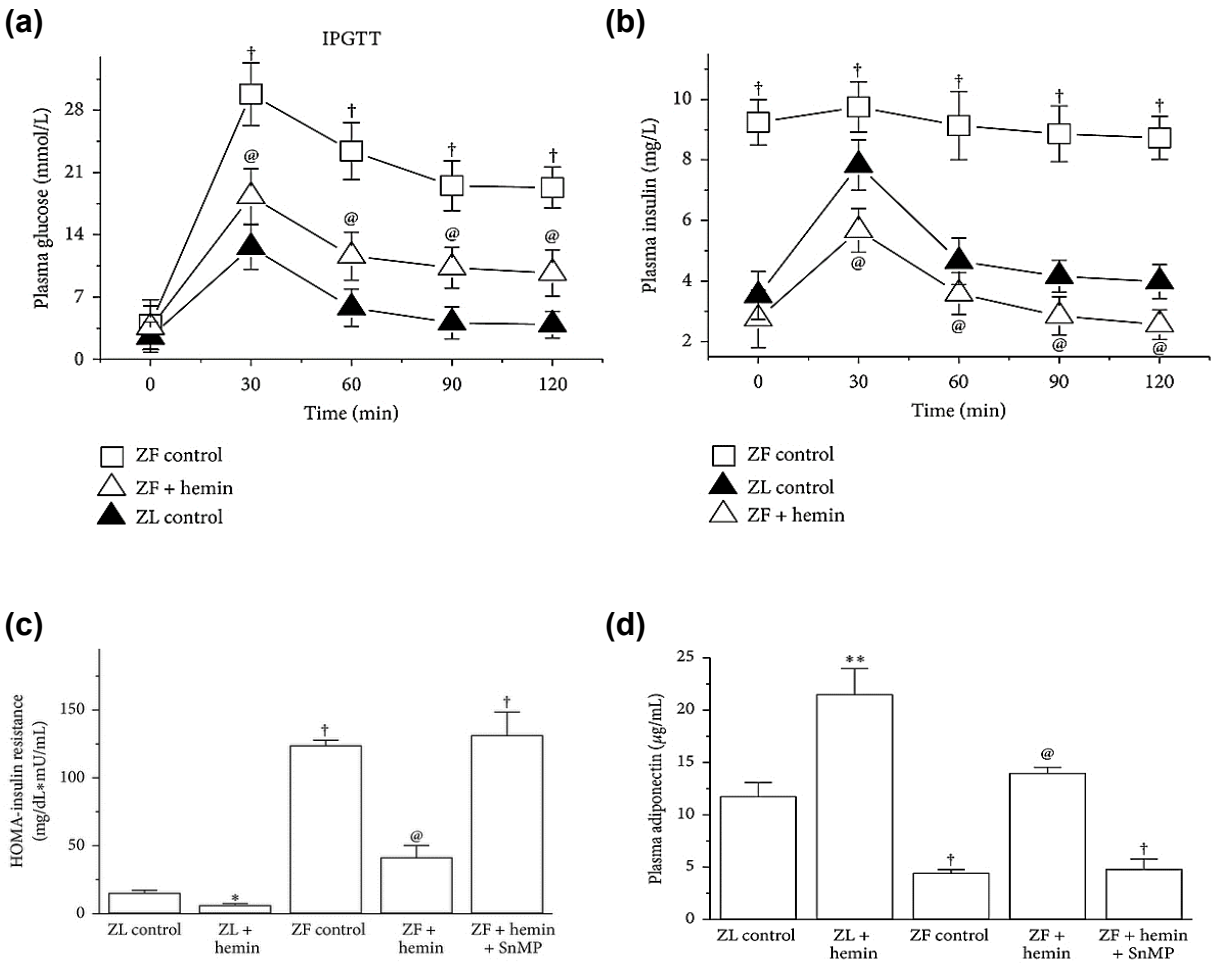

Figure 3-6: Effects of hemin on glucose tolerance, insulin resistance (HOMA-IR index), and adiponectin. Hemin therapy (a) improved glucose tolerance (IPGTT), (b) increased glucose-stimulated insulin release, (c) reduced insulin resistance, and (d) increased adiponectin. Bars represent means ± SEM; n = 6 rats per group (*p<0.05, **p<0.01 versus ZL control; †p<0.01 versus ZL control; $^{@}$p<0.01 versus ZF + hemin + SnMP or ZF control).

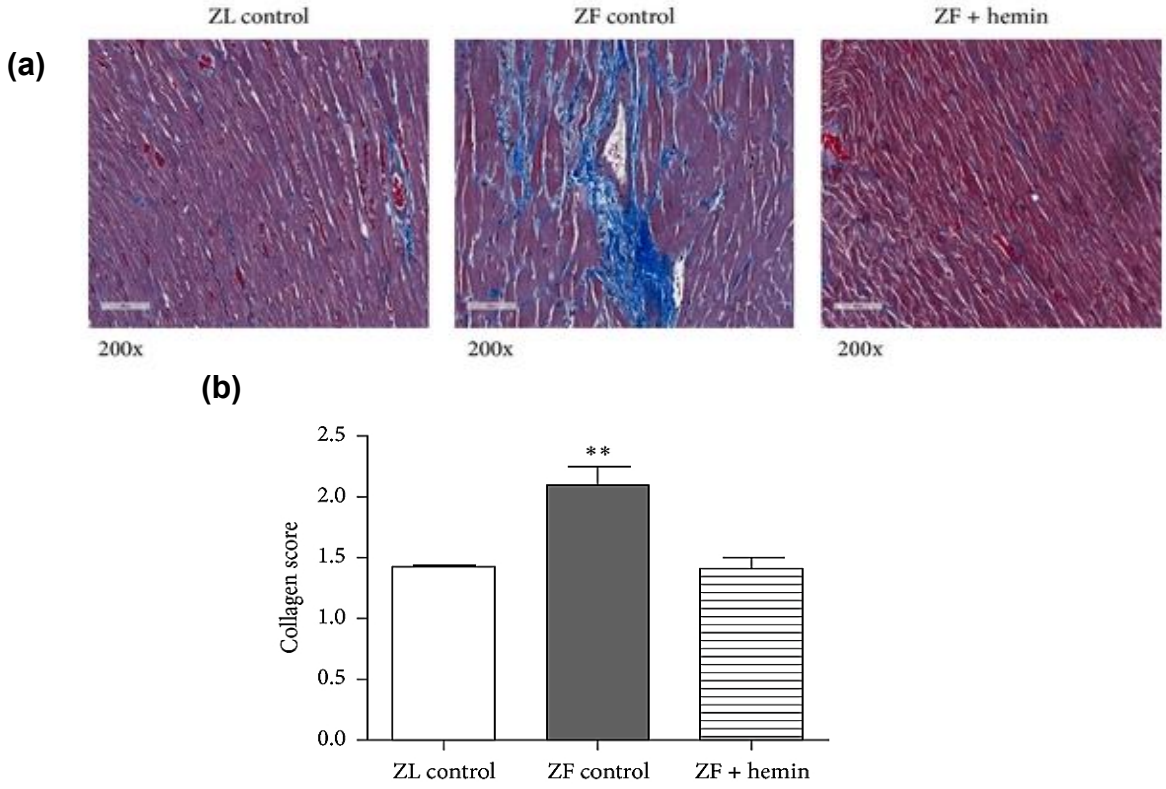
(a)
ZL control
ZF control
ZF + hemin
200x
200x
200x
(b)
Collagen score
2.5
2.0
1.5
1.0
0.5
0.0
**
ZL control
ZF control
ZF + hemin
(c)
ZL control
ZF control
ZF + hemin
200x
200x
200x
(d)
Myocytes thickness (μm)
30
20
10
0
*
ZL control
ZF control
ZF + hemin

Figure 3-7: Effect of hemin on histological lesions in the left ventricle of ZLs and ZFs. (a) Representative Mason's trichrome-stained images revealing severe cardiac muscle scaring and collagen deposition in ZFs. (b) Semi-quantitative evaluation showed that hemin therapy reduced collagen deposition in ZFs. (c) Representative hematoxylin and eosin-stained images revealing severe longitudinal muscle-fiber thickness in ZFs. (d) Quantitative evaluation showed that hemin reduced longitudinal muscle-fiber thickness. ± SEM; n = 6 rats per group (*p<0.05, **p<0.01 versus all groups).

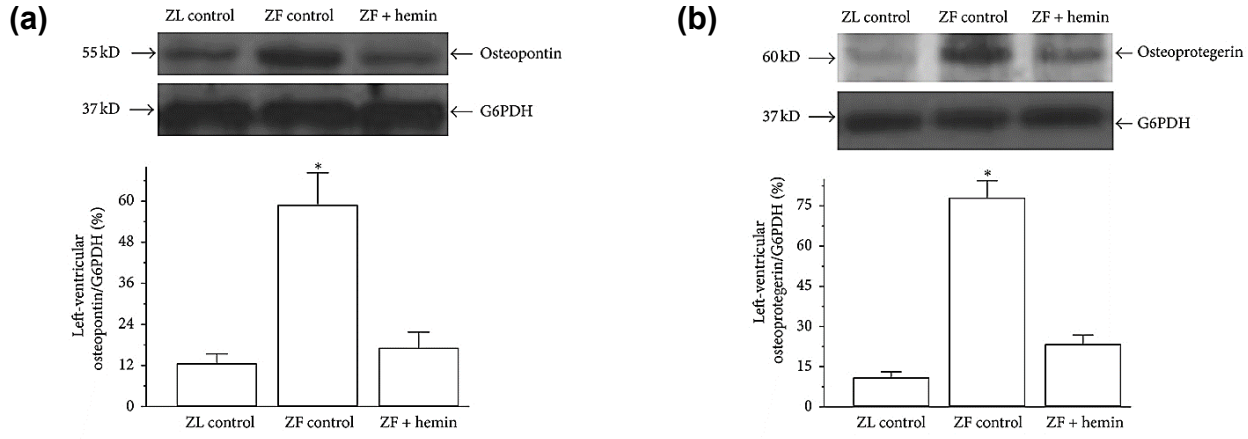

Figure 3-8: Effect of hemin on markers of heart failure such as osteopontin and osteoprotogerin in the left ventricle of ZLs and ZFs. Representative Western immunoblotting and relative densitometry of the expressed proteins normalized by G6PDH indicates that hemin therapy significantly (a) abated osteopontin and (b) reduced osteoprotogerin in ZFs. Bars represent means ± SEM; n = 4 rats per group (*p<0.01 versus all groups).

3.7 References

1. V. S. Malik, W. C. Willett, and F. B. Hu, “Global obesity: trends, risk factors and policy implications,” Nature Reviews Endocrinology, vol. 9, no. 1, pp. 13-27, 2013.

2. J. C. Han, D. A. Lawlor, and S. Y. Kimm, “Childhood obesity,” The Lancet, vol. 375, no. 9727, pp. 1737-1748, 2010.

3. S. Tiwari and J. F. Ndisang, “The role of obesity in cardiomyopathy and nephropathy,” Current Pharmaceutical Design. In press.

4. B. Mittendorfer and L. R. Peterson, “Cardiovascular consequences of obesity and targets for treatment,” Drug Discovery Today, vol. 5, no. 1, pp. 53-61, 2008.

5. J. F. Ndisang and R. Wang, “Novel therapeutic strategies for impaired endothelium-dependent vascular relaxation,” Expert Opinion on Therapeutic Patents, vol. 12, no. 8, pp. 1237-1247, 2002.

6. M. Bluher, “Are there still healthy obese patients?” Current Opinion in Endocrinology, Diabetes and Obesity, vol. 19, no. 5, pp. 341-346, 2012.

7. C. den Engelsen, K. J. Gorter, P. L. Salom´e, and G. E. Rutten, “Development of metabolic syndrome components in adults with a healthy obese phenotype: a three-year follow-up,” Obesity, vol. 21, no. 5, pp. 1025-1030, 2013.

8. Y. Hirata, M. Tabata, H. Kurobe et al., “Coronary atherosclerosis is associated with macrophage polarization in epicardial adipose tissue,” Journal of the American College of Cardiology, vol. 58, no. 3, pp. 248-255, 2011.

9. S. Gordon, “Alternative activation of macrophages,” Nature Reviews Immunology, vol. 3, no. 1, pp. 23-35, 2003.

10. S. Lallukka, K. Sevastianova, J. Perttila et al., “Adipose tissue is inflamed in NAFLD due to obesity but not in NAFLD due to genetic variation in PNPLA3,” Diabetologia, vol. 56, no. 4, pp. 886-892, 2013.

11. M. Neumeier, S. Bauer, H. Br¨uhl et al., “Adiponectin stimulates release of CCL2, -3, -4 and -5 while the surface abundance of CCR2 and -5 is simultaneously reduced in primary human monocytes,” Cytokine, vol. 56, no. 3, pp. 573-580, 2011.

12. J. F. Ndisang, “Role of heme oxygenase in inflammation, insulin-signalling, diabetes and obesity,” Mediators of Inflammation, vol. 2010, Article ID 359732, 18 pages, 2010.

13. A. Jadhav, S. Tiwari, P. Lee, and J. F. Ndisang, “The heme oxygenase system selectively enhances the anti-inflammatory macrophage-m2 phenotype, reduces pericardial adiposity, and ameliorated cardiac injury in diabetic cardiomyopathy in Zucker Diabetic Fatty rats,” Journal of Pharmacology and Experimental Therapeutics, vol. 345, no. 2, pp. 239-249, 2013.

14. M. Rosenberg, C. Zugck, M. Nelles et al., “Osteopontin, a new prognostic biomarker in patients with chronic heart failure,” Circulation, vol. 1, no. 1, pp. 43-49, 2008.

15. T. Ueland, C. P. Dahl, J. Kjekshus et al., “Osteoprotegerin predicts progression of chronic heart failure: results from CORONA,” Circulation, vol. 4, no. 2, pp. 145-152, 2011.

16. M. Zeyda, K. Gollinger, J. Todoric et al., “Osteopontin is an activator of human adipose tissue macrophages and directly affects adipocyte function,” Endocrinology, vol. 152, no. 6, pp. 2219-2227, 2011.

17. E. S. Oh, E.-J. Rhee, K.W. Oh et al., “Circulating osteoprotegerin levels are associated with age, waist-to-hip ratio, serum total cholesterol, and low-density lipoprotein cholesterol levels in healthy Korean women,” Metabolism, vol. 54, no. 1, pp. 49-54, 2005.

18. M. Keophiphath, V. Achard, C. Henegar, C. Rouault, K. Cl´ement, and D. L. Lacasa, “Macrophage-secreted factors promote a profibrotic phenotype in human preadipocytes,” Molecular Endocrinology, vol. 23, no. 1, pp. 11-24, 2009.

19. H. J. Duckers, M. Boehm, A. L. True et al., “Heme oxygenase-1 protects against vascular constriction and proliferation,” Nature Medicine, vol. 7, no. 6, pp. 693-698, 2001.

20. M. Mishra and J. F. Ndisang, “A critical and comprehensive insight on heme oxygenase and related products including carbon monoxide, bilirubin, biliverdin and ferritin in type-1 and type-2 diabetes,” Current Pharmaceutical Design. In press.

21. S. Tiwari and J. F. Ndisang, “The Heme oxygenase system and type-1 diabetes,” Current Pharmaceutical Design. In press.

22. S. Tiwari and J. F. Ndisang, “Heme oxygenase system and hypertension: a comprehensive insight,” Current Pharmaceutical Design. In press.

23. J. F. Ndisang, N. Lane, N. Syed, and A. Jadhav, “Up-regulating the heme oxygenase system with hemin improves insulin sensitivity and glucose metabolism in adult spontaneously hypertensive rats,” Endocrinology, vol. 151, no. 2, pp. 549-560, 2010.

24. J. F. Ndisang, “The Heme oxygenase system selectively modulates proteins implicated in metabolism, oxidative stress and inflammation in spontaneously hypertensive rats,” Current Pharmaceutical Design. In press.

25. J. F. Ndisang and A. Jadhav, “Upregulating the Heme oxygenase system suppresses left ventricular hypertrophy in adult spontaneously hypertensive rats for 3 months,” Journal of Cardiac Failure, vol. 15, no. 7, pp. 616-628, 2009.

26. J. F. Ndisang, N. Lane, and A. Jadhav, “Upregulation of the heme oxygenase system ameliorates postprandial and fasting hyperglycemia in type 2 diabetes,” The American Journal of Physiology, vol. 296, no. 5, pp. E1029-E1041, 2009.

27. J. F. Ndisang and R. Wang, “Age-related alterations in soluble guanylyl cyclase and cGMP pathway in spontaneously hypertensive rats,” Journal of Hypertension, vol. 21, no. 6, pp. 1117-1124, 2003.

28. J. F. Ndisang, H. E. N. Tabien, and R. Wang, “Carbon monoxide and hypertension,” Journal of Hypertension, vol. 22, no. 6, pp. 1057-1074, 2004.

29. I. G. Poornima, P. Parikh, and R. P. Shannon, “Diabetic cardiomyopathy: the search for a unifying hypothesis,” Circulation Research, vol. 98, no. 5, pp. 596-605, 2006.

30. J. F. Ndisang, N. Lane, and A. Jadhav, “The heme oxygenase system abates hyperglycemia in zucker diabetic fatty rats by potentiating insulin-sensitizing pathways,” Endocrinology, vol.150, no. 5, pp. 2098-2108, 2009.

31. J. F. Ndisang and A. Jadhav, “Hemin therapy suppresses inflammation and retroperitoneal adipocyte hypertrophy to improve glucose metabolism in obese rats co-morbid with insulin resistant type-2 diabetes,” Diabetes, Obesity and Metabolism, vol.15, no. 11, pp. 1029-1039, 2013.

32. A. Jadhav, E. Torlakovic, and J. F. Ndisang, “Interaction among heme oxygenase, nuclear factor-κB, and transcription activating factors in cardiac hypertrophy in hypertension,” Hypertension, vol. 52, no. 5, pp. 910-917, 2008.

33. J. F. Ndisang and M. Mishra, “The Heme oxygenase system selectively suppresses the proinflammatory macrophage M1 phenotype and potentiates insulin signaling in spontaneously hypertensive rats,” The American Journal of Hypertension, vol. 26, no. 9, pp. 1123-1131, 2013.

34. J. F. Ndisang and A. Jadhav, “Hemin therapy improves kidney function in male streptozotocin-induced diabetic rats: role of the heme oxygenase/atrial-natriuretic peptide/adiponectin axis,” Endocrinology. In press.

35. A. Jadhav and J. F. Ndisang, “Treatment with heme arginate alleviates adipose tissue inflammation and improves insulin sensitivity and glucose metabolism in a rat model of Human primary aldosteronism,” Free Radical Biology and Medicine, vol. 53, no. 12, pp. 2277-2286, 2012.

36. A. Jadhav, E. Torlakovic, and J. F. Ndisang, “Hemin therapy attenuates kidney injury in deoxycorticosterone acetate-salt hypertensive rats,” The American Journal of Physiology, vol. 296, no. 3, pp. F521-F534, 2009.

37. H. Mos´en, A. Salehi, P. Almet al., “Defective glucose-stimulated insulin release in the diabetic Goto-Kakizaki (GK) rat coincides with reduced activity of the islet carbon monoxide signaling pathway,” Endocrinology, vol. 146, no. 3, pp. 1553-1558, 2005.

38. M. L. Muiesan, M. Salvetti, C. Monteduro et al., “Left ventricular concentric geometry during treatment adversely affects cardiovascular prognosis in hypertensive patients,” Hypertension, vol.43, no. 4, pp. 731-738, 2004.

39. M. Fukunaga, T. Yura, and K. F. Badr, “Stimulatory effect of 8-Epi-PGF(2α), an F2-isoprostane, on endothelin-1 release,” Journal of Cardiovascular Pharmacology, vol. 26, supplement 3, pp. S51-S52, 1995.

40. N. Delanty, M. P. Reilly, D. Pratico et al., “8-epi PGF(2α) generation during coronary reperfusion: a potential quantitative marker of oxidant stress in vivo,” Circulation, vol. 95, no. 11, pp. 2492-2499, 1997.

41. M. Piechota, M. Banach, R. Irzma´nski et al., “N-terminal brain natriuretic propeptide levels correlate with procalcitonin and C reactive protein levels in septic patients,” Cellular and Molecular Biology Letters, vol. 12, no. 2, pp. 162-175, 2007.

42. K. Aki, A. Shimizu, Y. Masuda et al., “ANG II receptor blockade enhances anti-inflammatory macrophages in anti-glomerular basement membrane glomerulonephritis,” The American Journal of Physiology, vol. 298, no. 4, pp. F870-F882, 2010.

43. A. Anzai, T. Anzai, S. Nagai et al., “Regulatory role of dendritic cells in postinfarction healing and left ventricular remodeling,” Circulation, vol. 125, no. 10, pp. 1234-1245, 2012.

44. M. Heusinkveld, P. J. de vos van Steenwijk, R. Goedemans et al., “M2 macrophages induced by prostaglandin E2 and IL-6 from cervical carcinoma are switched to activated M1 macrophages by CD4+ Th1 cells,” Journal of Immunology, vol. 187, no. 3, pp. 1157-1165, 2011.

45. A. Bhattacharjee, S. Pal, G. M. Feldman, and M. K. Cathcart, “Hck is a key regulator of gene expression in alternatively activated human monocytes,” Journal of Biological Chemistry, vol. 286, no. 42, pp. 36709-36723, 2011.

46. S. Gibbings, N. D. Elkins, H. Fitzgerald et al., “Xanthine oxidoreductase promotes the inflammatory state of mononuclear phagocytes through effects on chemokine expression, peroxisome proliferator-activated receptor-γ sumoylation, and HIF-1α,” Journal of Biological Chemistry, vol. 286, no. 2, pp. 961-975, 2011.

47. G. A. Rosito, J. M. Massaro, U. Hoffmann et al., "Pericardial fat, visceral abdominal fat, cardiovascular disease risk factors, and vascular calcification in a community-based sample the framingham heart study," Circulation, vol. 117, no. 5, pp. 605-613, 2008.

48. H. Sell, C. Habich, and J. Eckel, "Adaptive immunity in obesity and insulin resistance," Nature Reviews, vol. 8, no. 12, pp. 709-716, 2012.

49. P. Li, D. Wang, J. Lucas et al., "Atrial natriuretic peptide inhibits transforming growth factor β-induced Smad signaling and myofibroblast transformation in mouse cardiac fibroblasts," Circulation Research, vol. 102, no. 2, pp. 185-192, 2008.

50. F. Fang, L. Liu, Y. Yang et al., "The adipokine adiponectin has potent anti-fibrotic effects mediated via adenosine monophosphate-activated protein kinase: novel target for fibrosis therapy," Arthritis Research and Therapy, vol. 14, no. 5, article R229, 2012.

51. M. Dobaczewski, C. Gonzalez-Quesada, and N. G. Frangogiannis, "The extracellular matrix as a modulator of the inflammatory and reparative response following myocardial infarction," Journal of Molecular and Cellular Cardiology, vol. 48, no. 3, pp. 504-511, 2010.

52. E. J. Folco, V. Z. Rocha, M. L´opez-Ilasaca, and P. Libby, "Adiponectin inhibits pro-inflammatory signaling in human macrophages independent of interleukin-10," Journal of Biological Chemistry, vol. 284, no. 38, pp. 25569-25575, 2009.

53. K. Robinson, J. Prins, and B. Venkatesh, "Clinical review: adiponectin biology and its role in inflammation and critical illness," Critical Care, vol. 15, no. 2 article 221, 2011.

54. T. A. McKinsey and E. N. Olson, "Toward transcriptional therapies for the failing heart: chemical screens to modulate genes," Journal of Clinical Investigation, vol. 115, no. 3, pp. 538-546, 2005.

55. M. Konishi, S. Sugiyama, Y. Sato et al., "Pericardial fat inflammation correlates with coronary artery disease," Atherosclerosis, vol. 213, no. 2, pp. 649-655, 2010.

56. M. O. Al Chekakie, C. C. Welles, R. Metoyer et al., "Pericardial fat is independently associated with human atrial fibrillation," Journal of the American College of Cardiology, vol. 56, no. 10, pp.784-788, 2010.

57. J. Ren, M. Yang, G. Qi et al., "Proinflammatory protein CARD9 is essential for infiltration of monocytic fibroblast precursors and cardiac fibrosis caused by angiotensin II infusion," The American Journal of Hypertension, vol. 24, no. 6, pp. 701-707, 2011.

58. X. Shi-Wen, L. Kennedy, E. A. Renzoni et al., "Endothelin is a downstream mediator of profibrotic responses to transforming growth factor β in human lung fibroblasts," Arthritis and Rheumatism, vol. 56, no. 12, pp. 4189-4194, 2007.

59. C. Moro, E. Klimcakova, K. Lolm`ede et al., “Atrial natriuretic peptide inhibits the production of adipokines and cytokines linked to inflammation and insulin resistance in human subcutaneous adipose tissue,” Diabetologia, vol. 50, no. 5, pp. 1038-1047, 2007.

60. Y. Chien, Y.-H. Lai, C. F. Kwok, and L.-T. Ho, “Endothelin-1 suppresses long-chain fatty acid uptake and glucose uptake via distinct mechanisms in 3T3-L1 adipocytes,” Obesity, vol. 19, no.1, pp. 6-12, 2011.

61. O. Tsukamoto, M. Fujita, M. Kato et al., “Natriuretic peptides enhance the production of adiponectin in human adipocytes and in patients with chronic heart failure,” Journal of the American College of Cardiology, vol. 53, no. 22, pp. 2070-2077, 2009.

62. K. N. Pandey, “Biology of natriuretic peptides and their receptors,” Peptides, vol. 26, no. 6, pp. 901-932, 2005.

63. R. Riba, B. Patel, A. Aburima, and K. M. Naseem, “Globular adiponectin increases cGMP formation in blood platelets independently of nitric oxide,” Journal of Thrombosis and Haemostasis, vol. 6, no. 12, pp. 2121-2131, 2008.

64. A. K. Kiemer, N. Bildner, N. C. Weber, and A. M. Vollmar, “Characterization of heme oxygenase 1 (heat shock protein 32) induction by atrial natriuretic peptide in human endothelial cells,” Endocrinology, vol. 144, no. 3, pp. 802-812, 2003.

65. T. Polte, A. Hemmerle, G. Berndt, N. Grosser, A. Abate, and H. Schr¨oder, “Atrial natriuretic peptide reduces cyclosporin toxicity in renal cells: role of cGMP and heme oxygenase-1,” Free Radical Biology and Medicine, vol. 32, no. 1, pp. 56-63, 2002.

66. J. F. Ndisang and A. Jadhav, “Heme arginate therapy enhanced adiponectin and atrial natriuretic peptide, but abated endothelin-1 with attenuation of kidney histopathological lesions in mineralocorticoid-induced hypertension,” Journal of Pharmacology and Experimental Therapeutics, vol. 334, no. 1, pp. 87-98, 2010.

67. J. Liu, C. S. Fox, D. A. Hickson et al., “Pericardial fat and echocardiographic measures of cardiac abnormalities: the Jackson heart study,” Diabetes Care, vol. 34, no. 2, pp. 341-346, 2011.

CHAPTER 4

The heme oxygenase system rescues hepatic deterioration in the condition of obesity co-morbid with type-2 Diabetes

Tatiana Ntube Salley, Manish Mishra, Shuchita Tiwari, Ashok Jadhav,

Joseph Fomusi Ndisang

This chapter has been published as a research paper in

PLOS ONE, November 2013, Volume 8, Issue 11, e79270

Contribution: The article, ***PLoS One. 2013****;8(11): e79270,* was co-authored with Tatiana Ntube Salley, Shuchita Tiwari, Ashok Jadhav and my supervisor Joseph Fomusi Ndisang. This chapter describes the effects of hemin-induced HO system on obesity-induced inflammation and associated hepatic deterioration in an obese rat model of T2D. This study collectively suggested that increasing obesity is a deterministic factor for development of non-alcoholic fatty liver disease in obese diabetic subjects that severely affect hepatic architecture. In this condition, the cytoprotective effects of upregulated HO system can be explored to counteract against these tissue comorbidities. In this study, I performed the animal and biochemical experiments and statistical analyses along with other co-authors. The idea of this study was conceived by my supervisor Joseph Fomusi Ndisang and was financially supported by the Heart and Stroke Foundation of Saskatchewan, Canada grant to Dr. Ndisang.

4.1 Abstract

The prevalence of non-alcoholic fatty-liver disease (NAFLD) is increasing globally. NAFLD is a spectrum of related liver diseases that progressive from simple steatosis to serious complications like cirrhosis. The major pathophysiological driving of NAFLD includes elevated hepatic adiposity, increased hepatic triglycerides/cholesterol, excessive hepatic inflammation, and hepatocyte ballooning injury is a common histo-pathological denominator. Although, heme-oxygenase (HO) is cytoprotective, its effects on hepatocyte ballooning injury have not been reported. We investigated the effects of upregulating HO with hemin or inhibiting it with stannous-mesoporphyrin (SnMP) on hepatocyte ballooning injury, hepatic adiposity and inflammation in Zucker diabetic fatty rats (ZDFs), an obese type-2-diabetic model. Hemin administration to ZDFs abated hepatic/plasma triglycerides and cholesterol, and suppressed several pro-inflammatory cytokines and chemokines including, TNF-α, IL-6, IL-1β, macrophage-inflammatory-protein-1α (MIP-1α) and macrophage-chemoattractant-protein-1 (MCP-1), with corresponding reduction of the pro-inflammatory M1-phenotype marker, ED1 and hepatic macrophage infiltration. Correspondingly, hemin concomitantly potentiated the protein expression of several markers of the anti-inflammatory macrophage-M2-phenotype including ED2, IL-10 and CD206, alongside components of the HO-system including HO-1, HO-activity and cGMP, whereas the HO-inhibitor, SnMP abolished the effects. Furthermore, hemin attenuated liver histo-pathological lesions like hepatocyte ballooning injury and fibrosis, and reduced extracellular-matrix/profibrotic proteins implicated in liver injury such as osteopontin, TGF-β1, fibronectin and collagen-IV. We conclude that hemin restore hepatic morphology by abating hepatic adiposity, suppressing macrophage infiltration, inflammation and fibrosis. The selective enhancement of anti-inflammatory macrophage-M2-phenotype with parallel reduction of pro-inflammatory macrophage M1-

phenotype and related chemokines/cytokines like TNF-α, IL-6, IL-1β, MIP-1α and MCP-1 are among the multifaceted mechanisms by which hemin restore hepatic morphology.

4.2 Introduction

Obesity is associated with many health complications including, type-2 diabetes, hyperlipidemia, dyslipidemia, hypertension and non-alcoholic fatty liver disease (NAFLD) (1-6). NAFLD is a wide spectrum of related liver diseases that progressive from simple a condition like steatosis to a more serious complication like cirrhosis, and elevated hepatic adiposity, high levels of hepatic triglycerides and hepatic cholesterol and hepatocyte ballooning injury are common denominators of NAFLD (1-5), (7-9). Besides hepatic adiposity, inflammation is crucial in the pathogenesis of NAFLD. Elevated levels of pro-inflammatory cytokines such as tumor necrosis factor (TNF-α), interleukin (IL)-6, IL-1β are amongst the pathophysiological driving force of NAFLD (10, 11). Similarly, pro-inflammatory chemokines such as macrophage-inflammatory-protein-1 alpha (MIP-1α) and macrophage-chemoattractant-protein-1 (MCP-1) are known to trigger macrophage infiltration to accentuate hepatic inflammatory insults (12, 13) and compromise hepatic morphology and function. Generally, two common forms of macrophages have been described (14, 15). These include the pro-inflammatory macrophage M1-phenotype that is stimulated by cytokines and chemokines like TNF-α, IL-6, IL-1β, MIP-1α and MCP-1 (16, 17) and the anti-inflammatory M2-phenotype that is associated with IL-10 (18-20). Therefore, substances capable of selectively modulating the polarization of macrophages towards the anti-inflammatory M2-phenotype and concomitantly reducing the pro-inflammatory M1-phenotype and its related secretagogues like TNF-α, IL-6, IL-1β, MIP-1α, MCP-1 and abates excessive

hepatic triglycerides and hepatic cholesterol may suppress and/or retard the progression of NAFLD to more severe conditions like hepatic cirrhosis.

Fatty liver contributes significantly to obesity-related morbidity and mortality (21-23). Pharmacological agents that can rescue the liver from lipotoxicity by restoring adipose tissue insulin sensitivity or preventing activation of inflammatory and oxidative insults hold promise in the treatment and management of NAFLD, although, their long-term safety and efficacy remains to be clearly established (24). The soaring prevalence of NAFLD necessitates the development of new therapeutic modalities to improve and possibly reverse the clinical symptoms of NAFLD. An interesting physiological enzyme that could be explored in this regard is heme-oxygenase (HO). HO is a microsomal enzyme with two active isoforms HO-1 (inducible) and HO-2 (constitutive), while the third isoform, HO-3 is a pseudo-transcript of HO-2 without catalytic activity (14). The HO-system can be pharmacologically enhanced to modulate physiological functions and combat adversity in tissue (14), (25-27). Although, emerging evidence indicates that an upregulated HO-system is capable of suppressing visceral adiposity (28-29), however, the effect of the HO-system on hepatic adiposity has not been reported. More-importantly, the role of the HO system on hepatocyte ballooning injury has not been reported. Similarly, the pathophysiology of hepatocyte ballooning injury in Zucker diabetic fatty rats (ZDFs), a model characterized by obesity and type-2 diabetes, with aberrant hepatic response to insulin (30) and impaired hepatic lipid metabolism (31) remains largely unclear. Furthermore, the role of the HO-system on macrophage M1/M2-phenotype in hepatic tissue from ZDFs has not been reported. Understanding the pathophysiological perturbations that accompanies hepatic impairment would have important implications for the prevention and treatment of diseases associated with fatty liver.

Therefore, this study will examine the effects of the HO-system on the pathophysiology of hepatocyte ballooning, macrophage M1/M2-phenotypes and related cytokines and chemokines such as TNF-α, IL-6, IL-1β, MIP-1α and MCP-1α, IL-10 in the liver of ZDFs. In addition, the effects of hemin therapy on extracellular-matrix/profibrotic proteins implicated in hepatic injury like osteopontin, transforming growth factor-beta (TGF-β1), fibronectin and collagen-IV (32-36) were examined.

4.3 Materials and methods

4.3.1 Animals and treatment groups

Our experimental protocol was approved by the Animal Care and Research Ethics Committee of University of Saskatchewan, which is in conformity with the Guide for Care and Use of Laboratory Animals by the Canadian Council on Animal Care and the National Institutes of Health (NIH Publication No. 85-23, revised 1996). Male ZDFs of twelve weeks and age/sex-matched Zucker-lean (ZL) littermates were bought from Charles River (Willington, MA, USA), and housed at 21°C with 12-hour light/dark cycles, fed with Purina 5008 diet and had access to drinking water *ad libitum*. The animals were allowed to accommodate for two weeks. At 14 weeks of age, the animals were randomly assigned to the following experimental groups (n = 6 per group): (A) controls (ZDF and ZL), (B) hemin-treated ZDF and ZL, (C) ZDF + hemin + SnMP, (D) ZDF + SnMP, and (E) ZDF + vehicle dissolving hemin and SnMP. The HO-inducer, hemin (Sigma, St Louis, MO) was administered twice weekly for a duration of eight weeks at a dose of 30 mg/kg intraperitoneally, while the HO-inhibitor, stannous-mesoporphyrin (SnMP, Porphyrin Products, Logan, UT) was given at a dose of (2 mg/100 g body weight) by intraperitoneal injection twice weekly for 8 weeks as we previously reported (29). During the treatment period body weight and glucose levels were determined on a weekly routine after 6 hrs

of fasting in metabolic cages using glucose-meter (BD, Franklin Lakes, NJ, USA). The experiments were terminated at the end of the 8-week treatment period, and the age of the animals was 22 weeks. Before killing, the animals were weighed and anaesthetized with pentobarbital sodium (50 mg/kg i.p.), and when the animals were fully unconscious blood was obtained by cardiac puncture. Subsequently, an incision was made in the peritoneum and the liver was carefully isolated, cleaned in ice-cold phosphate-buffered saline and weighed using an analytical balance (Precisa Instruments Ltd, Switzerland) as previously reported (37-39). The liver and plasma were used for biochemical assays.

4.3.2 Histological, morphological and immunohistochemical analysis of liver tissue

Histological and morphometric studies were done as we previously reported (28). Liver sections of 5 μm were cut and treated with Masson's trichrome staining to assess collagen deposition and hepatocyte ballooning injury using a microscope (Aperio Scan Scope, Model CS, Aperio Technology Inc, CA). Morphologic assessment of hepatocyte ballooning injury was done by a blinded researcher using a microscope (Aperio Scan Scope, Model CS, Aperio Technology Inc, CA), and analyzed using Aperio Image Scope V11.2.0.780 software (Aperio, e-Pathology Solution, CA). Liver sections were magnified at 200X, and 20 random snaps shots were taken per slide for each experimental group of 4-6 animals (80-120 images per group). The images were scored semi-quantitatively by a blinded researcher as we previously reported (28, 29).

Immunohistochemistry was done as we previously reported (40). Sections of 5 μm of whole liver sections were treated with bovine serum albumin in phosphate buffered saline to block non-specific staining and incubated overnight with ED1 antibody (1:500 dilution, Santa Cruz Biotechnology, CA). Subsequently, the liver sections were incubated with goat anti-mouse IgG

for 30 minutes (1:200 dilution; Jackson ImmunoResearch Laboratories, Inc., ME, USA). Immunohistochemical staining was done using the standard avidin-biotin complex method with the chromagen 3,3′-diaminobenzidine (DAB) at the final detection step. The liver sections were scanned using a virtual microscope (Aperio Scan Scope, Model CS, Aperio Technology Inc, CA). Macrophages (brown from immune-stained sections) were quantified by a blinded researcher by manually counting the positively-stained ED1 cells under 200 X magnification in 15 randomized non-overlapping fields, and only distinct ED1-stained cells from all experimental groups were taken into consideration.

4.3.3 Determination of HO activity and HO-1 concentration

Liver HO activity was measured as bilirubin production using our established method (41-43). The amount of bilirubin in each sample was determined spectrophotometrically (extinction coefficient for bilirubin 40 $mM^{-1}cm^{-1}$), and expressed as nmole/mg protein/hour. Hepatic HO-1 concentration was determined using enzyme-linked immunosorbent assay (ELISA, Stressgen-Assay Design, Ann Arbor, MI, USA) as we previously reported (41-43).

4.3.4 Measurement of TNF-α, IL-6 and IL-1β

The levels of TNF-α, IL-6 and IL-1β in the liver was assessed by using ELISA kits (Immuno-Biological Laboratories Co Ltd, Takasaki-shi, Gunma, Japan) following to the manufacturer's instructions and read at 450 nm in a plate reader (SpectraMax 340PC, Molecular Device, CA, USA) as we previously reported (29).

4.3.5 Western immunoblotting

The liver was homogenized (1:10, w:v) in 10 mM Tris-buffered saline (20 mM Tris-HCl, pH 7.4, 0.25 M sucrose, and 1 mM EDTA) in the presence of a cocktail of protease inhibitors, centrifuged, and proteins extracted and quantified as we previously reported (44, 45). Aliquots of 50 µg of proteins were loaded on SDS-polyacrylamide gel, and the fractionated proteins were electrophoretically transferred to nitrocellulose paper. Non-specific bindings were blocked with 3% non-fat milk, and incubated overnight with primary antibodies against ED1, ED2, CD206, IL-10, TGF-β1/2/3, collagen-IV, fibronectin and osteopontin (Santa Cruz Biotechnology, CA, USA). Anti-mouse Beta-actin (Sigma St Louis, MO, USA) was used as control to ascertain equivalent loading. After washing, blots were incubated with anti-rabbit IgG conjugated to horseradish peroxide (Bio-Rad, CA, USA), and the immuno-reactivity visualized using enhanced horseradish peroxide/luminol chemiluminescence reagent (Perkin Elmer Life Sciences, Boston, MA, USA). Densitometric analysis was done with UN-SCAN-IT software (Silk Scientific, Utah, USA).

4.3.6 Determination of cGMP

The concentration of cGMP in the liver determined using an enzyme-immunoassay kit (Cayman Chemical, Ann Arbor, MI, USA) as previously described (41, 42). Briefly, homogenized liver tissue was treated with 6% trichloroacetic acid at 4°C in the presence of 3′-isobutyl-1-methylxanthine to inhibit phosphodiesterase activity. The samples were subsequently centrifuged at 2000 *g* for 15 minutes and the supernatant was recovered, washed with water-saturated diethyl ether and the upper ether layer aspired and discarded while the aqueous layer containing cGMP was recovered and lyophilized. The dry extract was dissolved in 1-ml assay buffer and the cGMP

was assessed according to the manufacturer's instruction and expressed as picomol per mg of protein.

4.3.7 Determination of MCP-1 and MIP-1α

The concentrations of macrophage-inflammatory-protein-1-alpha (MIP-1α) and macrophage-chemoattractant-protein-1 (MCP-1) in the liver were determined using ELISA kits (OmniKine™, Assay Biotechnology Company Inc, Sunnyvale, CA). All samples were assayed in triplicates following the manufacturer's instructions.

4.3.8 Determination of triglycerides and total cholesterol

Total-cholesterol and triglycerides were measured in liver homogenates and plasma using cholesterol and triglycerides assay kits (Cayman Chemical, Ann Arbor, MI, USA) following instructions from the manufacturer.

4.3.9 Statistical analysis

All data are expressed as means ± SEM from at least four independent experiments unless otherwise stated. Statistical analyses were done using two-way ANOVA, by means of Statistical Analysis System (SAS), software, version 9.3 (SAS Institute Inc., Cary, NC, USA) and Student's *t-test*. Group differences at the level of $p<0.05$ were considered statistically significant.

4.4 Results

4.4.1 Hemin therapy potentiates the HO-system, normalized glycaemia and reduced liver hypertrophy

The administration of the HO-inducer, hemin, to ZDFs normalized glycemia (26.3 ± 2.5 vs 8.3 ± 1.4 mmol/L, $p<0.01$) and reduced liver-to-body weight ratio, an important index of liver hypertrophy (46) (54.8 ± 1.8 vs 40.7 ± 1.5 g/kg body weight, $p<0.01$) (Table 4-1). In contrast, co-administrating hemin and the HO-inhibitor, SnMP abolished the effect of hemin on liver hypertrophy (54.8 ± 1.8 vs 55.2 ± 2.3 g/kg body weight) and glycaemia (26.3 ± 2.5 vs 29.4 ± 3.7 mmol/L). On the other hand, treatment with hemin together with SnMP resulted in a slight reduction of body-weight, which was less than 10% (Table 4-1). The body-weight loss may not be due to toxicity because we recently reported that important indices of toxicity such as gamma-glutamyltransferase, plasma alanine aminotransferase and aspartate aminotransferase were within normal range (42).

Although, body-weight loss may affect glucose levels, it is unlikely in this situation because the slight loss of body-weight in hemin-treated ZDFs and hemin + SnMP-treated ZDFs were accompanied by opposing glycemic effects (Table 4-1). Accordingly, in hemin-treated ZDFs there was reduction of hyperglycemia, whereas co-administering hemin and the HO-blocker, SnMP abolished the effects of hemin on glycaemia, suggesting that the HO system may have an intrinsic anti-diabetic effect.

To further investigate the role of the HO system on hyperglycemia and liver hypertrophy, we measured important components of the HO system such as HO-1 and HO-activity in the liver. Our results indicate that in ZDF-control, the basal HO-1 and HO-activity were significantly depressed as compared to the ZL-controls (Figs. 4-1A and 4-1B). Interestingly, hemin

administration greatly enhanced the aberrant HO-1 and HO activity in ZDFs, whereas the co-administration of hemin together with the HO inhibitor, SnMP nullified the effect of hemin.

Since enhanced HO activity is accompanied by increased production of endogenous of carbon monoxide that would in turn enhance cGMP (42), we measured cGMP. Moreover, both cGMP and carbon monoxide are known to enhance glucose metabolism (47, 48). In ZDF-controls, the basal levels of cGMP were markedly reduced as compared to ZL-controls **(**Fig. 4-1C). However, treatment with hemin robustly enhanced cGMP in ZDFs (Fig. 4-1C), suggesting a role of the HO-cGMP axis in the normalization of hyperglycemia in hemin-treated ZDFs (Table 4-1). In contrast, co-administering hemin with SnMP reversed the effects of hemin.

Hemin therapy also enhanced HO-1, HO-activity and cGMP levels in ZL-controls, although, the magnitude was smaller as compared to ZDFs, suggesting greater selectivity of hemin in diseased condition. The vehicle dissolving hemin and SnMP had no effect on any of the measured parameters.

4.4.2 Hemin therapy abated the elevated basal levels of inflammatory cytokines in the liver of ZDFs

Given that elevated inflammation due to TNF-α, IL-6 and IL-1β are amongst the causative factors of liver fibrosis and liver steatosis (10), and high levels of TNF-α, IL-6 and IL-1β are known to deregulate glucose metabolism (14, 49), we measured the levels of these cytokines in the liver. Our results indicate that the basal levels of TNF-α, IL-6 and IL-1β in ZDF-controls were significantly elevated as compared to the ZL-controls (Figs. 4-2A, 4-2B and 4-2C). Interestingly, the normalization of glycaemia in hemin-treated ZDFs was accompanied by the attenuation of TNF-α, IL-6 and IL-1β, whereas co-treatment of hemin and the HO-inhibitor, SnMP, reversed the

effects of hemin (Figs. 4-2A, 4-2B and 4-2C). Hemin therapy also attenuated TNF-α, IL-6 and IL-1β in the ZL-controls, although to a lesser extent as compared to ZDFs.

4.4.3 Treatment with hemin abated inflammatory chemokines such as MCP-1 and MIP-1α in hepatic tissue of ZDFs

To further investigate the effects of hemin therapy on liver inflammation and hepatic lesions, we measured MIP-1α and MCP-1 since these chemokines trigger macrophage infiltration and cause hepatic injury (12, 13). In ZDF-controls, the basal levels of MCP-1 levels were markedly elevated as compared to ZL-controls (Fig. 4-3A), but were abated by hemin, whereas the co-treatment of hemin with SnMP nullified the effects of hemin (Fig. 4-3A). Hemin therapy was also effective against MIP-1α in ZDFs (Fig. 4-3B). In ZDF-controls, the basal levels of MIP-1α were significantly enhanced as compared to ZL-controls but were reduced by hemin, whereas the co-administration of hemin with SnMP abolished the effects of hemin (Fig. 4-3B). Hemin therapy also reduced MCP-1 and MIP-1α in ZL-controls, although, the effect in hemi-treated ZLs was smaller as compared to hemin-treated ZDFs.

4.4.4 Hemin therapy abated plasma and hepatic triglycerides and cholesterol in ZDFs

Since elevated hepatic triglycerides and high levels of hepatic cholesterol are common denominators of liver disease (7-9), we investigated the effects of hemin therapy on hepatic triglycerides and hepatic cholesterol. In ZDF-controls, the basal levels of liver triglycerides and liver cholesterol were significantly elevated as compared to ZL-controls (Figs. 4-4A and 4-4B). Similarly, the basal levels of plasma triglycerides and plasma cholesterol in ZDF-controls were markedly elevated (Figs. 4-4C and 4-4D). Interestingly, treatment with hemin greatly reduced the

elevated basal levels of liver triglycerides/cholesterol and plasma triglycerides/cholesterol (Fig. 4-4). Hemin therapy also reduced triglycerides and cholesterol in ZL-controls, though to a lesser extent as compared to ZDFs.

4.4.5 Hemin therapy abated the expression of markers for the pro-inflammatory M1-macrophage, while enhancing markers for the anti-inflammatory M2-phenotype in hepatic tissue

Given that macrophage infiltration is implicated in hepatic impairment (50-52), we used specific markers namely, ED1 to quantify the pro-inflammatory M1-phenotype, and ED2, CD206 and IL-10 for the assessment of anti-inflammatory M2-phenotype (19, 53, 54). Moreover, IL-10 is protective against fatty liver disease (18). Our Western immunoblotting and relative densitometry revealed that the basal expression of ED1 in the liver of ZDF-controls was significantly elevated as compared to the ZL-controls (Fig. 4-5A). Interestingly hemin therapy significantly attenuated the elevated expression of the pro-inflammatory M1-phenotype marker, ED1 (Fig. 4-5A).

To further investigate the effects of hemin on inflammation, we also determined the expression of the M2-phenotype. Our results indicate that the basal expression levels of different anti-inflammatory M2-phenotype markers including ED2, CD206 and IL-10 were markedly reduced in ZDF-controls as compared to ZL-controls (Figs. 4-5B, 4-5C and 4-5D). Interestingly, hemin therapy robustly enhanced the depressed basal expression levels of ED2 (Fig. 4-5B), CD206 (Fig. 4-5C) and IL-10 (Fig. 4-5D), suggesting that hemin therapy may selectively modulate the polarization of macrophage toward the M2-phenotype that dampens inflammation.

4.4.6 Hemin therapy suppressed macrophage infiltration in the liver

Since our Western immunoblotting data indicated that hemin therapy abated the expression of ED1 a marker of the pro-inflammatory macrophage M1-phenotype (Fig. 4-5A), we did immunohistochemistry to assess macrophage infiltration in hepatic tissue (Fig. 4-6A). Images of hepatic sections from ZL-controls were almost devoid of cells with the characteristic dark-brown ED1-positive staining. In contrast, liver sections from ZDF-controls showed marked increase of ED1-positive dark-brown cells as compared to ZL-controls, suggesting increased macrophage infiltration in ZDFs (Fig. 4-6A). Interestingly, hemin therapy greatly attenuated the number of dark-brown stained macrophages, suggesting reduction of macrophage infiltration in hemin-treated ZDFs. These observations were further confirmed by quantitative ED1 scoring (Fig. 4-6B), which showed a significant reduction of ED1-positive cells in hemin-treated ZDFs as compared to ZDF-controls.

4.4.7 Hemin reduced the expression of profibrotic and extracellular matrix proteins in the liver

Since elevated deposition of extracellular matrix is implicated in liver damage (32-36), we measured the levels of profibrotic and extracellular matrix proteins such as osteopontin, collagen, fibronectin and TGF-β in the liver. Moreover, TGF-β is known to activate hepatic fat to accentuate the deposition of extracellular matrix proteins (34). In ZDF-controls the basal expression of TGF-β was significantly elevated as compared to ZL-controls (Fig. 4-7A), but was greatly attenuated by hemin.

Since TGF-β mobilizes the extracellular the matrix by stimulating fibronectin and collagen to cause fibrosis (55), so we also measured the expressions of fibronectin and collagen-IV. In ZDF-

controls, the basal expressions of fibronectin and collagen-IV were significantly elevated as compared to ZL-controls, but were attenuated by hemin therapy (Figs. 4-7B and 4-7C). It is noteworthy that hemin effectively restored fibronectin to comparable levels as in the ZL-control, but collagen-IV was not reinstated to the levels of ZL-controls, suggesting that hemin may have greater selectivity against fibronectin. The reason for the selective effect is unknown.

We also assessed the expression of osteopontin because osteopontin is implicated in hepatic fibrosis and injury (32). In ZDF-controls, the basal expression of osteopontin was markedly elevated as compared to ZL-controls, but was significantly reduced by hemin therapy, although, similar levels as observed in the ZL-controls were not reinstated (Fig. 4-7D).

4.4.8 Hemin therapy suppressed hepatic histo-pathological lesions

Hepatocyte ballooning injury and fibrosis are common histo-physiological denominators in fatty-liver diseases such as NAFLD (1, 5, 32, 34-36) To further investigate the effects of hemin therapy on liver lesions, we did histological and morphometric analyses using Masson's trichrome staining. Our results indicate that sections from liver tissue obtained from ZL-controls had normal appearance and the central vein region was without hepatocyte ballooning injury (Fig. 4-8A). However, in ZDF-controls, there was greater hepatocyte ballooning injury with inflammatory cell infiltration around the central vein region, which interestingly were greatly attenuated in hemin-treated ZDF (Fig. 4-8A). These observations were further confirmed by quantitative ballooning scoring (Fig. 4-8B), which showed a significant reduction of hepatocyte ballooning injury in hemin-treated ZDFs as compared to untreated ZDF-controls.

To further investigate the effects of hemin therapy on hepatic morphology, fibrosis was assessed by Masson's trichrome staining. Our results show that images of liver sections from the

ZL-controls appeared relatively healthy with little Mason's trichrome staining (blue coloration), suggesting little fibrosis (Fig. 4-9). However, in ZDF-controls, greater fibrotic activity was observed, particularly around the portal spaces with some extension towards center-lobular zones. Interestingly, hemin therapy greatly reduced the fibrotic activity in ZDF (Fig. 4-9).

4.5 Discussion

The present study unveils several novel and/or important insights on the hepatoprotective effects of hemin therapy in the condition of obesity and type-2 diabetes including; (i) the hemin-dependent suppression of hepatic levels of chemokines and cytokines such as MCP-1, MIP-1α, TNF-α, IL-6 and IL-1β implicated in hepatic injury; (ii) the reduction of plasma and hepatic triglycerides/cholesterol; (iii) the abrogation of extracellular matrix/profibrotic proteins in hepatic tissue including osteopontin, TGF-β, fibronectin and collagen; and (iv) the attenuation of hepatocyte ballooning injury to preserve hepatic morphology and function in ZDFs. Impaired hepatic function is a common phenomenon in non-alcoholic fatty liver disease (56), and with the rising prevalence and incidence of non-alcoholic fatty liver disease following the dramatic escalation of obesity, insulin resistance and overt diabetes worldwide (57), novel pharmacological agents capable of preserving hepatic function are needed. Accordingly, this study demonstrates that upregulating the HO-system with hemin abates inflammation, suppress hepatic adiposity and attenuate hepatocyte ballooning injury in ZDF, a model characterized by obesity, aberrant hepatic response to insulin, type-2 diabetes and impaired hepatic lipid metabolism (30, 31). Hepatic adiposity and inflammation are the hallmarks of non-alcoholic fatty liver disease (9, 56, 58). Therefore, the elevated basal levels of hepatic triglycerides, hepatic cholesterol, macrophage infiltration, pro-inflammatory cytokines/chemokines including, TNF-α, IL-6, IL-1β, MIP-1α and

MCP-1 are among the multifaceted pathophysiological factors that accentuate inflammation during the progressive deterioration of hepatic morphology and function in ZDFs.

In the present study, a signature of the ailing hepatic morphology in ZDFs was evidenced the severe hepatocyte ballooning injury. However, the administration of hemin therapy to ZDFs abated macrophage infiltration and pro-inflammatory mediators and improved hepatic morphology, whereas treatment with the HO-inhibitor, SnMP accentuated the levels of inflammatory cytokines and chemokines. Importantly, the hemin-induced selective enhancement the anti-inflammatory macrophage-M2-phenotype with parallel reduction of pro-inflammatory macrophage M1-phenotype observed in our study is an alternative anti-inflammatory mechanism by which the HO-system protects hepatic tissue. Although, one study had previously reported the effects of HO-1 promoter in macrophage polarization (59), the actual expression levels of M1 and M2 macrophage phenotypes were not measured, so our study provides more solid evidence on the role of the HO system on M1 and M2 during macrophage polarization. However, the present study may be just the tip of an iceberg and further investigations are needed to fully characterize the effects of upregulating the HO system with hemin on macrophage polarization in ZDF.

Besides its effects against inflammation, hemin also suppressed osteopontin, an extracellular matrix-proteins is implicated in hepatic fibrosis and injury (32). Similarly, other extracellular matrix/profibrotic proteins such as TFG-β, collagen and fibronectin that impair liver function (32-36), were also reduced in hemi-treated ZDFs, with corresponding reduction of hepatic histo-pathological lesions like hepatocyte ballooning injury and fibrosis. Hemin therapy also potentiated the HO-system and cGMP in ZL-control rats and abated MIP-1α, MCP-1, TNF-α, IL-6 and IL-1β although, the effect of hemin was less-intense in ZLs as compared to ZDFs with aberrant HO-system. Although, the reasons for this selective effect of hemin remain unclear, it is

possible that the HO-system in healthy ZLs is more stable than in unhealthy ZDFs with depressed HO-activity. Nevertheless, future studies should be designed to investigate this observation.

The emerging cytoprotective role of the HO system in non-alcoholic fatty liver disease has been well-acknowledged (60, 61). Accordingly, the HO system has been shown to alleviate hepatic steatosis and necroinflammation in a mice model of experimental nutritional steatohepatitis (60). Similarly, the anti-oxidant effect of the HO system was amongst the mechanisms conferred protection against non-alcoholic fatty liver disease in mice and humans (61, 62). Therefore, the present study is a further testimony of the important hepatoprotective role of the HO system.

Collectively, our study indicates that hemin therapy restores hepatic morphology by abating hepatic adiposity, suppressing liver macrophage infiltration, inflammation, fibrosis and extracellular/profibrotic proteins implicated in hepatic lesions. The selective enhancement of anti-inflammatory macrophage-M2-phenotype with parallel reduction of pro-inflammatory macrophage M1-phenotype and related chemokines/cytokines like TNF-α, IL-6, IL-1β, MIP-1α and MCP-1 are among the multifaceted mechanisms by which hemin restore hepatic morphology.

Funding: This work was supported by a grant from the Heart & Stroke Foundation of Saskatchewan, Canada to Dr. Joseph Fomusi Ndisang. The funders had no role in study design, data collection and analysis, decision to publish, or preparation of the manuscript.

Competing Interests: The authors have declared that no competing interests exist.

Table 4-1: Effect of hemin and stannous mesoporphyrin (SnMP) on physiological parameters in ZDF and ZL rats.

Physiological Parameters	Animal groups					
	Control ZL	ZL + Hemin	Control ZDF	ZDF + Hemin	ZDF + Hemin + SnMP	ZDF + Vehicle
Body weight (g)	348.6 ± 5.9	341.2 ± 10.5	406.3 ± 5.2†	382.5 ± 4.8*	369.2 ± 5.5$^{\#}$	396.5 ± 9.3
Fasting glucose (mmol/L)	6.5 ± 0.2	5.9 ± 0.3*	26.3 ± 2.5††	8.3 ± 1.4**	29.4 ± 3.7$^{\#}$	25.7 ± 2.6
Liver weight (g/Kg body weight)	45.4 ± 1.4	42.2 ± 4.6	54.8 ± 1.8†	40.7 ± 1.5*	55.2 ± 2.3$^{\#}$	53.6 ± 2.8

*$p<0.05$, **$p<0.01$ vs Control ZDF or control ZL; $^{\#}p<0.05$ vs ZDF + Hemin; $^{\dagger}p<0.05$, $^{\dagger\dagger}p<0.01$ vs control ZL; n = 6 per group.

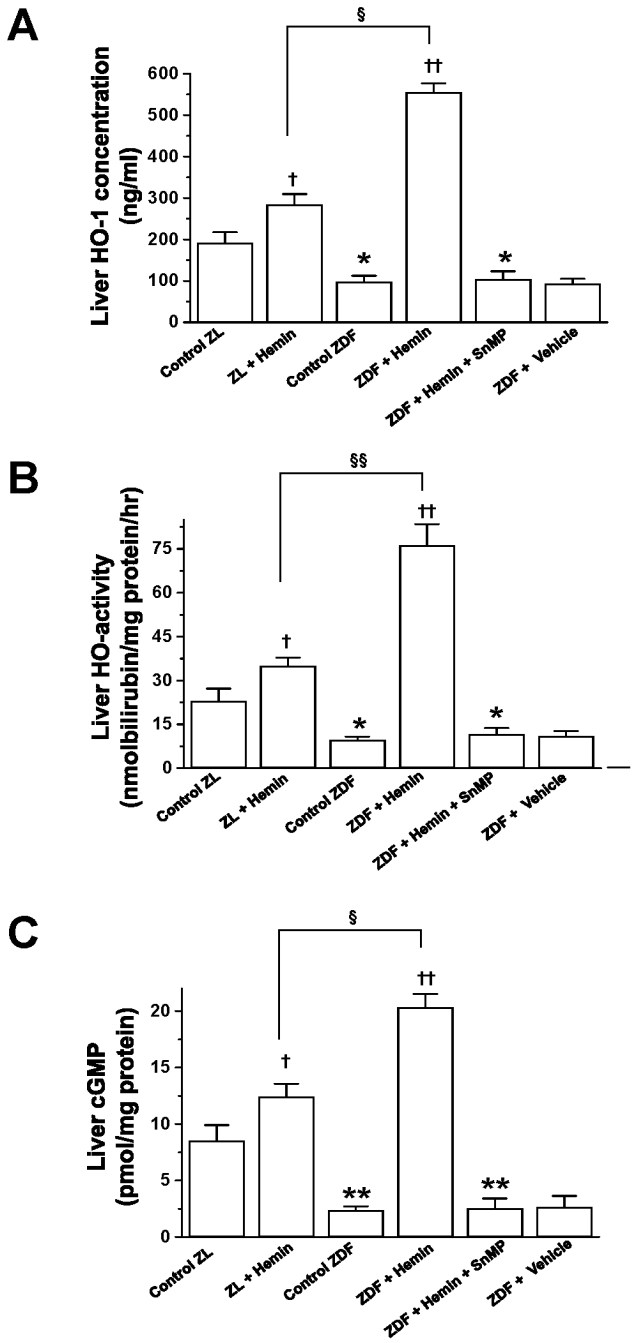

Figure 4-1: Effects of the HO-inducer, hemin and the HO inhibitor SnMP, on hepatic levels of HO-1, HO activity and cGMP. Hemin therapy greatly increased the depressed (A) HO-1 concentration, (B) HO-activity, and (C) cGMP levels in ZDFs, whereas the HO blocker, SnMP nullified the effects. Treatment of hemin to ZL also resulted to increased levels of HO-1, HO-activity and cGMP in ZLs, thought less effectively as compared to ZDFs. Bars represent means ±

SEM; n = 6 rats per group (*p<0.05, **p<0.01 vs Control-ZL; †p<0.05, ††p<0.01 vs Control-ZL or Control-ZDF; §p<0.05, §§p<0.01 vs ZL + Hemin).

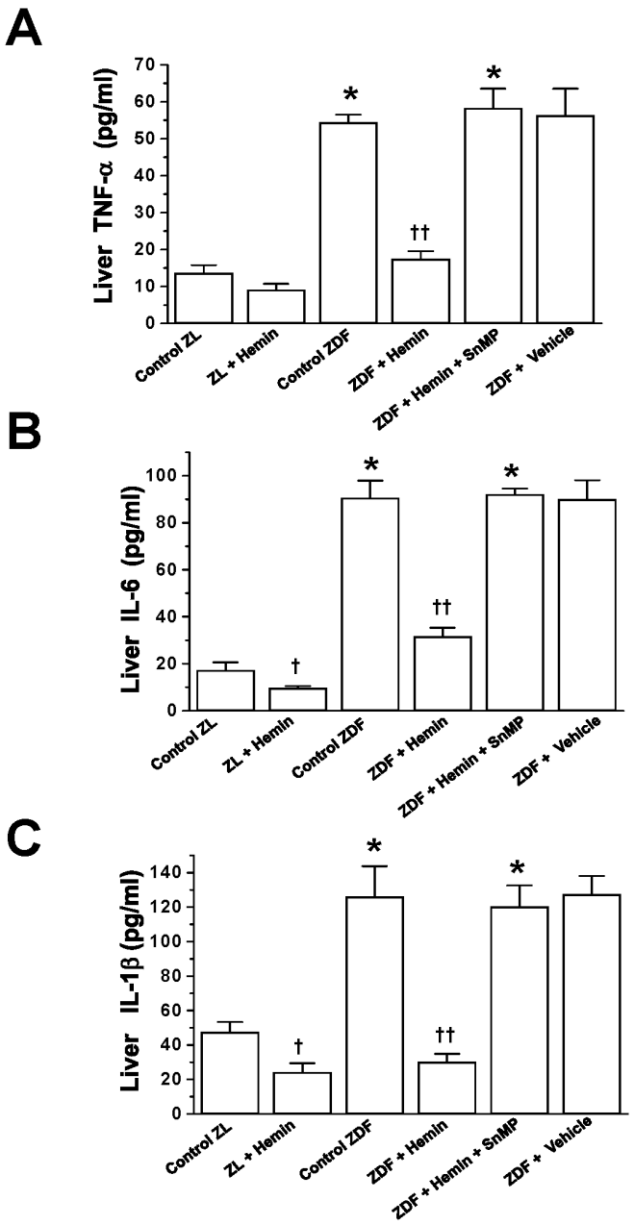

Figure 4-2: Effects of hemin, the HO inducer and SnMP, the HO inhibitor on liver levels of TNF-α, IL-6 and IL-1β. Hemin therapy attenuated the elevated basal levels of (A) TNF-α, (B) IL-6 and (C) IL-1β in ZDFs, while the HO blocker, SnMP reversed the effects. Hemin therapy also lowered

TNF-α, IL-6 and IL-1β levels in ZLs. Bars represent means ± SEM; *n* = 6 rats per group (*p<0.01 vs Control-ZL; †p<0.05, ††p<0.01 vs Control-ZL or Control-ZDF).

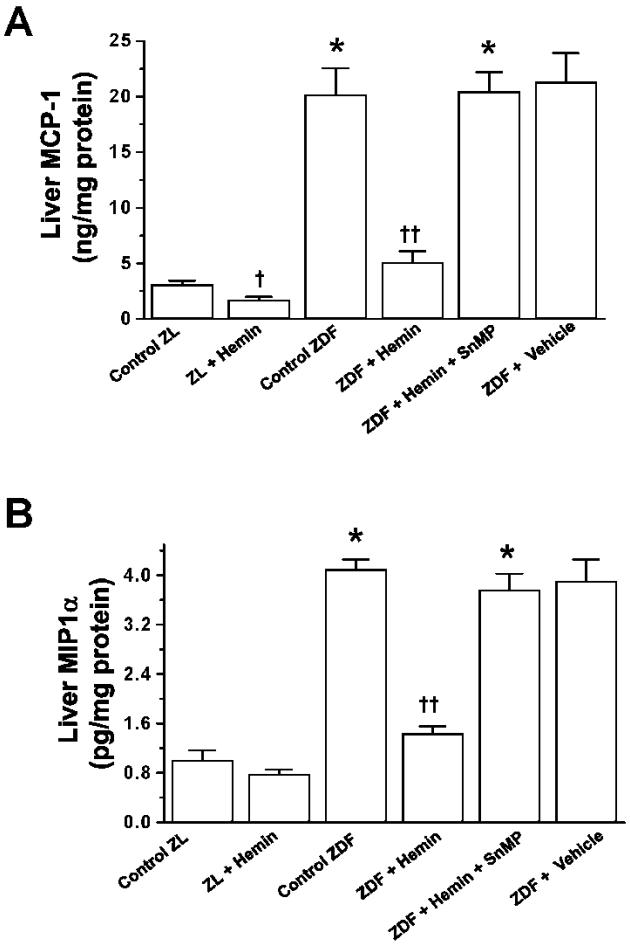

Figure 4-3: Effects of hemin, the HO inducer and SnMP, the HO inhibitor on hepatic levels of MCP-1 and MIP-1α. Hemin therapy suppressed the elevated basal levels of (A) MCP-1 and (B) MIP-1α in ZDFs, but the HO blocker, SnMP abolished the effects of hemin. Treatment with hemin also reduced MCP-1 and MIP-1α in ZLs. Bars represent means ± SEM; *n* = 6 rats per group (*****p<0.01 vs Control-ZL; †p<0.05, ††p<0.01 vs Control-ZL or Control-ZDF).

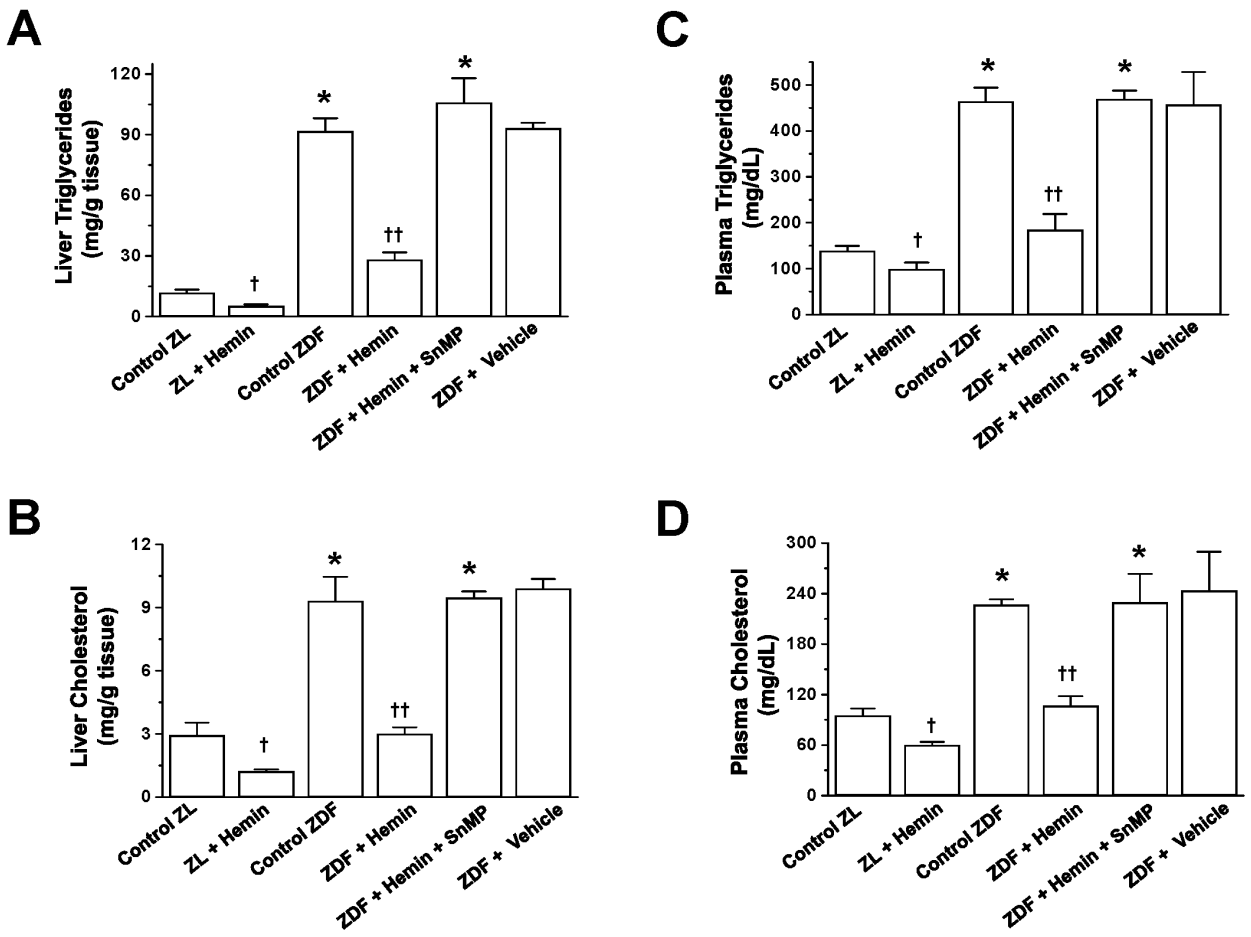

Figure 4-4: Effects of hemin, the HO inducer and SnMP, the HO inhibitor on hepatic triglycerides, hepatic cholesterol, plasma triglycerides and plasma cholesterol. Hemin therapy markedly reduced the elevated basal levels of (A) liver triglycerides, (B) liver cholesterol, (C) plasma triglycerides and (D) plasma cholesterol in ZDFs, whereas the HO blocker, SnMP nullified the effects. Hemin therapy also lowered hepatic triglycerides/cholesterol and plasma triglycerides/cholesterol in ZLs. Bars represent means ± SEM; *n* = 6 rats per group (*$p<0.01$ vs Control-ZL; $^{\dagger}p<0.05$, $^{\dagger\dagger}p<0.01$ vs Control-ZL or Control-ZDF).

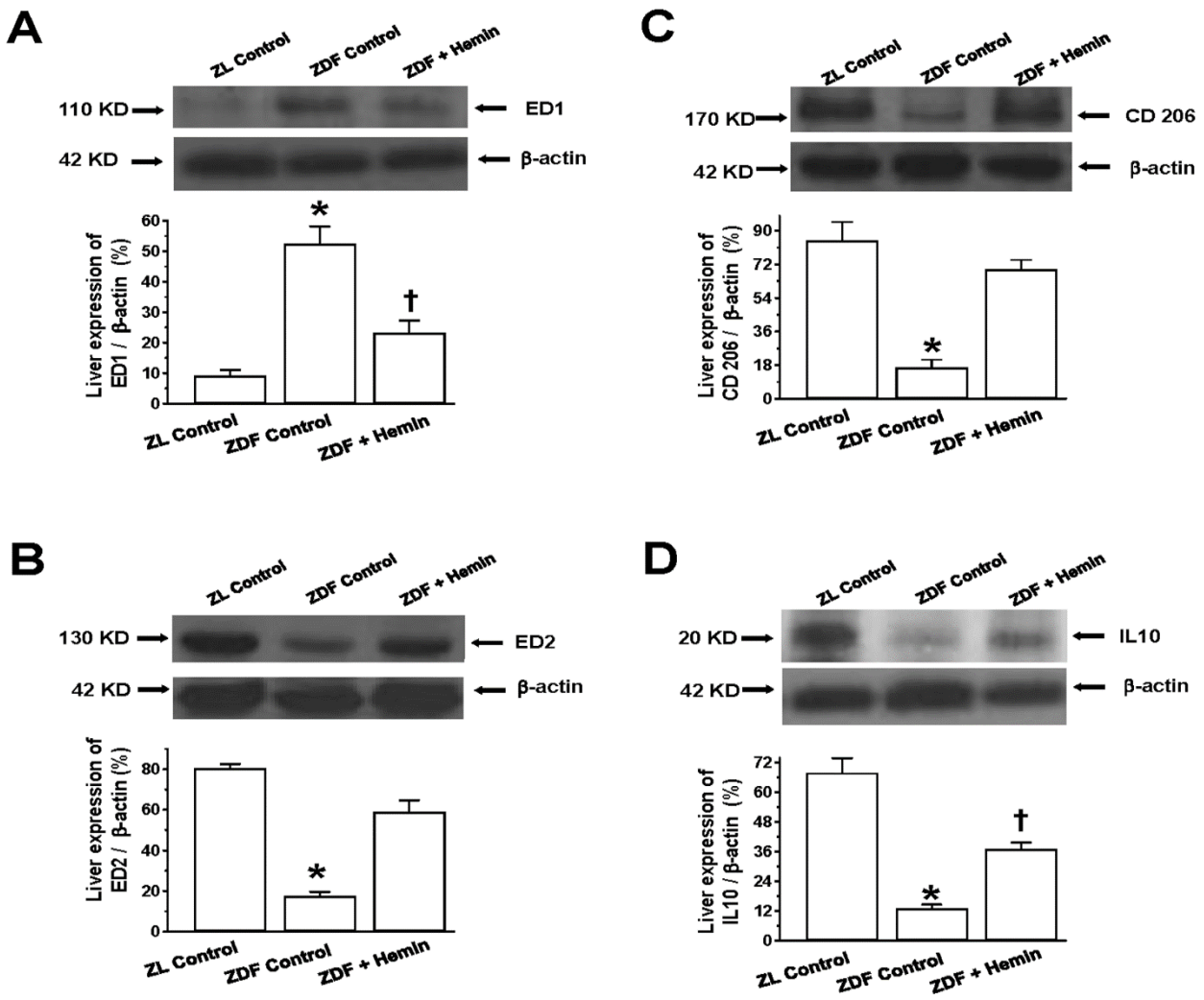

Figure 4-5: Effects of hemin on hepatic expression of ED1, ED2, CD206 and IL-10. Representative Western immunoblot and relative densitometric analyses of expressed protein normalized with b-actin indicates that hemin therapy suppressed the elevated basal expression of (A) the pro-inflammatory macrophage M1-phenotype marker, ED, but enhanced the expression of several anti-inflammatory macrophage M2-phenotye markers such as (B) ED2, (C) CD206 and (D) IL-10 in ZDFs. Bars represent means ± SEM; *n* = 4 rats per group (*p<0.01 vs Control-ZL, †p<0.05 vs Control-ZL).

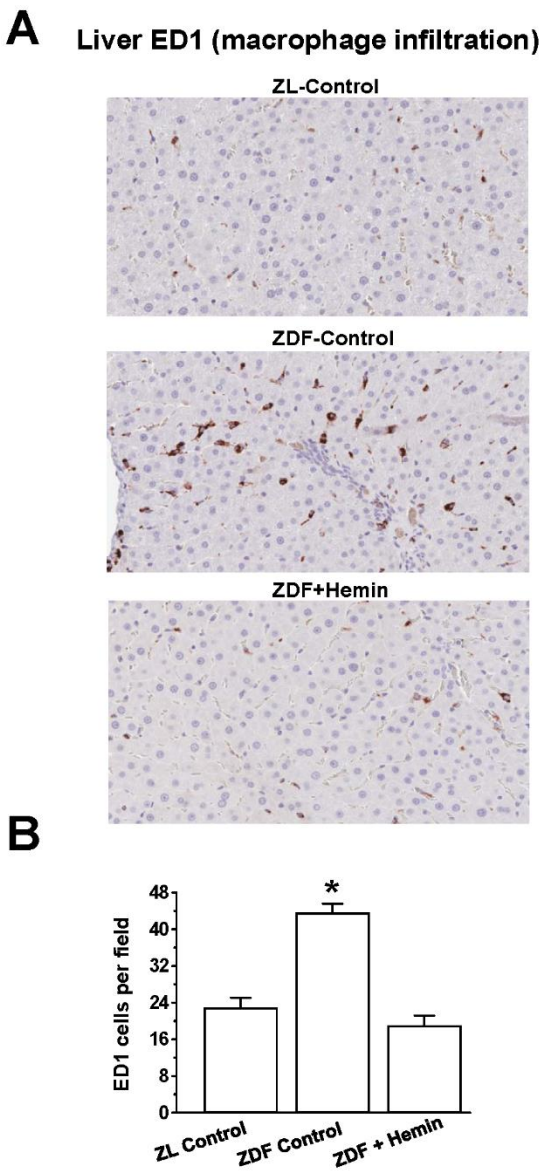

Figure 4-6: Effect of hemin therapy on macrophage infiltration in the liver. (A) Representative image indicates that macrophage infiltration (ED1-positive cells stained dark brown) in liver sections were elevated in ZDF-controls as compared to ZL-controls, but were reduced in hemi-treated ZDFs. (Magnification x200). (B) Quantitative analyses per field revealed that in ZDF-controls, macrophage infiltration was markedly elevated as compared to ZL-control, but was significantly reduced in hemi-treated ZDFs. Bars represent means ± SEM; *n* = 4-6 rats per group (*p<0.01 vs all groups).

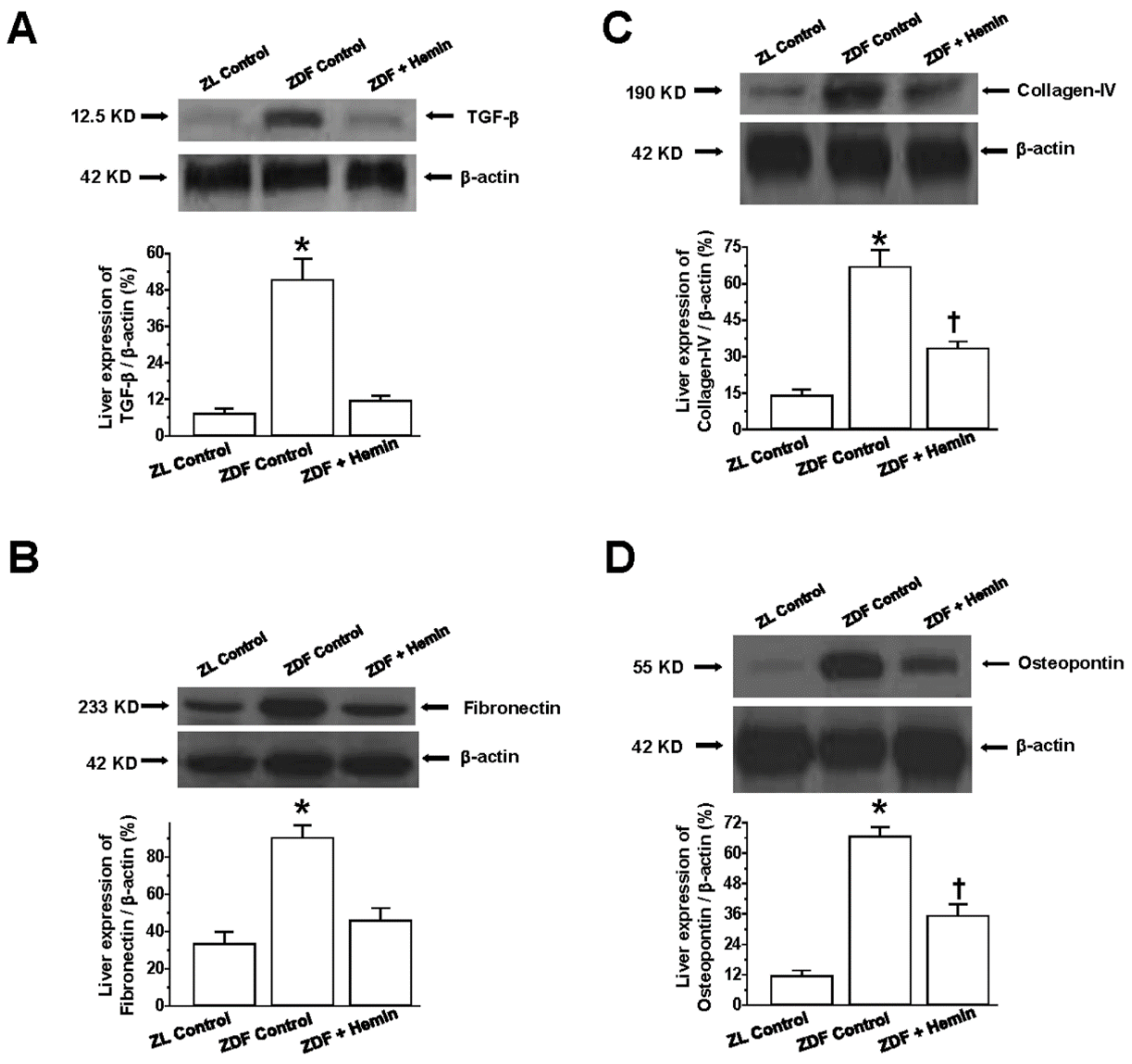

Figure 4-7: Effect of hemin therapy on liver expression of TGF-β, fibronectin, collagen-IV and osteopontin in ZDFs. Representative Western immunoblots, and relative densitometry revealed that hemin therapy markedly reduced the elevated basal expression of (A) TGF-β, (B) fibronectin, (C) collagen-IV and (D) osteopontin in ZDFs. Bars represent means ± SEM; *n* = 4 rats per group (*$p<0.01$ vs Control-ZL; †$p<0.05$ vs Control-ZL).

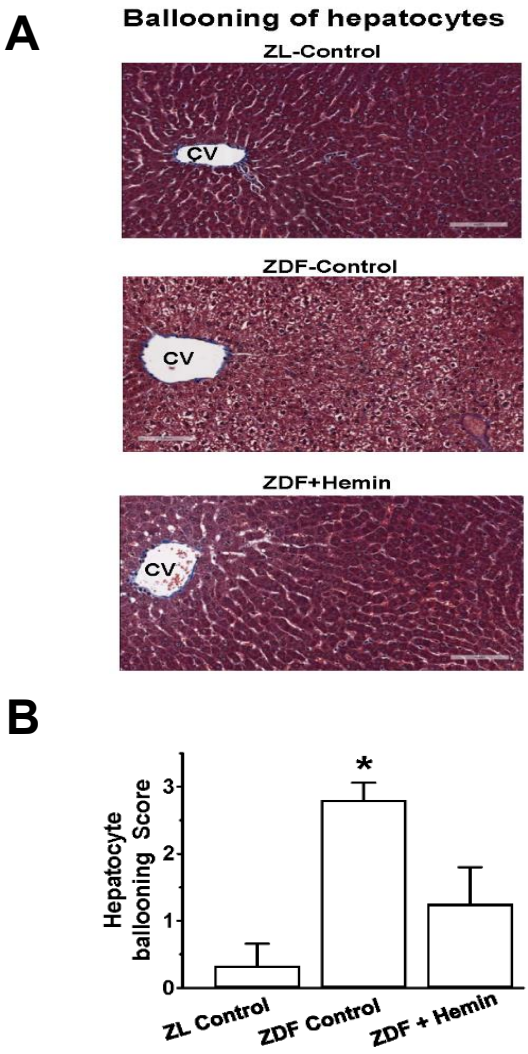

Figure 4-8: Effect of hemin therapy on hepatic histo-pathological lesions. (A) Representative image after Masson's trichrome staining revealed severe hepatocyte ballooning injury with inflammatory cell infiltration around the central vein (CV) region in ZDFs, which interestingly were attenuated in hemin-treated ZDF (Magnification x200). (B) Semi-quantitative evaluation showed that hemin therapy significantly reduced hepatocyte ballooning injury in ZDFs. Bars represent means ± SEM; *n* = 4-6 rats per group (*p<0.01 vs all groups).

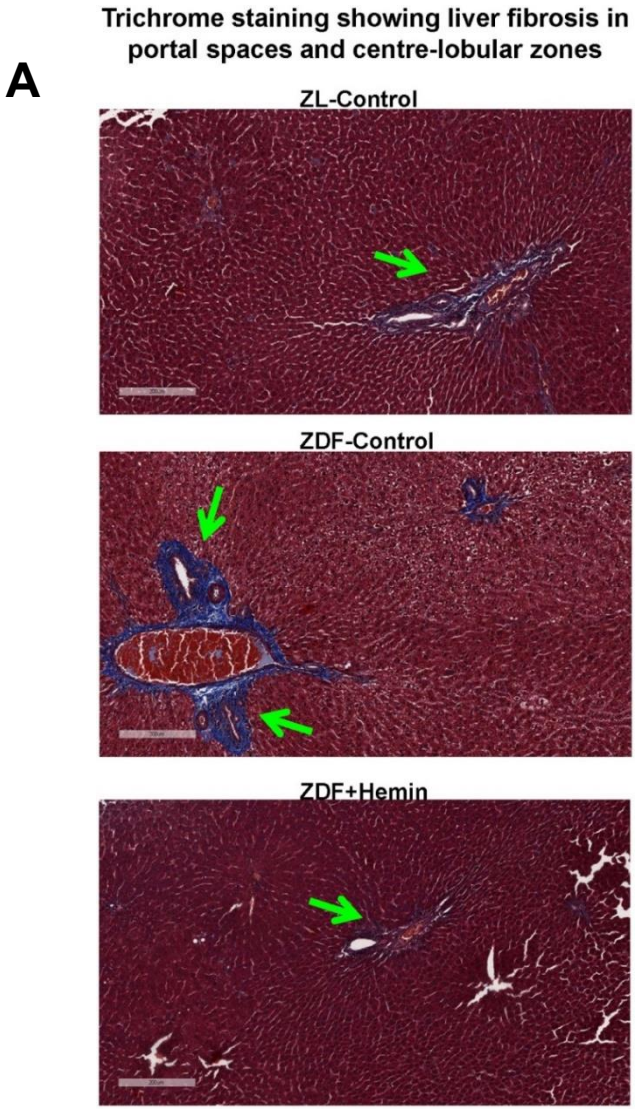

Figure 4-9: Effect of hemin therapy on hepatic fibrosis, determined by Masson'' trichrome staining. (A) Representative image following Masson's trichrome staining revealed greater fibrotic activity (blue coloration), particularly around the portal spaces with some extension toward center-lobular zones in sections from ZDFs, but interestingly were reduced in hemin-treated ZDF (Magnification x200).

4.6 References

1. Lackner C (2011) Hepatocellular ballooning in nonalcoholic steatohepatitis: the pathologist's perspective. Expert Rev Gastroenterol Hepatol 5: 223-231.

2. Haynes P, Liangpunsakul S, Chalasani N (2004) Nonalcoholic fatty liver disease in individuals with severe obesity. Clin Liver Dis 8: 535-547, viii.

3. Abrams GA, Kunde SS, Lazenby AJ, Clements RH (2004) Portal fibrosis and hepatic steatosis in morbidly obese subjects: A spectrum of nonalcoholic fatty liver disease. Hepatology 40: 475-483.

4. Tarantino G, Saldalamacchia G, Conca P, Arena A (2007) Non-alcoholic fatty liver disease: further expression of the metabolic syndrome. J Gastroenterol Hepatol 22: 293-303.

5. Machado MV, Cortez-Pinto H (2011) Cell death and nonalcoholic steatohepatitis: where is ballooning relevant? Expert Rev Gastroenterol Hepatol 5: 213-222.

6. Ndisang JF, Wang R (2002) Novel therapeutic strategies for impaired endothelium-dependent vascular relaxation. Expert Opin Ther Patents 12: 1237-1247.

7. Liu Y, Dang H, Li D, Pang W, Hammock BD, et al. (2012) Inhibition of soluble epoxide hydrolase attenuates high-fat-diet-induced hepatic steatosis by reduced systemic inflammatory status in mice. PLoS One 7: e39165.

8. Pathil A, Mueller J, Warth A, Chamulitrat W, Stremmel W (2012) Ursodeoxycholyl lysophosphatidylethanolamide improves steatosis and inflammation in murine models of nonalcoholic fatty liver disease. Hepatology 55: 1369-1378.

9. Gentile CL, Pagliassotti MJ (2008) The role of fatty acids in the development and progression of nonalcoholic fatty liver disease. J Nutr Biochem 19: 567-576.

10. Barbuio R, Milanski M, Bertolo MB, Saad MJ, Velloso LA (2007) Infliximab reverses steatosis and improves insulin signal transduction in liver of rats fed a high-fat diet. J Endocrinol 194: 539-550.

11. Mathur A, Marine M, Lu D, Swartz-Basile DA, Saxena R, et al. (2007) Nonalcoholic fatty pancreas disease. HPB (Oxford) 9: 312-318.

12. Gordon S (2003) Alternative activation of macrophages. Nat Rev Immunol 3: 23-35.

13. Antoniades CG, Quaglia A, Taams LS, Mitry RR, Hussain M, et al. (2012) Source and characterization of hepatic macrophages in acetaminophen-induced acute liver failure in humans. Hepatology 56: 735-746.

14. Ndisang JF (2010) Role of heme oxygenase in inflammation, insulin-signalling, diabetes and obesity. Mediators Inflamm 2010: 359732.

15. Gordon S, Martinez FO (2010) Alternative activation of macrophages: mechanism and functions. Immunity 32: 593-604.

16. Navarro-Gonzalez JF, Mora-Fernandez C, Muros de Fuentes M, Garcia-Perez J (2011) Inflammatory molecules and pathways in the pathogenesis of diabetic nephropathy. Nat Rev Nephrol 7: 327-340.

17. Navarro-Gonzalez JF, Mora-Fernandez C (2011) Inflammatory pathways. Contrib Nephrol 170: 113-123.

18. Cintra DE, Pauli JR, Araujo EP, Moraes JC, de Souza CT, et al. (2008) Interleukin-10 is a protective factor against diet-induced insulin resistance in liver. J Hepatol 48: 628-637.

19. Aki K, Shimizu A, Masuda Y, Kuwahara N, Arai T, et al. (2010) ANG II receptor blockade enhances anti-inflammatory macrophages in anti-glomerular basement membrane glomerulonephritis. Am J Physiol Renal Physiol 298: F870-882.

20. Satoh-Asahara N, Shimatsu A, Sasaki Y, Nakaoka H, Himeno A, et al. (2012) Highly purified eicosapentaenoic acid increases interleukin-10 levels of peripheral blood monocytes in obese patients with dyslipidemia. Diabetes Care 35: 2631-2639.

21. Mauricio MD, Aldasoro M, Ortega J, Vila JM (2013) Endothelial dysfunction in morbid obesity. Curr Pharm Des.

22. Shen C, Zhao CY, Zhang R, Qiao L (2012) Obesity-related hepatocellular carcinoma: roles of risk factors altered in obesity. Front Biosci 17: 2356-2370.

23. Tiwari S, Ndisang JF (2013) The Role of Obesity in Cardiomyopathy And Nephropathy. Curr Pharm Des.

24. Cusi K (2012) Role of obesity and lipotoxicity in the development of nonalcoholic steatohepatitis: pathophysiology and clinical implications. Gastroenterology 142: 711-725 e716.

25. Tiwari S, Ndisang JF (2013) The Heme Oxygenase System and Type-1 Diabetes. Curr Pharm Des.

26. Mishra M, Ndisang JF (2013) A critical and comprehensive insight on heme oxygenase and related products including carbon monoxide, bilirubin, biliverdin and ferritin in type-1 and type-2 diabetes. Curr Pharm Des.

27. Tiwari S, Ndisang JF (2013) Heme Oxygenase System and Hypertension: A Comprehensive Insight. Curr Pharm Des.

28. Jadhav A, Ndisang JF (2012) Treatment with heme arginate alleviates adipose tissue inflammation and improves insulin sensitivity and glucose metabolism in a rat model of Human primary aldosteronism. Free Radic Biol Med 53: 2277-2286.

29. Jadhav A, Tiwari S, Lee P, Ndisang JF (2013) The heme oxygenase system selectively enhances the anti-inflammatory macrophage-m2 phenotype, reduces pericardial adiposity, and ameliorated cardiac injury in diabetic cardiomyopathy in zucker diabetic Fatty rats. J Pharmacol Exp Ther 345: 239-249.

30. Shiota M, Printz RL (2012) Diabetes in Zucker diabetic fatty rat. Methods Mol Biol 933: 103-123.

31. Satapati S, He T, Inagaki T, Potthoff M, Merritt ME, et al. (2008) Partial resistance to peroxisome proliferator-activated receptor-alpha agonists in ZDF rats is associated with defective hepatic mitochondrial metabolism. Diabetes 57: 2012-2021.

32. Yang YY, Tsai TH, Huang YT, Lee TY, Chan CC, et al. (2012) Hepatic endothelin-1 and endocannabinoids-dependent effects of hyperleptinemia in nonalcoholic steatohepatitis-cirrhotic rats. Hepatology 55: 1540-1550.

33. Okamoto T, Park CH, Noh JS, Toriizuka K, Sei Y, et al. (2011) Hepato2/renoprotective activity of Chinese prescription Kangen-karyu through inhibition of AGE formation and fibrosis-related protein expression in type 2 diabetes. J Pharm Pharmacol 63: 952-959.

34. Flisiak R, Pytel-Krolczuk B, Prokopowicz D (2000) Circulating transforming growth factor beta (1) as an indicator of hepatic function impairment in liver cirrhosis. Cytokine 12: 677-681.

35. Kleiner DE, Brunt EM, Van Natta M, Behling C, Contos MJ, et al. (2005) Design and validation of a histological scoring system for nonalcoholic fatty liver disease. Hepatology 41: 1313-1321.

36. Hayashi H, Sakai T (2011) Animal models for the study of liver fibrosis: new insights from knockout mouse models. Am J Physiol Gastrointest Liver Physiol 300: G729–738.

37. Reed DR, Duke FF, Ellis HK, Rosazza MR, Lawler MP, et al. (2011) Body fat distribution and organ weights of 14 common strains and a 22-strain consomic panel of rats. Physiol Behav 103: 523-529.

38. Lee HJ, Choi SS, Park MK, An YJ, Seo SY, et al. (2002) Fenofibrate lowers abdominal and skeletal adiposity and improves insulin sensitivity in OLETF rats. Biochem Biophys Res Commun 296: 293-299.

39. Morel OE, Aubert R, Richalet JP, Chapelot D (2005) Simulated high altitude selectively decreases protein intake and lean mass gain in rats. Physiol Behav 86: 145-153.

40. Jadhav A, Torlakovic E, Ndisang JF (2009) Hemin therapy attenuates kidney injury in deoxycorticosterone acetate-salt hypertensive rats. Am J Physiol Renal Physiol 296: F521-F534.

41. Ndisang JF, Jadhav A (2009) Heme oxygenase system enhances insulin sensitivity and glucose metabolism in streptozotocin-induced diabetes. Am J Physiol Endocrinol Metab 296: E829-841.

42. Ndisang JF, Lane N, Jadhav A (2009) The heme oxygenase system abates hyperglycemia in Zucker diabetic fatty rats by potentiating insulin-sensitizing pathways. Endocrinology 150: 2098-2108.

43. Ndisang JF (2013) The Heme Oxygenase System Selectively Modulates Proteins Implicated in Metabolism, Oxidative Stress and Inflammation in Spontaneously Hypertensive Rats. Curr Pharm Des.

44. Ndisang JF, Lane N, Jadhav A (2008) Crosstalk between the heme oxygenase system, aldosterone, and phospholipase C in hypertension. J Hypertens 26: 1188-1199.

45. Ndisang JF, Wu L, Zhao W, Wang R (2003) Induction of heme oxygenase-1 and stimulation of cGMP production by hemin in aortic tissues from hypertensive rats. Blood 101: 3893-3900.

46. Gupte RS, Floyd BC, Kozicky M, George S, Ungvari ZI, et al. (2009) Synergistic activation of glucose-6-phosphate dehydrogenase and NAD(P)H oxidase by Src kinase elevates superoxide in type 2 diabetic, Zucker fa/fa, rat liver. Free Radic Biol Med 47: 219-228.

47. Mosen H, Salehi A, Alm P, Henningsson R, Jimenez-Feltstrom J, et al. (2005) Defective glucose-stimulated insulin release in the diabetic Goto-Kakizaki (GK) rat coincides with reduced activity of the islet carbon monoxide signaling pathway. Endocrinology 146: 1553-1558.

48. Mosen H, Salehi A, Henningsson R, Lundquist I (2006) Nitric oxide inhibits, and carbon monoxide activates, islet acid alpha-glucoside hydrolase activities in parallel with glucose-stimulated insulin secretion. J Endocrinol 190: 681-693.

49. Moro C, Klimcakova E, Lolmede K, Berlan M, Lafontan M, et al. (2007) Atrial natriuretic peptide inhibits the production of adipokines and cytokines linked to inflammation and insulin resistance in human subcutaneous adipose tissue. Diabetologia 50: 1038-1047.

50. Kang JH, Goto T, Han IS, Kawada T, Kim YM, et al. (2010) Dietary capsaicin reduces obesity-induced insulin resistance and hepatic steatosis in obese mice fed a high-fat diet. Obesity (Silver Spring) 18: 780-787.

51. Barnes MA, McMullen MR, Roychowdhury S, Pisano SG, Liu X, et al. (2013) Macrophage migration inhibitory factor contributes to ethanol-induced liver injury by mediating cell injury, steatohepatitis, and steatosis. Hepatology 57: 1980-1991.

52. Deng C, Liu J, Wang G, Ma L, Xie C, et al. (2012) A novel small molecule, (E)-5-(2,4-di-tert-butyl-6-((2,4-dioxothiazolidin-5-ylidene) methyl) phenyl)-59-methyl-7,79-dimethoxy-4,49-bibenzo[d][1,3] dioxole-5,59-dicarboxylate(7k), alleviates the development of D-galactosamine/lipopolysaccharide-induced acute liver failure by inhibiting macrophage infiltration and regulating cytokine expression. J Pharmacol Exp Ther 341: 146-155.

53. Anzai A, Anzai T, Nagai S, Maekawa Y, Naito K, et al. (2012) Regulatory role of dendritic cells in postinfarction healing and left ventricular remodeling. Circulation 125: 1234-1245.

54. Jing F, Mogi M, Min LJ, Ohshima K, Nakaoka H, et al. (2013) Effect of Angiotensin II Type 2 Receptor-Interacting Protein on Adipose Tissue Function via Modulation of Macrophage Polarization. PLoS One 8: e60067.

55. Finer G, Schnaper HW, Kanwar YS, Liang X, Lin HY, et al. (2012) Divergent roles of Smad3 and PI3-kinase in murine adriamycin nephropathy indicate distinct mechanisms of proteinuria and fibrogenesis. Kidney Int 82: 525-536.

56. Fabbrini E, Sullivan S, Klein S (2010) Obesity and nonalcoholic fatty liver disease: biochemical, metabolic, and clinical implications. Hepatology 51: 679-689.

57. Masuoka HC, Chalasani N (2013) Nonalcoholic fatty liver disease: an emerging threat to obese and diabetic individuals. Ann N Y Acad Sci 1281: 106-122.

58. Fracanzani AL, Valenti L, Bugianesi E, Vanni E, Grieco A, et al. (2011) Risk of nonalcoholic steatohepatitis and fibrosis in patients with nonalcoholic fatty liver disease and low visceral adiposity. J Hepatol 54: 1244-1249.

59. Weis N, Weigert A, von Knethen A, Brune B (2009) Heme oxygenase-1 contributes to an alternative macrophage activation profile induced by apoptotic cell supernatants. Mol Biol Cell 20: 1280-1288.

60. Wang RQ, Nan YM, Han F, Zhao SX, Fu N, et al. (2010) [The role of heme oxygenase-1 in non-alcoholic steatohepatitis]. Zhonghua Gan Zang Bing Za Zhi 18: 680-684.

61. Kathirvel E, Chen P, Morgan K, French SW, Morgan TR (2010) Oxidative stress and regulation of anti-oxidant enzymes in cytochrome P4502E1 transgenic mouse model of non-alcoholic fatty liver. J Gastroenterol Hepatol 25: 1136-1143.

62. Malaguarnera L, Madeddu R, Palio E, Arena N, Malaguarnera M (2005) Heme oxygenase-1 levels and oxidative stress-related parameters in non-alcoholic fatty liver disease patients. J Hepatol 42: 585-591.

CHAPTER 5

The heme oxygenase system suppresses perirenal visceral adiposity, abates renal inflammation and ameliorates diabetic nephropathy in Zucker diabetic fatty rats

Joseph Fomusi Ndisang, Ashok Jadhav, Manish Mishra

This chapter has been published as a research paper in

PLOS One, January 2014, Volume 9, Issue 1, e87936

Contribution: The article, ***PLoS One. 2014****;9(1): e87936* was co-authored with my supervisor Joseph Fomusi Ndisang and Ashok Jadhav. This chapter describes the effects of the hemin-induced HO system on perirenal visceral obesity-induced diabetic nephropathy in an obese rat model of T2D. This study collectively suggested that both visceral and perirenal obesity severely affect the renal architecture and physiological functions and participates in development of nephropathy in obese-diabetic individuals. In this condition, HO upregulation not only reduce the renal injuries but also improved renal functions and suppress the development of nephropathy. In this study, I was involved in performing the experiments and statistical analyses along with other co-authors. The idea of this study was conceived by my supervisor Joseph Fomusi Ndisang and financially supported by the Heart and Stroke Foundation of Saskatchewan, Canada grant to Dr. Ndisang.

5.1 Abstract

The growing incidence of chronic kidney disease remains a global health problem. Obesity is a major risk factor for type-2 diabetes and renal impairment. Perirenal adiposity, by virtue of its anatomical proximity to the kidneys may cause kidney disease through paracrine mechanisms that include increased production of inflammatory cytokines. Although, heme-oxygenase (HO) is cytoprotective, its effects on perirenal adiposity and diabetic nephropathy in Zucker-diabetic fatty rats (ZDFs) remains largely unclear. Upregulating the HO-system with hemin normalized glycemia, reduced perirenal adiposity and suppressed several pro-inflammatory/oxidative mediators in perirenal fat including macrophage-inflammatory-protein-1α (MIP-1α), endothelin (ET-1), 8-isoprostane, TNF-α, IL-6 and IL-1β. Furthermore, hemin reduced ED1, a marker of proinflammatory macrophage M1-phenotype, but interestingly, enhanced markers associated with anti-inflammatory M2-phenotype such as ED2, CD206 and IL-10, suggesting that hemin selectively modulates macrophage polarization towards the anti-inflammatory M2-phenotype. These effects were accompanied by increased adiponectin, HO-1, HO-activity, atrial-natriuretic peptide (ANP), and its surrogate marker, urinary-cGMP. Furthermore, hemin reduced renal histological lesions and abated pro-fibrotic/extracellular-matrix proteins like collagen and fibronectin that deplete nephrin, an important transmembrane protein which forms the scaffolding of the podocyte slit-diaphragm allowing ions to filter but not massive excretion of proteins, hence proteinuria. Correspondingly, hemin increased nephrin expression in ZDFs, reduced markers of renal damage including, albuminuria/proteinuria, but increased creatinine-clearance, suggesting improved renal function. Conversely, the HO-blocker, stannous-mesoporphyrin nullified the hemin effects, aggravating glucose metabolism, and exacerbating renal injury and function. The hemin effects were less-pronounced in Zucker-lean controls with healthy status, suggesting greater

selectivity of HO in ZDFs with disease. We conclude that the concomitant reduction of proinflammatory/oxidative mediators, macrophage infiltration and profibrotic/extracellular-matrix proteins, coupled to increased nephrin, adiponectin, ANP, cGMP and creatinine clearance may account for improved renal function in hemin-treated ZDFs. These findings suggest that HO-inducers like hemin may be explored against the co-morbidity of perirenal adiposity and diabetic nephropathy.

5.2 Introduction

Recent epidemiological data indicates that more than 1.6 billion adults worldwide are overweight and over 400 million are obese (1, 2). Obesity is a major risk factor for insulin-resistant type-2 diabetes mellitus (T2D), dyslipidemia, hypertension and impaired renal function (3-6). One of the common causes of morbidity and mortality in T1D and T2D patients is diabetic nephropathy, a micro-vascular complication of diabetes that may lead to end-stage-renal-disease (ESRD) [7]. The growing incidence of chronic kidney disease is widely recognized as a global health problem. The prevalence and incidence of ESRD is greater in patients co-morbid with obesity and diabetes (8). Moreover, perirenal adiposity is an independent predictor of kidney dysfunction in T2D (9). Thus, novel strategies that could simultaneously combat obesity, insulin resistant T2D and diabetic nephropathy are needed.

It is widely acknowledged that the site of fat accumulation may be more critical for health than the overall amount of fat tissue (10). Moreover, adipocytes from different body compartments have distinct inflammatory phenotype based on their anatomical location (10). Generally, visceral or intra-abdominal adiposity is more-malignant than subcutaneous adiposity, although, they are both implicated in the pathogenesis of obesity-related cardio-metabolic complications like insulin

resistance, T2D and renal disease (10, 11). Perirenal adiposity, in comparison to central obesity is a greater risk factor for renal complications (9). Emerging evidence indicates that perirenal adiposity may better reflect the risks commonly associated with increased visceral fat accumulation and particularly those related to impaired renal function (9). By virtue of its anatomical and functional proximity to the kidney, perirenal adiposity may be even more malignant than central adiposity. Perirenal adiposity can lead to renal impairment through paracrine mechanisms that include increased production of inflammatory cytokines including tumor necrosis factor alpha (TNF-α), interleukin (IL)-6 and IL-1β and interestingly, these cytokines are also implicated in dysfunctional glucose metabolism (12-16). Moreover, increased perirenal adiposity has been shown to compress renal vessels and renal parenchyma, causing elevated renal interstitial hydrostatic fluid with reduction of renal and tubular flow rates (17). Therefore, novel formulations capable of reducing perirenal adiposity and its deleterious cytokines are needed to safeguard renal morphology and function.

In diabetic nephropathy, the expression of nephrin is deregulated (18), and elevated levels of pro-fibrotic/extracellular matrix proteins such as collagen and fibronectin are implicated in the aberrant expression of nephrin (19). Nephrin is an important transmembrane zipper-like protein which is critical for the formation of the scaffolding of the podocyte slit diaphragm of the glomerular barrier, a structure that regulates the aperture size of the renal filtration barrier, selectively allowing the filtration of small molecules like ions, but not larger molecules like proteins (20-22). A defect in nephrin may cause massive excretion of proteins, hence proteinuria (20-22). Therefore, agents capable of reducing excessive deposition of pro-fibrotic/extracellular matrix proteins may be useful to preserve nephrin, and thus improve renal dysfunction due to proteinuria.

Although, we recently reported the insulin sensitizing and cytoprotective effects of the heme oxygenase (HO) inducer, hemin, in Zucker diabetic fatty rats (ZDFs) (23, 24), the effects of the HO system on perirenal adiposity remains largely unclear. Similarly, the effects of upregulating the HO system with hemin on macrophage polarization in renal tissue have not been reported. The two common polarized macrophage phenotypes are the pro-inflammatory M1-phenotype and anti-inflammatory M2-phenotype, and these subtypes are often referred to as classically activated macrophages (M1-macrophages) and alternatively activated macrophages (M2 macrophages) (13, 25, 26). Importantly, we will investigate whether hemin therapy can selectively modulate M1 and M2 macrophages in the kidneys to counteract inflammatory insults. Whether the effects of hemin therapy on M2 macrophage will be accompanied by increased expression of the anti-inflammatory cytokine, IL-10 (27) will also be investigated. Given that macrophage-inflammatory-protein-1α (MIP-1α) is a chemokine implicated in macrophage infiltration (28), we will also assess the effect of hemin therapy on this protein.

Therefore, this study will unveil the effects of hemin therapy on renal expression of the anti-inflammatory macrophage M2-phenotye, the pro-inflammatory macrophage M1-phenotype and related chemokines/cytokines including MIP-1α, TNF-α, IL-6 and IL-1β as well as nephrin and pro-fibrotic/extracellular matrix proteins such as collagen and fibronectin. Importantly, the effects of the HO-system on perirenal adiposity, MIP-1α, M1/M2 macrophage and nephrin in ZDFs have not been reported. Since the mechanisms by which hemin therapy improves renal function in the co-morbid conditions of obesity and insulin-resistant diabetes have not been completely characterized, this study will unmask novel effects of hemin on perirenal adiposity and diabetic nephropathy in ZDFs, and add more insights in the multifaceted complication of diabetic nephropathy.

5.3 Materials and methods

5.3.1 Animals groups and plasma measurements

The experimental protocol was approved by University of Saskatchewan Standing Committee on Animal Care and Research Ethics. Male ZDF of 12 weeks and age/sex-matched litter Zucker lean (ZL) rats were purchased from Charles River (Willington, MA, USA). The animals were housed at 21°C with 12-hour light/dark cycles, fed with fed with Purina 5008 diet and had access to drinking water *ad libitum*. After a week of acclimation, the animals were randomly assigned to the following experimental groups: (A) controls (ZDF and ZL), (B) hemin-treated ZDF, (C) hemin-treated ZL, (D) ZDF treated with hemin and the HO inhibitor, stannous mesoporphyrin (SnMP), (E) ZDF treated with SnMP alone, and (F) ZDF and ZL treated with vehicle dissolving hemin and SnMP. Hemin (15 mg/kg i.p.) and SnMP (5 mg/100 g body weight, i.p.) were prepared and administered twice weekly for a duration of 8 weeks as we previously described (24, 29, 30). Fasting glucose was monitored weekly with a diagnostic auto-analyzer (BD, Franklin Lakes, NJ) after 6 hrs of fasting as previously reported (31-34). At the end of the 8-week treatment, the animals were placed in metabolic cages for 24 hrs urine collection. Proteinuria, albuminuria and creatinine were measured as previously reported (35). A day prior to killing, the animals were weighed, anaesthetized with pentobarbital sodium (50 mg/kg i.p.), killed and the perirenal fat pads dissected free, blotted off water and weighed using an analytical balance (Precisa XR 205SM-DR, Precisa Instruments Ltd, Switzerland).

5.3.2 HO-1 concentration and HO activity assay

HO activity in the perirenal adipose tissue was measured as bilirubin production using our established method (24, 36, 37). Briefly, the perirenal fat was homogenized on ice in 4 volumes

of 5:1 K/Na 100 mmol/L phosphate buffer with 2 mmol/L $MgCl_2$ (HO-activity buffer), centrifuged at 13,000 rpm for 15 minutes. Aliquots of 100 µl were collected from the supernatant and transferred into another beaker containing 500 µl of a mixture of 0.8 mmol/L nicotinamide dinucleotide phosphate, 20 µmol/L hemin, 2 mmol/L glucose-6-phosphate, 0.002 U/µl glucose-6-phosphate dehydrogenase and 100 µl liver cytosol as source of biliverdin reductase. The reaction was done in darkness for 1 hour at 37°C, and was stopped by adding 500 µl of chloroform.

Thereafter, bilirubin was extracted by vigorously agitating the tubes and centrifuging at 13,000 rpm for 5 minutes, and the chloroform layer collected and read on a spectrophotometer at 464 nm minus the background at 530 nm. The amount of bilirubin in each sample was determined spectrophotometrically (extinction coefficient for bilirubin 40 $mM^{-1}cm^{-1}$), and expressed as nmole/mg protein/hour. The protein content was measured using Bradford assay. As a positive control, spleen tissue was used.

Perirenal fat HO-1 concentration was determined by enzyme-linked immunosorbent assay (ELISA) (EKS-810A, Stressgen-Assay Design, Ann Arbor, MI, USA) according to the manufacturer's instructions as we previously reported (34, 38, 39).

5.3.3 Histological, morphological and immunohistochemical analyses of kidney tissue

Histology and morphometric analyses were done as we previously described (40). Whole kidney sections of 5 µm were cut and treated with Masson's trichrome staining to assess collagen deposition. Morphologic assessment of collagen deposition was determined by a blinded researcher using a virtual microscope (Aperio Scan Scope Model CS, Aperio Technology Inc, CA), and analyzed using Aperio Image Scope V11.2.0.780 software (Aperio, e-Pathology Solution, CA). Each kidney section was magnified at 200x, and 20 random snaps were taken per

slide per group of 4-6 animals (80-120 images per group), and subsequently scored semi-quantitatively by a blinded researcher as we previously reported (29, 40).

Immunohistochemistry was done as we previously reported (35). Sections of 5 µm of whole kidney sections were treated with bovine serum albumin in phosphate buffered saline to block non-specific staining and incubated overnight with ED1 (1:500 dilution, sc-59103, Santa Cruz Biotechnology, CA, USA) or HO-1 (1:200 dilution, OSA-150, Stressgen Biotechnologies, Ann Arbor, MI, USA). Thereafter, the kidney sections were incubated with goat anti-mouse IgG for 30 min (1:200 dilution; Jackson ImmunoResearch Laboratories, Inc., ME, USA). Immunohistochemical staining was performed using the standard avidin-biotin complex method with the chromagen 3,3′-diaminobenzidine (DAB) used at the final detection step. The kidney sections were scanned using a microscope (Aperio Scan Scope Model CS, Aperio Technology Inc, CA). Macrophages (brown from immune-stained sections) were quantified by manually counting the positively stained cells under a standard light microscope under 200X magnification in 20-22 randomized non-overlapping fields in the cortical region of kidney section, macrophages were infiltrated between intertubular spaces, in the glomeruli and perivascular region.

5.3.4 Western immunoblotting

The kidney was homogenized (1:10, w:v) in 10 mM Tris-buffered saline (20 mM Tris-HCl, pH 7.4, 0.25 M sucrose, and 1 mM EDTA) in the presence of freshly prepared cocktail of protease inhibitors, centrifuged, and proteins extracted as we previously described (36, 41). The proteins were extracted and quantified by Bradford assay, and aliquots of 50 µg were loaded on SDS-polyacrylamide gel.

The fractionated proteins were electrophoretically transferred to nitrocellulose paper and non-specific bindings blocked with 3% non-fat milk, and incubated overnight with primary antibodies against ED1, ED2, CD206, IL-10, nephrin, collagen-IV, and fibronectin (Santa Cruz Biotechnology, CA, USA). Anti-mouse glucose-6-phosphate dehydrogenase (G6PDH) antibody (Sigma St Louis, MO, USA) was used as control (42, 43) to ascertain equivalent loading. After washing, blots were incubated with anti-rabbit IgG conjugated to horseradish peroxide (Bio-Rad, CA, USA), and the immuno-reactivity visualized using enhanced horseradish peroxide/luminol chemiluminescence reagent (Perkin Elmer Life Sciences, Boston, MA, USA). Densitometric analysis was done with UN-SCAN-IT software (Silk Scientific, Utah, USA).

5.3.5 Determination of endothelin-1

Perirenal fat ET-1 was determined by EIA (Cayman Chemical, Ann Arbor, MI, USA) as we previously reported (38, 39). This immunometric assay is based on a double-antibody 'sandwich' technique that detects ET-1 within the range of 0-250 pg/ml. In brief, supernatants from homogenized perirenal fat tissues were purified by cold spike extraction, concentrated and the absorbance read at 405 nm in a plate reader (SpectraMax 340PC, Molecular Device, CA, USA) as we previously reported (29).

5.3.6 Determination of TNF-α, IL-6 and IL-1β

Perirenal fat TNF-α, IL-6 and IL-1β were assessed by ELISA (Immuno-Biological Laboratories Co Ltd, Takasaki-shi, Gunma, Japan) according to the manufacturer's instructions and read at 450 nm in a plate reader (SpectraMax 340PC, Molecular Device, CA, USA) as we previously reported (29).

5.3.7 Determination of 8-isoprostane

8-isoprostane is a non-invasive index of oxidative stress. This was determined by EIA (Cayman Chemical, Ann Arbor, MI) as we previously reported (37). The tissues were homogenized in phosphate buffer containing 0.005% butylated hydroxy toluene in a ratio of 10 µL buffer/mg tissue. Subsequently, an equal volume of 15% KOH was added to the homogenate. The samples were incubated at 40°C for an hour, followed by centrifugation, and the supernatant neutralized with KH_2PO4 and the absorbance read at a wavelength of 412 nm in a microplate reader (SpectraMax 340PC, Molecular Device, CA, USA) and expressed as picograms per milligram of protein.

5.3.8 Determination of atrial natriuretic peptide (ANP)

Perirenal fat ANP was quantified by EIA (Cayman Chemical, Ann Arbor, MI, USA) as we previously reported (38). This assay is based on the competition between unlabeled rat ANP and a tracer, acetylcholinesterase, linked to rat ANP for limited specific rabbit anti-rat ANP antiserum sites. The complex rabbit antiserum-rat ANP (free ANP or tracer) binds to the mouse monoclonal anti-rabbit antibody that is attached to a well. Briefly, supernatants from homogenized tissue were aliquoted wells containing unlabeled rat ANP and a tracer. After washing, Ellman's Reagent (enzymatic substrate for acetylcholinesterase) and a chromogen added to the wells forming a yellow coloration that was read at 405 nm in a plate reader (SpectraMax 340PC, Molecular Device, CA, USA).

5.3.9 Measurement of cGMP

The concentration of urinary cGMP was measured by EIA (Cayman Chemical, Ann Arbor, MI, USA) as previously described (36, 44). Urine samples were treated with 6% trichloroacetic acid at 4°C in the presence of 3′-isobutyl-1-methylxanthine to inhibit phosphodiesterase activity and centrifuged at 2000 g for 15 mins. The supernatant was recovered, washed three times with water-saturated diethyl ether and the upper ether layer was aspired and discarded while the aqueous layer containing cGMP was recovered and lyophilized. The dry extract was dissolved in 1 ml assay buffer and the cGMP content measured according to the manufacturer's protocol and expressed as picomol per mg of protein.

5.3.10 Determination of macrophage-inflammatory-protein-1α (MIP-1α)

The concentration of MIP-1α was determined in homogenized perirenal and kidney tissues using ELISA kits (OmniKine™, Assay Biotechnology Company Inc, Sunnyvale, CA). All samples were assayed in triplicates following the manufacturer's instructions.

5.3.11 Determination of Plasma Adiponectin

Adiponectin was measured by ELISA (Phenix Pharmaceuticals, Inc, Burlingame, CA, USA) as we previously reported (23, 31-33). In brief, plasma was aliquoted into wells of a microplate containing adiponectin antibody, followed by treatment with horseradish peroxidase-conjugated secondary antibody and streptavidin. Thereafter, the absorbance was read at 450 nm with a microplate (SpectraMax-340PC, Molecular Device, CA, USA).

5.3.12 Statistical analyses

All data are expressed as means ± SEM from at least four independent experiments unless otherwise stated. Statistical analyses were done using two-way ANOVA and Student's *t-test*. Group differences at the level of $p<0.05$ were considered statistically significant.

5.4 Results

5.4.1 Hemin therapy abated perirenal adiposity and reinstated normoglycemia in ZDFs

The administration of hemin to ZDFs significantly reduced perirenal adiposity (Table 5-1). This was accompanied by a parallel reduction of hyperglycemia to normal levels (26.8 ± 4.9 vs 7.1 ± 1.5 mmol/L, $p<0.01$). In contrast, the co-administration of hemin and the HO-blocker, SnMP abolished the effect of hemin on perirenal adiposity and blood glucose, whereas treatment with SnMP alone aggravated perirenal adiposity and hyperglycemia suggesting a role of the HO system on the regulation of perirenal adiposity and glucose metabolism. The vehicle dissolving hemin and SnMP had no effect on blood glycemic and perirenal adiposity (Table 5-1).

Hemin therapy was also administered to ZL control rats. In hemin-treated ZLs, a slight but significant reduction of perirenal adiposity and blood glucose was observed (Table 5-1). In hemin-treated ZDFs, perirenal adiposity and glycemia were reduced by 56.1 and 73.5% respectively whereas in ZLs these same parameters were reduced by 21.9 and 11.4% respectively. These effects were abolished by the HO-blocker, SnMP. Interestingly, the effect of hemin was more-intense in unhealthy ZDFs than in the healthy ZLs, suggesting greater selectivity of the actions in ZDFs with disease.

Hemin and SnMP treatment caused a small reduction of body-weight (<9%) (Table 5-1). In ZL + hemin, ZDF + hemin, and ZDF + hemin + SnMP the loss of body-weight were 2.3, 4.6

and 8.7% respectively. Although, body-weight loss may cause reduction of glycemia, it is unlikely in this case because the slight body-weight loss in hemin- and SnMP-treated animals were accompanied by opposite effects on glycemia; that is a reduction of glycemia in hemin-treated animals, but an increase in SnMP-treated animals (Table 5-1), suggesting that the HO system may be endowed with intrinsic anti-diabetic effects. The loss of body-weight may not be due to toxicity since we recently showed that indices of toxicity such as plasma alanine aminotransferase, gamma-glutamyltransferase and aspartate aminotransferase and were within normal range (23).

In order to examine the role of the HO system on renal function, important indices of renal function including urinary proteins like proteinuria and albuminuria (34) were assayed. Our results indicate that the levels of proteinuria and albuminuria were significantly elevated in untreated ZDFs (Table 5-1). Interestingly, hemin therapy markedly abated proteinuria and albuminuria by 74 and 64% respectively, whereas co-treatment of hemin and SnMP abolished the effects of hemin, while treatment SnMP alone exacerbated the excretion of these urinary proteins (Table 5-1). Furthermore, hemin therapy enhanced creatinine clearance in ZDFs, and thus improved renal function, whereas the HO-inhibitor, SnMP, nullified the effects of hemin on creatinine clearance. The vehicle dissolving hemin and SnMP had no effect on any of the measured parameters measured in ZDFs and ZLs.

5.4.2 Hemin therapy enhanced HO-1 and HO activity in perirenal adipose tissue of ZDFs

To investigate the role of the HO system on perirenal adiposity and diabetic nephropathy, we measured HO-1 concentration and HO activity. Our results indicate that the basal levels of HO-1 and HO-activity in control-ZDFs were significantly reduced as compared to control-ZLs (Figs. 5-1A and 5-1B**)**. Interestingly, hemin therapy greatly enhanced the depressed levels of HO-1 and

HO activity in ZDFs, whereas the co-treatment with the HO inhibitor, SnMP reversed the effects of the HO inducer, hemin, while treatment with SnMP alone depleted the basal levels of HO-1 and HO activity (Figs. 5-1A and 5-1B).

Hemin therapy also enhanced the levels of HO-1 and HO activity in ZL rats, although, a greater increment was observed in hemin-treated ZDFs (Figs. 5-1A and 5-1B). In hemin-treated ZLs, HO-1 and HO-activity were increased by 3.8-and 2.6-fold respectively, while the increment observed in ZDFs for HO-1 and HO-activity were 13.5- and 11.2-fold respectively. The higher increment of HO-1 and HO-activity may account for the more accentuated effects against hyperglycemia and nephropathy observed in ZDFs (Table 5-1). The vehicle dissolving hemin and SnMP had no effect on HO-1 and HO-activity in ZDFs and ZLs.

5.4.3 Hemin therapy abated 8-isoprostane and ET-1 in perirenal adipose tissue of ZDF

Given that elevated oxidative stress is among the causative factors of insulin resistance and tissue dysfunction, we measured 8-isoprostane, an important marker of oxidative stress (45). Moreover, ET-1 is implicated in cardiac and renal insufficiency (46). In untreated ZDFs, the basal levels of perirenal adipose tissue 8-isoprostane were markedly elevated, suggesting enhanced oxidative stress (Fig. 5-2A). However, hemin therapy significantly reduced the elevated levels of 8-isoproatane by in ZDFs, whereas the co-treatment of hemin with SnMP nullified the effects of hemin while treatment with SnMP alone further increased 8-isoprostane levels, suggesting that oxidative stress is further potentiated by blockade of basal HO activity (Fig. 5-2A). Hemin therapy also reduced 8-isoprostane in ZL rats, although, less-intensely as compared to ZDFs. In hemin-treated ZLs, 8-isoprostane was reduced by 2.7-fold as compared to a reduction of 3.3-fold in hemin-treated ZDFs (Fig. 5-2A).

Since 8-isoprostane stimulates ET-1 (47), and both ET-1 and 8-isoprostane are involved in the oxidative destruction of tissue, we also measured ET-1 in perirenal adipose tissue. Our results indicate that the levels of ET-1 in untreated ZDFs were significantly elevated as compared to the control-ZLs (Fig. 5-2B). Interestingly, hemin therapy significantly abated the elevated levels of ET-1 in ZDFs, while co-treatment of hemin and SnMP annulled the effect of hemin (Fig. 5-2B), whereas, treatment with SnMP alone further accentuated the levels of ET-1. Hemin therapy also reduced ET-1 in ZLs although, to a lesser magnitude as compared to ZDFs. Accordingly, a reduction of 2.2-fold of ET-1 was observed in hemin-treated ZLs as compared to 2.8% hemin-treated ZDFs. The vehicle dissolving hemin and SnMP had no effect on 8-isoprostane and ET-1 in ZDFs and ZLs.

5.4.4 Hemin therapy suppressed pro-inflammatory cytokines in perirenal adipose tissue

TNF-α, IL-6 and IL-1β are cytokines that impair renal function and glucose metabolism (12-15), so we investigated whether the improvement of renal function and glucose metabolism in hemin-treated ZDFs would be accompanied by reduction of these cytokines. Our results indicate that the levels of TNF-α, IL-6 and IL-1β in perirenal adipose tissue of untreated ZDFs were significantly elevated as compared to control-ZLs (Fig. 5-3A, 5-3B and 5-3C). Treatment with hemin greatly reduced TNF-α, IL-6 and IL-1β, whereas the co-application of the HO-inhibitor, SnMP with hemin reversed the effects of hemin, while treatment of SnMP alone further increased the levels of these cytokines. Hemin therapy also reduced the levels of TNF-α, IL-6 and IL-1β in the ZLs, although, less intensely. A reduction of 1.7-, 1.9-, and 2.5-fold of TNF-α, IL-6 and IL-1β respectively was observed in hemin-treated ZLs as compared to 2.2-, 2.6-, and 3.0-fold in hemin-

treated ZDFs. The vehicle dissolving hemin and SnMP had no effect on TNF-α, IL-6 and IL-1β in ZDFs and ZLs.

5.4.5 Hemin therapy potentiated ANP, its surrogate marker, urinary cGMP and adiponectin

Given that ET-1 and ANP interact reciprocally (48), we investigated whether the hemin-induced reduction of ET-1 will affect the levels of ANP. Our results indicate that the reduction of ET-1 (Fig. 5-2B) by hemin was accompanied by the concomitant potentiation of ANP levels (Figs. 5-4A)**.** Consistently, urinary cGMP, a surrogate marker of ANP (49) was significantly increased by hemin, while co-treatment with the HO-inhibitor, SnMP reversed the effects of hemin (Fig. 5-4B), whereas, treatment with SnMP alone further depleted the basal levels of urinary cGMP.

Since adiponectin is an anti-inflammatory protein (50) with renoprotective effects and insulin sensitizing effects (51, 52), we investigated the effects of hemin on adiponectin in ZDFs. In ZDFs, the basal levels of adiponectin were depressed (Fig. 5-4C). Interestingly, hemin therapy significantly enhanced adiponectin (Fig. 5-4A). In contrast, co-treatment of hemin with the HO-inhibitor, SnMP annulled the hemin effects on adiponectin, while treatment with SnMP alone further reduced the levels of adiponectin. The vehicle dissolving hemin and SnMP had no effect on ANP and urinary cGMP.

5.4.6 Hemin therapy abated MIP-1α in perirenal adipose tissue and kidneys

To further evaluate the effects of the HO system on macrophage infiltration, we determined the levels of MIP-1α, a chemokine implicated in macrophage infiltration (28). The basal levels of MIP-1α in perirenal adipose tissue from control ZDFs were significantly elevated as compared to the ZL controls (Fig. 5-5A). Interestingly, treatment with hemin greatly attenuated the high levels

of MIP-1α in ZDFs although, comparable levels in ZL-controls were not reinstated. In contrast, the co-application of the HO-inducer, hemin with the HO-blocker, SnMP abolished the effects of hemin (Fig. 5-5A). Similarly, treatment with the SnMP alone exacerbated the levels of perirenal MIP-1α (Fig. 5-5A).

We also investigated the effects of hemin on kidney MIP-1α levels. In kidney tissues from control ZDFs, MIP-1α was markedly elevated as compared to ZL control rats (Fig. 5-5B), but was significantly attenuated by hemin therapy. On the other hand, the co-administration of SnMP and hemin nullified the effects of hemin (Fig. 5-5B), while SnMP alone further increased the levels of MIP-1α in ZDFs. It is noteworthy that hemin appeared to be more effective in the abrogating kidney MIP-1α as the hemin-dependent reduction of MIP-1α reinstated comparable levels as observed in ZL control rats. The reasons for this selective effect remain unclear, although, tissue selectivity might be implicated.

Hemin therapy also reduced MIP-1α in perirenal adipose tissue and the kidney from ZL control rats (Figs. 5-5A and 5-5B). The vehicle dissolving hemin and SnMP had no effect on MIP-1α in ZDFs and ZLs.

5.4.7 Hemin therapy abated inflammatory proteins implicated in insulin resistance and renal dysfunction

Given that macrophage infiltration is implicated in the development of insulin-resistant T2D and kidney dysfunction (13, 53-56) we used specific markers such as ED1 to quantify the pro-inflammatory M1-phenotype, and ED2, CD206 and IL10 for the assessment of anti-inflammatory M2-phenotype (27, 56-58) Our Western immunoblotting and relative densitometric analyses revealed that the basal expression of ED1 in the kidneys of ZDF-controls were significantly

elevated (Fig. 5-6A). Interestingly hemin therapy significantly attenuated the elevated expression of the pro-inflammatory M1-phenotype marker ED1 and restored ED1 to comparable levels as observed in ZL-controls (Fig. 5-6A). To determine whether the suppression of the pro-inflammatory M1-phenotype by hemin would be accompanied by changes in the anti-inflammatory M2-phenotype, we determined the expression of macrophage-M2 using specific M2 markers such as ED2, CD206 and IL-10. Our results indicate that the basal expression levels of ED2, CD206 and IL-10 were markedly reduced in ZDF-controls as compared to ZL-controls. Interestingly, hemin therapy robustly enhanced the depressed basal expressions of ED-2 (Figs. 5-6B), CD206 (Figs. 5-6C) and, IL-10 (Figs. 5-6D), suggesting that hemin therapy may selectively modulate the polarization of macrophage toward the M2-phenotype that dampens inflammation. It is noteworthy that hemin therapy reinstated ED2 and IL-10 to the levels of ZL-controls, but enhanced CD206 to levels even beyond ZL-controls. Hemin therapy also reduced ED1 in ZLs, and enhanced CD206 and IL-10, but did not affect ED2 in ZLs.

5.4.8 Hemin therapy suppresses pro-fibrotic proteins in the kidney but enhanced nephrin

To further explore the mechanisms by which hemin therapy reduces proteinuria, and thus improve renal function, we assessed the expression levels of nephrin, an important transmembrane protein which forms the scaffolding of the podocyte slit diaphragm, a structure that regulates the aperture size of the renal filtration barrier, allowing the filtration of small molecules like ions, but not larger molecules like proteins (18). A defect in nephrin causes massive excretion of proteins, hence proteinuria (18).

Our Western immunoblotting data indicates that in ZDF-controls, the basal expression of nephrin in the kidneys was markedly depressed as compared to the ZL-controls (Fig. 5-7A), and

this coincided with marked increased in proteinuria and albuminuria, suggesting renal dysfunction (Table 5-1). However, treatment with hemin robustly enhanced the depressed expression of nephrin in ZDFs (Fig. 5-7A), reinstating comparable levels as observed in ZLs, with reduction of proteinuria and albuminuria (Table 5-1), and thus improved renal function. Hemin therapy did not affect the expression of nephrin in the healthy ZLs.

Since, the expression of nephrin is deregulated in diabetic nephropathy (18, 56), and elevated levels of pro-fibrotic/extracellular matrix proteins such as collagen and fibronectin are implicated in the aberrant expression of nephrin (19, 56), we investigated the effects of hemin therapy on the expression of collagen-IV and fibronectin. Our results indicate that in ZDFs, the basal expression levels of collagen-IV and fibronectin were significantly elevated as compared to the ZL-controls (Figs. 5-7B and 5-7C). Interestingly, the administration of hemin to ZDFs significantly reduced the elevated expression of collagen-IV and fibronectin to levels even lower than in the ZL-controls (Figs. 5-7B and 5-7C). Hemin therapy also reduced fibronectin expression in ZLs, but did not affect collagen-IV in ZLs. The reason for this selective effect is unknown, and should be further investigated. It is important to note that although hemin reduced fibronectin in healthy ZLs, it was more effective in unhealthy ZDFs because fibronectin was reduced by 4.3-fold in ZDFs as opposed to 1.5-fold in ZLs.

5.4.9 Hemin therapy suppressed renal fibrosis

Histological study using Masson's trichrome staining and morphometric analyses were done to further confirm the renoprotective effects of hemin. As observed in (Fig. 5-8A), ZDF-controls displayed severe tubulo-interstitial, perivascular and glomerular fibrosis around the cortex and medullar as compared to ZL-controls. Similarly, kidney sections from ZDF-controls showed

tubular vacuolization and glomerulosclerosis. Interestingly, these renal lesions were greatly attenuated by hemin therapy as hemin-treated ZDFs showed reduction of glomerular, tubulo-interstitial and perivascular fibrosis. Correspondingly, semi-quantitative analysis showed that hemin therapy significantly abated the elevated collagen deposition and perivascular fibrosis in ZDFs, reinstating similar levels as observed in ZL-controls (Fig. 5-8B).

5.4.10 Hemin therapy suppressed macrophage infiltration in renal tissue by abating ED1

Since data from our Western immunoblot experiment indicated that hemin therapy abated ED1 expression in the kidney (Fig. 5-6A), we use the ED1 antibody to determine macrophage infiltration in the kidneys by immunohistochemistry (Fig. 5-9A). Our results indicate that kidney sections from ZL-controls were almost devoid of the dark brown ED1 positive staining that characterizes macrophage infiltration. However, in untreated ZDF-controls, greater numbers of ED1 positive staining for macrophage was observed in several structures located in the cortex and medullar of the kidney including the tubulointerstitial, perivascular and glomeruli as compared to ZL-controls (Fig. 5-9A and 5-9B). Interestingly, in hemin-treated ZDFs, there was a significant reduction in the number of ED1 positively stained macrophage, suggesting reduction of macrophage infiltration. Correspondingly, hemin therapy significantly reduced the quantitative ED1 score of kidney sections (Fig. 5-9B), although, the levels of ZL-controls were not reinstated.

5.4.11 Immuno-labeling of HO-1 shows elevated HO-1 in tubulointerstitial, perivascular area and around the glomeruli of hemin-treated ZDFs

To further confirm the localization of HO-1 in the kidney, we did immunohistochemistry. Our immunohistochemical data shows very little expression of HO-1 was observed in kidney

tissues of ZDF control (Fig. 5-10). However, in hemin-treated ZDF, HO-1 was very conspicuous and widely expressed in the renal parenchyma, with particularly high expressions in the tubulointerstitium, perivascular area and around the glomeruli.

5.5 Discussion

The present study unveils several novel findings. These include (i) the hemin-induced enhancement of the anti-inflammatory macrophage M2-phenotype and corresponding reduction of the pro-inflammatory M1-phenotype; (ii) the suppression of perirenal adiposity and MIP-1α, a chemokine implicated in macrophage infiltration; (iii) the enhancement of nephrin, of nephrin, an important transmembrane protein critical for the formation of the podocyte slit diaphragm that regulates the aperture size of the glomerular filtration barrier, selectively allowing the filtration of small molecules like ions, but not larger molecules like proteins; and (iv) the corresponding reduction of proteinuria and albuminuria that was, interestingly, accompanied by increased creatinine clearance and thus improved renal function in ZDFs. The role of nephrin in glomerular filtration cannot be overemphasized. A defect in nephrin may cause massive excretion of proteins, hence proteinuria and renal dysfunction (20-22, 56). It is possible that in ZDFs, the high levels of profibrotic/extracellular matrix proteins would aggravate histological renal lesions, and this defect was evidenced by increased tubular vacuolization, glomerulosclerosis with severe tubulo-interstitial, perivascular and glomerular fibrosis, all of which pathophysiological factors that together with the aberrant expression of nephrin may account for proteinuria and renal impairment. Therefore, another important observation from our study is that hemin therapy significantly reduced the expression of pro-fibrotic/extracellular matrix proteins such as collagen and fibronectin. Moreover, excessive collagen and fibronectin are among the factors that deplete

nephrin (17), a zipper-like protein that plays a fundamental role in the formation of the podocyte slit diaphragm of the glomerular barrier (18-20).

Although, it is widely acknowledged that obesity and insulin resistant T2D are common causes of diabetic nephropathy and renal failure (3-5, 7), emerging evidence indicate that the anatomical location of adiposity reflects its adversity (10). Therefore, the presence of excessive visceral adipose tissue like perirenal adiposity may constitute an independent prognostic factor of kidney malfunction in T2D (9). Thus, the concomitant suppression of perirenal adiposity alongside the reduction of macrophage infiltration, the abrogation of mediators of oxidative stress like 8-isoprostane and ET-1 (45, 59), and the attenuation of pro-inflammatory cytokines like TNF-α, IL-6 and IL-1β (12-15) in perirenal adipose tissue by hemin are among the multifaceted mechanisms by which the HO system attenuates renal damage. In addition, the selective enhancement of anti-inflammatory M2-phenotype macrophage and corresponding reduction of the pro-inflammatory M1-phenotype in renal tissue from hemin-treated animals may be indicative of a novel mechanism by which the HO system counteracts tissue inflammation. In addition, it may also suggest a role of hemin therapy in the modulation of macrophage polarization.

During inflammation blood monocytes are recruited into the tissues where they differentiate into macrophages. Macrophage heterogeneity is a well-known phenomenon (13, 25, 26). Generally, macrophages heterogeneity reflects the specialization of tissue-resident macrophages in the different microenvironments in distinct tissues like liver, adipose tissue, kidney and other tissues (25, 26). Within such microenvironment, macrophages can acquire distinct functional phenotypes (25, 26). Importantly, macrophage polarization is driven by a wide variety of stimuli and signals in the tissue microenvironment, and these stimuli include cytokines, growth factors and other agents (25, 26). The presence of these signals dictates the transcriptional

response that shapes the phenotype and function of the macrophages on the basis of the physiological or pathophysiological role acquired by the macrophage in a given tissue (25, 26). Therefore, changes in the levels of the pro-inflammatory cytokines observed in hemin-treated animals may be responsible for the selective enhancement of the anti-inflammatory M2-phenotype. Moreover, during macrophage polarization, there is a switch of the gene expression program from a pro-inflammatory M1 signature to an anti-inflammatory M2-phenotype, depending on the tissue microenvironment and the presence of different stimuli including cytokines (25, 26). Interestingly, hemin therapy suppressed the levels of several cytokines including TNF-α, IL-6 and IL-1β, and thus there is a possibility that in the microenvironment of the perirenal adipose tissue, the abrogation of these cytokines may account for the selective polarization of macrophage towards the anti-inflammatory M2-phenotype. Nevertheless, these preliminary observations made in this study are just the tip of an iceberg and more-intense research is needed to address the many challenging questions that would be necessary for characterizing the role of the HO system in macrophage polarization. Moreover, the suppression of macrophage infiltration and reduction of extracellular matrix/profibrotic proteins reported here are consistent with previous studied showing that upregulating the HO system is renoprotective (35, 56, 60).

Besides the selective enhancement of M2-phenotype, other mechanisms may account for the suppression of inflammation in hemin treated animals. These include the potentiation of ANP and the enhancement of adiponectin (50, 61, 62). Interestingly, our results indicate that hemin therapy enhanced ANP and its surrogate marker, urinary cGMP (49), and adiponectin has been shown to enhance cGMP (63). The stimulation of cGMP is an important mechanism by which ANP elicit its effects (64). Given that impairment of cGMP-signalling leads to anti-thy1 glomerulonephritis (65), and the cGMP-signal transduction pathway has been shown to abate

inflammation (66), the enhancement of ANP and cGMP by hemin may counter-regulate the effects of elevated renal inflammation to improve renal function. Thus, the cGMP secondary messenger system is a common denominator between the HO system, ANP and adiponectin. Therefore, the HO-adiponectin-ANP axis may constitute a synergistic protective axis with relevance for tissue defence and glucose metabolism. Moreover, hemin therapy may also abate inflammation and improve glucose metabolism by enhancing adiponectin, an anti-inflammatory protein with renoprotective and insulin sensitizing effects (50-52, 67-69). Given that an ANP-mediated reduction of TNF-α, IL-6 and IL-1β have been linked to reduced insulin resistance (61), the suppression of these cytokines and potentiation of HO-adiponectin-ANP axis is important for enhanced glucose metabolism and improved kidney function observed in ZDFs. Therefore, the multifaceted mechanisms responsible for the renoprotection evoked by hemin include the potentiation of the HO system and related cellular targets like cGMP, ANP and adiponectin, which interestingly was accompanied by the reduction of collagen and fibronectin. The HO-adiponectin-ANP axis may suppress the adverse effects of ET-1. The interaction between ET-1 and ANP is well known (48). For example, ANP inhibits ET-1 (70), and interestingly, the hemin-induced increase of ANP was accompanied by a parallel reduction of ET-1. On the other hand, ANP attenuates fibrosis by abating extracellular matrix/profibrotic proteins including fibronectin and TGF-β1 (70), while ET-1 acts in concert with TGF-β1 to stimulate fibronectin synthesis (71). Since ANP can also stimulate the production of adiponectin (72), a cytoprotective adipokine with anti-inflammatory effects (50), and the present study indicates that hemin therapy enhances adiponectin and ANP but abates ET-1 with the reduction of renal fibrosis, it could be envisaged that the potentiation of the HO-adiponectin-ANP axis is an important renoprotective mechanism.

Our study also indicates that the effect of hemin therapy was less-pronounced in ZL-control rats with healthy status, suggesting greater selectivity of the HO system in ZDFs with disease. Alternatively, the HO system in healthy ZL-control rats may be more stable given that HO-1 and HO-activity in ZDFs were depressed as compared to ZLs, and interestingly, the effect of hemin on HO-1 and HO-activity was more accentuated in ZDFs than ZLs. It is also possible that the higher magnitude of HO-signalling in hemin-treated ZDFs may be responsible for the more intense anti-diabetic and reno-protective effect in ZDFs as compared to ZLs. This is reflected in the physiological variables measured (Table 5-1). In hemin-treated ZDFs, fasting glucose, perirenal adiposity, proteinuria and albuminuria were reduced by 73.5, 56.1, 74.1 and 64.6% respectively, while creatinine clearance was increased by 41.7%. On the other hand, fasting glucose, perirenal adiposity, proteinuria and albuminuria were only reduced in hemin-treated ZLs by 11.4, 21.9, 5.9 and 17.4% respectively, with only a 4.7% increase in creatinine clearance. It is important to note that although, these physiological variables in ZLs were affected by hemin, they were still within the acceptable physiological range. Similarly, most of the other biochemical parameters measured in this study were more accentuated in hemin-treated ZDFs than hemi-treated ZLs. Therefore, the hemin-mediated changes in physiological variables and biochemical parameters reported in this study are more intense in unhealthy ZDFs than healthy ZLs, suggesting greater selectivity of hemin in diseased conditions. Nevertheless, further investigations need to clarify the selectivity of hemin therapy in unhealthy ZDFs.

Immunohistochemical labeling of HO-1 in kidney has been widely reported (60, 73-75). These studies indicate that HO-1 is expressed all over the renal parenchyma, with higher levels in tubular epithelial cells, vascular wall smooth muscle cells and the interstitium of the cortex and medulla (60, 73-75). Consistently, our immunohistochemical results show high HO-1 expression

in many areas of the renal parenchyma including the tubulointerstitium and perivascular area of the cortex and medullar. Interestingly, these areas intense HO-1 expression coincided with areas of the kidney where lesions were hemin therapy significantly reduced histopathological lesions. Moreover, in our study, renal lesions and kidney insufficiency was associated with severe histopathological lesions in tubular epithelial cells, the interstitium and other regions of the cortex and medullar in untreated ZDFs. These renal lesions were evidenced by increased tubular vacuolization, glomerulosclerosis with severe tubulo-interstitial, perivascular and glomerular fibrosis, and were associated with elevated macrophage infiltration and increased deposition of collagen, an extracellular matrix protein in untreated ZDFs. Moreover, the elevated collagen deposition in untreated ZDFs was associated with increased expression of fibronectin, another extracellular matrix protein that together with collagen are known to deplete nephrin causing proteinuria and renal insufficiency (19-22, 56). Given that previous studies have reported increased HO-1 expression in the interstitium and tubular epithelium of the cortex following the administration of HO-inducers (60, 74), and incidentally the interstitium and tubular epithelium were among the areas with significant lesion in untreated ZDF, the present study and previous reports in literature strongly suggest that the HO system alleviates not only tubulo-interstitial injury, but also suppress perivascular and glomerular fibrosis to improve renal function.

Generally, HO-1 is activated by a wide variety of physical, chemical and pathophysiological stimuli (76-81). Accordingly, HO-1 may be considered a sensitive index that is triggered during the onset of pathophysiological alterations in tissues as an attempt to counteract the adverse changes. However, the pathophysiological activation of HO-1 has been shown to evoke only a transient or sub-threshold value of HO-activity that is incapable of activating important downstream signaling components of the HO system like cGMP (36, 41, 56, 80, 82-85), suggesting

the necessity for a more robust enhancement of HO-1 by pharmacological agents like cobalt proptoporphyrin and hemin (36, 41, 82-85). Thus, the transient up-regulation of HO-1 that accompanies many pathophysiological conditions may represent the first line of defense mounted by the HO system against tissue injury. Accordingly, the high expression of HO-1 in interstitial macrophages and tubular epithelial cells reported in the cortex and outer medullar regions of dysfunctional kidneys (60, 73) may be indicative of the manifestation of pathophysiological alterations in the kidneys. Similarly, in our study we observed renal insufficiency characterized by elevated proteinuria/albuminuria and reduced creatinine clearance in untreated ZDFs. However, these renal defects were attenuated by potentiating the HO system and its downstream signaling molecule cGMP by hemin therapy.

Collectively, the present findings indicate that the concomitant enhancement of ANP, cGMP, adiponectin and creatinine clearance, alongside the corresponding reduction of perirenal adiposity and the suppression of pro-inflammatory/oxidative mediators, macrophage infiltration, albuminuria and proteinuria may account for the improved glucose metabolism and improved renal function in hemin-treated ZDFs. These data suggest that HO-inducers like hemin may be explored against the co-morbidity of perirenal adiposity and diabetic nephropathy.

5.6 Limitations

Although, the present study underscores the renoprotective effects of hemin therapy in diabetic nephropathy, and suggest that the suppression of extracellular matrix proteins like collagen-IV and fibronectin in hemin-treated ZDF are accompanied by increased expression of nephrin and improved renal function, these observations should be cautiously interpreted because

this study does not provide unequivocal data that demonstrate the interaction among HO-1, collagen-IV, fibronectin and nephrin in the glomeruli.

Funding: This work was supported by Heart & Stroke Foundation of Saskatchewan of Canada. The funders had no role in study design, data collection and analysis, decision to publish, or preparation of the manuscript.

Competing Interests: The authors have declared that no competing interests exist.

Table 5-1: Effect of hemin and stannous mesoporphyrin (SnMP) on physiological variables in Zucker diabetic fatty rats (ZDF)

Physiological variables	Animal groups							
	Control ZL	ZL + Hemin	ZL + Vehicle	Control ZDF	ZDF + Hemin	ZDF + Hemin + SnMP	ZDF + SnMP	ZDF + Vehicle
Body weight (g)	366.4 ± 7.5	357.8 ± 6.4	361.5 ± 4.9	389.5 ± 8.6	371.5 ± 5.7†	355.7 ± 7.1§	363.9 ± 8.1§	384.2 ± 6.5
Fasting glucose (mmol/L)	7.0 ± 0.2	6.2 ± 0.3*	6.8 ± 0.2	26.8 ± 4.9	7.1 ± 1.5**	23.5 ± 5.1§	29.4 ± 5.3§	25.8 ± 4.2
Perirenal adiposity (g/Kg body weight	10.5 ± 2.7	8.2 ± 1.2*	10.2 ± 2.5	28.7 ± 4.6	12.6 ± 3.8**	26.4 ± 5.6§	30.5 ± 6.2§	29.5 ± 5.3
Albuminuria (mg/24 hrs)	2.3 ± 0.4	1.9 ± 0.7	2.5 ± 0.6	25.1 ± 1.7	8.9 ± 1.2**	27.1 ± 2.8§	32.8 ± 2.6§	26.7 ± 3.9
Proteinuria (mg/24 hrs)	5.1 ± 1.5	4.8 ± 2.3	5.9 ± 2.1	87.3 ± 8.1	22.6 ± 2.5**	90.7 ± 7.8§	102.4 ± 6.9§	91.5 ± 10.6
Creatinine Clearance (ml.min/g kidney)	4.1 ± 0.7	4.3 ± 1.3	4.2 ± 0.9	2.1 ± 0.5	3.6 ± 0.7**	2.4 ± 0.5§	1.8 ± 0.4§	1.9 ± 0.6

†$p<0.05$ vs controls; *$p<0.05$, **$p<0.01$ *vs* control ZDF or control ZL, §$p<0.05$ *vs* ZDF + Hemin, $n = 6$ per group.

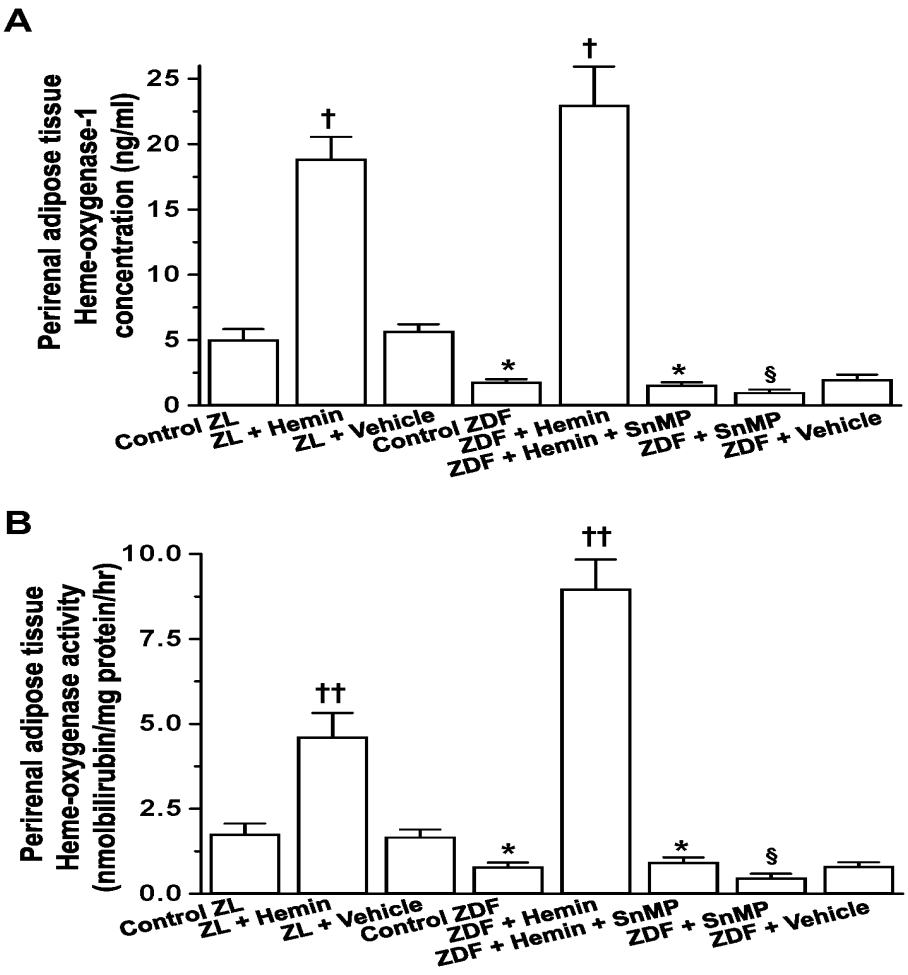

Figure 5-1: Effects of hemin, the HO inducer and SnMP, the HO inhibitor on HO-1 and HO activity of perirenal adipose tissue from ZDF and ZL rats. (A) The basal HO-1 levels in ZDF rats were lower than in age/sex-matched ZL-control rats, but were increased by hemin, whereas SnMP nullified the hemin effect. (B) The basal HO activity in ZDF rats was depressed as compared to ZL-control rats. Treatment with hemin markedly enhanced HO activity, whereas SnMP annulled the hemin effect. Hemin also enhanced HO-1 and HO activity in ZL rats, though less effectively as compared to ZDF rats. Bars represent means ± SEM; $n = 6$ rats per group (*$p<0.05$ vs all groups, $^{\dagger}p<0.05$, $^{\dagger\dagger}p<0.01$ vs all groups; $^{\S}p<0.05$ vs all groups).

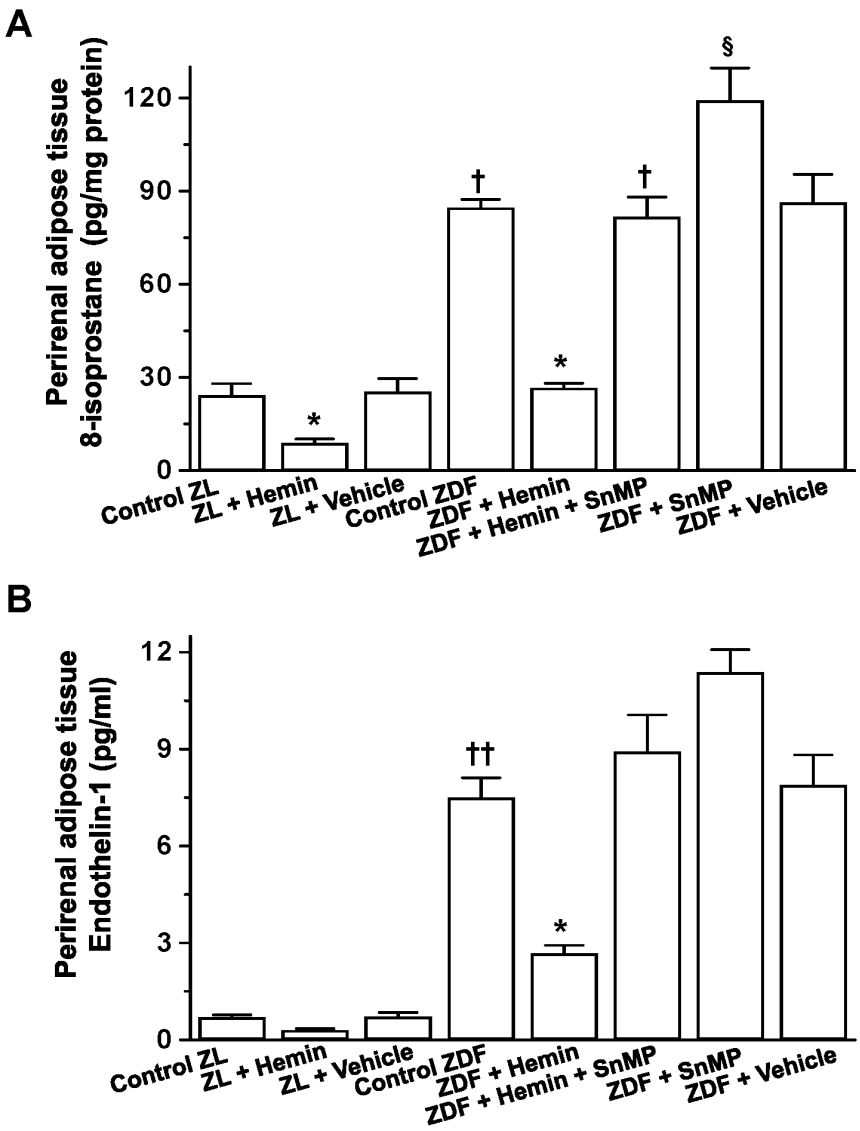

Figure 5-2: Effects of hemin, the HO inducer and SnMP, the HO inhibitor on 8-isoprostane and ET-1 of the perirenal adipose tissue from ZDF and ZL rats. (A) The basal 8-isoprostane levels in ZDF rats were markedly elevated as compared to ZL-control rats, but were significantly reduced by hemin, whereas SnMP nullified the hemin effect. (B) The basal ET-1 levels in ZDF rats were significantly elevated as compared to ZL-control rats, but were reduced by hemin, whereas SnMP nullified the hemin effect. Hemin also reduced 8-isoprostane and ET-1 in ZL rats, but less effectively as compared to ZDF rats. Bars represent means ± SEM; $n = 6$ rats per group (*$p<0.05$ vs all groups, $^{\dagger}p<0.05$, $^{\dagger\dagger}p<0.01$ vs all groups; $^{\S}p<0.05$ vs all groups).

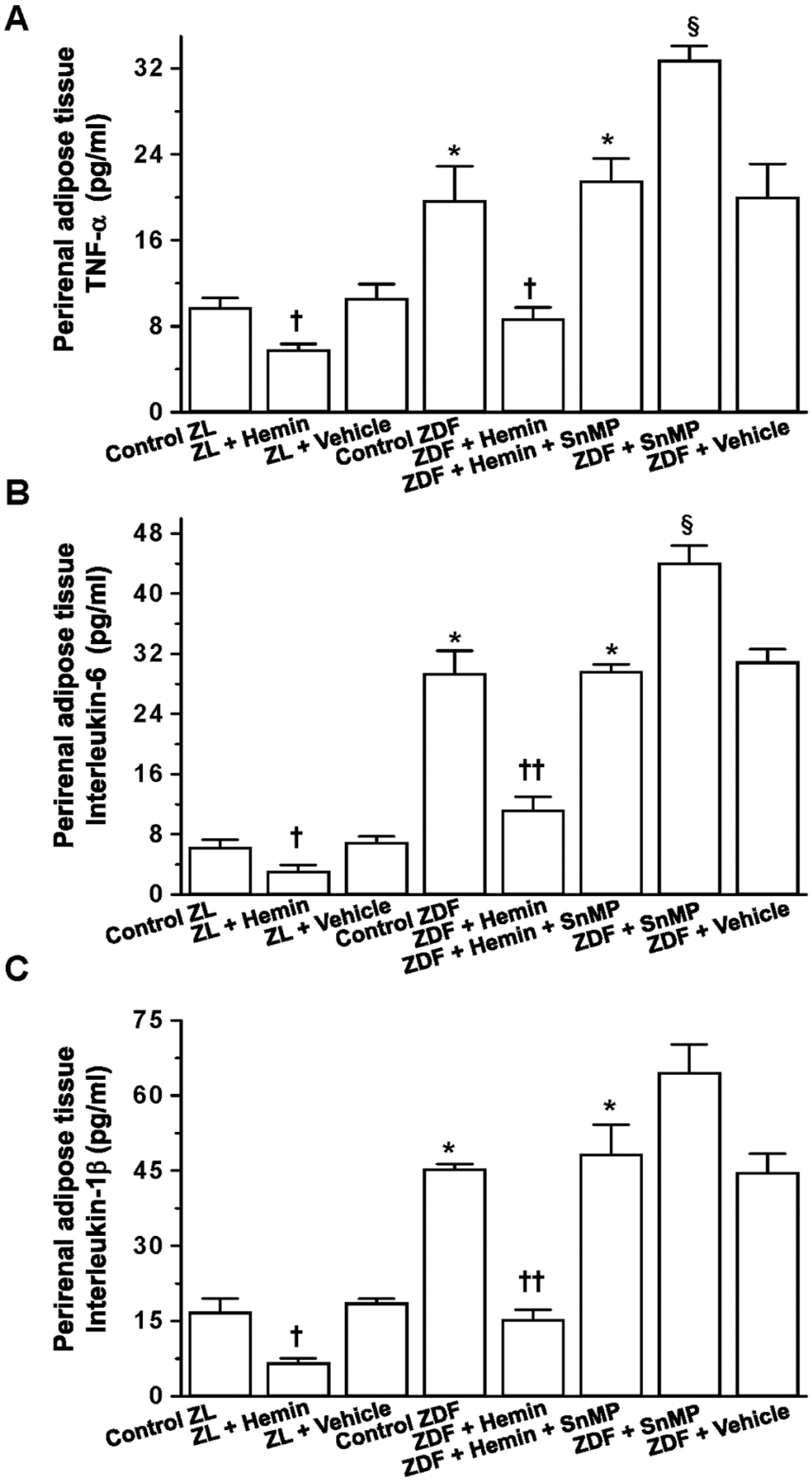
A
Perirenal adipose tissue
TNF-α (pg/ml)
0
8
16
24
32
*
†
§
Control ZL
ZL + Hemin
ZL + Vehicle
Control ZDF
ZDF + Hemin
ZDF + Hemin + SnMP
ZDF + SnMP
ZDF + Vehicle
B
Perirenal adipose tissue
Interleukin-6 (pg/ml)
0
8
16
24
32
40
48
*
†
††
§
Control ZL
ZL + Hemin
ZL + Vehicle
Control ZDF
ZDF + Hemin
ZDF + Hemin + SnMP
ZDF + SnMP
ZDF + Vehicle
C
Perirenal adipose tissue
Interleukin-1β (pg/ml)
0
15
30
45
60
75
*
†
††
Control ZL
ZL + Hemin
ZL + Vehicle
Control ZDF
ZDF + Hemin
ZDF + Hemin + SnMP
ZDF + SnMP
ZDF + Vehicle

Figure 5-3: Effects of hemin, the HO inducer and SnMP, the HO inhibitor on TNF-α, IL-6 and IL-1β, of the perirenal adipose tissue from ZDF and ZL rats. Hemin therapy significantly reduced the elevated levels of (A) TNF-α, (B) IL-6 and (C) IL-1β in ZDF rats, but the hemin effects were reversed by co-treatment with the HO blocker SnMP, while treatment with SnMP alone further increased the levels. Hemin also reduced TNF-α, IL-6 and IL-1β in ZL rats, but less effectively as compared to ZDF rats. Bars represent means ± SEM; $n = 6$ rats per group (*$p<0.05$, **$p<0.01$ vs all groups; $^{\dagger}p<0.05$, $^{\dagger\dagger}p<0.01$ vs all groups; $^{\S}p<0.05$, $^{\S\S}p<0.01$ vs all groups).

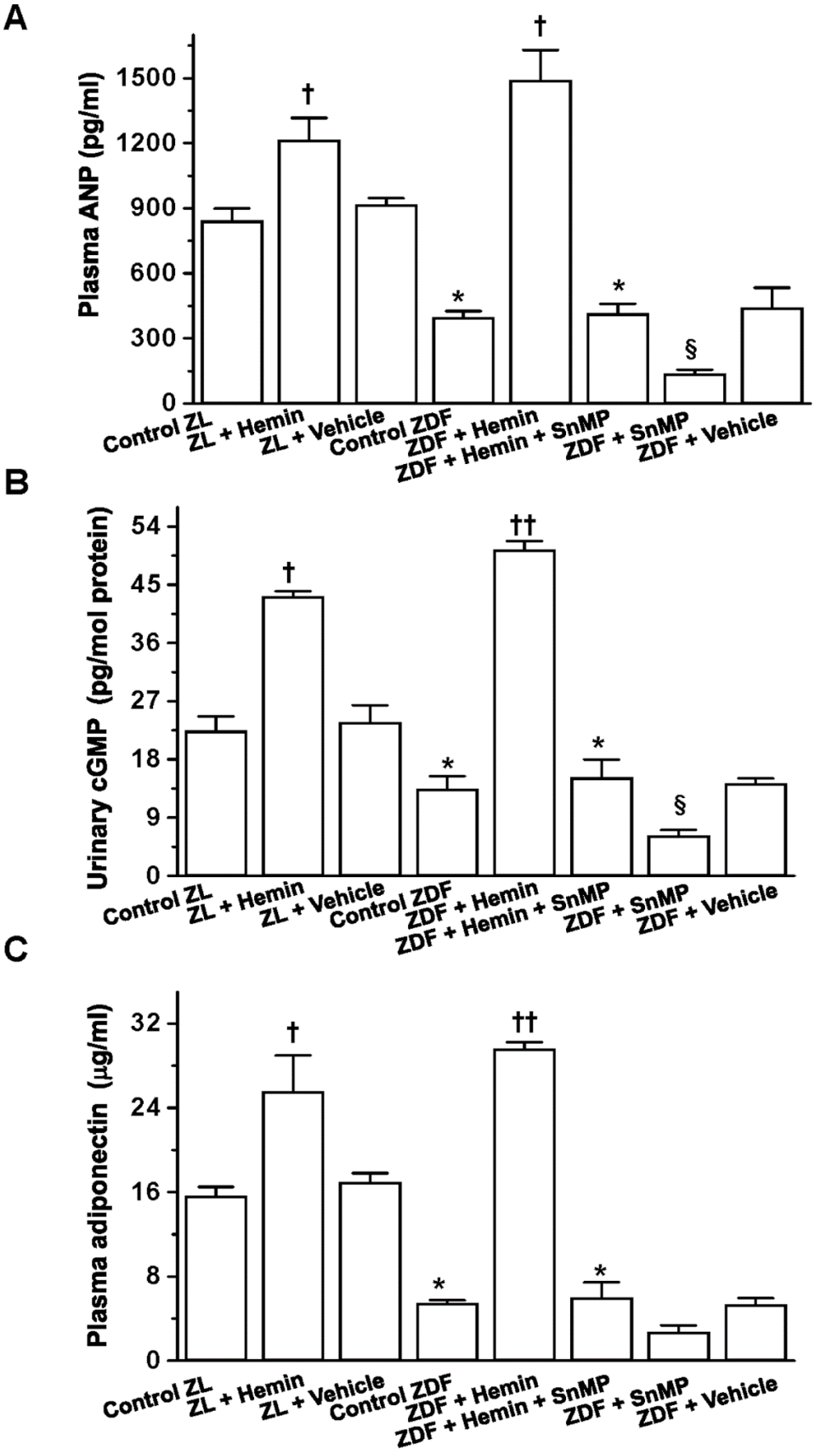
A
Plasma ANP (pg/ml)
0
300
600
900
1200
1500
†
†
*
*
§
Control ZL
ZL + Hemin
ZL + Vehicle
Control ZDF
ZDF + Hemin
ZDF + Hemin + SnMP
ZDF + SnMP
ZDF + Vehicle
B
Urinary cGMP (pg/mol protein)
0
9
18
27
36
45
54
†
††
*
*
§
Control ZL
ZL + Hemin
ZL + Vehicle
Control ZDF
ZDF + Hemin
ZDF + Hemin + SnMP
ZDF + SnMP
ZDF + Vehicle
C
Plasma adiponectin (μg/ml)
0
8
16
24
32
†
††
*
*
Control ZL
ZL + Hemin
ZL + Vehicle
Control ZDF
ZDF + Hemin
ZDF + Hemin + SnMP
ZDF + SnMP
ZDF + Vehicle

Figure 5-4: Effect of hemin, the HO inducer and SnMP, the HO inhibitor on plasma ANP, urinary cGMP and plasma adiponectin in ZDFs and ZLs. Hemin therapy significantly increased the depressed basal levels of (A) ANP, (B) urinary cGMP and (C) plasma adiponectin in ZDF rats, but was reversed by co-treatment with the HO blocker SnMP, while treatment with SnMP alone further depleted the basal levels. Hemin also increased plasma ANP, urinary cGMP and plasma adiponectin in ZL rats. Bars represent means ± SEM; n=6 rats per group (*$p<0.05$ vs all groups, $^{\dagger}p<0.01$ vs all groups, $^{\S}p<0.05$ vs all groups).

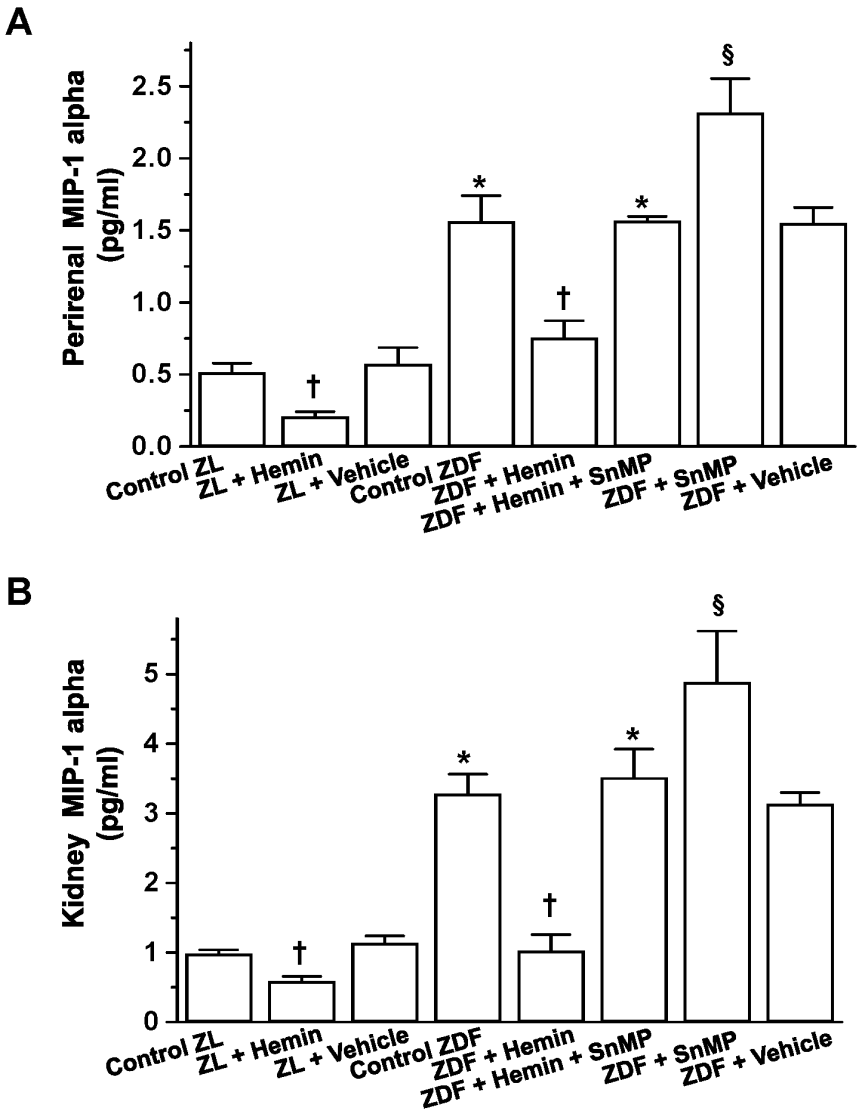

Figure 5-5: Effect of hemin on macrophage-inflammatory-protein-1 alpha (MIP-1α) in perirenal adipose tissue and the kidneys of ZDF. Hemin therapy significantly reduced the elevated levels of MIP-1α in (A) perirenal adipose tissues and (B) kidney from ZDF, but the hemin-effect was annulled by co-treatment with the HO blocker SnMP, while treatment with SnMP alone further increased the levels Bars represent means ± SEM; $n = 6$ rats per group (*$p<0.01$ vs all groups; $^{\dagger}p<0.05$ vs all groups; $^{\S}p<0.01$ vs all groups).

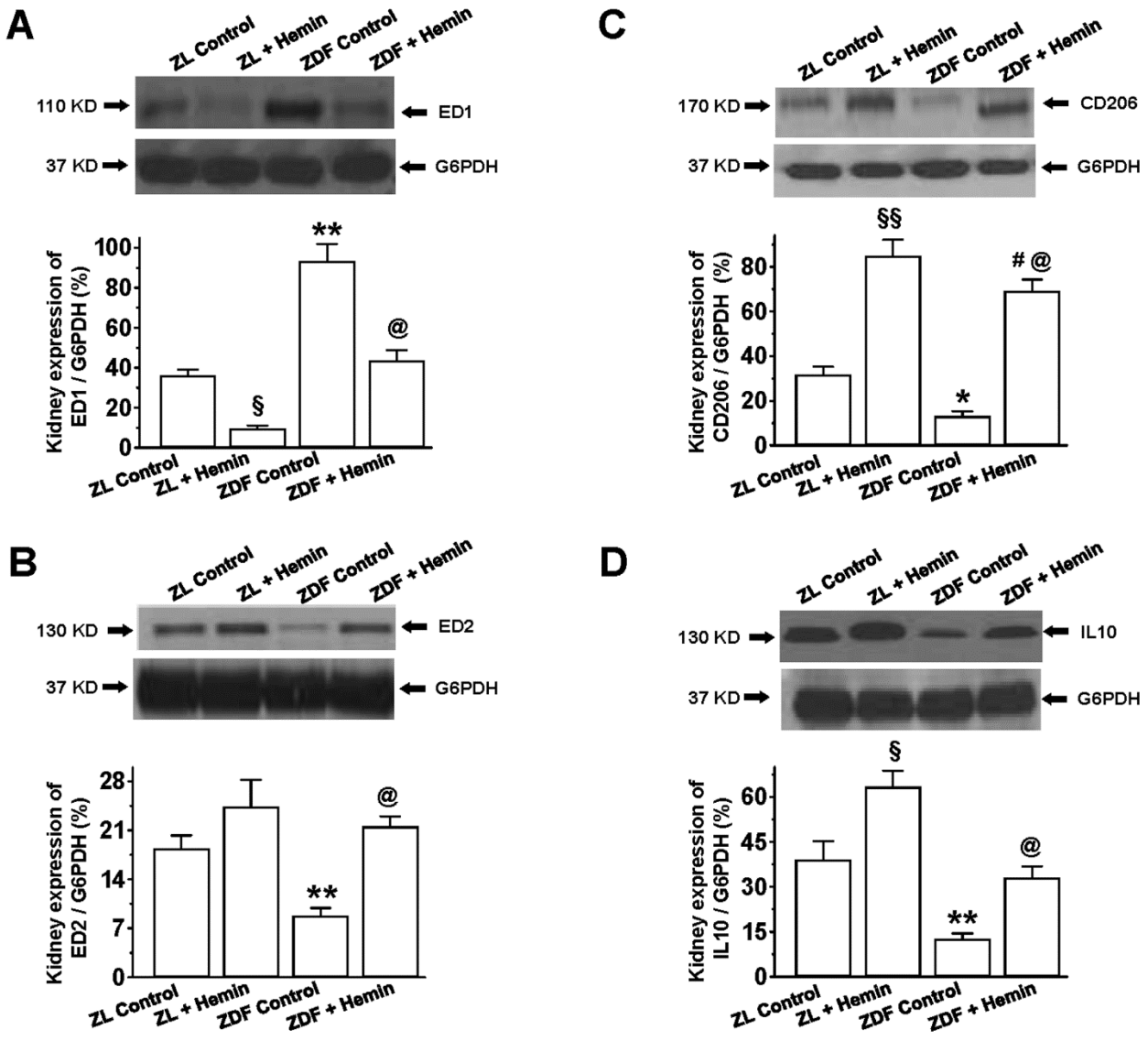

Figure 5-6: Effect of hemin on the expression of ED-1, ED2, CD206 and IL-10 in renal tissues of ZDF. Representative Western immunoblots, and relative densitometry indicates that hemin therapy significantly (A) reduced ED-1, but (B) enhanced ED2, (C) increased CD206, and (D) enhanced IL-10 expression in ZDF. Bars represent means ± SEM; $n = 4$ rats per group (*$p<0.05$, **$p<0.01$ vs ZL-Control; $^{\S}p<0.05$, $^{\S\S}p<0.01$ vs ZL-Control; $^{\#}p<0.01$ vs ZL-Control; $^{@}p<0.01$ vs ZDF Control).

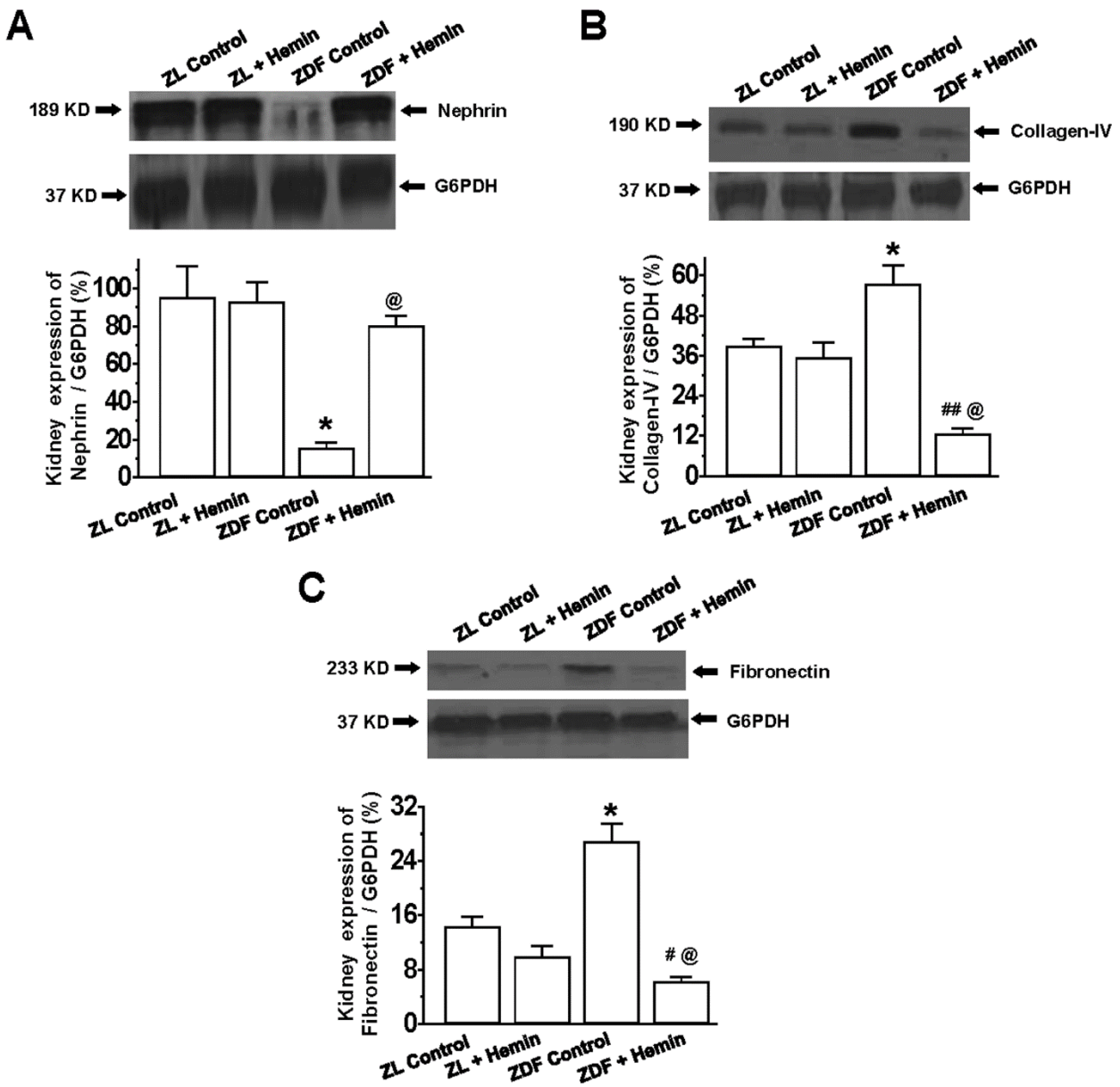

Figure 5-7: Effect of hemin on the expression of collagen-IV, fibronectin and nephrin in renal tissues of ZDF. Representative Western immunoblots, and relative densitometry indicates that hemin therapy significantly (A) enhanced the expression of nephrin but, (B) abated collagen-IV expression, and (C) reduced the expression of fibronectin in ZDF. Bar represent means ± SEM; *n* = 4 rats per group (*$p<0.01$ vs all groups; $^{\#}p<0.05$, $^{\#\#}p<0.01$ vs ZL-Control; $^{@}p<0.01$ vs ZDF-Control).

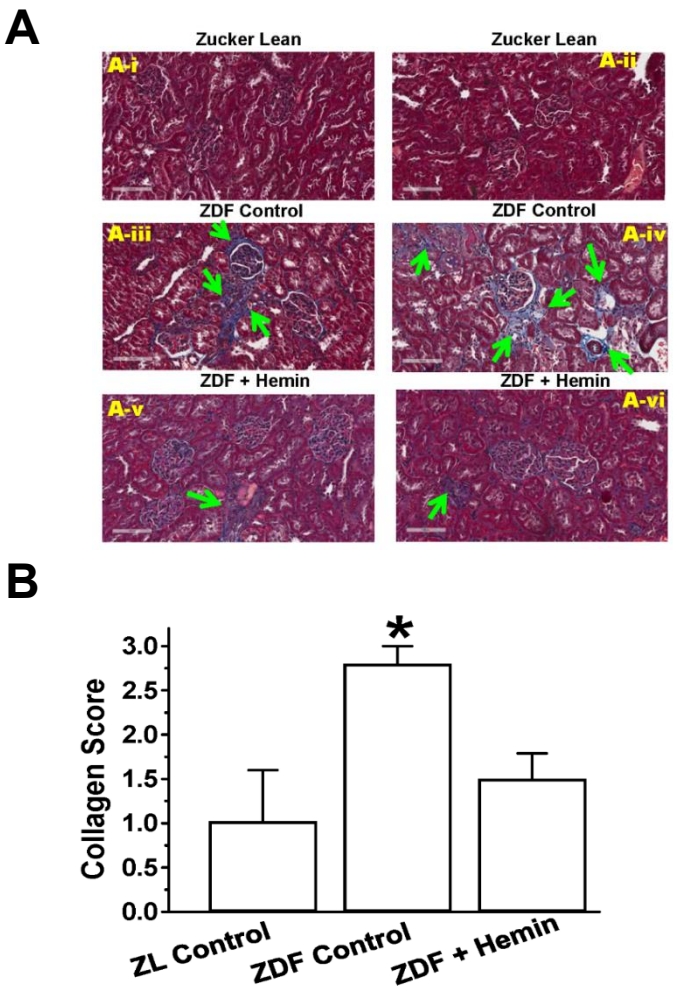

Figure 5-8: Masson's trichrome staining of collagen deposition and fibrosis the in kidney. (A) Representative images of kidney section from two different rats. Sections from untreated ZDF-controls (panels A-iii and A-iv) indicate severe fibrosis in tubulointerstitial, perivascular and glomerulus as compared with ZL-control rats (panels A-i and A-ii), which interestingly were attenuated by hemin (panels A-v and A-vi). (Magnification×200) (B) Semi-quantitative evaluation showed that hemin reduced collagen deposition. Bars represent means ± SEM; n =4-6 rats per group (*$p<0.05$ vs all groups).

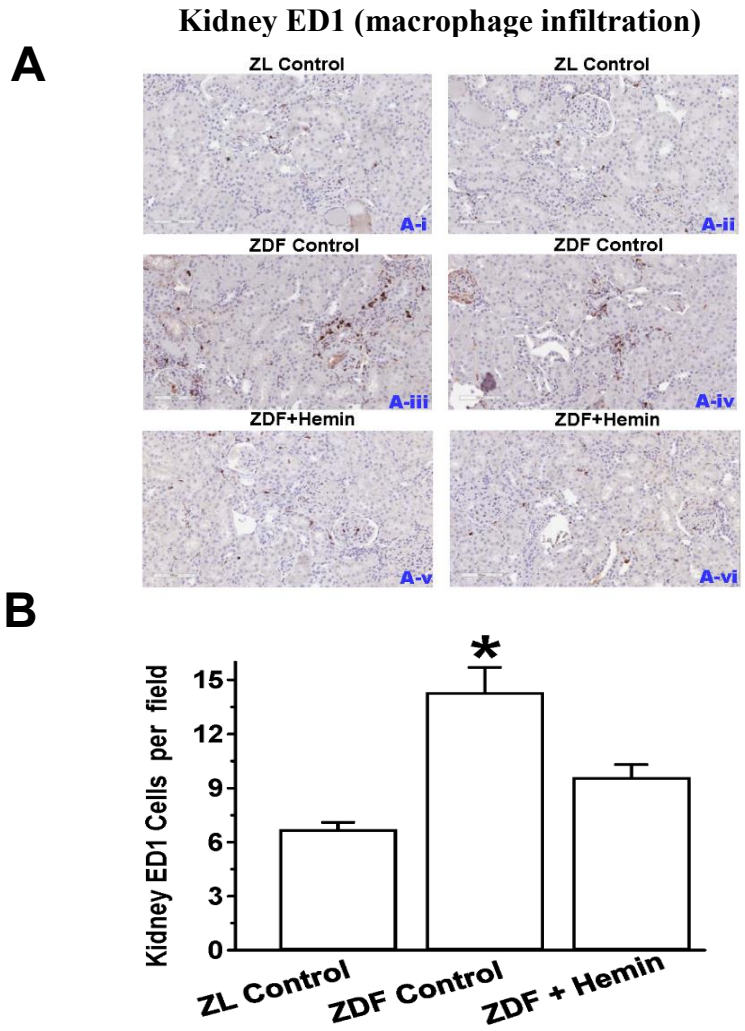

Figure 5-9: Effect of hemin therapy on kidney macrophage infiltration (A) Representative images of kidney section from different rats. The images reveal that macrophage infiltration (ED1-positive cells stained dark brown in kidney sections were elevated in ZDF-controls (panels A-iii and A-iv) as compared to ZL-controls (panels A-i and A-ii), but interestingly were reduced by hemin (panels A-v and A-vi). (Magnification×200). (B) Quantitative analyses per field indicating that in ZDF-controls macrophage infiltration was significantly elevated as compared to ZL-control, but was significantly attenuated by hemin therapy. Bars represent means ± SEM; n = 4-6 rats per group (*p<0.01 vs all groups).

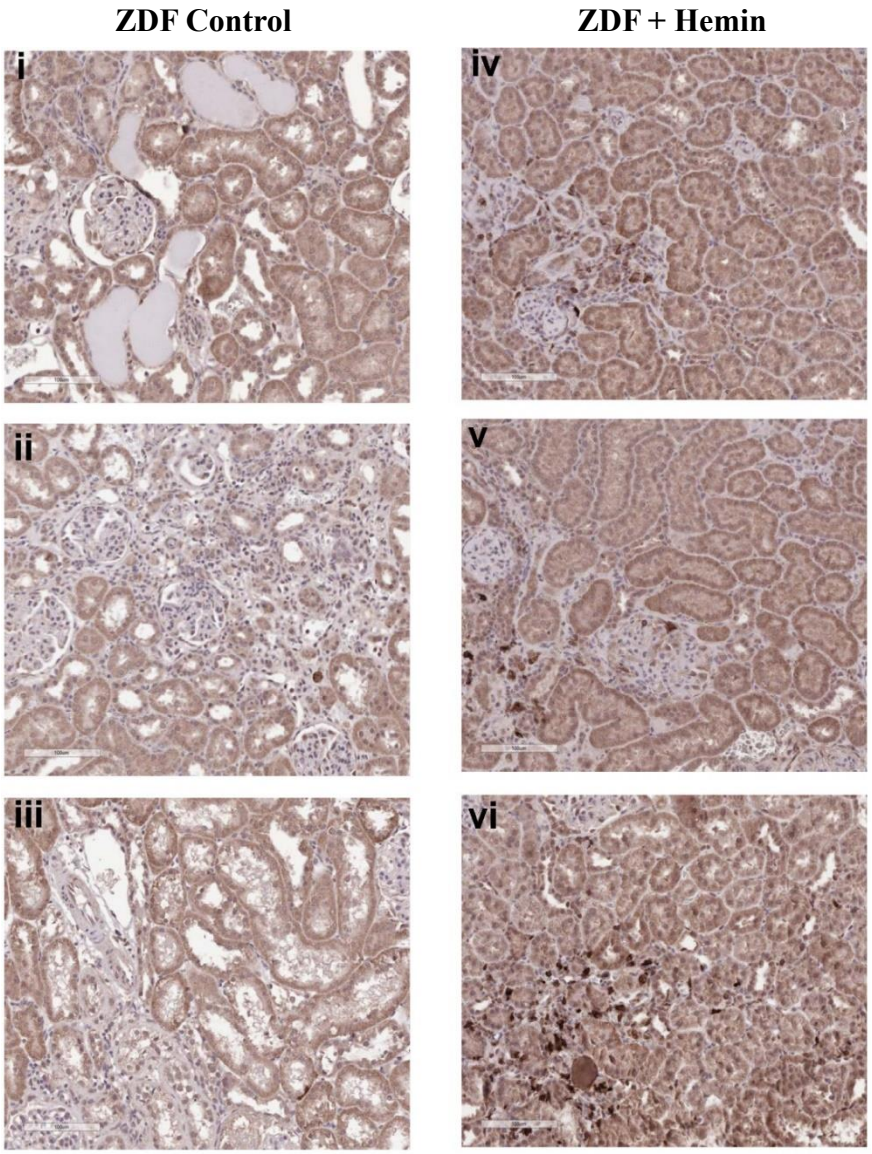

Figure 5-10: Immunolabelling of HO-1 in the kidney of ZDF-control and ZDF-treated with hemin therapy. Representative images of kidney section from different rats reveal that HO-1 is more expressed in ZDF + hemin group (panels iv-vi) as compared to the ZDF-control group (panels i-iii). (Magnification×200).

5.7 References

1. Hossain P, Kawar B, El Nahas M (2007) Obesity and diabetes in the developing world–a growing challenge. N Engl J Med 356: 213-215.

2. WHO (2006) Obesity and overweight. Fact Sheet No. 311, World Health Organization.

3. Ford ES, Mokdad AH, Giles WH (2003) Trends in waist circumference among U.S. adults. Obes Res 11: 1223-1231.

4. Mokdad AH, Ford ES, Bowman BA, Dietz WH, Vinicor F, et al. (2003) Prevalence of obesity, diabetes, and obesity-related health risk factors, 2001. Jama 289: 76-79.

5. Odermatt A (2011) The Western-style diet: a major risk factor for impaired kidney function and chronic kidney disease. Am J Physiol Renal Physiol 301: F919-931.

6. Tiwari S, Ndisang JF (2013) The Role of Obesity in Cardiomyopathy And Nephropathy. Curr Pharm Des.

7. Giunti S, Barit D, Cooper ME (2006) Mechanisms of diabetic nephropathy: role of hypertension. Hypertension 48: 519-526.

8. Ting SM, Nair H, Ching I, Taheri S, Dasgupta I (2009) Overweight, obesity and chronic kidney disease. Nephron Clin Pract 112: c121-127; discussion c127.

9. Lamacchia O, Nicastro V, Camarchio D, Valente U, Grisorio R, et al. (2011) Para- and perirenal fat thickness is an independent predictor of chronic kidney disease, increased renal resistance index and hyperuricaemia in type-2 diabetic patients. Nephrol Dial Transplant 26: 892-898.

10. Hamdy O, Porramatikul S, Al-Ozairi E (2006) Metabolic obesity: the paradox between visceral and subcutaneous fat. Curr Diabetes Rev 2: 367-373.

11. Postorino M, Marino C, Tripepi G, Zoccali C, Group CW (2009) Abdominal obesity and all-cause and cardiovascular mortality in end-stage renal disease. J Am Coll Cardiol 53: 1265-1272.

12. Li Y, Takemura G, Okada H, Miyata S, Maruyama R, et al. (2006) Reduction of inflammatory cytokine expression and oxidative damage by erythropoietin in chronic heart failure. Cardiovasc Res 71: 684-694.

13. Ndisang JF (2010) Role of heme oxygenase in inflammation, insulin-signalling, diabetes and obesity. Mediators Inflamm 2010: 359732.

14. Burgess A, Li M, Vanella L, Kim DH, Rezzani R, et al. (2010) Adipocyte heme oxygenase-1 induction attenuates metabolic syndrome in both male and female obese mice. Hypertension 56: 1124-1130.

15. Pan Y, Wang Y, Cai L, Cai Y, Hu J, et al. (2012) Inhibition of high glucose-induced inflammatory response and macrophage infiltration by a novel curcumin derivative prevents renal injury in diabetic rats. Br J Pharmacol 166: 1169-1182.

16. Ndisang JF (2013) The Heme Oxygenase System Selectively Modulates Proteins Implicated in Metabolism, Oxidative Stress and Inflammation in Spontaneously Hypertensive Rats. Curr Pharm Des.

17. Sanches FM, Avesani CM, Kamimura MA, Lemos MM, Axelsson J, et al. (2008) Waist circumference and visceral fat in CKD: a cross-sectional study. Am J Kidney Dis 52: 66-73.

18. Jim B, Ghanta M, Qipo A, Fan Y, Chuang PY, et al. (2012) Dysregulated nephrin in diabetic nephropathy of type 2 diabetes: a cross sectional study. PLoS One 7: e36041.

19. Wang Y, Wang DH (2011) Protective effect of TRPV1 against renal fibrosis via inhibition of TGF-beta/Smad signaling in DOCA-salt hypertension. Mol Med 17: 1204-1212.

20. Marshall SM (2007) The podocyte: a potential therapeutic target in diabetic nephropathy? Curr Pharm Des 13: 2713-2720.

21. Menne J, Meier M, Park JK, Boehne M, Kirsch T, et al. (2006) Nephrin loss in experimental diabetic nephropathy is prevented by deletion of protein kinase C alpha signaling in-vivo. Kidney Int 70: 1456-1462.

22. Satchell SC, Tooke JE (2008) What is the mechanism of microalbuminuria in diabetes: a role for the glomerular endothelium? Diabetologia 51: 714-725.

23. Ndisang JF, Lane N, Jadhav A (2009) The heme oxygenase system abates hyperglycemia in Zucker diabetic fatty rats by potentiating insulin-sensitizing pathways. Endocrinology 150: 2098-2108.

24. Salley TN, Mishra M, Tiwari S, Jadhav A, Ndisang JF (2013) The heme oxygenase system rescues hepatic deterioration in the condition of obesity comorbid with type-2 diabetes. PLoS One 8: e79270.

25. Finucane OM, Reynolds CM, McGillicuddy FC, Roche HM (2012) Insights into the role of macrophage migration inhibitory factor in obesity and insulin resistance. Proc Nutr Soc: 1-12.

26. Lawrence T, Natoli G (2011) Transcriptional regulation of macrophage polarization: enabling diversity with identity. Nat Rev Immunol 11: 750-761.

27. Jing F, Mogi M, Min LJ, Ohshima K, Nakaoka H, et al. (2013) Effect of Angiotensin II Type 2 Receptor-Interacting Protein on Adipose Tissue Function via Modulation of Macrophage Polarization. PLoS One 8: e60067.

28. Kim DH, Sandoval D, Reed JA, Matter EK, Tolod EG, et al. (2008) The role of GM-CSF in adipose tissue inflammation. Am J Physiol Endocrinol Metab 295: E1038-1046.

29. Jadhav A, Tiwari S, Lee P, Ndisang JF (2013) The heme oxygenase system selectively enhances the anti-inflammatory macrophage-m2 phenotype, reduces pericardial adiposity, and ameliorated cardiac injury in diabetic cardiomyopathy in zucker diabetic Fatty rats. J Pharmacol Exp Ther 345: 239-249.

30. Ndisang JF, Jadhav A (2013) Hemin therapy suppresses inflammation and retroperitoneal adipocyte hypertrophy to improve glucose metabolism in obese rats co-morbid with insulin resistant type-2 diabetes. Diabetes Obes Metab.

31. Ndisang JF, Jadhav A (2009) Heme oxygenase system enhances insulin sensitivity and glucose metabolism in streptozotocin-induced diabetes. Am J Physiol Endocrinol Metab 296: E829-841.

32. Ndisang JF, Jadhav A (2009) Up-regulating the hemeoxygenase system enhances insulin sensitivity and improves glucose metabolism in insulin-resistant diabetes in Goto-Kakizaki rats. Endocrinology 150: 2627-2636.

33. Ndisang JF, Lane N, Jadhav A (2009) Upregulation of the heme oxygenase system ameliorates postprandial and fasting hyperglycemia in type 2 diabetes. Am J Physiol Endocrinol Metab 296: E1029-1041.

34. Ndisang JF, Lane N, Syed N, Jadhav A (2010) Up-regulating the heme oxygenase system with hemin improves insulin sensitivity and glucose metabolism in adult spontaneously hypertensive rats. Endocrinology 151: 549-560.

35. Jadhav A, Torlakovic E, Ndisang JF (2009) Hemin therapy attenuates kidney injury in deoxycorticosterone acetate-salt hypertensive rats. Am J Physiol Renal Physiol 296: F521-F534.

36. Ndisang JF, Lane N, Jadhav A (2008) Crosstalk between the heme oxygenase system, aldosterone, and phospholipase C in hypertension. J Hypertens 26: 1188-1199.

37. Jadhav A, Torlakovic E, Ndisang JF (2008) Interaction Among Heme Oxygenase, Nuclear factor kappa B and Transcription Activating Factors in Cardiac Hypertrophy in Hypertension. Hypertension 52: 910-917.

38. Ndisang JF, Jadhav A (2010) Heme arginate therapy enhanced adiponectin and atrial natriuretic peptide, but abated endothelin-1 with attenuation of kidney histopathological lesions in mineralocorticoid-induced hypertension. J Pharmacol Exp Ther 334: 87-98.

39. Ndisang JF, Jadhav A (2010) Heme-arginate suppresses phospholipase C and oxidative stress in the mesenteric arterioles of mineralcorticoid-induced hypertensive rats. Hypertens Res 33: 338-347.

40. Jadhav A, Ndisang JF (2012) Treatment with heme arginate alleviates adipose tissue inflammation and improves insulin sensitivity and glucose metabolism in a rat model of Human primary aldosteronism. Free Radic Biol Med 53: 2277-2286.

41. Ndisang JF, Wu L, Zhao W, Wang R (2003) Induction of heme oxygenase-1 and stimulation of cGMP production by hemin in aortic tissues from hypertensive rats. Blood 101: 3893-3900.

42. Rovira A, De Angioletti M, Camacho-Vanegas O, Liu D, Rosti V, et al. (2000) Stable in vivo expression of glucose-6-phosphate dehydrogenase (G6PD) and rescue of G6PD deficiency in stem cells by gene transfer. Blood 96: 4111-4117.

43. Notaro R, Afolayan A, Luzzatto L (2000) Human mutations in glucose 6-phosphate dehydrogenase reflect evolutionary history. Faseb J 14: 485-494.

44. Ndisang JF, Zhao W, Wang R (2002) Selective regulation of blood pressure by heme oxygenase-1 in hypertension. Hypertension 40: 315-321.

45. Delanty N, Reilly MP, Pratico D, Lawson JA, McCarthy JF, et al. (1997) 8-epiPGF2 alpha generation during coronary reperfusion. A potential quantitative marker of oxidant stress in vivo. Circulation 95: 2492-2499.

46. Ndisang JF, Wang R (2002) Novel therapeutic strategies for impaired endothelium-dependent vascular relaxation. Expert Opin Ther Patents 12: 1237-1247.

47. Fukunaga M, Yura T, Badr KF (1995) Stimulatory effect of 8-Epi-PGF2 alpha, an F2-isoprostane, on endothelin-1 release. J Cardiovasc Pharmacol 26 Suppl 3: S51-52.

48. Shirakami G, Nakao K, Saito Y, Magaribuchi T, Mukoyama M, et al. (1993) Low doses of endothelin-1 inhibit atrial natriuretic peptide secretion. Endocrinology 132: 1905-1912.

49. Benigni A, Zoja C, Zatelli C, Corna D, Longaretti L, et al. (2004) Vasopeptidase inhibitor restores the balance of vasoactive hormones in progressive nephropathy. Kidney Int 66: 1959-1965.

50. Folco EJ, Rocha VZ, Lopez-Ilasaca M, Libby P (2009) Adiponectin Inhibits Proinflammatory Signaling in Human Macrophages Independent of Interleukin-10. J Biol Chem 284: 25569-25575.

51. Kubota N, Terauchi Y, Yamauchi T, Kubota T, Moroi M, et al. (2002) Disruption of adiponectin causes insulin resistance and neointimal formation. J Biol Chem 277: 25863-25866.

52. Sharma K, Ramachandrarao S, Qiu G, Usui HK, Zhu Y, et al. (2008) Adiponectin regulates albuminuria and podocyte function in mice. J Clin Invest 118: 1645-1656.

53. Gordon S, Martinez FO (2010) Alternative activation of macrophages: mechanism and functions. Immunity 32: 593-604.

54. Furuta T, Saito T, Ootaka T, Soma J, Obara K, et al. (1993) The role of macrophages in diabetic glomerulosclerosis. Am J Kidney Dis 21: 480-485.

55. Tesch GH (2010) Macrophages and diabetic nephropathy. Semin Nephrol 30: 290-301.

56. Ndisang JF, Jadhav A (2013) Hemin therapy improves kidney function in male streptozotocin-induced diabetic rats: Role of the heme oxygenase/atrial-natriuretic peptide/adiponectin axis. Endocrinology.

57. Aki K, Shimizu A, Masuda Y, Kuwahara N, Arai T, et al. (2010) ANG II receptor blockade enhances anti-inflammatory macrophages in anti-glomerular basement membrane glomerulonephritis. Am J Physiol Renal Physiol 298: F870-882.

58. Anzai A, Anzai T, Nagai S, Maekawa Y, Naito K, et al. (2012) Regulatory role of dendritic cells in postinfarction healing and left ventricular remodeling. Circulation 125: 1234-1245.

59. Piechota A, Goraca A (2011) Influence of nuclear factor-kappaB inhibition on endothelin-1 induced lung edema and oxidative stress in rats. J Physiol Pharmacol 62: 183-188.

60. Iwai T, Kitamoto K, Teramoto K, Machida Y, Tamada S, et al. (2008) Cobalt protoporphyrin attenuates rat obstructive nephropathy: role of cellular infiltration. Urology 72: 432-438.

61. Moro C, Klimcakova E, Lolmede K, Berlan M, Lafontan M, et al. (2007) Atrial natriuretic peptide inhibits the production of adipokines and cytokines linked to inflammation and insulin resistance in human subcutaneous adipose tissue. Diabetologia 50: 1038-1047.

62. Roson MI, Toblli JE, Della Penna SL, Gorzalczany S, Pandolfo M, et al. (2006) Renal protective role of atrial natriuretic peptide in acute sodium overload-dinduced inflammatory response. Am J Nephrol 26: 590-601.

63. Riba R, Patel B, Aburima A, Naseem KM (2008) Globular adiponectin increases cGMP formation in blood platelets independently of nitric oxide. J Thromb Haemost 6: 2121-2131.

64. Pandey KN (2005) Biology of natriuretic peptides and their receptors. Peptides 26: 901-932.

65. Wang Y, Kramer S, Loof T, Martini S, Kron S, et al. (2005) Stimulation of soluble guanylate cyclase slows progression in anti-thy1-induced chronic glomerulosclerosis. Kidney Int 68: 47-61.

66. Li Y, Tong X, Maimaitiyiming H, Clemons K, Cao JM, et al. (2012) Overexpression of cGMP-dependent protein kinase I (PKG-I) attenuates ischemia-reperfusion-induced kidney injury. Am J Physiol Renal Physiol 302: F561-570.

67. Mishra M, Ndisang JF (2013) A critical and comprehensive insight on heme oxygenase and related products including carbon monoxide, bilirubin, biliverdin and ferritin in type-1 and type-2 diabetes. Curr Pharm Des.

68. Tiwari S, Ndisang JF (2013) The Heme Oxygenase System and Type-1 Diabetes. Curr Pharm Des.

69. Tiwari S, Ndisang JF (2013) Heme Oxygenase System and Hypertension: A Comprehensive Insight. Curr Pharm Des.

70. Piechota M, Banach M, Irzmanski R, Misztal M, Rysz J, et al. (2007) N-terminal brain natriuretic propeptide levels correlate with procalcitonin and C-reactive protein levels in septic patients. Cell Mol Biol Lett 12: 162-175.

71. Shi-Wen X, Kennedy L, Renzoni EA, Bou-Gharios G, du Bois RM, et al. (2007) Endothelin is a downstream mediator of profibrotic responses to transforming growth factor beta in human lung fibroblasts. Arthritis Rheum 56: 4189-4194.

72. Tsukamoto O, Fujita M, Kato M, Yamazaki S, Asano Y, et al. (2009) Natriuretic peptides enhance the production of adiponectin in human adipocytes and in patients with chronic heart failure. J Am Coll Cardiol 53: 2070-2077.

73. Ballarin J, Arce Y, Torra Balcells R, Diaz Encarnacion M, Manzarbeitia F, et al. (2011) Acute renal failure associated to paroxysmal nocturnal haemoglobinuria leads to intratubular haemosiderin accumulation and CD163 expression. Nephrol Dial Transplant 26: 3408-3411.

74. Bedard EL, Jiang J, Parry N, Wang H, Liu W, et al. (2005) Peritransplant treatment with cobalt protoporphyrin attenuates chronic renal allograft rejection. Transpl Int 18: 341-349.

75. de Jesus Soares T, Volpini RA, Francescato HD, Costa RS, da Silva CG, et al. (2007) Effects of resveratrol on glycerol-induced renal injury. Life Sci 81: 647-656.

76. Keyse SM, Tyrrell RM (1989) Heme oxygenase is the major 32-kDa stress protein induced in human skin fibroblasts by UVA radiation, hydrogen peroxide, and sodium arsenite. Proc Natl Acad Sci U S A 86: 99-103.

77. Abraham NG, Kappas A (2008) Pharmacological and clinical aspects of heme oxygenase. Pharmacol Rev 60: 79-127.

78. Wei Y, Liu XM, Peyton KJ, Wang H, Johnson FK, et al. (2009) Hypochlorous acid-induced heme oxygenase-1 gene expression promotes human endothelial cell survival. Am J Physiol Cell Physiol 297: C907-915.

79. Mohri T, Ogura H, Koh T, Fujita K, Sumi Y, et al. (2006) Enhanced expression of intracellular heme oxygenase-1 in deactivated monocytes from patients with severe systemic inflammatory response syndrome. J Trauma 61: 616-623; discussion 623.

80. Ndisang JF, Tabien HE, Wang R (2004) Carbon monoxide and hypertension. J Hypertens 22: 1057-1074.

81. Jonas JC, Guiot Y, Rahier J, Henquin JC (2003) Haeme-oxygenase 1 expression in rat pancreatic beta cells is stimulated by supraphysiological glucose concentrations and by cyclic AMP. Diabetologia 46: 1234-1244.

82. Ndisang JF, Masini E, Mannaioni PF, Wang R (2002) Carbon monoxide and cardiovascular inflammation. In: R I, editor. Carbon monoxide and cardiovascular functions. Boca Raton: CPC Press. 165-180.

83. Ndisang JF, Jadhav A (2009) Upregulating the heme oxygenase system suppresses left ventricular hypertrophy in adult spontaneously hypertensive rats for 3 months. J Card Fail 15: 616-628.

84. Ndisang JF, Jadhav A (2009) The heme oxygenase system attenuates pancreatic lesions and improves insulin sensitivity and glucose metabolism in deoxycorticosterone acetate hypertension. Am J Physiol Regul Integr Comp Physiol.

85. Ndisang JF, Wang R (2003) Alterations in heme oxygenase/carbon monoxide system in pulmonary arteries in hypertension. Exp Biol Med (Maywood) 228: 557-563.

CHAPTER 6

Role of the Nrf2/HO axis in pancreatic repair and/or regeneration in a type-1 diabetic rat model

(unpublished thesis work)

Manish Mishra and Joseph Fomusi Ndisang

6.1 Abstract

Nuclear factor-(erythroid-derived 2)-like 2 (Nrf2) and heme oxygenase (HO) synergism associated mechanisms are the crucial regulator of inflammation, oxidative stress and abnormal glucose metabolism, and tissue injury in type-1 diabetes mellitus (T1D). We previously reported that HO upregulation reduced pancreatic lesions and improved pancreatic functions in streptozotocin (STZ)-induced diabetes, however, the mechanisms of HO-mediated reduction in pancreatic lesions were not clear. To understand the HO-associated pancreatic repair mechanisms, the effects of upregulating the HO system on proteins implicated in pancreatic repair and/or regeneration were examined in STZ-induced diabetes. Diabetes was induced with STZ, while the HO system was upregulated with hemin. Our results demonstrate that the hemin-induced HO system enhanced the expression of stem cell markers (c-Kit and Sca-1), proteins of regeneration (β-catenin, Islet-1, GLUT2) and transcriptional factors (Oct3/4, Pax2, Nkx6.1) in the pancreas, suggesting their involvement in pancreatic repair and /or regeneration. Furthermore, hemin therapy effectively reduced inflammation through selective enhancement of ED2, CD206 and CD36 (anti-inflammatory M2-phenotype markers), while it suppressed ED1 (proinflammatory M1-phenotype

marker) expression. Additionally, hemin therapy ameliorated oxidative stress through enhancing total antioxidant capacity and through Nrf2 transcriptional factor activation. Hemin-mediated reduction of inflammation and oxidative stress was associated with improved glucose metabolism through augmentation of insulin signaling components such as IRS-1, IRS-2, PI3K and GLUT4 in the liver and soleus muscle. In conclusion, the present findings suggest that hemin-mediated activation of the Nrf2/HO axis is one of the mechanisms that enhance of expression of proteins of pancreatic repair and /or regeneration, and improve glucose metabolism.

6.2 Introduction

Type-1 diabetes (T1D) is an autoimmune condition of tissue injury and impaired glucose metabolism affecting 7-12% of the world's population (1,2). Increasing T-cell-mediated β-cell apoptosis, insulin insufficiency and hyperglycemia are the characteristic features of T1D that are associated with altered pancreatic morphology and functions (3,4). Additionally, hyperglycemia-induced systemic inflammation and oxidative stress equally contribute to tissue injury and metabolic dysfunction in several other vital organs such as liver, muscle and kidney that results in life threatening consequences (1,4,5).

Clinically, T1D is managed by insulin therapy and islet transplantation (2,6,7). However, insulin-mediated allergies, variability in insulin action and hypoglycemia and immune-mediated graft rejection and low efficiency are the major concerns that reduce the effectiveness of insulin therapy and islet transplantation in T1D treatment (2,6,7). In these dysfunctional conditions, development of strategies against tissue injuries and metabolic dysfunction are important priorities.

Experimental studies in rodents showed that the pancreas has a reasonable potential to repair and/ or regenerate in various conditions of injuries (8,9). During pancreatic injury, dying pancreatic cells are replaced by replication of pre-existing cells or through neogenesis (8-11). Thus, promoting pancreatic repair and /or regeneration by various means may be very beneficial to reduce T1D-induced comorbidities. However, the contribution of a slower replication process is thought to be insufficient for the required cellular replacement in pancreas because due to autoimmunity assault, only a marginal number of β-cells remain alive in the pancreatic islet (12,13).

Furthermore, studies in rodents showed that during pancreatic injury, there are a number of proteins and transcriptional factors such as c-Kit, Sca-1, octamer-binding transcription factor 3/4 (Oct3/4), paired homeodomain transcription factor-2 (Pax2), β-catenin, insulin gene enhancer protein-1 (Islet-1), homeobox protein Nkx6.1, and glucose transporter-2 (GLUT2) expressed in the pancreas and participates in pancreatic repair and/ or regenerative process (14-21). Thus, identification and characterization of these markers is very useful to define the repair and /or regenerative mechanism of the pancreas.

During the past, few years, several observations have supported the cytoprotective functions of heme oxygenase (HO) system in experimental T1D (22). Additionally, HO metabolites, biliverdin ferritin and carbon monoxide are shown to promote tissue health and functions in various conditions of diabetes-induced tissue inflammation and oxidative injuries (22). Interestingly, in our previous observations in streptozotocin (STZ)-induced diabetes and deoxycorticosterone-acetate-induced hypertension model, HO upregulation through hemin significantly reduced pancreatic injuries (vacuolization interstitial edema, monocyte infiltration and fibrosis) while insulin levels were improved (4,23). Similarly, hemin treatment reduced

pancreatic lesions in STZ diabetic rats (5). However, the mechanisms of HO-mediated tissue restoration of pancreatic morphology are unknown. It is reported that nuclear factor (erythroid-derived 2)-like 2 (Nrf2) governs several cytoprotective effects of the HO system via regulation of its transcriptional activation (24,25). However, during T1D, the modulatory role of Nrf2/HO synergism on inflammation and oxidative stress-induced pancreatic injury, and dysregulated glucose metabolism is not clearly understood.

Thus, to investigate the regulatory role of the Nrf2/HO axis in pancreatic injury, repair and/or regeneration and glucose metabolism in more depth, a rat model of STZ-induced diabetes is used that mimics several pathological features of T1D, such as increasing β-cell death, pancreatic inflammation and tissue injury and elevated levels of blood glucose (3,4). We hypothesized that Nrf2/HO synergism will modulate the negative consequences of inflammation, oxidative stress such as abnormal insulin signalling and pancreatic injuries while promoting pancreatic repair and/or regeneration in diabetic STZ animals.

6.3 Materials and methods

6.3.1 Animal treatment and biochemical parameters

All experimental procedures were followed in accordance with a protocol approved by the Animal Care Committee at the University of Saskatchewan and Canadian Council on Animal Care. Male 5-week old Sprague Dawley (SD) rats were purchased from Charles River Laboratories (Willington, MA) and kept at 12-hours of light and dark cycles and fed with a regular laboratory chow diet and given free access to drinking water ad libitum. Our experimental design included the following treatment groups: (i) controls (citrate buffer-treated SD rats), (ii) streptozotocin (STZ) group, (iii) STZ + hemin group, and (iv) STZ + hemin + CrMP group. Diabetes was induced with a single and high dose of streptozotocin (Sigma, St Louis, MO.) (150 mg/kg body weight,

intraperitoneal injection (ip) in 0.1 mol/L citrate buffer, pH 4.5) in animals of the STZ group, STZ + hemin group and STZ + hemin + CrMP group as previously reported (4). The citrate buffer-treated SD control group was also treated with 0.1 mol/L citrate buffer, pH 4.5 in which we dissolved the streptozotocin. After 72 hours of streptozotocin injection, the diabetic state of the animals is confirmed by the presence of polyuria, polydipsia, polyphagia and increased blood glucose levels (>20 mmol/L) using the blood glucose analyzer (Abbott Diabetes Care Inc. CA94502, USA). Animals whose glucose levels were >20 mmol/L were considered as diabetic and used in experiments.

HO-inducer hemin (30 mg/kg body weight i.p., Sigma, St Louis, MO) and HO-blocker chromium mesoporphyrin [(CrMP) 4 mol/kg body weight i.p.; Porphyrin Products (Logan, UT)] were prepared as previously reported and administered after 1 week of STZ administration, biweekly for 4 weeks (4). Physiological parameters (body weight, drinking water, urine) were measured weekly before and during the treatment period. Additionally, at the end of the study, the animals (11 weeks old) were fasted in metabolic cages and urine samples were collected for 24 hrs. Thereafter, the rats were weighed and anaesthetized with isoflurane (50 mg/kg i.p.) and blood and plasma samples were collected. After that animals were sacrificed and pancreas, liver, soleus muscle, were removed in pre-chilled PBS, cleaned and weighed and frozen in liquid nitrogen and stored at -80°C for further analysis.

Total antioxidant capacity of pancreatic tissue was measured by enzyme-linked immunoassay through using a commercial kit for total antioxidant (Cayman Chemicals) through an immunosorbent assay as previously reported (23). In brief, pancreatic tissue samples were homogenized in PBS buffer with a cocktail of protease inhibitors and treated with Trolox (6-hydroxy-2, 5, 7, 8-tetramethylchroman-2-carboxylic acid), met-myoglobin, and chromogen and

the absorbances were read at 750 nm with a microplate reader (Spectra Max, Molecular Devices). The results were expressed as Trolox equivalent antioxidant capacity (TEAC) per milligram of protein.

6.3.2 Western immunoblotting

Frozen (-80°C) liver, pancreas, soleus muscle was homogenized with radioimmunoprecipitation assay buffer (RIPA) (50 mM Tris-HCl pH 7.8, 150 mM NaCl, 0.1% SDS, 0.5% sodium deoxycholate, 1% triton x-100) in the presence of a freshly prepared cocktail of protease inhibitors. The total protein concentration in supernatant was quantified by a detergent compatible protein quantification kit (DC^{TM} Protein Assay Kit, Bio Rad). Here 50-75 μg of total protein was electrophoresed on 8-12% SDS-polyacrylamide gels. After electrophoresis of total proteins, the fractionated proteins were transferred to a nitrocellulose membrane (0.45 μm, Bio Rad) and blocked with 3-5% non-fat dry milk or bovine serum albumin for 1.5 hrs to prevent non-specific binding. Further, the membranes were incubated overnight at 4°C with primary antibodies against HO-1 (Stressgen-1:800), Nrf2, ED1, CD36, GLUT4, c-Kit and Sca-1, Oct3/4, Pax2, Nkx6.1 and GLUT2 (Santa Cruz-1:1000), ED2, CD206, PI3K, Islet-1 (Santa Cruz-1:800), IRS-1 and IRS-2 (Santa Crutz-1:750), β catenin (Abcam-1:5000). After primary antibody hybridization, blots were washed 3 times for 5 minutes each in 1x TBST (20 mM Tris-Cl, 150 mM NaCl, 0.1% tween 20, pH 7.6), and further incubated with secondary IgG horseradish peroxide conjugate antibody (Bio Rad) for 2 hrs at room temperature. After secondary antibody hybridization, blots were washed 3 times for 15 minutes each in 1x TBST to remove non-specific antibody. Finally, enhanced horseradish peroxide/luminol chemiluminescence reagent (Perkin Elmer Life Sciences, Boston, MA USA) was used to visualize the immuno-reactivity. β-actin antibody (Sigma St Louis,

MO, USA) was used as a housekeeping protein control to confirm uniform loading. Enhanced horseradish peroxide/luminol chemiluminescence reagent (Perkin Elmer Life Sciences, Boston, MA USA) was used to visualize the immuno-reactivity. Relative densitometry of respective bands on blots was done using UN-SCAN-IT software (Silk Scientific, Utah, USA).

6.3.3 Statistical analysis

All data were expressed as mean ± SEM from at least four independent experiments unless otherwise stated. Statistical analyses were done using Student's *t-test*, analysis of variance (ANOVA) and analysis of variance for repeated measures followed by post-hoc analysis (Bonferroni post hoc analysis) wherever appropriate (IBM SPSS Statistics, IBM Analytics, USA). Group differences at the level of $p<0.05$ were considered statistically significant.

6.4 Results

6.4.1 Hemin therapy enhanced HO-1 and Nrf2 in STZ-rats

Our data showed that diabetic STZ-rats, exhibited several enhanced parameters of the diabetic state such as polydipsia, polyurea and fasting blood glucose. Hemin-treatment significantly reduced these parameters due to its intrinsic antidiabetic effects (4). In contrast, in the CrMP group, hemin-induced reduction of these parameters was greatly attenuated (Table 6-1).

Diabetes significantly reduced the body weight in STZ-rats. Body weight was also lower in the hemin-treated and CrMP group (Table 6-1). However, there was no significant difference in body weight between the diabetic STZ-group and the hemin-treated group or CrMP group. Moreover, all three study groups showed a higher pancreatic weight (g/kg body weight) compared to controls. The increase in pancreatic weights were comparatively lower in hemin-treated and CrMP-group of animals. The differences in pancreatic weight (g/kg body weight) were not

statistical significant between STZ-rats and hemin-treated rats. In contrast, in CrMP group, the reduction of pancreatic weights was statistically significant compared to diabetic animals. Since we observed an increase in pancreatic weight (g/kg body weight) in diabetic STZ-rats which may be due to presence of pancreatic edema that characterised by increasing fluid retention and pancreatic swelling in response of STZ-induced toxicity (4,26).

We further investigated the effects of hemin therapy on expression of HO-1 and Nrf2 proteins which are known to have modulatory impact on tissue injuries and glucose metabolism (25). Our results indicated that the basal expression of HO-1 and Nrf2 in the control group was 8.8- and 11.01-fold lower than the hemin-treated group and there was no significant increase in HO-1 and Nrf2 expression in the diabetic STZ-group compared to the control group. Hemin-treatment significantly augmented the supressed basal expression of both HO-1 and Nrf2 in pancreatic tissue by 5.3-fold, and 13.7-fold compared to the STZ-group (Figs. 6-1A, 6-2A) respectively.

6.4.2 Hemin therapy counteracted inflammation in STZ-rats

Enhanced macrophage infiltration is a primary cause of tissue injury and dysfunctional metabolism in T1D (5, 27, 28). To determine the effects of hemin-therapy on macrophage-induced inflammation in STZ rats, several markers of macrophages ED1 (M1-macrophages), ED2, CD206, CD36 (M2-macrophage) were analysed (29, 30). Immunoblotting data indicated that the expression of ED1 is highly elevated in pancreas and liver of the diabetic STZ-group (14.1-fold and 4.3-fold) compared to the controls (Figs.6-3A, Fig 6-4A). Although, hemin did not completely supress the ED1 expression to the control level (5.6-fold, and 1.49-fold higher), it was significantly

attenuated in both pancreas and liver tissues (1.3-fold, 1.12-fold), compared to the diabetic STZ-group.

To investigate further hemin-induced effects on inflammation, the expressions of ED2, CD206 and CD36 markers (M2-phenotype) were analyzed in the pancreas and liver tissue that are shown to be associated with maintenance of the anti-inflammatory status (30). Our results showed that the expressions of ED2 and CD206 markers were significantly supressed in the diabetic STZ-group compared to the controls and hemin treated group (Figs. 6-3B, C, Fig 6-4B, C). There was no significant difference in the expression of ED2, CD206 markers in the hemin treated- group compared to the controls in pancreas and liver. However, the hemin-treated group showed a significant enhanced expression of ED2 in both pancreas and liver (2.56-fold, 1.53-fold) (Figs. 6-3B, Fig 6-4B), while enhanced CD206 expression is only documented in the liver (1.55-fold) compared to the diabetic STZ-group (Fig. 6-4C).

Furthermore, in the diabetic STZ-group, the expression of CD36 markers in the pancreas and liver did not differ significantly, compared to the control group (Figs. 6-3C, Fig 6-4D). However, the hemin-treated group showed a significant increase of CD36 expression in both pancreas and the liver compared to the control and the diabetic STZ-group. These observations, collectively suggest that hemin-induced enhanced selectivity towards M2 macrophages is the underlying mechanism through which hemin counteracts inflammation in STZ-rats.

6.4.3 Hemin therapy potentiates insulin signaling components in STZ-rats

Given that increasing inflammation and oxidative stress are negative modulators of insulin signalling and glucose metabolism in diabetes (4, 22). To elucidate the effects of hemin therapy on insulin signalling and glucose metabolism in diabetic STZ-rats, major insulin signaling

components (IRS-1, IRS-2, PI3K and GLUT4) were examined in metabolically active liver and soleus muscle.

Our results showed that the diabetic conditions significantly attenuated the expressions of IRS-1, IRS-2, PI3K and GLUT4 in liver of diabetic STZ-liver compared to the control group (Fig. 6-5 A-D). Similar reduction of these components was also observed in soleus muscle for IRS-1, IRS-2 and GLUT4, however, the decrease of PI3K expression was not statistically significant (Fig. 6-6 A-D). In contrast, hemin therapy significantly enhanced the expression of these components in both liver and soleus muscle compared to diabetic STZ-rats. The increases in the expression of IRS-1 were (1.28-fold, 10.5-fold), IRS-2 (0.56-fold, 2.3-fold), PI3K (1.0-fold, 1.3-fold) and GLUT4 (2.1-fold, 2.9-fold) higher in the liver and soleus muscle compared to diabetic STZ-rats (Figs.6-5 A-D, Fig. 6.6 A-D). Interestingly, the expressions of IRS-2, GLUT4 in liver and IRS-1 in soleus muscle were significantly increased in hemin-treated animals than control counterparts.

6.4.4 Enhancement of total antioxidant capacity with hemin in the pancreas of STZ-rats

Since, pancreatic tissues are more susceptible to oxidative stress-induced comorbidities due to low antioxidant levels (31), we also examined the effect of hemin on total antioxidant capacity in the pancreas which is an important index of oxidative stress (23). Our results indicate that the diabetic STZ-group (1.83-fold) and CrMP-group (1.7-fold) showed a significantly lower total antioxidant capacity than controls (Fig. 6-7). In contrast, in the hemin-treated group, the total antioxidant capacity was significantly increased by 2.9-fold and 2.7-fold compared to diabetic STZ-rat and CrMP groups. However, the differences in the values of total antioxidant capacity between either the hemin treated group and control group or diabetic STZ-group and CrMP group were not significant. These results suggested that hemin therapy reduced the oxidative stress

through potentiation of total antioxidant capacity. In contrast, hemin-mediated effects on enhancement of pancreatic total antioxidant capacity were abated by CrMP treatment.

6.4.5 Hemin therapy enhanced the expression of markers of pancreatic repair and/or regeneration in STZ-rats

Given that T1D is an abnormal condition of increasing tissue injury and metabolic dysregulation (4,5) and enhancement of pancreatic repair and/or regenerative capabilities have cytoprotective benefits. To examine the effects of hemin on pancreatic repair and/or regeneration and functions during T1D, several markers (c-Kit, Sca-1, Oct3/4, Pax2, β-catenin, Islet-1, Nkx6.1, and GLUT2) that are implicated in pancreatic repair and/ or regeneration were analysed in pancreas of STZ-rats (14-21). Our results showed that the expressions of c-Kit and Sca-1, Oct3/4, Pax2, β-catenin, Islet-1, Nkx6.1, and GLUT2 were significantly lower in diabetic STZ-rats compared to controls (Figs. 6-8 A, B, 6-9 A, B, D, 6-10 A, B).

The expressions of c-Kit, Oct3/4 and Islet-1, and Pax2, Nkx6.1 and GLUT2 in hemin treated group were not statistically different compared to the control group. However, the expression of Sca-1 and β-catenin were significantly lower in the hemin-treated group than controls (Figs. 6-8 B, 6-9 C). Interestingly, hemin-treatment significantly increased the expressions of c-Kit, Sca-1, Oct3/4, Pax2, β-catenin and Islet-1, Nkx6.1 and GLUT4 in pancreas compared to diabetic STZ-rats. The expressions of c-Kit (4.8-fold), Sca-1 (5.9-fold), Oct3/4 (3.8-fold), Pax2 (5.9-fold), β-catenin (2.1-fold), Islet-1 (2.2-fold), Nkx6.1 (1.03-fold) and GLUT4 (2.8-fold) were higher in hemin-treated rats compared to diabetic STZ-rats (Figs. 6-8, 6-9, 6-10). These results suggested that hemin therapy has significant modulatory effects on the expression of markers of

pancreatic repair and/or regeneration. These effects of hemin therapy on expression of pancreatic markers are novel and have not been previously reported.

6.5 Discussion

The data from our study suggested the multifaceted mechanisms of hemin through which it counteracts inflammation, oxidative stress and potentiates insulin signalling to improve glucose metabolism in STZ rats, a model of T1D (4). Treatment with hemin upregulated both Nrf2 and HO-1. This was associated with the enhancement of several proteins implicated in pancreatic repair and regeneration including c-Kit, Sca-1, Oct3/4, Pax2, β-catenin, Islet-1, Nkx6.1 and GLUT2.

Interestingly, recent studies underscore a regulatory role of Nrf2 in diabetic wound repair and the tissue regeneration process in various organs such as skeletal muscle, kidney and liver (32-36). Similarly, the HO system has been implicated in tissue regeneration (37,38), thus, it is possible that Nrf2/HO synergism may play a reasonable role in pancreatic repair. To test this hypothesis, we analysed several proteins, markers and transcriptional factors in pancreatic homogenates that are implicated in pancreatic repair and /or the regeneration process, such as stem cell marker (c-Kit, Sca-1), markers of early β-cells and islet development (Oct3/4, Pax2, β-catenin, Islet-1), and functional markers of β-cells maturation and functions (Nkx6.1, GLUT2) (14-21). A depressed expression of these markers was observed in the STZ-treated diabetic group, suggesting that the diabetic condition negatively regulates the expression of these markers in the pancreas and due to this reason, the tissue regenerative capabilities of the pancreas is markedly reduced during diabetes. The enhancement of c-Kit, Sca-1, Oct3/4, Pax2, β-catenin, Islet-1, Nkx6.1, GLUT2 in pancreas of STZ rats is a novel observation.

It is evident that enhanced macrophage infiltration is the primary characteristic of injured pancreas during T1D (28-39). In our experiments, diabetes induction through STZ was associated with several folds increased expression of proinflammatory M1 markers of macrophages in the STZ-group in both pancreas and liver which is indicative of inflammatory injury. In contrast, hemin-induced Nrf2/HO axis was associated with reduction of inflammation in pancreas and liver. It is reported that during inflammation, macrophages can exhibit distinct phenotypes i.e. the classical M1-phenotype which is pro-inflammatory and the alternative-activated M2-phenotype that is known to have anti-inflammatory effects (30, 40). To resolve inflammation, these macrophages can switch their existing phenotype, for example M1-M2 transition, through a polarisation process (30,40).

In our experiments, Nrf2/HO-mediated anti-inflammatory effects were executed through selective enhancement of M2-phenotype expression of macrophage (ED2, CD206 and CD36) which are known to be anti-inflammatory and participate in tissue repair (30,40). The selective enhancement of M2-markers (ED2, CD206 and CD36) and parallel reduction in M1-phenotypic expression of ED1 is a novel mechanism by which upregulated Nrf2/HO reduced inflammation in STZ-rats which has not been previously reported in pancreas and liver of STZ-rats.

Elevated oxidative stress also a major contributor of tissue injury and metabolic dysfunction in T1D (4,5,41) and pancreatic tissue is highly vulnerable against oxidative stress in T1D due to their intrinsic weaker antioxidant defence (31). In this situation, potentiation of antioxidant capacity of the pancreas will have cytoprotective benefits. The data from the present study showed that hemin-mediated upregulation of the Nrf2/HO axis was associated with enhanced total antioxidant capacity of the pancreas, which is a measurement of several important antioxidant enzymes (superoxide dismutase, catalase, and glutathione peroxidase) and antioxidant

molecules (albumin, ceruloplasmin, ferritin, ascorbic acid, α-tocopherol, β-carotene, reduced glutathione, uric acid, and bilirubin). Our data indicated that the diabetic condition is associated with reduced levels of antioxidant status in STZ-rats compared to controls and the hemin-treated group and HO blockage further supressed the expression of antioxidant levels in pancreatic tissue. In contrast, antioxidant capacity of the pancreas is significantly augmented through hemin treatment.

It is reported that HO-metabolites biliverdin and ferritin have potent antioxidant effects (22), in addition, hemin therapy also enhanced the expression of antioxidant response transcriptional factor Nrf2 in pancreas which is a positive modulator of not only HO-mediated cytoprotective functions but also confers cytoprotection through production of antioxidant enzymes (24,25). Since, hemin augmented both HO and Nrf2 in pancreas, it is obvious that hemin-induced enhanced antioxidant capacity is a direct effect of Nrf2/HO axis upregulation and associated enhancement of antioxidant enzymes. The lower basal expression level of Nrf2 in control subjects may be due to downregulation of Nrf2 activation through Kelch-like erythroid cell-derived factor which is only known to activate Nrf2 in various conditions of inflammation and oxidative stress (24,25). In contrast, suppressed expression of Nrf2 in the STZ-treated diabetic group was indicative of a dysregulated Nrf2 activation mechanism during diabetes (24,25, 42).

It is known that inflammation and oxidative stress are negative modulators of glucose metabolism through suppression of insulin signaling components such as IRS-1, IRS-2, PI3K and GLUT4, in metabolic important tissues (4,43-47), and for physiological regulation of glucose, optimal functions of insulin signaling components are an essential requirement. Since hemin-induced Nrf2/HO axis attenuated inflammation and oxidative stress in diabetic animals, it is expected that these cytoprotective effects would be accompanied by improvement in the insulin signalling

mechanism and glucose metabolism. The data from the present study indicate that the diabetic condition significantly supressed the expression levels of insulin signaling components (IRS1, IRS2, PI3K, and GLUT4) in the liver and soleus muscle. However, hemin-mediated Nrf2/HO axis upregulation enhanced the expression of these components compared to the diabetic STZ-group in both liver and soleus muscle. Furthermore, hemin-mediated potentiation of insulin signalling components was associated with lowering of fasting blood glucose levels in diabetic animals (Table 6-1). These observations collectively indicated that although, hemin-treatment did not completely normalize the fasting blood glucose levels to the control levels, 4 wks of hemin regimen showed an effective suppression of the elevation of blood glucose level in STZ rats that is suggestive of improved glucose metabolism and increased insulin contents in diabetic animals. These observations were in line with previously published reports that during diabetes reduction of inflammatory and oxidative mechanisms have a positive impact on glucose metabolism in various conditions of inflammatory and oxidative-stress-induced tissue insult (4).

Taken together, the present study implicates the role of Nrf2/HO axis in regulation and maintenance of glucose metabolism through enhanced expression of insulin signalling components and reduction of hyperglycemia in the STZ-induced diabetes condition.

6.6 Conclusion

In conclusion, upregulation of Nrf2/HO axis, selective enhancement of M2-macrophage markers (ED2, CD206, CD36), potentiation of antioxidant capacity and insulin signalling components (IRS-1, IRS-2, PI3K, GLUT4) are the multifaceted mechanisms through which hemin suppresses tissue insults while improving glucose metabolism in STZ rats. The hemin-mediated potentiation of the Nrf2/HO axis and reduction of tissue comorbidities and dysfunctional

metabolism is associated with enhancement of several markers (c-Kit, Sca-1, Oct3/4, Pax2, β-catenin, Islet-1, Nkx6.1, GLUT2) implicated in pancreatic repair and/or regeneration in STZ rats. Thus, our present study underscores the important modulatory role of hemin therapy in improvement of tissue repair and metabolism during T1D and suggested that hemin-based strategies will be part of therapeutic protocols for T1D treatment in the future.

Table 6-1: Effects of hemin (HO-1 inducer) and CrMP (HO-1 blocker) treatment on physiological variables in STZ-induced diabetic Sprague Dawley (SD) rats

	Animal groups			
Physiological Variables	**SD + Citrate buffer**	**STZ**	**STZ + Hemin**	**STZ + Hemin + CrMP**
Body weight (g)	354.83 ± 11.04	198.96 ± 13.52[b]	221.53 ± 11.04[b]	241.52 ± 12.09[b]
Pancreas weight (g/Kg body weight)	0.528 ± 0.020	0.842 ± 0.049[b f]	0.690 ± 0.046[a]	0.642 ± 0.036[c]
Fasting glucose (mmol/L)	4.52 ± 0.15	23.23 ± 0.37[b e g]	12.20 ± 0.27[b d g]	19.66 ± 1.05[b d g]
Water intake (mL/24hrs)	39.37 ± 4.00	138.86 ± 4.90[b e]	87.98 ± 4.0[b d g]	131.58 ± 4.37[b e]
Urine volume (mL/24hrs)	14.98 ± 3.60	125.26 ± 4.4[b e f]	79.69 ± 3.6[b d g]	106.29 ± 3.94[b c e]

Table 6-1: Effects of hemin and CrMP-treatment in STZ-treated diabetic rats. Statistical analysis was done using analysis of variance (ANOVA) and analysis of variance for repeated measures

followed by post hoc analysis. Values are means ± SEM for *n*=4-6 rats per group. STZ, streptozotocin-induced diabetic; CrMP, chromium mesoporphyrin [a]p<0.05 vs control group; [b]p<0.01 vs control group; [c]p<0.05 vs STZ group; [d]p<0.01 vs STZ group; [e]p<0.01 vs STZ + hemin group; [f]p<0.05 vs STZ + hemin + CrMP group; [g]p<0.01 vs STZ + hemin + CrMP group.

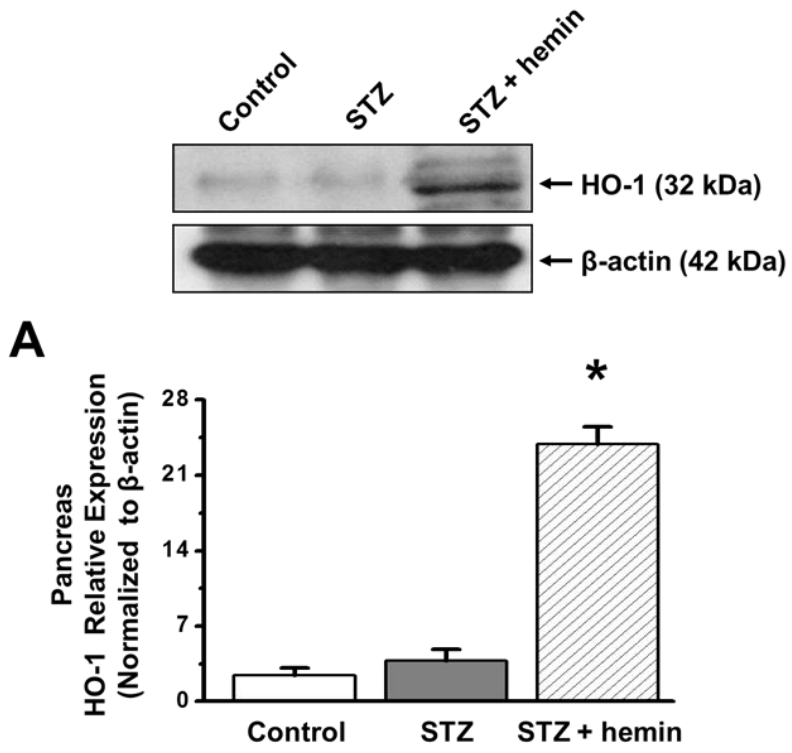

Figure 6-1: Effects of the HO-1 inducer, hemin on HO-1 expression in the pancreas of diabetic STZ-rats. (A) Hemin treatment enhanced HO-1, whereas the control group showed lower basal expression of HO-1 and there was no increase in HO-1 expression in the STZ-treated diabetic rats. Statistical analysis was done using Student's *t-test*. Bars represent means ± SEM; *n* = 4 rats per group (*p<0.01 vs control group and STZ group).

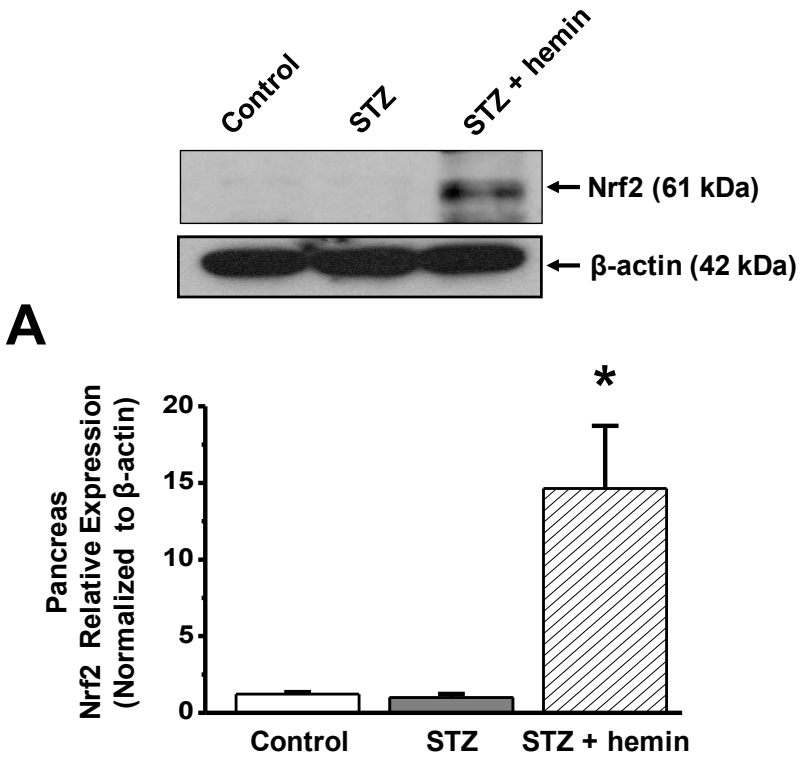

Figure 6-2: Effects of the HO-1 inducer, hemin on Nrf2 expression in the pancreas of diabetic STZ-rats. (A) Hemin enhanced Nrf2, whereas the basal level of Nrf2 was significantly lower in control group while significantly abated in STZ-treated diabetic group compared to hemin-treated group. Statistical analysis was done using Student's *t-test*. Bars represent means ± SEM; n = 4 rats per group (*$p<0.05$ vs control group and STZ group).

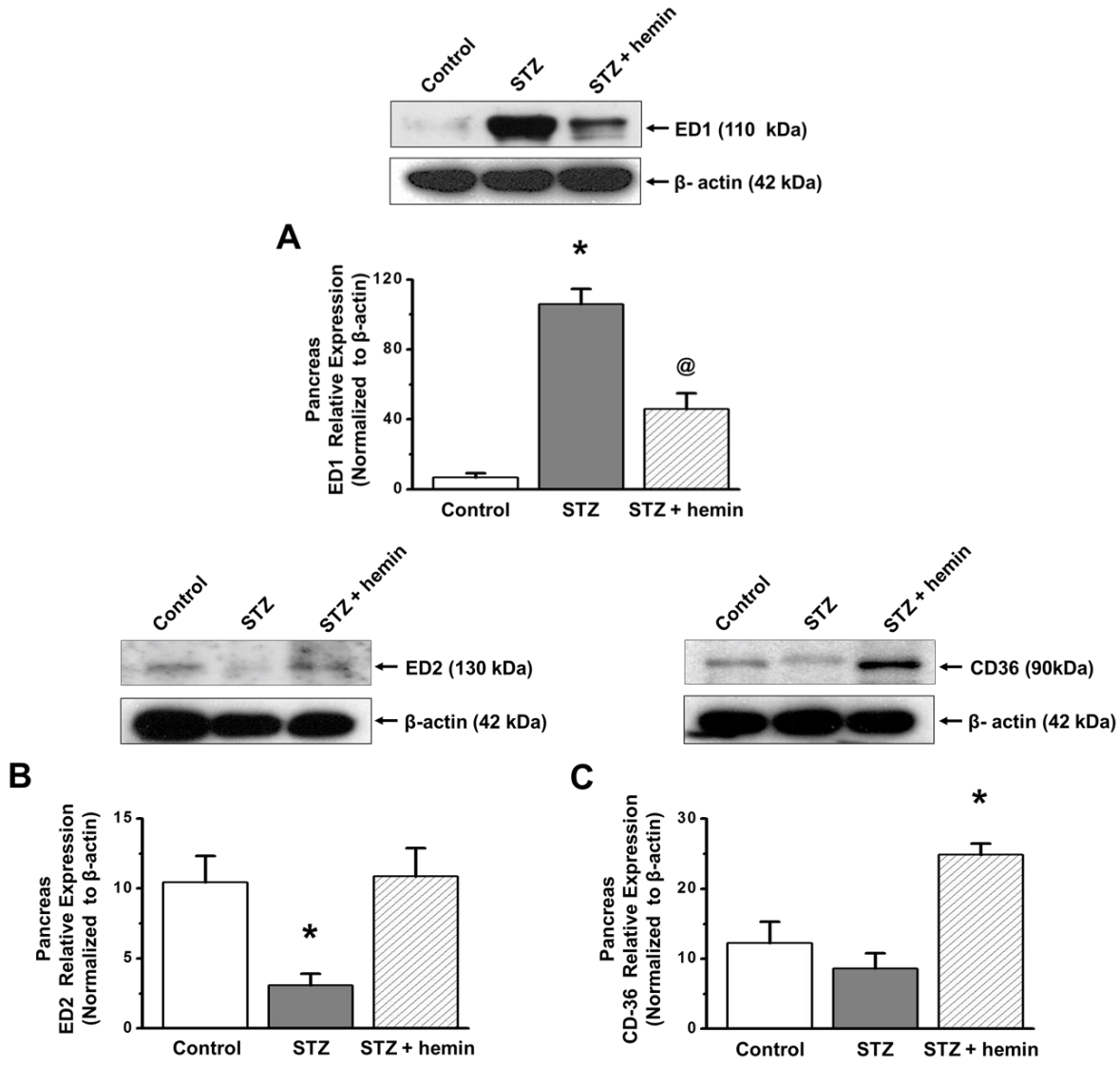

Figure 6-3: Effects of HO-1 inducer, hemin on ED1, ED2, and CD36 in the pancreatic tissue of diabetic STZ-rats. Hemin therapy (A) reduced ED1, but (B) enhanced ED2, (C) increased CD36 in STZ-treated diabetic rats. Statistical analysis was done using Student's *t-test*. Bars represent means ± SEM; n = 4 rats per group (*$p<0.05$ vs all groups; $^{@}p<0.05$ vs all groups).

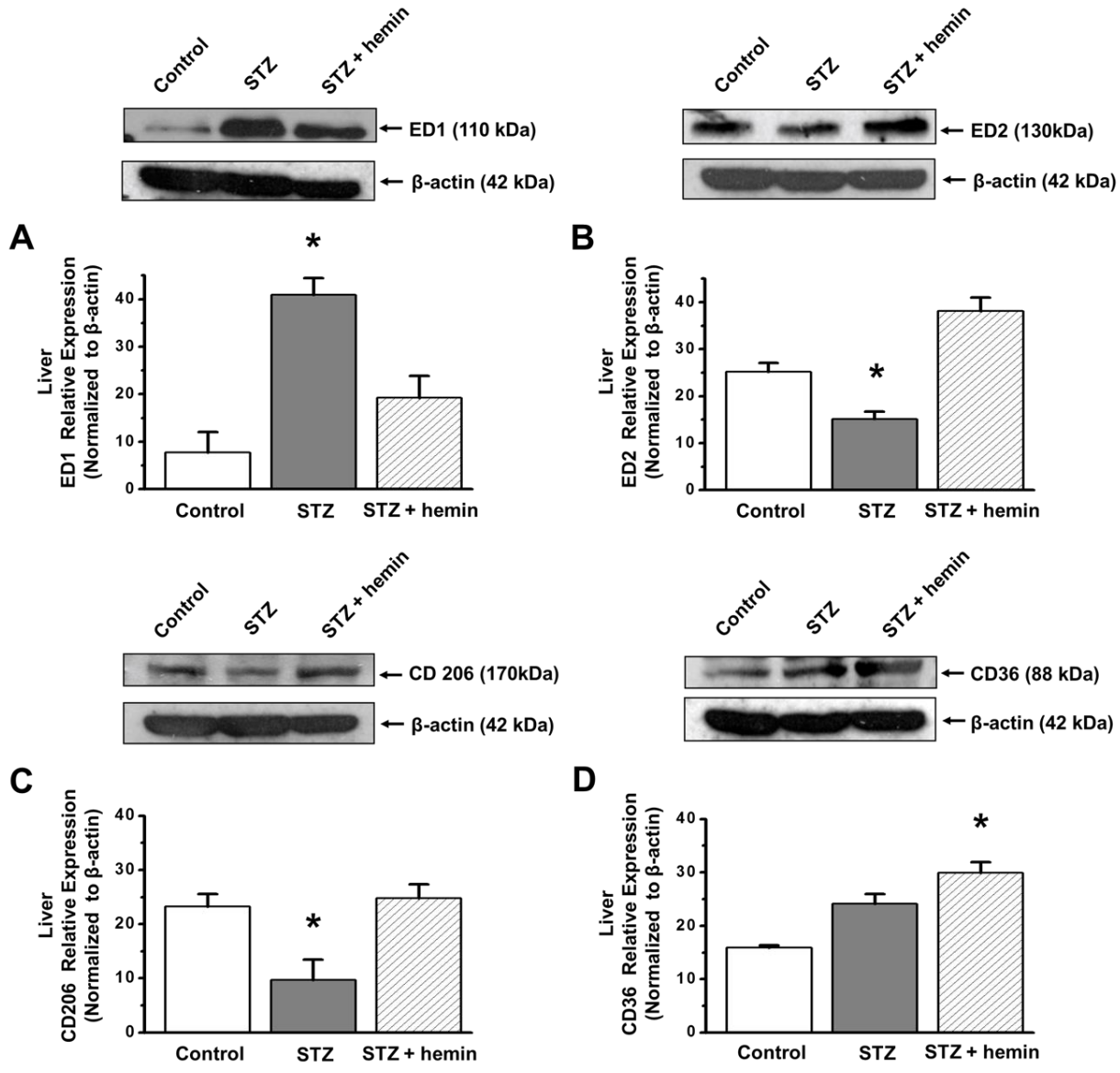

Figure 6-4: Effects of HO-1 inducer, hemin on ED1, ED2, CD206 and CD36 in the liver of diabetic STZ-rats. Hemin therapy (A) reduced ED1, but (B) enhanced ED2, (C) increased CD206 (D) enhanced CD36 in STZ-treated diabetic rats. Statistical analysis was done using Student's *t-test*. Bars represent means ± SEM; n = 4 rats per group (*$p<0.05$ vs all groups).

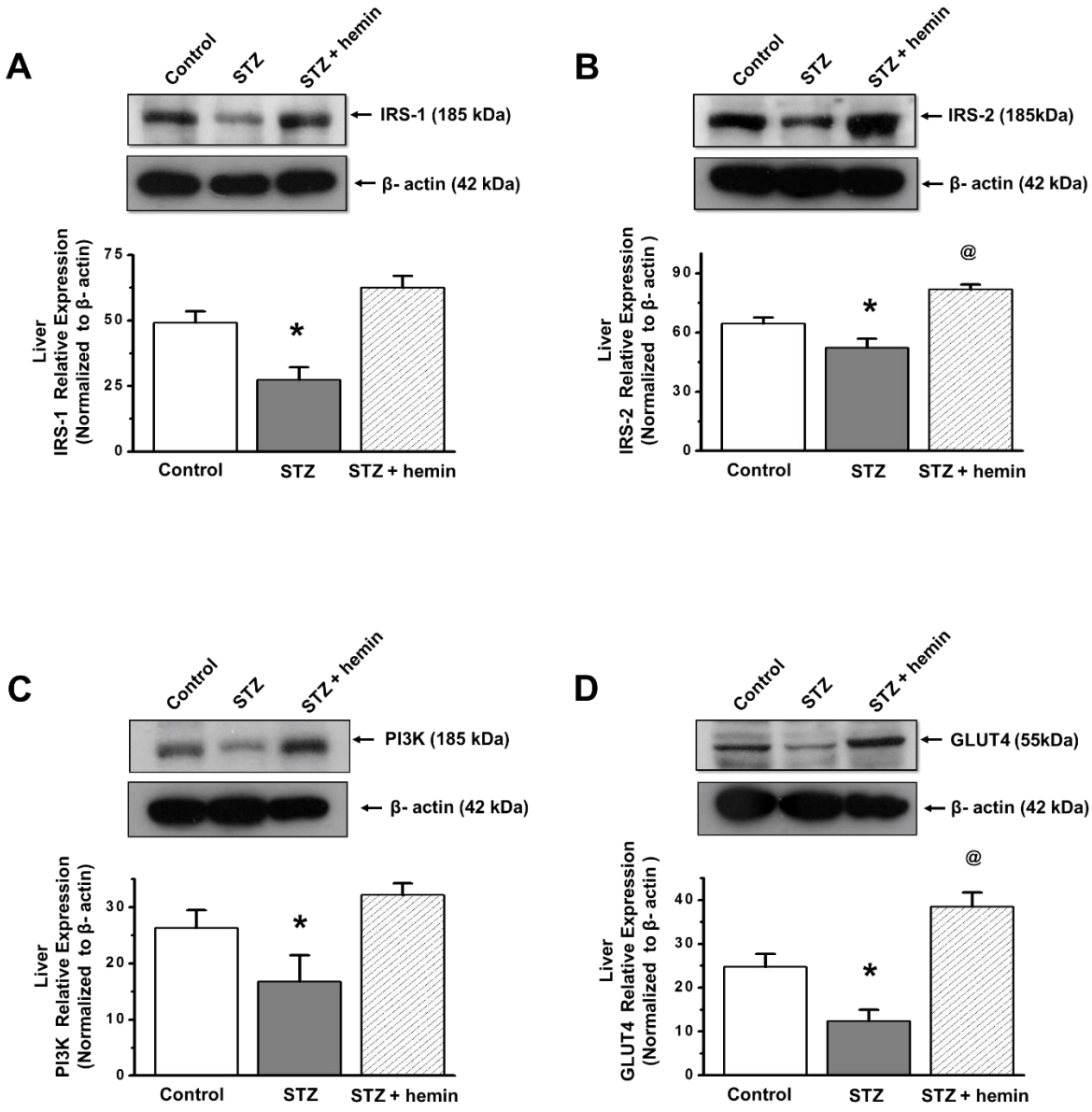

Figure 6-5: Effects of HO-1 inducer, hemin on IRS-1, IRS-2, PI3K and GLUT4 in the liver of diabetic STZ-rats. Hemin therapy significantly enhanced the expression of insulin components (A) IRS-1, (B) IRS-2, (C) PI3K, and (D) GLUT4 in STZ-treated diabetic rats. Statistical analysis was done using Student's *t-test*. Bars represent means ± SEM; n = 4 rats per group (*$p<0.05$ vs all groups, $^{@}p<0.05$ vs all groups).

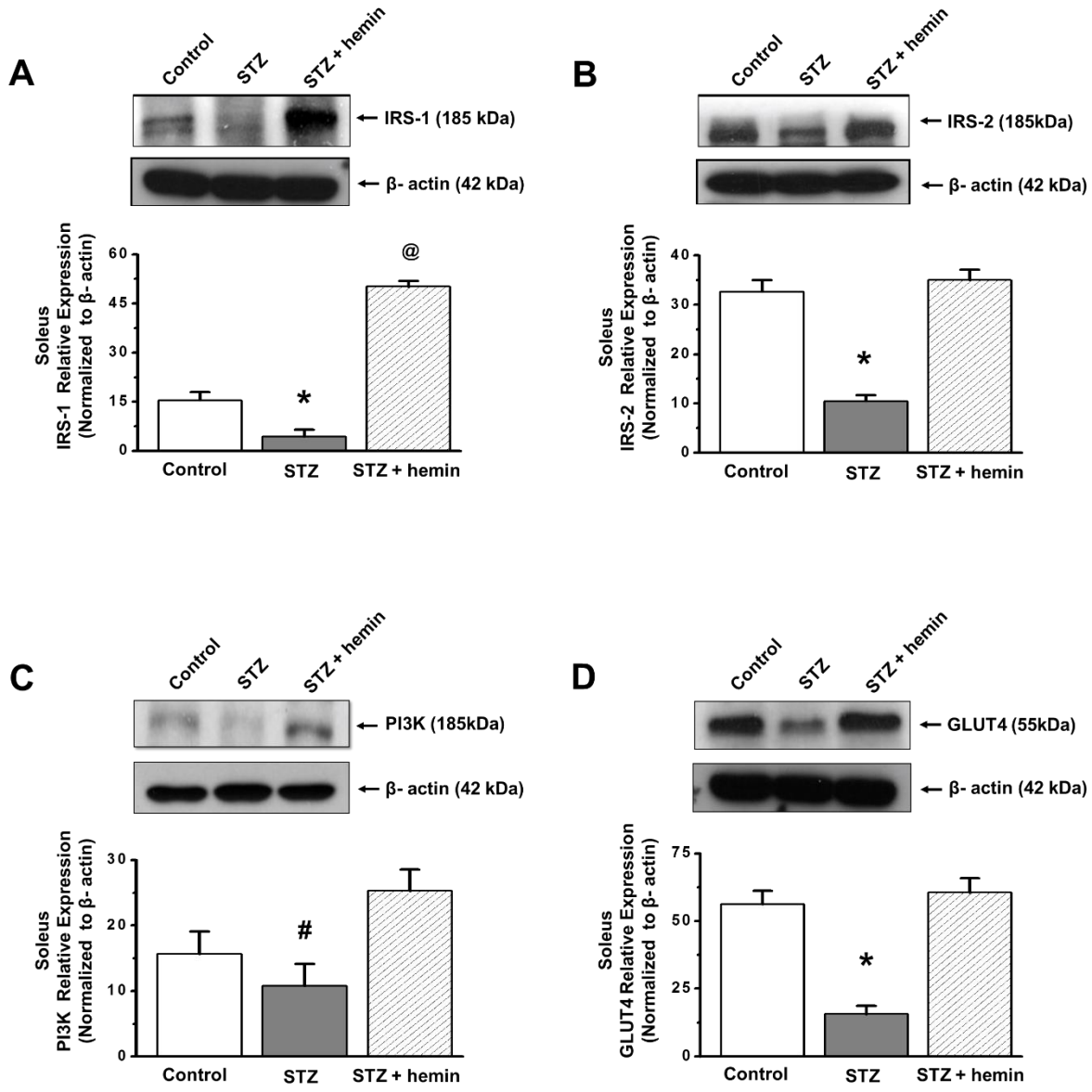

Figure 6-6: Effects of HO-1 inducer, hemin on IRS-1, IRS-2, PI3K and GLUT4 in the soleus muscle of diabetic STZ-rats. Hemin therapy significantly enhanced the expression of insulin components (A) IRS-1, (B) IRS-2, (C) PI3K, and (D) GLUT4 in STZ-treated rats. Statistical analysis was done using Student's *t-test*. Bars represent means ± SEM; *n* = 4 rats per group (*$p<0.01$ vs all groups, $^{@}p<0.01$ vs all groups, $^{\#}p<0.05$ vs STZ+ hemin group only).

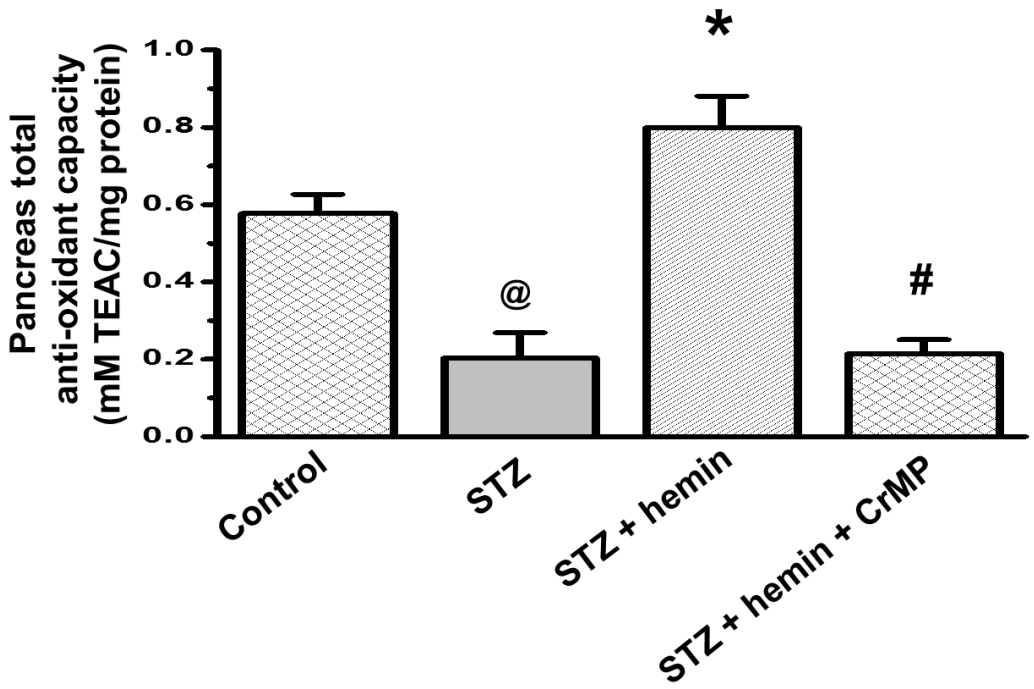

Figure 6-7: Effects of hemin on total antioxidant capacity in the pancreas of diabetic STZ-rats. Hemin therapy significantly enhanced the total antioxidant capacity of pancreas in STZ-treated diabetic rats. Statistical analysis was done using analysis of variance (ANOVA) followed by post hoc analysis. Bars represent means ± SEM; n = 6 rats, control and hemin group, n = 4, STZ-treated diabetic rats and n = 5 rats, CrMP group (*$p<0.01$ vs STZ and STZ + hemin + CrMP group; $^{@}p<0.01$ vs control group and STZ + hemin group, $^{\#}p<0.01$ vs control group).

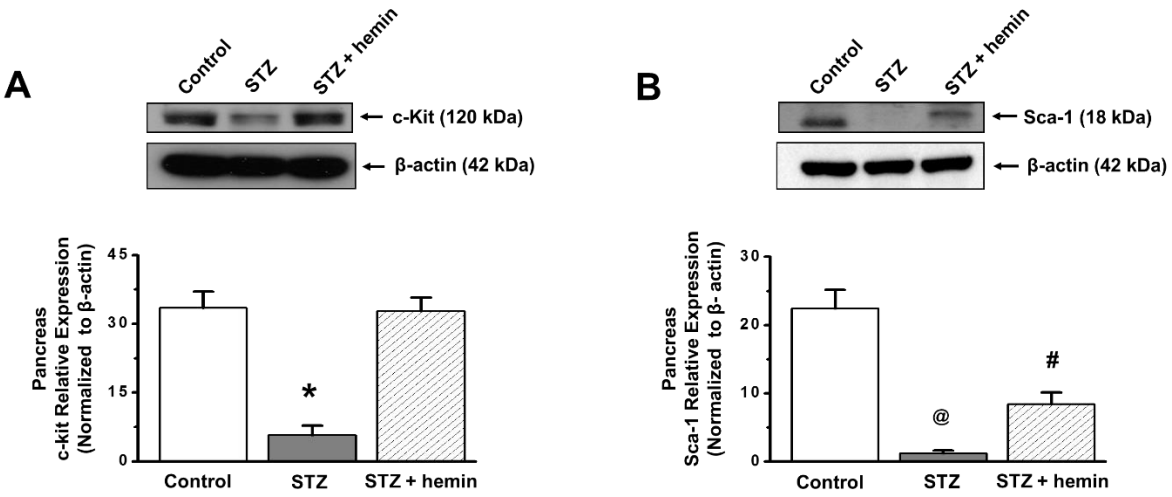

Figure 6-8: Effects of hemin on expression of stem cell markers in the pancreatic tissue of diabetic STZ-rats. Hemin therapy significantly enhanced the expression of stem cell markers (A) c-Kit and (B) Sca-1 in STZ-treated diabetic rats. Statistical analysis was done using Student's *t-test*. Bars represent means ± SEM; n = 4 rats per group (*$p<0.01$ vs all groups, $^{\#}p<0.05$ vs control and STZ group, $^{@}p<0.01$ vs control group only).

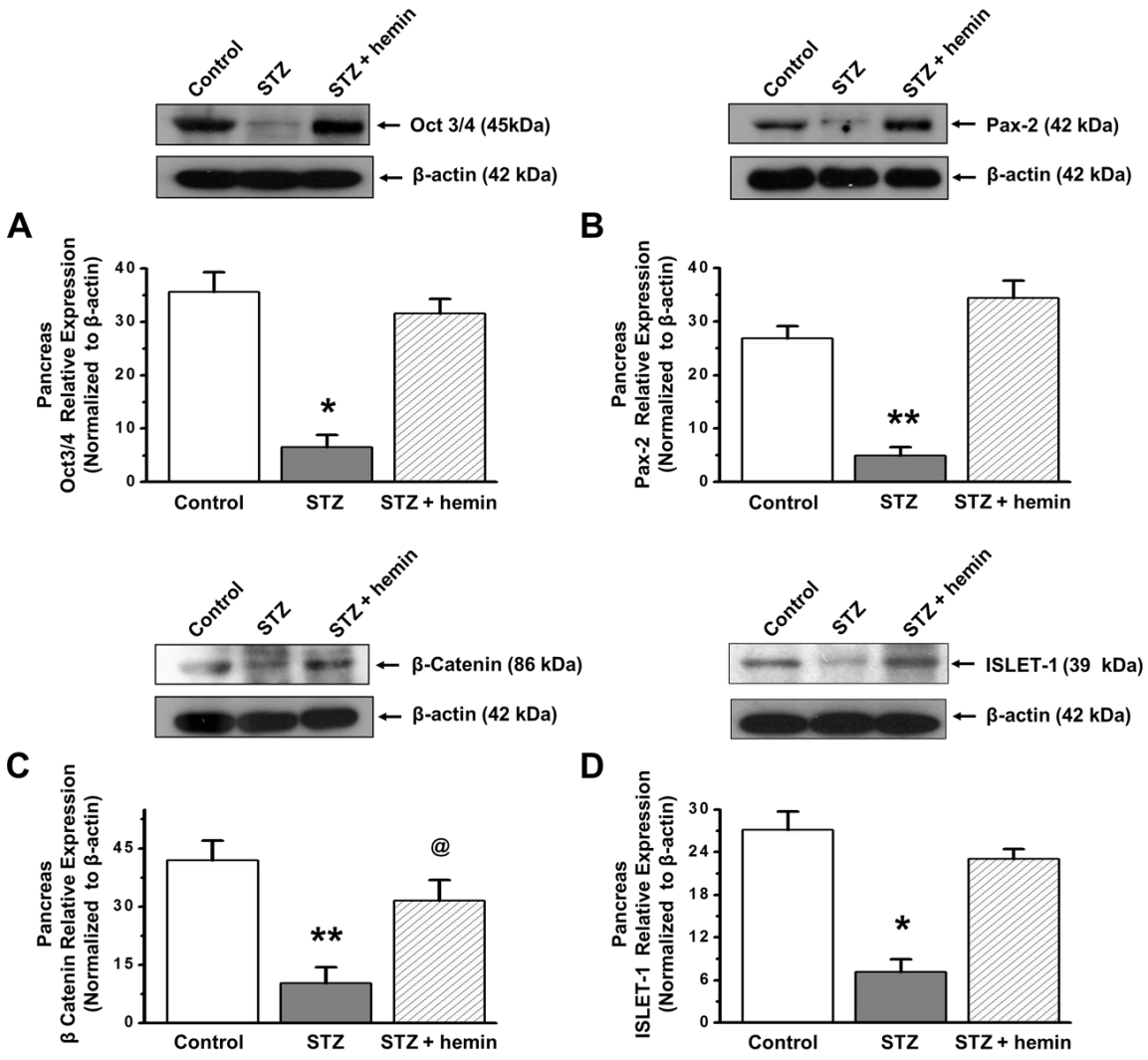

Figure 6-9: Effects of hemin on expression of markers of early β-cells development in pancreatic tissue of diabetic STZ-rats. Hemin therapy significantly enhanced the expression of (A) Oct3/4 (B) Pax2, (C) β-catenin and (D) Islet-1 in STZ-treated rats. Statistical analysis was done using Student's *t-test*. Bars represent means ± SEM; n = 4 rats per group (**p<0.05 vs all groups, *p<0.01 vs all groups, $^{@}$p<0.05 vs all groups).

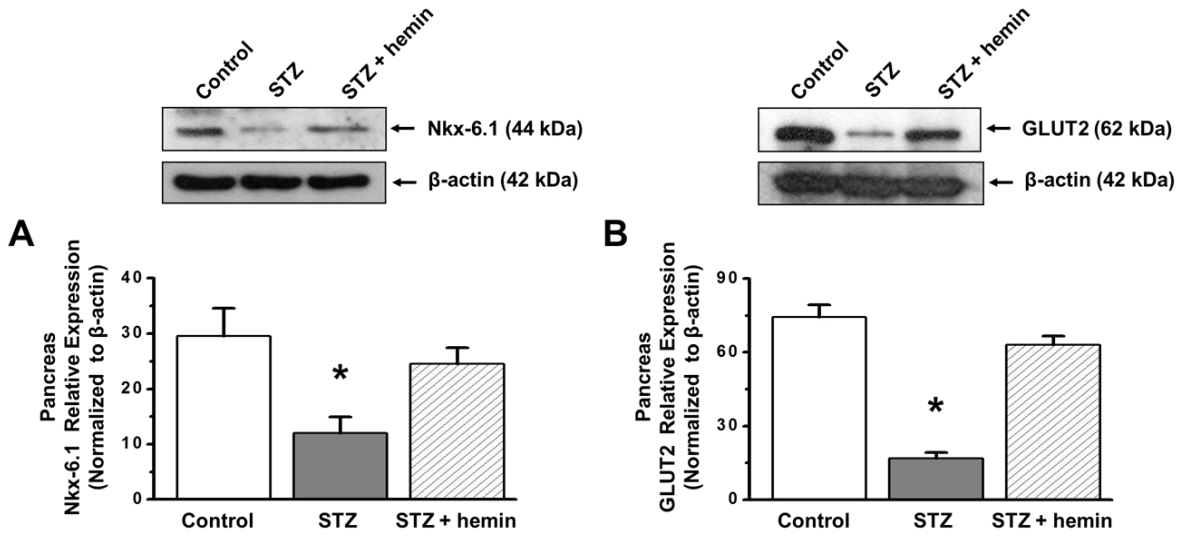

Figure 6-10: Effects of hemin on expression of markers of β-cells maturation and functions in the pancreatic tissue of diabetic STZ-rats. Hemin therapy significantly enhanced the expression of (A) Nkx6.1 and (B) GLUT2 in STZ-treated diabetic rats. Statistical analysis was done using Student's *t-test*. Bars represent means ± SEM; n = 4 rats per group (*p<0.01 vs all groups).

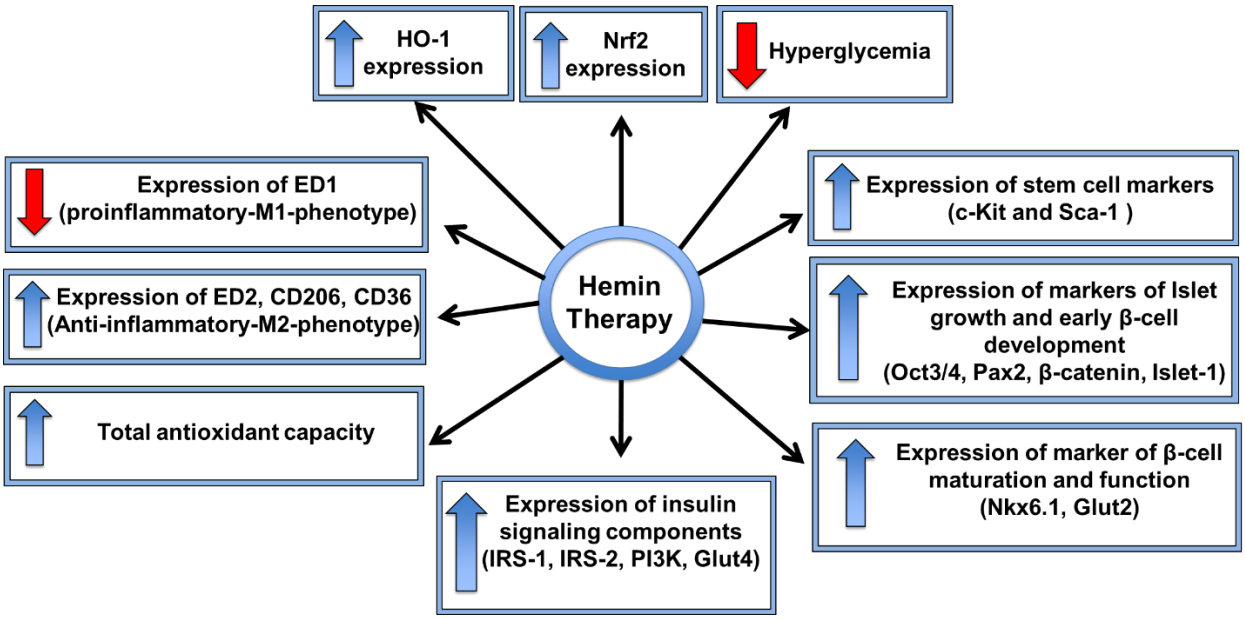

Figure 6-11: Summary of results. **Abbreviations used**; Heme oxygenase-1 (HO-1), Nuclear factor-(erythroid-derived 2)-like 2 factor (Nrf2), Classical M1-macrophages; Alternative-activated M2-macrophages; Cluster of differentiation-68 (ED1) macrophages; Cluster of differentiation-163 (ED2) macrophages; Cluster of differentiation-206 (CD206) macrophages; Cluster of differentiation-14 (CD14) macrophages; Cluster of differentiation-36 (CD36) macrophages; Tyrosine-protein kinase protein (c-Kit); Stem cell antigen-1 (Sca-1); Octamer-binding transcription factor-3/4 (Oct3/4); Paired homeodomain transcription factor-2 (Pax2); Beta catenin (β-catenin); Insulin gene enhancer protein-1 (Islet-1); Homeobox protein Nkx6.1; Glucose transporter 2 (GLUT2); Insulin receptor substrate-1 (IRS-1); Insulin receptor substrate-2 (IRS-2); Phosphoinositide 3-kinase (PI3K); Glucose transporter 4 (GLUT4).

6.7 References

1. International Diabetes Federation. IDF Diabetes Atlas, 7th edn. Brussels, Belgium: International Diabetes Federation, 2015.

2. Daneman D. Type 1 diabetes. Lancet 2006; 367:847-858

3. Kurrer MO, Pakala SV, Hanson HL, Katz JD. Beta cell apoptosis in T cell-mediated autoimmune diabetes. Proc Natl Acad Sci U S A 1997; 94:213-218

4. Ndisang JF, Jadhav A. Heme oxygenase system enhances insulin sensitivity and glucose metabolism in streptozotocin-induced diabetes. Am J Physiol Endocrinol Metab 2009; 296:E829-841

5. Ndisang JF, Jadhav A. Hemin therapy improves kidney function in male streptozotocin-induced diabetic rats: role of the heme oxygenase/atrial natriuretic peptide/adiponectin axis. Endocrinology 2014; 155:215-229

6. Lechleitner M, Hoppichler F. Insulin therapy. Wien Med Wochenschr 2011; 161:300-304

7. Shapiro AM, Lakey JR, Ryan EA, Korbutt GS, Toth E, Warnock GL, Kneteman NM, Rajotte RV. Islet transplantation in seven patients with type 1 diabetes mellitus using a glucocorticoid-free immunosuppressive regimen. N Engl J Med 2000; 343:230-238

8. Xu X, D'Hoker J, Stange G, Bonne S, De Leu N, Xiao X, Van de Casteele M, Mellitzer G, Ling Z, Pipeleers D, Bouwens L, Scharfmann R, Gradwohl G, Heimberg H. Beta cells can be generated from endogenous progenitors in injured adult mouse pancreas. Cell 2008; 132:197-207

9. Li WC, Rukstalis JM, Nishimura W, Tchipashvili V, Habener JF, Sharma A, Bonner-Weir S. Activation of pancreatic-duct-derived progenitor cells during pancreas regeneration in adult rats. J Cell Sci 2010; 123:2792-2802

10. Dor Y, Brown J, Martinez OI, Melton DA. Adult pancreatic beta-cells are formed by self-duplication rather than stem-cell differentiation. Nature 2004; 429:41-46

11. Georgia S, Bhushan A. Beta cell replication is the primary mechanism for maintaining postnatal beta cell mass. J Clin Invest 2004; 114:963-968

12. Teta M, Long SY, Wartschow LM, Rankin MM, Kushner JA. Very slow turnover of beta-cells in aged adult mice. Diabetes 2005; 54:2557-2567

13. Kushner JA. The role of aging upon beta cell turnover. J Clin Invest 2013; 123:990-995

14. Gong J, Zhang G, Tian F, Wang Y. Islet-derived stem cells from adult rats participate in the repair of islet damage. J Mol Histol 2012; 43:745-750

15. Rovira M, Scott SG, Liss AS, Jensen J, Thayer SP, Leach SD. Isolation and characterization of centroacinar/terminal ductal progenitor cells in adult mouse pancreas. Proc Natl Acad Sci U S A 2010; 107:75-80

16. Zhao M, Amiel SA, Christie MR, Muiesan P, Srinivasan P, Littlejohn W, Rela M, Arno M, Heaton N, Huang GC. Evidence for the presence of stem cell-like progenitor cells in human adult pancreas. J Endocrinol 2007; 195:407-414

17. Ritz-Laser B, Estreicher A, Gauthier B, Philippe J. The paired homeodomain transcription factor Pax-2 is expressed in the endocrine pancreas and transactivates the glucagon gene promoter. J Biol Chem 2000; 275:32708-32715

18. Figeac F, Uzan B, Faro M, Chelali N, Portha B, Movassat J. Neonatal growth and regeneration of beta-cells are regulated by the Wnt/beta-catenin signaling in normal and diabetic rats. Am J Physiol Endocrinol Metab 2010; 298:E245-256

19. Du A, Hunter CS, Murray J, Noble D, Cai CL, Evans SM, Stein R, May CL. Islet-1 is required for the maturation, proliferation, and survival of the endocrine pancreas. Diabetes 2009; 58:2059-2069

20. Guillam MT, Hummler E, Schaerer E, Yeh JI, Birnbaum MJ, Beermann F, Schmidt A, Deriaz N, Thorens B. Early diabetes and abnormal postnatal pancreatic islet development in mice lacking Glut-2. Nat Genet 1997; 17:327-330

21. Sander M, Sussel L, Conners J, Scheel D, Kalamaras J, Dela Cruz F, Schwitzgebel V, Hayes-Jordan A, German M. Homeobox gene Nkx6.1 lies downstream of Nkx2.2 in the major pathway of beta-cell formation in the pancreas. Development 2000; 127:5533-5540

22. Mishra M, Ndisang JF. A critical and comprehensive insight on heme oxygenase and related products including carbon monoxide, bilirubin, biliverdin and ferritin in type-1 and type-2 diabetes. Curr Pharm Des 2014; 20:1370-1391

23. Ndisang JF, Jadhav A. The heme oxygenase system attenuates pancreatic lesions and improves insulin sensitivity and glucose metabolism in deoxycorticosterone acetate hypertension. Am J Physiol Regul Integr Comp Physiol 2010; 298:R211-223

24. Srisook K, Kim C, Cha YN. Molecular mechanisms involved in enhancing HO-1 expression: de-repression by heme and activation by Nrf2, the "one-two" punch. Antioxid Redox Signal 2005; 7:1674-1687

25. Ndisang JF. Synergistic Interaction Between Heme Oxygenase (HO) and Nuclear-Factor E2-Related Factor-2 (Nrf2) against Oxidative Stress in Cardiovascular Related Diseases. Curr Pharm Des 2017; 23:1465-1470

26. Suman RK, Ray Mohanty I, Borde MK, Maheshwari U, Deshmukh YA. Development of an Experimental Model of Diabetes Co-Existing with Metabolic Syndrome in Rats. Adv Pharmacol Sci 2016; 2016:9463476

27. Jorns A, Arndt T, Meyer zu Vilsendorf A, Klempnauer J, Wedekind D, Hedrich HJ, Marselli L, Marchetti P, Harada N, Nakaya Y, Wang GS, Scott FW, Gysemans C, Mathieu C, Lenzen S. Islet infiltration, cytokine expression and beta cell death in the NOD mouse, BB rat, Komeda rat, LEW.1AR1-iddm rat and humans with type 1 diabetes. Diabetologia 2014; 57:512-521

28. Kolb H, Burkart V, Appels B, Hanenberg H, Kantwerk-Funke G, Kiesel U, Funda J, Schraermeyer U, Kolb-Bachofen V. Essential contribution of macrophages to islet cell destruction in vivo and in vitro. J Autoimmun 1990; 3 Suppl 1:117-120

29. Damoiseaux JG, Dopp EA, Calame W, Chao D, MacPherson GG, Dijkstra CD. Rat macrophage lysosomal membrane antigen recognized by monoclonal antibody ED1. Immunology 1994; 83:140-147

30. Ndisang JF, Mishra M. The heme oxygenase system selectively suppresses the proinflammatory macrophage m1 phenotype and potentiates insulin signaling in spontaneously hypertensive rats. Am J Hypertens 2013; 26:1123-1131

31. Tiedge M, Lortz S, Drinkgern J, Lenzen S. Relation between antioxidant enzyme gene expression and antioxidative defense status of insulin-producing cells. Diabetes 1997; 46:1733-1742

32. Soares MA, Cohen OD, Low YC, Sartor RA, Ellison T, Anil U, Anzai L, Chang JB, Saadeh PB, Rabbani PS, Ceradini DJ. Restoration of Nrf2 Signaling Normalizes the Regenerative Niche. Diabetes 2016; 65:633-646

33. Long M, Rojo de la Vega M, Wen Q, Bharara M, Jiang T, Zhang R, Zhou S, Wong PK, Wondrak GT, Zheng H, Zhang DD. An Essential Role of NRF2 in Diabetic Wound Healing. Diabetes 2016; 65:780-793

34. Zhaleh F, Amiri F, Mohammadzadeh-Vardin M, Bahadori M, Harati MD, Roudkenar MH, Saki S. Nuclear factor erythroid-2 related factor 2 overexpressed mesenchymal stem cells transplantation, improves renal function, decreases injuries markers and increases repair markers in glycerol-induced Acute kidney injury rats. Iran J Basic Med Sci 2016; 19:323-329

35. Shelar SB, Narasimhan M, Shanmugam G, Litovsky SH, Gounder SS, Karan G, Arulvasu C, Kensler TW, Hoidal JR, Darley-Usmar VM, Rajasekaran NS. Disruption of nuclear factor (erythroid-derived-2)-like 2 antioxidant signaling: a mechanism for impaired activation of stem cells and delayed regeneration of skeletal muscle. FASEB J 2016; 30:1865-1879

36. Dayoub R, Vogel A, Schuett J, Lupke M, Spieker SM, Kettern N, Hildt E, Melter M, Weiss TS. Nrf2 activates augmenter of liver regeneration (ALR) via antioxidant response element and links oxidative stress to liver regeneration. Mol Med 2013; 19:237-244

37. Ndisang JF, Tiwari S. Featured article: induction of heme oxygenase with hemin improves pericardial adipocyte morphology and function in obese Zucker rats by enhancing proteins of regeneration. Exp Biol Med (Maywood) 2015; 240:45-57

38. Ndisang JF, Tiwari S. Mechanisms by which heme oxygenase rescue renal dysfunction in obesity. Redox Biol 2014; 2:1029-1037

39. Kolb-Bachofen V, Schraermeyer U, Hoppe T, Hanenberg H, Kolb H. Diabetes manifestation in BB rats is preceded by pan-pancreatic presence of activated inflammatory macrophages. Pancreas 1992; 7:578-584

40. Gordon S. Alternative activation of macrophages. Nat Rev Immunol 2003; 3:23-35

41. Kaur G, Padiya R, Adela R, Putcha UK, Reddy GS, Reddy BR, Kumar KP, Chakravarty S, Banerjee SK. Garlic and Resveratrol Attenuate Diabetic Complications, Loss of beta-Cells, Pancreatic and Hepatic Oxidative Stress in Streptozotocin-Induced Diabetic Rats. Front Pharmacol 2016; 7:360

42. Aleksunes LM, Reisman SA, Yeager RL, Goedken MJ, Klaassen CD. Nuclear factor erythroid 2-related factor 2 deletion impairs glucose tolerance and exacerbates hyperglycemia in type 1 diabetic mice. J Pharmacol Exp Ther 2010; 333:140-151

43. Norquay LD, D'Aquino KE, Opare-Addo LM, Kuznetsova A, Haas M, Bluestone JA, White MF. Insulin receptor substrate-2 in beta-cells decreases diabetes in nonobese diabetic mice. Endocrinology 2009; 150:4531-4540

44. Kelleher AR, Fairchild TJ, Keslacy S. STZ-induced skeletal muscle atrophy is associated with increased p65 content and downregulation of insulin pathway without NF-kappaB canonical cascade activation. Acta Diabetol 2010; 47:315-323

45. Folli F, Saad MJ, Backer JM, Kahn CR. Regulation of phosphatidylinositol 3-kinase activity in liver and muscle of animal models of insulin-resistant and insulin-deficient diabetes mellitus. J Clin Invest 1993; 92:1787-1794

46. Ekladous D, Mehdi MZ, Costa M, Srivastava AK, Chiasson JL, Coderre L. Tissue- and fibre-specific modifications of insulin-signalling molecules in cardiac and skeletal muscle of diabetic rats. Clin Exp Pharmacol Physiol 2008; 35:971-978

47. Bahr I, Bazwinsky-Wutschke I, Wolgast S, Hofmann K, Streck S, Muhlbauer E, Wedekind D, Peschke E. GLUT4 in the endocrine pancreas-indicating an impact in pancreatic islet cell physiology? Horm Metab Res 2012; 44:442-450

CHAPTER 7

GENERAL DISCUSSION

The data presented in this thesis strongly suggest that inflammation and oxidative stress are among the major pathophysiological driving forces that cause tissue injury and compromise function in metabolic diseases, and unveil novel multi-faceted mechanisms through which upregulation of the HO-system potentiate insulin signaling, enhance glucose and lipid metabolism with corresponding improvement of pancreas, liver, kidney and heart function in animal models of obesity, diabetes, and hypertension.

7.1 Role of HO against inflammation

It is known that obesity, diabetes, and hypertension are the inflammatory conditions and macrophages are the major cellular entity that participates in both inflammation initiation and progression. Enhanced macrophage accumulation of proinflammatory M1-macrophages and augmentation of proinflammatory cytokines and chemokines (TNF-α, IL-6, IL-1β, MCP-1, MIP-1α) are the key events during these conditions that not only initiate tissue injury but also define the severity and progression of these conditions (5-7,27-29,347-351). During these conditions, excessive adiposity and elevated levels of lipid derivatives such as triglycerides and cholesterol are leading causes of inflammation initiation in metabolic tissues. In response, macrophages accumulate in fat laden tissues and initiate inflammation-induced tissue injury mechanisms through overproduction of proinflammatory cytokines and chemokines (5,7,27-29,347-351). In several studies related to obesity, diabetes, and hypertension an increased accumulation of macrophages and elevated levels of proinflammatory cytokines and chemokines have been observed (5,7,27-29,347-351). The availability of protein markers for proinflammatory macrophages, such as ED1, give a great opportunity to trace this phenomenon in various tissue

(27,28). The present study shows that the condition of obesity, diabetes and hypertension are characterized by enhanced expression of pro-inflammatory ED1 macrophages in various inflamed tissues such as liver, heart, kidney, and pancreas that suggests increased inflammatory events in response to increasing obesity, diabetes and blood pressure elevation (10,15,16). However, HO upregulation through hemin is associated with marked reduction of ED1 expression that is suggestive of reduction in inflammation. Although, hemin-associated HO upregulation was associated with abated ED1, the mechanism through which hemin executed this protective effect was not known. In the scientific literature, it is reported that M2-macrophages, distinct functional subsets of resident macrophages, are involved in tissue repair and lowering of inflammation (22-24). Based on this information, several M2 macrophage markers (ED2, CD206, CD36, and CD14) were selected to investigate the hemin-induced anti-inflammatory mechanism in the present study (352-355). The data from the present study indicate that hemin treated animals showed an enhanced expression of M2-macrophages. This selective enhanced expression of M2-macrophages is suggestive of HO-mediated regulation of macrophage polarization event. Thus, the data of the present study indicate that hemin-induced HO upregulation was associated with regulation of macrophage polarization through which it selectively enhanced the anti-inflammatory M2 macrophages while restricted proinflammatory M1-macrophages in the injured tissue. The collective effect of this selectivity is a marked suppression of inflammation induced injuries in the vital organs liver, heart, kidney, and pancreas.

Chemokines and cytokines are implicated in the inflammatory effects of the M1-macrophage phenotype. It is known that M1-macrophages are the major producers of proinflammatory cytokines and chemokines (TNF-α, IL-6, IL-1β) and (MCP-1, MIP-1α) during tissue inflammation (22-24), and the data presented in this thesis confirmed the presence of the

proinflammatory cytokines and chemokines in liver, kidney and cardiac tissue. Thus, it is expected that HO-associated reduction of proinflammatory ED1 macrophages will be accompanied with a parallel reduction of macrophage associated enhanced production of TNF-α, IL-6, IL-1β, MCP-1, MIP-1α. The data indicated that HO upregulation significantly inhibited the TNF-α, IL-6, IL-1β, MCP-1, MIP-1α expression levels in liver, heart and kidney. These observations further supported the role of HO-associated modulation of inflammation during obesity, diabetes, and hypertension.

Based on these observations, the presented data collectively suggested that the hemin-induced selective inhibition of M1-macrophages was associated with augmentation of M2-macrophage markers (ED2, CD206, CD36, CD14) which is one mechanism by which the HO-system may reduce the elevated levels of inflammatory cytokines and chemokines associated cytotoxic tissue injury in metabolic dysfunctional states like obesity, diabetes, and hypertension. Thus, the data from the present study indicate that during metabolic tissue injury, hemin-mediated suppression of inflammation signalling has a protective significance that leads to improved tissue health and physiological functions during obesity, diabetes, and hypertension.

7.2 Role of HO against oxidative stress

Oxidative stress is another major player of tissue destruction of liver, heart, kidney and pancreas that governs tissue injury through induction of inflammation via proinflammatory cytokines and tissue fibrotic response in obesity, diabetes, and hypertension (109-114). In addition, during the conditions of obesity, diabetes, and hypertension, elevated levels of oxidative stress mediators also inhibit the insulin signalling mechanism and assist in development of insulin resistance and altered glucose metabolism, which collectively result in tissue dysfunction and failure (109-114).

Elevated fat derivatives, like triglycerides, cholesterol and hyperglycemia are detrimental to tissue morphology and functions via production of oxidative stress (109-114). During conditions of obesity and diabetes, overproduction of these oxidative stress generating molecules have been documented and suggest their participation in oxidative tissue injuries (109-114). In addition, tissue infiltrating macrophages are also shown to produce oxidative stress in the local tissue environment (5,7,115-118). Thus, collectively elevated oxidative stress participates in oxidative damage to tissue. Moreover, during T1D, where the pancreatic tissue has a low antioxidant capacity compared to other tissues, elevated oxidative stress causes significant damage to both endocrine and exocrine tissues (8,160,161), thus, in this condition, enhancement of an antioxidant defense mechanism is necessary.

The data of the present study also shows oxidative stress-induced injury in liver, kidney, and heart through elevation of a marker of lipid peroxidation and vascular oxidative stress (8-isoprostane and ET-1) (8,16,17,19,144,150-153,356). In both obesity and diabetes, elevated levels of 8-isoprostane and ET-1 are observed that is suggestive of the presence of an oxidative environment. However, in hemin-treated animals these markers were significantly attenuated in liver, kidney and cardiac tissue. Interestingly, the data in STZ rats indicated that hemin therapy significantly augmented the total antioxidant capacity of pancreatic tissue and upregulates the antioxidant related transcriptional factor Nrf2. But the question arises how the hemin induced HO-system participates in reduction of oxidative stress. It is reported that catabolic functions of the HO-system generates anti-inflammatory molecules like carbon monoxide and antioxidants like biliverdin and ferritin (356). In addition, the Nrf2/HO axis is shown to activate transcription of a number of antioxidant enzymes (357,358). Thus, the augmentation of antioxidant Nrf2 signaling and production of antioxidant molecules such as biliverdin and ferritin are the mechanisms through

which the hemin induced HO-system protects the tissue from oxidative injuries and this beneficial impact results in improvement of tissue morphology and functions.

7.3 Role of HO upregulation on body weight

Hemin therapy has been shown to be associated with a slight reduction in body weight measurements in all rat models (ZF, ZDF, SHR, STZ). The inhibition of HO either with CrMP or SnMP also further slightly decreased body weight in all experimental animals. Interestingly, hemin therapy also caused a weight reduction in the WKY genetic control of SHR rats or Zucker lean control rats. Due to this body weight reducing effect of hemin, one may consider the toxic effects of hemin in experimental animals. However, our previous experimental observations suggested that the above reduction in body weight was not due to an effect of hemin toxicity since toxicity parameters such as plasma gamma-glutamyl transferase, aspartate aminotransferase, and alanine aminotransferase were in the normal range (359).

7.4 Role of HO upregulation on blood glucose and blood pressure

Although, SHR rats and ZF rats were normoglycemic, hemin treatment further decreased glucose levels while HO inhibition in the CrMP group enhanced glycemic levels. Interestingly, hemin-mediated reduction of glucose levels was also seen in control Zucker lean animals, while HO-inhibitor group was associated with elevated blood glucose.

The data from the present study showed that hemin-therapy significantly reduced the fasting blood glucose levels in hyperglycemic ZDF and STZ rats, in contrast HO- inhibition through either CrMP group or SnMP acerbated the hemin-mediated glucose lowering effects. These observations collectively suggested the potent regulatory role of the HO-system in blood glucose lowering and

matched previously published reports where the HO-system metabolite carbon monoxide participates in insulin release through stimulation of islets (360-362). Furthermore, in hypertensive SHR-rats, hemin-induced HO upregulation effectively regulated blood pressure elevation while HO blockage through CrMP ameliorates the hemin-mediated lowering effect on blood pressure. The blood pressure regulating effects of hemin was in line with our previously published reports (363,364), and was associated with HO-mediated increased expression of sGC proteins and increased cGMP levels in SHR rats. Thus, the HO-induced lowering of blood glucose and blood pressure is suggestive of reduction of hyperglycemic-induced and pressure induced tissue injury during hypertension and diabetes.

7.5 Role of HO upregulation on tissue injury

The comorbid conditions of oxidative stress and inflammation in obesity, diabetes, and hypertension negatively affect the tissue morphology of liver, kidney and heart. Moreover, the physiological functions of these tissue are greatly disturbed and collectively develop into pathological conditions of fatty liver disease, nephropathy and cardiomyopathy if not managed efficiently. Data from the present study indicate that elevated adiposity in ZF rats resulted in significant enhancement of heart tissue weight which is indicative of hypertrophied changes of cardiac tissue (365-367). In addition, adiposity also greatly disturbed several functional hemodynamic parameters in cardiac tissue such as an increase in arterial systolic and diastolic pressure, mean arterial pressure, left ventricular (LV) developed pressure, total peripheral resistances, $+dp/dt_{(max)}$, heart rate and LV diastolic and systolic wall thickness (365-367). Furthermore, obesity downregulated the cardiac functional parameters such as decreased LV end-diastolic and systolic volume, stroke volume, and cardiac output. The obesity-induced cardiac

tissue injury was associated with enhanced expression of profibrotic mediators such as collagen-IV, fibronectin and TGF-β (368,369). Cardiac histological and morphometric analyses of obese ZF rats showed increased cardiomyocyte longitudinal muscle-fiber thickness and cardiac hypertrophy (365-367). In contrast, hemin therapy, significantly reduced heart weight close to the lean counterpart. Left ventricular thickness and expression of profibrotic collagen-IV, fibronectin and TGF-β that are the important factors for cardiac hypertrophy were greatly attenuated by hemin (365,366,368,369). Histological analysis further confirmed these observations, where hemin therapy significantly reduced cardiomyocyte longitudinal muscle-fiber thickness, scarring and interstitial and perivascular collagen deposition which are the important indices of cardiac hypertrophy (367), while HO blockage enhanced the hypertrophied cardiac tissue. Additionally, hemin associated reduction of cardiac hypertrophy was associated with improvement in hemodynamic parameters which were deviated in response to obesity. Hemodynamic parameters such as increased arterial systolic and diastolic pressure, mean arterial pressure, left ventricular (LV) developed pressure, total peripheral resistances, $+dp/dt_{(max)}$, heart rate and LV diastolic and systolic wall thickness were suppressed by hemin therapy while cardiac functions (LV end diastolic and systolic volume, stroke volume and cardiac output) were improved (365-367). Similarly, in obese diabetic ZDF animals, hemin-treatment reduced hepatic hypertrophy as indicated by a reduced liver-to-body weight ratio which is an important indicator hypertrophic liver (370) and reduction of profibrotic mediators such as TGF-β, fibronectin and collagen-IV implicated in hepatic fibrosis (371-376). However, hemin therapy showed a greater selectivity for reduction of fibronectin compared to collagen-IV. In addition, histological measurement showed that hemin therapy significantly reduced histopathological lesions of liver tissue as evident by hepatocyte ballooning injury and fibrosis in ZDF control animal (377,378).

Increasing perirenal adiposity is a critical factor in renal dysfunction and injury and renal failure in obesity and diabetes (379-381). Hemin therapy significantly reduced perirenal adiposity in obese diabetic ZDF rats while HO inhibition nullified the hemin-mediated suppressive effect on perirenal adiposity. Enhanced renal fibrosis is a major event during obesity and diabetes that severely affected renal functions and reduced the expression of nephrin which is an important protein of podocyte functions (10,382-386). In addition, renal pathological features such as albuminuria, proteinuria and creatinine clearance were greatly affected (10,382-386). The data from the present study showed that hemin treatment in ZDF animals was associated with marked reduction of profibrotic fibronectin and collagen-IV expression. Histological analysis further showed that in hemin treated ZDF animals, renal histopathological lesions were greatly reduced through suppression of collagen deposition, tubular vacuolization, glomerulosclerosis, and perivascular fibrosis while nephrin expression was enhanced. The collective effect of these reduced renal pathologies through hemin treatment was associated with suppression of albuminuria, proteinuria with enhanced creatinine clearance. Thus, the data from the present study indicate that hemin-mediated HO-induction has a cytoprotective role in hepatic, renal and cardiac injuries during obesity and diabetes, that collectively results in improved cardiac, renal and hepatic functions.

7.6 Role of HO upregulation on insulin signaling

In obese, diabetic and hypertensive subjects, elevated levels of inflammatory and oxidative stress mediators are negative regulators of insulin signalling and glucose metabolism and during these conditions, insulin signalling is greatly attenuated (5,6,54-57,61,73,77,85,91,120,167-169,179-181,308).

Additionally, these inflammatory/oxidative mediators cause effective suppression of insulin-receptor-phosphorylation-mediated activation, thus, interfering in insulin-mediated activation of the insulin signalling mechanism (5,6,54-57,61,73,77,85,91,120,167-169,179-181,308). Moreover, the expression of important insulin signalling components such as IRS-1, IRS-2, PI3K and GLUT4 is also reduced that collectively results in abnormal or suppressed insulin signalling and development of insulin resistance in metabolically active tissues (5,6,54-57,61,73,77,85,91,120,167-169,179-181,308). The data from the present study showed the role of the above described negative consequences of inflammation and oxidative stress in dysregulated insulin signalling during obesity, diabetes, and hypertension. In hypertensive animals (SHR), obese animals (ZF-rats), and T1D-diabetic (STZ-rats) animals, the expression of insulin signalling components such as IRS-1, IRS-2, PI3K and GLUT4 was greatly attenuated in liver, soleus muscle and heart leading to abnormal glucose metabolism. Similarly, the altered or low expression of insulin signalling components were reported in our previous published report in ZDF model of T2D (15,341,359). However, hemin treatment greatly enhanced the expression of these components and potentiated the insulin signaling mechanism in both the obese and diabetic models.

Furthermore, it is reported that, enhanced HO-1 activity and increased production of carbon monoxide has a potent stimulating effect on cGMP expression, that is an important mediator of improved insulin signalling and metabolism (346,359,387). Hemin-treatment also increased cGMP levels in SHR, ZDF, ZF rats. In contrast, the ablation of HO greatly suppressed the expression and levels of these homeostatic and functional components of insulin signalling. In addition, in obese ZF-rats, the glucose tolerance test and a homeostasis model assessment of insulin resistance experiments showed that hemin therapy was associated with improvement of

insulin sensitivity, and glucose tolerance with suppressed the insulin resistance. Hemin treatment also enhanced adiponectin in ZF and ZDF rats that was shown to have a potent role in the insulin sensitizing mechanism during obesity and diabetes and hypertension (18,388,389).The data from the present study collectively suggested that hemin associated reduction of inflammation, oxidative stress and potentiation of insulin signalling components (IRS-1, IRS-2, PI3K, GLUT4) and augmentation of cGMP and adiponectin are the major mechanisms through which HO improves glucose metabolism in conditions of obesity, diabetes and hypertension.

7.7 Role of HO upregulation on markers of pancreatic repair and/or regeneration

Increasing inflammation and oxidative stress and low antioxidant capacity are key contributors to enhanced pancreatic injuries during T1D (160,161). In this condition, reduction of these tissue destructive conditions and enhancement of pancreatic repair would have cytoprotective advantage. Our previous studies showed that hemin therapy significantly reduced pancreatic lesions in both T1D and hypertensive rats through suppression of vacuolization, interstitial edema, mononuclear infiltration and acinar cell necrosis (8,9), however, the underlying mechanisms behind this cytoprotection and repair was unknown. It is reported in several models of rodents that during pancreatic injuries, several tissue repair and regeneration processes are activated and participate in resolution of tissue injuries.

The data from the present study showed that, hemin treatment not only reduced pancreatic inflammation and oxidative injuries but also enhanced several protein markers and transcriptional factors that are implicated in pancreatic repair and regeneration. The immunoblotting data from the present study in STZ rats showed that 4-wks hemin treatment significantly enhanced several markers implicated in pancreatic repair or regeneration, such as stem cell markers (c-Kit, Sca-1), markers of early β-cell growth and islet development (Oct3/4, Pax2, β-catenin, Islet-1) and β-cell

maturation and function (Nkx6.1, GLUT2) in the STZ pancreas. In contrast, the expression of these markers was greatly attenuated in diabetic STZ rats. The collective effect of the enhanced markers of pancreatic repair and or/ regeneration was associated with reduction in hyperglycemia. Thus, it is suggested that the hemin-induced HO-upregulation, participates in the enhancement of pancreatic repair and/or regeneration markers that may be a reason for reduction of pancreatic injury observed in our previous study (8,9).

Although, the data from present study indicate the enhancement of several markers of pancreatic repair and/ or regeneration, it seems that hemin therapy induced pancreatic regeneration by which it enhances the repair of injured pancreas. However, our study has some limitations. The present study only evaluated the effect of hemin-therapy on several markers of pancreatic repair and/ or regeneration at a whole animal level through measurement of expression of marker, in this situation, it is hard to confirm the individual contribution of these markers in pancreatic repair since the present study lacks the other data support. In addition, the present study did not use any genetic cellular tagging methods to trace the effect of hemin therapy on individual cells, for example β-cells. However, in the present study and past observation from our laboratory (359), hemin-mediated potentiation of insulin signalling, insulin levels and reduction of hyperglycemia are indicative of a positive influence of hemin therapy on pancreatic regeneration. Since, in recent years, pancreatic regeneration in the adult stage is greatly challenged by a number of studies (205,207,226,234-237,239-244), more investigation and data support are required at the molecular level to confirm the regenerative potency of hemin therapy.

CONCLUSION

My thesis represented a comprehensive study on the novel and multifaceted effects of the upregulated HO system on hepatic, renal, cardiac, pancreatic tissue injury, glucose homeostasis and tissue functions in conditions of obesity, diabetes, and hypertension. The data presented in this thesis demonstrated the potential role of the HO-inducer hemin in reduction of inflammation and oxidative stress-induced tissue comorbidities such as fibrosis and histopathological lesions in hepatic, renal and cardiac tissue while enhancement of repair and/or regenerative markers in the pancreas was observed. Additionally, hemin-mediated HO upregulation was associated with improvement in glucose metabolism through reduction of insulin resistance, hyperglycemia and potentiation of insulin signaling components.

The novel observations of the present study are as follows;

1) The hemin-induced HO system significantly reduced the inflammatory macrophage infiltration through the enhancement of macrophage polarization in which HO selectively enhanced the expression of anti-inflammatory M2-phenotype with corresponding suppression of the pro-inflammatory M1-phenotype in obese, diabetic and hypertensive rats.
2) Hemin-induced HO system attenuates pro-inflammatory chemokines/cytokines (TNF-α, IL-6, IL-1β, MCP-1, MIP-1α) and oxidative mediators (8-isoprostane and ET-1), while it enhanced antioxidant capacity and the antioxidant signalling transcriptional factor Nrf2 in obese, diabetic and hypertensive rats.
3) Hemin-mediated HO upregulation attenuates fibrosis, hypertrophy and histopathological lesions in the liver, cardiac and renal tissue via marked suppression of both ECM and profibrotic mediators, collagen-IV, fibronectin and TGF-β in obese and diabetic rats.

4) Hemin-induced HO significantly enhanced the glucose metabolism through potentiation of insulin signaling components (IRS1, IRS2, PI3K and GLUT4) and adiponectin while suppressing hyperglycemia, insulin resistance and glucose intolerance in obese, diabetic and hypertensive rats

5) Hemin-induced HO significantly enhanced the expression of Nrf2 transcription factor, and markers implicated in pancreatic repair and/or regeneration, such as stem cell markers (c-Kit, Sca-1), markers of early β-cell development (Oct3/4, Pax2, β-catenin, Islet-1), and markers of β-cell maturity and functions (Nkx6.1 and GLUT2) in pancreas of diabetic rats.

6) Collectively, these data suggest that HO reduced tissue inflammation (TNF-α, IL-1β, IL-6, MCP-1, MIP-1α), oxidative mediators (8-isoprostane, ET-1), profibrotic mediators (TGF-β, collagen-IV, fibronectin) and improved glucose metabolism through potentiation of the components of insulin signaling (IRS-1, IRS-2, PI3K, GLUT4) and adiponectin are the major mechanisms through which HO confers cytoprotection and metabolic regulation in conditions of tissue injury and metabolic dysfunction such as obesity, diabetes, and hypertension.

SIGNIFICANCE

Cellular injury and metabolic dysfunction are the hallmark features of obesity, hypertension and diabetes. Increasing inflammation and oxidative stress are considered as the major driving forces behind this altered cellular homeostasis and present a life-threatening risk. Several pharmaceutical advancements are currently in use to counteract these abnormal situations, but the desired outcome is still lacking due to intrinsic complexity and multigenic origin of these metabolic complications. Additionally, these conditions not only cause local tissue dysfunctions

but also systemically affect the whole physiological system. Thus, in this vulnerable condition, an effective alternative management tool is urgently required that efficiently counteracts these metabolic abnormalities at both the local and systemic levels.

In this context, the present study, provide a reasonable support for the use of hemin based therapeutic protocols in treatment of obesity, diabetes and hypertension associated metabolic tissue injury and dysfunction. Although, the hemin-based drug Penhematin® is already approved for treatment for the blood related disorder porphyria by the Food and Drug Administration, its use in metabolic disease is still restricted to rodent research. The data presented in this study provide valuable information regarding the potential beneficial effects of hemin therapy in rodents that could overcome tissue injury and metabolic dysregulation during obesity, diabetes and hypertensive conditions without any related drug toxicity. Thus, it is expected that in the future, hemin based strategies will be part of the pharmaceutical interventions for treatment of complications related to obesity, diabetes and hypertension in humans.

APPENDICES

Appendix A: **Mishra M,** Ndisang JF. A critical and comprehensive insight on heme oxygenase and related products including carbon monoxide, bilirubin, biliverdin and ferritin in type-1 and type-2 diabetes. ***Curr Pharm Des. 2014;*** 20(9):1370-91.

REFERENCES

1. International Diabetes Federation. IDF Diabetes Atlas, 7th edn. Brussels, Belgium: International Diabetes Federation, 2015.

2. WHO. A global brief on hypertension, A global brief on hypertension, Silent killer, global public health crisis, 2013.

3. Timar R, Timar B, Degeratu D, Serafinceanu C, Oancea C. Metabolic syndrome, adiponectin and proinflammatory status in patients with type 1 diabetes mellitus. J Int Med Res 2014; 42:1131-1138

4. Chillaron JJ, Sales MP, Flores-Le-Roux JA, Murillo J, Benaiges D, Castells I, Goday A, Cano JF, Pedro-Botet J. Insulin resistance and hypertension in patients with type 1 diabetes. J Diabetes Complications 2011; 25:232-236

5. Weisberg SP, McCann D, Desai M, Rosenbaum M, Leibel RL, Ferrante AW, Jr. Obesity is associated with macrophage accumulation in adipose tissue. J Clin Invest 2003; 112:1796-1808

6. Hotamisligil GS, Shargill NS, Spiegelman BM. Adipose expression of tumor necrosis factor-alpha: direct role in obesity-linked insulin resistance. Science 1993; 259:87-91

7. Xu H, Barnes GT, Yang Q, Tan G, Yang D, Chou CJ, Sole J, Nichols A, Ross JS, Tartaglia LA, Chen H. Chronic inflammation in fat plays a crucial role in the development of obesity-related insulin resistance. J Clin Invest 2003; 112:1821-1830

8. Ndisang JF, Jadhav A. Heme oxygenase system enhances insulin sensitivity and glucose metabolism in streptozotocin-induced diabetes. Am J Physiol Endocrinol Metab 2009; 296:E829-841

9. Ndisang JF, Jadhav A. The heme oxygenase system attenuates pancreatic lesions and improves insulin sensitivity and glucose metabolism in deoxycorticosterone acetate hypertension. Am J Physiol Regul Integr Comp Physiol 2010; 298:R211-223

10. Ndisang JF, Jadhav A. Hemin therapy improves kidney function in male streptozotocin-induced diabetic rats: role of the heme oxygenase/atrial natriuretic peptide/adiponectin axis. Endocrinology 2014; 155:215-229

11. Ndisang JF, Mishra M. The heme oxygenase system selectively suppresses the proinflammatory macrophage m1 phenotype and potentiates insulin signaling in spontaneously hypertensive rats. Am J Hypertens 2013; 26:1123-1131

12. Kim MJ, Lim NK, Choi SJ, Park HY. Hypertension is an independent risk factor for type 2 diabetes: the Korean genome and epidemiology study. Hypertens Res 2015; 38:783-789

13. Tiwari S, Mishra M, Jadhav A, Gerger C, Lee P, Weber L, Ndisang JF. The risk of heart failure and cardiometabolic complications in obesity may be masked by an apparent healthy status of normal blood glucose. Oxid Med Cell Longev 2013; 2013:253657

14. Salley TN, Mishra M, Tiwari S, Jadhav A, Ndisang JF. The heme oxygenase system rescues hepatic deterioration in the condition of obesity co-morbid with type-2 diabetes. PLoS One 2013; 8:e79270

15. Jadhav A, Tiwari S, Lee P, Ndisang JF. The heme oxygenase system selectively enhances the anti-inflammatory macrophage-M2 phenotype, reduces pericardial adiposity, and ameliorated cardiac injury in diabetic cardiomyopathy in Zucker diabetic fatty rats. J Pharmacol Exp Ther 2013; 345:239-249

16. Jadhav A, Torlakovic E, Ndisang JF. Hemin therapy attenuates kidney injury in deoxycorticosterone acetate-salt hypertensive rats. Am J Physiol Renal Physiol 2009; 296:F521-534

17. Ndisang JF, Jadhav A, Mishra M. The heme oxygenase system suppresses perirenal visceral adiposity, abates renal inflammation and ameliorates diabetic nephropathy in Zucker diabetic fatty rats. PLoS One 2014; 9:e87936

18. Ndisang JF, Lane N, Syed N, Jadhav A. Up-regulating the heme oxygenase system with hemin improves insulin sensitivity and glucose metabolism in adult spontaneously hypertensive rats. Endocrinology 2010; 151:549-560

19. Ndisang JF, Chibbar R. Heme Oxygenase Improves Renal Function by Potentiating Podocyte-Associated Proteins in Nomega-Nitro-l-Arginine-Methyl Ester (l-NAME)-Induced Hypertension. Am J Hypertens 2015; 28:930-942

20. Wynn TA, Chawla A, Pollard JW. Macrophage biology in development, homeostasis and disease. Nature 2013; 496:445-455

21. Murray PJ, Wynn TA. Protective and pathogenic functions of macrophage subsets. Nat Rev Immunol 2011; 11:723-737

22. Biswas SK, Chittezhath M, Shalova IN, Lim JY. Macrophage polarization and plasticity in health and disease. Immunol Res 2012; 53:11-24

23. Sica A, Mantovani A. Macrophage plasticity and polarization: in vivo veritas. J Clin Invest 2012; 122:787-795

24. Gordon S. Alternative activation of macrophages. Nat Rev Immunol 2003; 3:23-35

25. Van den Bossche J, Neele AE, Hoeksema MA, de Winther MP. Macrophage polarization: the epigenetic point of view. Curr Opin Lipidol 2014; 25:367-373

26. Ivashkiv LB. Epigenetic regulation of macrophage polarization and function. Trends Immunol 2013; 34:216-223

27. Damoiseaux JG, Dopp EA, Calame W, Chao D, MacPherson GG, Dijkstra CD. Rat macrophage lysosomal membrane antigen recognized by monoclonal antibody ED1. Immunology 1994; 83:140-147

28. Kolb H, Burkart V, Appels B, Hanenberg H, Kantwerk-Funke G, Kiesel U, Funda J, Schraermeyer U, Kolb-Bachofen V. Essential contribution of macrophages to islet cell destruction in vivo and in vitro. J Autoimmun 1990; 3 Suppl 1:117-120

29. Sato S, Mukai Y, Yamate J, Kato J, Kurasaki M, Hatai A, Sagai M. Effect of polyphenol-containing azuki bean (Vigna angularis) extract on blood pressure elevation and macrophage infiltration in the heart and kidney of spontaneously hypertensive rats. Clin Exp Pharmacol Physiol 2008; 35:43-49

30. Seok SJ, Lee ES, Kim GT, Hyun M, Lee JH, Chen S, Choi R, Kim HM, Lee EY, Chung CH. Blockade of CCL2/CCR2 signalling ameliorates diabetic nephropathy in db/db mice. Nephrol Dial Transplant 2013; 28:1700-1710

31. Zwadlo G, Voegeli R, Schulze Osthoff K, Sorg C. A monoclonal antibody to a novel differentiation antigen on human macrophages associated with the down-regulatory phase of the inflammatory process. Exp Cell Biol 1987; 55:295-304

32. Etzerodt A, Moestrup SK. CD163 and inflammation: biological, diagnostic, and therapeutic aspects. Antioxid Redox Signal 2013; 18:2352-2363

33. Fujisaka S, Usui I, Bukhari A, Ikutani M, Oya T, Kanatani Y, Tsuneyama K, Nagai Y, Takatsu K, Urakaze M, Kobayashi M, Tobe K. Regulatory mechanisms for adipose tissue M1 and M2 macrophages in diet-induced obese mice. Diabetes 2009; 58:2574-2582

34. Martinez-Pomares L. The mannose receptor. J Leukoc Biol 2012; 92:1177-1186

35. Rodgaard-Hansen S, Rafique A, Christensen PA, Maniecki MB, Sandahl TD, Nexo E, Moller HJ. A soluble form of the macrophage-related mannose receptor (MR/CD206) is present in human serum and elevated in critical illness. Clin Chem Lab Med 2014; 52:453-461

36. Sun H, Tian J, Xian W, Xie T, Yang X. Pentraxin-3 Attenuates Renal Damage in Diabetic Nephropathy by Promoting M2 Macrophage Differentiation. Inflammation 2015; 38:1739-1747

37. Mirza R, Koh TJ. Dysregulation of monocyte/macrophage phenotype in wounds of diabetic mice. Cytokine 2011; 56:256-264

38. Finn AV, Nakano M, Polavarapu R, Karmali V, Saeed O, Zhao X, Yazdani S, Otsuka F, Davis T, Habib A, Narula J, Kolodgie FD, Virmani R. Hemoglobin directs macrophage differentiation and prevents foam cell formation in human atherosclerotic plaques. J Am Coll Cardiol 2012; 59:166-177

39. Boyle JJ, Harrington HA, Piper E, Elderfield K, Stark J, Landis RC, Haskard DO. Coronary intraplaque hemorrhage evokes a novel atheroprotective macrophage phenotype. Am J Pathol 2009; 174:1097-1108

40. Endemann G, Stanton LW, Madden KS, Bryant CM, White RT, Protter AA. CD36 is a receptor for oxidized low density lipoprotein. J Biol Chem 1993; 268:11811-11816

41. Moore KJ, Kunjathoor VV, Koehn SL, Manning JJ, Tseng AA, Silver JM, McKee M, Freeman MW. Loss of receptor-mediated lipid uptake via scavenger receptor A or CD36 pathways does not ameliorate atherosclerosis in hyperlipidemic mice. J Clin Invest 2005; 115:2192-2201

42. Aouadi M, Vangala P, Yawe JC, Tencerova M, Nicoloro SM, Cohen JL, Shen Y, Czech MP. Lipid storage by adipose tissue macrophages regulates systemic glucose tolerance. Am J Physiol Endocrinol Metab 2014; 307:E374-383

43. Yuasa-Kawase M, Masuda D, Yamashita T, Kawase R, Nakaoka H, Inagaki M, Nakatani K, Tsubakio-Yamamoto K, Ohama T, Matsuyama A, Nishida M, Ishigami M, Kawamoto T, Komuro I, Yamashita S. Patients with CD36 deficiency are associated with enhanced atherosclerotic cardiovascular diseases. J Atheroscler Thromb 2012; 19:263-275

44. Miyaoka K, Kuwasako T, Hirano K, Nozaki S, Yamashita S, Matsuzawa Y. CD36 deficiency associated with insulin resistance. Lancet 2001; 357:686-687

45. Kuwasako T, Hirano K, Sakai N, Ishigami M, Hiraoka H, Yakub MJ, Yamauchi-Takihara K, Yamashita S, Matsuzawa Y. Lipoprotein abnormalities in human genetic CD36 deficiency associated with insulin resistance and abnormal fatty acid metabolism. Diabetes Care 2003; 26:1647-1648

46. Kim W, Lee HN, Jang JH, Kim SH, Lee YH, Hahn YI, Ngo HK, Choi Y, Joe Y, Chung HT, Chen Y, Cha YN, Surh YJ. 15-Deoxy-Delta12,14-Prostaglandin J2 Exerts Proresolving Effects Through Nuclear Factor E2-Related Factor 2-Induced Expression of CD36 and Heme Oxygenase-1. Antioxid Redox Signal 2017

47. Kern PA, Ranganathan S, Li C, Wood L, Ranganathan G. Adipose tissue tumor necrosis factor and interleukin-6 expression in human obesity and insulin resistance. Am J Physiol Endocrinol Metab 2001; 280:E745-751

48. Maachi M, Pieroni L, Bruckert E, Jardel C, Fellahi S, Hainque B, Capeau J, Bastard JP. Systemic low-grade inflammation is related to both circulating and adipose tissue TNFalpha, leptin and IL-6 levels in obese women. Int J Obes Relat Metab Disord 2004; 28:993-997

49. Filho AG, Kinote A, Pereira DJ, Renno A, dos Santos RC, Ferreira-Melo SE, Velloso LA, Bordin S, Anhe GF, Moreno Junior H. Infliximab prevents increased systolic blood pressure and upregulates the AKT/eNOS pathway in the aorta of spontaneously hypertensive rats. Eur J Pharmacol 2013; 700:201-209

50. Sahraoui A, Dewachter C, de Medina G, Naeije R, Aouichat Bouguerra S, Dewachter L. Myocardial Structural and Biological Anomalies Induced by High Fat Diet in Psammomys obesus Gerbils. PLoS One 2016; 11:e0148117

51. Tosello-Trampont AC, Landes SG, Nguyen V, Novobrantseva TI, Hahn YS. Kuppfer cells trigger nonalcoholic steatohepatitis development in diet-induced mouse model through tumor necrosis factor-alpha production. J Biol Chem 2012; 287:40161-40172

52. Chung CH, Fan J, Lee EY, Kang JS, Lee SJ, Pyagay PE, Khoury CC, Yeo TK, Khayat MF, Wang A, Chen S. Effects of Tumor Necrosis Factor-alpha on Podocyte Expression of Monocyte Chemoattractant Protein-1 and in Diabetic Nephropathy. Nephron Extra 2015; 5:1-18

53. Awad AS, You H, Gao T, Cooper TK, Nedospasov SA, Vacher J, Wilkinson PF, Farrell FX, Brian Reeves W. Macrophage-derived tumor necrosis factor-alpha mediates diabetic renal injury. Kidney Int 2015; 88:722-733

54. Cai D, Yuan M, Frantz DF, Melendez PA, Hansen L, Lee J, Shoelson SE. Local and systemic insulin resistance resulting from hepatic activation of IKK-beta and NF-kappaB. Nat Med 2005; 11:183-190

55. Arkan MC, Hevener AL, Greten FR, Maeda S, Li ZW, Long JM, Wynshaw-Boris A, Poli G, Olefsky J, Karin M. IKK-beta links inflammation to obesity-induced insulin resistance. Nat Med 2005; 11:191-198

56. Hirosumi J, Tuncman G, Chang L, Gorgun CZ, Uysal KT, Maeda K, Karin M, Hotamisligil GS. A central role for JNK in obesity and insulin resistance. Nature 2002; 420:333-336

57. Park EJ, Lee JH, Yu GY, He G, Ali SR, Holzer RG, Osterreicher CH, Takahashi H, Karin M. Dietary and genetic obesity promote liver inflammation and tumorigenesis by enhancing IL-6 and TNF expression. Cell 2010; 140:197-208

58. Jiang JX, Chen X, Fukada H, Serizawa N, Devaraj S, Torok NJ. Advanced glycation endproducts induce fibrogenic activity in nonalcoholic steatohepatitis by modulating TNF-alpha-converting enzyme activity in mice. Hepatology 2013; 58:1339-1348

59. de Meijer VE, Le HD, Meisel JA, Sharma AK, Popov Y, Puder M. Tumor necrosis factor alpha-converting enzyme inhibition reverses hepatic steatosis and improves insulin sensitivity markers and surgical outcome in mice. PLoS One 2011; 6:e25587

60. da Costa RM, Neves KB, Mestriner FL, Louzada-Junior P, Bruder-Nascimento T, Tostes RC. TNF-alpha induces vascular insulin resistance via positive modulation of PTEN and decreased Akt/eNOS/NO signaling in high fat diet-fed mice. Cardiovasc Diabetol 2016; 15:119

61. Lagathu C, Yvan-Charvet L, Bastard JP, Maachi M, Quignard-Boulange A, Capeau J, Caron M. Long-term treatment with interleukin-1beta induces insulin resistance in murine and human adipocytes. Diabetologia 2006; 49:2162-2173

62. Nagareddy PR, Kraakman M, Masters SL, Stirzaker RA, Gorman DJ, Grant RW, Dragoljevic D, Hong ES, Abdel-Latif A, Smyth SS, Choi SH, Korner J, Bornfeldt KE, Fisher EA, Dixit VD, Tall AR, Goldberg IJ, Murphy AJ. Adipose tissue macrophages promote myelopoiesis and monocytosis in obesity. Cell Metab 2014; 19:821-835

63. Dixon LJ, Flask CA, Papouchado BG, Feldstein AE, Nagy LE. Caspase-1 as a central regulator of high fat diet-induced non-alcoholic steatohepatitis. PLoS One 2013; 8:e56100

64. Negrin KA, Roth Flach RJ, DiStefano MT, Matevossian A, Friedline RH, Jung D, Kim JK, Czech MP. IL-1 signaling in obesity-induced hepatic lipogenesis and steatosis. PLoS One 2014; 9:e107265

65. Ehses JA, Lacraz G, Giroix MH, Schmidlin F, Coulaud J, Kassis N, Irminger JC, Kergoat M, Portha B, Homo-Delarche F, Donath MY. IL-1 antagonism reduces hyperglycemia and tissue inflammation in the type 2 diabetic GK rat. Proc Natl Acad Sci U S A 2009; 106:13998-14003

66. Kamari Y, Shaish A, Vax E, Shemesh S, Kandel-Kfir M, Arbel Y, Olteanu S, Barshack I, Dotan S, Voronov E, Dinarello CA, Apte RN, Harats D. Lack of interleukin-1alpha or interleukin-1beta inhibits transformation of steatosis to steatohepatitis and liver fibrosis in hypercholesterolemic mice. J Hepatol 2011; 55:1086-1094

67. Maedler K, Sergeev P, Ris F, Oberholzer J, Joller-Jemelka HI, Spinas GA, Kaiser N, Halban PA, Donath MY. Glucose-induced beta cell production of IL-1beta contributes to glucotoxicity in human pancreatic islets. J Clin Invest 2002; 110:851-860

68. Sauter NS, Schulthess FT, Galasso R, Castellani LW, Maedler K. The antiinflammatory cytokine interleukin-1 receptor antagonist protects from high-fat diet-induced hyperglycemia. Endocrinology 2008; 149:2208-2218

69. Bracey NA, Beck PL, Muruve DA, Hirota SA, Guo J, Jabagi H, Wright JR, Jr., Macdonald JA, Lees-Miller JP, Roach D, Semeniuk LM, Duff HJ. The Nlrp3 inflammasome promotes myocardial dysfunction in structural cardiomyopathy through interleukin-1beta. Exp Physiol 2013; 98:462-472

70. Luo B, Li B, Wang W, Liu X, Xia Y, Zhang C, Zhang M, Zhang Y, An F. NLRP3 gene silencing ameliorates diabetic cardiomyopathy in a type 2 diabetes rat model. PLoS One 2014; 9:e104771

71. Ndisang JF, Chibbar R, Lane N. Heme oxygenase suppresses markers of heart failure and ameliorates cardiomyopathy in L-NAME-induced hypertension. Eur J Pharmacol 2014; 734:23-34

72. Vallejo S, Palacios E, Romacho T, Villalobos L, Peiro C, Sanchez-Ferrer CF. The interleukin-1 receptor antagonist anakinra improves endothelial dysfunction in streptozotocin-induced diabetic rats. Cardiovasc Diabetol 2014; 13:158

73. Gao D, Madi M, Ding C, Fok M, Steele T, Ford C, Hunter L, Bing C. Interleukin-1beta mediates macrophage-induced impairment of insulin signaling in human primary adipocytes. Am J Physiol Endocrinol Metab 2014; 307:E289-304

74. Shahzad K, Bock F, Dong W, Wang H, Kopf S, Kohli S, Al-Dabet MM, Ranjan S, Wolter J, Wacker C, Biemann R, Stoyanov S, Reymann K, Soderkvist P, Gross O, Schwenger V, Pahernik S, Nawroth PP, Grone HJ, Madhusudhan T, Isermann B. Nlrp3-inflammasome activation in non-myeloid-derived cells aggravates diabetic nephropathy. Kidney Int 2015; 87:74-84

75. Koenen TB, Stienstra R, van Tits LJ, Joosten LA, van Velzen JF, Hijmans A, Pol JA, van der Vliet JA, Netea MG, Tack CJ, Stalenhoef AF, de Graaf J. The inflammasome and caspase-1 activation: a new mechanism underlying increased inflammatory activity in human visceral adipose tissue. Endocrinology 2011; 152:3769-3778

76. Lee HM, Kim JJ, Kim HJ, Shong M, Ku BJ, Jo EK. Upregulated NLRP3 inflammasome activation in patients with type 2 diabetes. Diabetes 2013; 62:194-204

77. Vandanmagsar B, Youm YH, Ravussin A, Galgani JE, Stadler K, Mynatt RL, Ravussin E, Stephens JM, Dixit VD. The NLRP3 inflammasome instigates obesity-induced inflammation and insulin resistance. Nat Med 2011; 17:179-188

78. Daousi C, Pinkney JH, Cleator J, Wilding JP, Ranganath LR. Acute peripheral administration of synthetic human GLP-1 (7-36 amide) decreases circulating IL-6 in obese patients with type 2 diabetes mellitus: a potential role for GLP-1 in modulation of the diabetic pro-inflammatory state? Regul Pept 2013; 183:54-61

79. Kozono M, Uto H, Ibusuki R, Arima S, Oda K, Taguchi H, Sasaki F, Nasu Y, Hashimoto S, Setoyama H, Kanmura S, Numata M, Tsubouchi H, Ido A. Antihypertensive therapy improves insulin resistance and serum levels of interleukin-6 and -10 in spontaneously hypertensive rats with steatohepatitis. Mol Med Rep 2016; 14:5385-5394

80. Mohamed-Ali V, Goodrick S, Rawesh A, Katz DR, Miles JM, Yudkin JS, Klein S, Coppack SW. Subcutaneous adipose tissue releases interleukin-6, but not tumor necrosis factor-alpha, in vivo. J Clin Endocrinol Metab 1997; 82:4196-4200

81. Fain JN, Madan AK, Hiler ML, Cheema P, Bahouth SW. Comparison of the release of adipokines by adipose tissue, adipose tissue matrix, and adipocytes from visceral and subcutaneous abdominal adipose tissues of obese humans. Endocrinology 2004; 145:2273-2282

82. Karavanaki K, Kakleas K, Georga S, Bartzeliotou A, Mavropoulos G, Tsouvalas M, Vogiatzi A, Papassotiriou I, Karayianni C. Plasma high sensitivity C-reactive protein and its relationship with cytokine levels in children with newly diagnosed type 1 diabetes and ketoacidosis. Clin Biochem 2012; 45:1383-1388

83. Dimas G, Iliadis F, Tegos T, Spiroglou S, Kanellos I, Karamouzis I, Savopoulos C, Hatzitolios A, Grekas D. 4b.08: Serum Levels of Timp-1 and Il-6 Are Associated with Hypertension and Atherosclerosis in Patients with Early Stages of Chronic Kidney Disease and Type 2 Diabetic Nephropathy. J Hypertens 2015; 33 Suppl 1:e55

84. Nonogaki K, Fuller GM, Fuentes NL, Moser AH, Staprans I, Grunfeld C, Feingold KR. Interleukin-6 stimulates hepatic triglyceride secretion in rats. Endocrinology 1995; 136:2143-2149

85. Klover PJ, Clementi AH, Mooney RA. Interleukin-6 depletion selectively improves hepatic insulin action in obesity. Endocrinology 2005; 146:3417-3427

86. Ramadoss P, Unger-Smith NE, Lam FS, Hollenberg AN. STAT3 targets the regulatory regions of gluconeogenic genes in vivo. Mol Endocrinol 2009; 23:827-837

87. Matthews VB, Allen TL, Risis S, Chan MH, Henstridge DC, Watson N, Zaffino LA, Babb JR, Boon J, Meikle PJ, Jowett JB, Watt MJ, Jansson JO, Bruce CR, Febbraio MA. Interleukin-6-deficient mice develop hepatic inflammation and systemic insulin resistance. Diabetologia 2010; 53:2431-2441

88. Mauer J, Chaurasia B, Goldau J, Vogt MC, Ruud J, Nguyen KD, Theurich S, Hausen AC, Schmitz J, Bronneke HS, Estevez E, Allen TL, Mesaros A, Partridge L, Febbraio MA, Chawla A, Wunderlich FT, Bruning JC. Signaling by IL-6 promotes alternative activation of macrophages to limit endotoxemia and obesity-associated resistance to insulin. Nat Immunol 2014; 15:423-430

89. Wunderlich FT, Strohle P, Konner AC, Gruber S, Tovar S, Bronneke HS, Juntti-Berggren L, Li LS, van Rooijen N, Libert C, Berggren PO, Bruning JC. Interleukin-6 signaling in liver-parenchymal cells suppresses hepatic inflammation and improves systemic insulin action. Cell Metab 2010; 12:237-249

90. Awazawa M, Ueki K, Inabe K, Yamauchi T, Kubota N, Kaneko K, Kobayashi M, Iwane A, Sasako T, Okazaki Y, Ohsugi M, Takamoto I, Yamashita S, Asahara H, Akira S, Kasuga M, Kadowaki T. Adiponectin enhances insulin sensitivity by increasing hepatic IRS-2 expression via a macrophage-derived IL-6-dependent pathway. Cell Metab 2011; 13:401-412

91. Sabio G, Das M, Mora A, Zhang Z, Jun JY, Ko HJ, Barrett T, Kim JK, Davis RJ. A stress signaling pathway in adipose tissue regulates hepatic insulin resistance. Science 2008; 322:1539-1543

92. Glund S, Deshmukh A, Long YC, Moller T, Koistinen HA, Caidahl K, Zierath JR, Krook A. Interleukin-6 directly increases glucose metabolism in resting human skeletal muscle. Diabetes 2007; 56:1630-1637

93. Carey AL, Steinberg GR, Macaulay SL, Thomas WG, Holmes AG, Ramm G, Prelovsek O, Hohnen-Behrens C, Watt MJ, James DE, Kemp BE, Pedersen BK, Febbraio MA. Interleukin-6 increases insulin-stimulated glucose disposal in humans and glucose uptake and fatty acid oxidation in vitro via AMP-activated protein kinase. Diabetes 2006; 55:2688-2697

94. Kelly M, Gauthier MS, Saha AK, Ruderman NB. Activation of AMP-activated protein kinase by interleukin-6 in rat skeletal muscle: association with changes in cAMP, energy state, and endogenous fuel mobilization. Diabetes 2009; 58:1953-1960

95. White PJ, St-Pierre P, Charbonneau A, Mitchell PL, St-Amand E, Marcotte B, Marette A. Protectin DX alleviates insulin resistance by activating a myokine-liver glucoregulatory axis. Nat Med 2014; 20:664-669

96. Ellingsgaard H, Hauselmann I, Schuler B, Habib AM, Baggio LL, Meier DT, Eppler E, Bouzakri K, Wueest S, Muller YD, Hansen AM, Reinecke M, Konrad D, Gassmann M, Reimann F, Halban PA, Gromada J, Drucker DJ, Gribble FM, Ehses JA, Donath MY. Interleukin-6 enhances insulin secretion by increasing glucagon-like peptide-1 secretion from L cells and alpha cells. Nat Med 2011; 17:1481-1489

97. Pedersen BK, Fischer CP. Physiological roles of muscle-derived interleukin-6 in response to exercise. Curr Opin Clin Nutr Metab Care 2007; 10:265-271

98. Zhang YJ, Rutledge BJ, Rollins BJ. Structure/activity analysis of human monocyte chemoattractant protein-1 (MCP-1) by mutagenesis. Identification of a mutated protein that inhibits MCP-1-mediated monocyte chemotaxis. J Biol Chem 1994; 269:15918-15924

99. Kanda H, Tateya S, Tamori Y, Kotani K, Hiasa K, Kitazawa R, Kitazawa S, Miyachi H, Maeda S, Egashira K, Kasuga M. MCP-1 contributes to macrophage infiltration into adipose tissue, insulin resistance, and hepatic steatosis in obesity. J Clin Invest 2006; 116:1494-1505

100. Tamura Y, Sugimoto M, Murayama T, Ueda Y, Kanamori H, Ono K, Ariyasu H, Akamizu T, Kita T, Yokode M, Arai H. Inhibition of CCR2 ameliorates insulin resistance and hepatic steatosis in db/db mice. Arterioscler Thromb Vasc Biol 2008; 28:2195-2201

101. Kashyap S, Warner GM, Hartono SP, Boyilla R, Knudsen BE, Zubair AS, Lien K, Nath KA, Textor SC, Lerman LO, Grande JP. Blockade of CCR2 reduces macrophage influx and development of chronic renal damage in murine renovascular hypertension. Am J Physiol Renal Physiol 2016; 310:F372-384

102. Patsouris D, Cao JJ, Vial G, Bravard A, Lefai E, Durand A, Durand C, Chauvin MA, Laugerette F, Debard C, Michalski MC, Laville M, Vidal H, Rieusset J. Insulin resistance is associated with MCP1-mediated macrophage accumulation in skeletal muscle in mice and humans. PLoS One 2014; 9:e110653

103. Ishibashi M, Hiasa K, Zhao Q, Inoue S, Ohtani K, Kitamoto S, Tsuchihashi M, Sugaya T, Charo IF, Kura S, Tsuzuki T, Ishibashi T, Takeshita A, Egashira K. Critical role of monocyte chemoattractant protein-1 receptor CCR2 on monocytes in hypertension-induced vascular inflammation and remodeling. Circ Res 2004; 94:1203-1210

104. Tucci M, Quatraro C, Frassanito MA, Silvestris F. Deregulated expression of monocyte chemoattractant protein-1 (MCP-1) in arterial hypertension: role in endothelial inflammation and atheromasia. J Hypertens 2006; 24:1307-1318

105. de Zeeuw D, Bekker P, Henkel E, Hasslacher C, Gouni-Berthold I, Mehling H, Potarca A, Tesar V, Heerspink HJ, Schall TJ, Group CBDNS. The effect of CCR2 inhibitor CCX140-B on residual albuminuria in patients with type 2 diabetes and nephropathy: a randomised trial. Lancet Diabetes Endocrinol 2015; 3:687-696

106. Di Prospero NA, Artis E, Andrade-Gordon P, Johnson DL, Vaccaro N, Xi L, Rothenberg P. CCR2 antagonism in patients with type 2 diabetes mellitus: a randomized, placebo-controlled study. Diabetes Obes Metab 2014; 16:1055-1064

107. Kirk EA, Sagawa ZK, McDonald TO, O'Brien KD, Heinecke JW. Monocyte chemoattractant protein deficiency fails to restrain macrophage infiltration into adipose tissue [corrected]. Diabetes 2008; 57:1254-1261

108. Inouye KE, Shi H, Howard JK, Daly CH, Lord GM, Rollins BJ, Flier JS. Absence of CC chemokine ligand 2 does not limit obesity-associated infiltration of macrophages into adipose tissue. Diabetes 2007; 56:2242-2250

109. Nishikawa T, Edelstein D, Du XL, Yamagishi S, Matsumura T, Kaneda Y, Yorek MA, Beebe D, Oates PJ, Hammes HP, Giardino I, Brownlee M. Normalizing mitochondrial superoxide production blocks three pathways of hyperglycaemic damage. Nature 2000; 404:787-790

110. Murphy MP. How mitochondria produce reactive oxygen species. Biochem J 2009; 417:1-13

111. Paglialunga S, Ludzki A, Root-McCaig J, Holloway GP. In adipose tissue, increased mitochondrial emission of reactive oxygen species is important for short-term high-fat diet-induced insulin resistance in mice. Diabetologia 2015; 58:1071-1080

112. Ruiz-Ramirez A, Chavez-Salgado M, Peneda-Flores JA, Zapata E, Masso F, El-Hafidi M. High-sucrose diet increases ROS generation, FFA accumulation, UCP2 level, and proton leak in liver mitochondria. Am J Physiol Endocrinol Metab 2011; 301:E1198-1207

113. Manrique C, Lastra G, Gardner M, Sowers JR. The renin angiotensin aldosterone system in hypertension: roles of insulin resistance and oxidative stress. Med Clin North Am 2009; 93:569-582

114. Munoz-Durango N, Fuentes CA, Castillo AE, Gonzalez-Gomez LM, Vecchiola A, Fardella CE, Kalergis AM. Role of the Renin-Angiotensin-Aldosterone System beyond Blood Pressure Regulation: Molecular and Cellular Mechanisms Involved in End-Organ Damage during Arterial Hypertension. Int J Mol Sci 2016; 17

115. Furukawa S, Fujita T, Shimabukuro M, Iwaki M, Yamada Y, Nakajima Y, Nakayama O, Makishima M, Matsuda M, Shimomura I. Increased oxidative stress in obesity and its impact on metabolic syndrome. J Clin Invest 2004; 114:1752-1761

116. Fortuno A, San Jose G, Moreno MU, Beloqui O, Diez J, Zalba G. Phagocytic NADPH oxidase overactivity underlies oxidative stress in metabolic syndrome. Diabetes 2006; 55:209-215

117. Nishimura S, Manabe I, Nagasaki M, Eto K, Yamashita H, Ohsugi M, Otsu M, Hara K, Ueki K, Sugiura S, Yoshimura K, Kadowaki T, Nagai R. CD8+ effector T cells contribute to macrophage recruitment and adipose tissue inflammation in obesity. Nat Med 2009; 15:914-920

118. Xia Y, Zweier JL. Superoxide and peroxynitrite generation from inducible nitric oxide synthase in macrophages. Proc Natl Acad Sci U S A 1997; 94:6954-6958

119. Houstis N, Rosen ED, Lander ES. Reactive oxygen species have a causal role in multiple forms of insulin resistance. Nature 2006; 440:944-948

120. Fernandez-Veledo S, Vila-Bedmar R, Nieto-Vazquez I, Lorenzo M. c-Jun N-terminal kinase 1/2 activation by tumor necrosis factor-alpha induces insulin resistance in human visceral but not subcutaneous adipocytes: reversal by liver X receptor agonists. J Clin Endocrinol Metab 2009; 94:3583-3593

121. Matsuzawa-Nagata N, Takamura T, Ando H, Nakamura S, Kurita S, Misu H, Ota T, Yokoyama M, Honda M, Miyamoto K, Kaneko S. Increased oxidative stress precedes the onset of high-fat diet-induced insulin resistance and obesity. Metabolism 2008; 57:1071-1077

122. Minamino T, Orimo M, Shimizu I, Kunieda T, Yokoyama M, Ito T, Nojima A, Nabetani A, Oike Y, Matsubara H, Ishikawa F, Komuro I. A crucial role for adipose tissue p53 in the regulation of insulin resistance. Nat Med 2009; 15:1082-1087

123. Keaney JF, Jr., Larson MG, Vasan RS, Wilson PW, Lipinska I, Corey D, Massaro JM, Sutherland P, Vita JA, Benjamin EJ, Framingham S. Obesity and systemic oxidative stress: clinical correlates of oxidative stress in the Framingham Study. Arterioscler Thromb Vasc Biol 2003; 23:434-439

124. Pestana RM, Domingueti CP, Duarte RC, Foscolo RB, Reis JS, Rodrigues AM, Martins LB, Sousa LP, Lage DP, Ferreira CN, Ferreira AV, Fernandes AP, Gomes KB. Cytokines profile and its correlation with endothelial damage and oxidative stress in patients with type 1 diabetes mellitus and nephropathy. Immunol Res 2016; 64:951-960

125. Goodarzi MT, Navidi AA, Rezaei M, Babahmadi-Rezaei H. Oxidative damage to DNA and lipids: correlation with protein glycation in patients with type 1 diabetes. J Clin Lab Anal 2010; 24:72-76

126. Jones DA, Prior SL, Barry JD, Caplin S, Baxter JN, Stephens JW. Changes in markers of oxidative stress and DNA damage in human visceral adipose tissue from subjects with obesity and type 2 diabetes. Diabetes Res Clin Pract 2014; 106:627-633

127. Sundaresan S, Vijayagopal P, Mills N, Imrhan V, Prasad C. A mouse model for nonalcoholic steatohepatitis. J Nutr Biochem 2011; 22:979-984

128. Lo L, McLennan SV, Williams PF, Bonner J, Chowdhury S, McCaughan GW, Gorrell MD, Yue DK, Twigg SM. Diabetes is a progression factor for hepatic fibrosis in a high fat fed mouse obesity model of non-alcoholic steatohepatitis. J Hepatol 2011; 55:435-444

129. Jaskiewicz K, Rzepko R, Sledzinski Z. Fibrogenesis in fatty liver associated with obesity and diabetes mellitus type 2. Dig Dis Sci 2008; 53:785-788

130. Luo Y, Burrington CM, Graff EC, Zhang J, Judd RL, Suksaranjit P, Kaewpoowat Q, Davenport SK, O'Neill AM, Greene MW. Metabolic phenotype and adipose and liver features in a high-fat Western diet-induced mouse model of obesity-linked NAFLD. Am J Physiol Endocrinol Metab 2016; 310:E418-439

131. Paradis V, Perlemuter G, Bonvoust F, Dargere D, Parfait B, Vidaud M, Conti M, Huet S, Ba N, Buffet C, Bedossa P. High glucose and hyperinsulinemia stimulate connective tissue growth factor expression: a potential mechanism involved in progression to fibrosis in nonalcoholic steatohepatitis. Hepatology 2001; 34:738-744

132. Shams ME, Al-Gayyar MM, Barakat EA. Type 2 Diabetes Mellitus-Induced Hyperglycemia in Patients with NAFLD and Normal LFTs: Relationship to Lipid Profile, Oxidative Stress and Pro-Inflammatory Cytokines. Sci Pharm 2011; 79:623-634

133. Larter CZ, Yeh MM, Haigh WG, Van Rooyen DM, Brooling J, Heydet D, Nolan CJ, Teoh NC, Farrell GC. Dietary modification dampens liver inflammation and fibrosis in obesity-related fatty liver disease. Obesity (Silver Spring) 2013; 21:1189-1199

134. Noeman SA, Hamooda HE, Baalash AA. Biochemical study of oxidative stress markers in the liver, kidney and heart of high fat diet induced obesity in rats. Diabetol Metab Syndr 2011; 3:17

135. Panchal SK, Poudyal H, Iyer A, Nazer R, Alam MA, Diwan V, Kauter K, Sernia C, Campbell F, Ward L, Gobe G, Fenning A, Brown L. High-carbohydrate, high-fat diet-induced metabolic syndrome and cardiovascular remodeling in rats. J Cardiovasc Pharmacol 2011; 57:611-624

136. Ballal K, Wilson CR, Harmancey R, Taegtmeyer H. Obesogenic high fat western diet induces oxidative stress and apoptosis in rat heart. Mol Cell Biochem 2010; 344:221-230

137. Sverdlov AL, Elezaby A, Qin F, Behring JB, Luptak I, Calamaras TD, Siwik DA, Miller EJ, Liesa M, Shirihai OS, Pimentel DR, Cohen RA, Bachschmid MM, Colucci WS. Mitochondrial Reactive Oxygen Species Mediate Cardiac Structural, Functional, and Mitochondrial Consequences of Diet-Induced Metabolic Heart Disease. J Am Heart Assoc 2016; 5

138. Koncsos G, Varga ZV, Baranyai T, Boengler K, Rohrbach S, Li L, Schluter KD, Schreckenberg R, Radovits T, Olah A, Matyas C, Lux A, Al-Khrasani M, Komlodi T, Bukosza N, Mathe D, Deres L, Bartekova M, Rajtik T, Adameova A, Szigeti K, Hamar P, Helyes Z, Tretter L, Pacher P, Merkely B, Giricz Z, Schulz R, Ferdinandy P. Diastolic dysfunction in prediabetic male rats: Role of mitochondrial oxidative stress. Am J Physiol Heart Circ Physiol 2016; 311:H927-H943

139. Gastaldelli A, Morales MA, Marraccini P, Sicari R. The role of cardiac fat in insulin resistance. Curr Opin Clin Nutr Metab Care 2012; 15:523-528

140. Vincent HK, Powers SK, Dirks AJ, Scarpace PJ. Mechanism for obesity-induced increase in myocardial lipid peroxidation. Int J Obes Relat Metab Disord 2001; 25:378-388

141. Li SJ, Liu CH, Chu HP, Mersmann HJ, Ding ST, Chu CH, Wang CY, Chen CY. The high-fat diet induces myocardial fibrosis in the metabolically healthy obese minipigs-The role of ER stress and oxidative stress. Clin Nutr 2017; 36:760-767

142. Chen HM, Liu ZH, Zeng CH, Li SJ, Wang QW, Li LS. Podocyte lesions in patients with obesity-related glomerulopathy. Am J Kidney Dis 2006; 48:772-779

143. Poirier B, Lannaud-Bournoville M, Conti M, Bazin R, Michel O, Bariety J, Chevalier J, Myara I. Oxidative stress occurs in absence of hyperglycaemia and inflammation in the onset of kidney lesions in normotensive obese rats. Nephrol Dial Transplant 2000; 15:467-476

144. Quigley JE, Elmarakby AA, Knight SF, Manhiani MM, Stepp DW, Olearzcyk JJ, Imig JD. Obesity induced renal oxidative stress contributes to renal injury in salt-sensitive hypertension. Clin Exp Pharmacol Physiol 2009; 36:724-728

145. Kang HM, Ahn SH, Choi P, Ko YA, Han SH, Chinga F, Park AS, Tao J, Sharma K, Pullman J, Bottinger EP, Goldberg IJ, Susztak K. Defective fatty acid oxidation in renal tubular epithelial cells has a key role in kidney fibrosis development. Nat Med 2015; 21:37-46

146. Herman-Edelstein M, Scherzer P, Tobar A, Levi M, Gafter U. Altered renal lipid metabolism and renal lipid accumulation in human diabetic nephropathy. J Lipid Res 2014; 55:561-572

147. Fujii H, Kono K, Nakai K, Goto S, Komaba H, Hamada Y, Shinohara M, Kitazawa R, Kitazawa S, Fukagawa M. Oxidative and nitrosative stress and progression of diabetic nephropathy in type 2 diabetes. Am J Nephrol 2010; 31:342-352

148. Labuschagne CF, van den Broek NJ, Postma P, Berger R, Brenkman AB. A protocol for quantifying lipid peroxidation in cellular systems by F2-isoprostane analysis. PLoS One 2013; 8:e80935

149. Roberts LJ, Morrow JD. Measurement of F(2)-isoprostanes as an index of oxidative stress in vivo. Free Radic Biol Med 2000; 28:505-513

150. Laffer CL, Bolterman RJ, Romero JC, Elijovich F. Effect of salt on isoprostanes in salt-sensitive essential hypertension. Hypertension 2006; 47:434-440

151. Davi G, Chiarelli F, Santilli F, Pomilio M, Vigneri S, Falco A, Basili S, Ciabattoni G, Patrono C. Enhanced lipid peroxidation and platelet activation in the early phase of type 1 diabetes mellitus: role of interleukin-6 and disease duration. Circulation 2003; 107:3199-3203

152. Samjoo IA, Safdar A, Hamadeh MJ, Raha S, Tarnopolsky MA. The effect of endurance exercise on both skeletal muscle and systemic oxidative stress in previously sedentary obese men. Nutr Diabetes 2013; 3:e88

153. Del Ben M, Polimeni L, Carnevale R, Bartimoccia S, Nocella C, Baratta F, Loffredo L, Pignatelli P, Violi F, Angelico F. NOX2-generated oxidative stress is associated with severity of ultrasound liver steatosis in patients with non-alcoholic fatty liver disease. BMC Gastroenterol 2014; 14:81

154. Shen XH, Tang QY, Huang J, Cai W. Vitamin E regulates adipocytokine expression in a rat model of dietary-induced obesity. Exp Biol Med (Maywood) 2010; 235:47-51

155. Rodrigo R, Prat H, Passalacqua W, Araya J, Bachler JP. Decrease in oxidative stress through supplementation of vitamins C and E is associated with a reduction in blood pressure in patients with essential hypertension. Clin Sci (Lond) 2008; 114:625-634

156. Hodgkinson AD, Bartlett T, Oates PJ, Millward BA, Demaine AG. The response of antioxidant genes to hyperglycemia is abnormal in patients with type 1 diabetes and diabetic nephropathy. Diabetes 2003; 52:846-851

157. Lortz S, Tiedge M, Nachtwey T, Karlsen AE, Nerup J, Lenzen S. Protection of insulin-producing RINm5F cells against cytokine-mediated toxicity through overexpression of antioxidant enzymes. Diabetes 2000; 49:1123-1130

158. de Oliveira BF, Costa DC, Nogueira-Machado JA, Chaves MM. beta-Carotene, alpha-tocopherol and ascorbic acid: differential profile of antioxidant, inflammatory status and regulation of gene expression in human mononuclear cells of diabetic donors. Diabetes Metab Res Rev 2013; 29:636-645

159. Varsha MK, Thiagarajan R, Manikandan R, Dhanasekaran G. Vitamin K1 alleviates streptozotocin-induced type 1 diabetes by mitigating free radical stress, as well as inhibiting NF-kappaB activation and iNOS expression in rat pancreas. Nutrition 2015; 31:214-222

160. Tiedge M, Lortz S, Drinkgern J, Lenzen S. Relation between antioxidant enzyme gene expression and antioxidative defense status of insulin-producing cells. Diabetes 1997; 46:1733-1742

161. Grankvist K, Marklund SL, Taljedal IB. CuZn-superoxide dismutase, Mn-superoxide dismutase, catalase and glutathione peroxidase in pancreatic islets and other tissues in the mouse. Biochem J 1981; 199:393-398

162. Kubisch HM, Wang J, Bray TM, Phillips JP. Targeted overexpression of Cu/Zn superoxide dismutase protects pancreatic beta-cells against oxidative stress. Diabetes 1997; 46:1563-1566

163. Chen H, Li X, Epstein PN. MnSOD and catalase transgenes demonstrate that protection of islets from oxidative stress does not alter cytokine toxicity. Diabetes 2005; 54:1437-1446

164. Saltiel AR, Kahn CR. Insulin signalling and the regulation of glucose and lipid metabolism. Nature 2001; 414:799-806

165. Leibiger IB, Leibiger B, Berggren PO. Insulin signaling in the pancreatic beta-cell. Annu Rev Nutr 2008; 28:233-251

166. Chang L, Chiang SH, Saltiel AR. Insulin signaling and the regulation of glucose transport. Mol Med 2004; 10:65-71

167. Uysal KT, Wiesbrock SM, Marino MW, Hotamisligil GS. Protection from obesity-induced insulin resistance in mice lacking TNF-alpha function. Nature 1997; 389:610-614

168. Hotamisligil GS, Peraldi P, Budavari A, Ellis R, White MF, Spiegelman BM. IRS-1-mediated inhibition of insulin receptor tyrosine kinase activity in TNF-alpha- and obesity-induced insulin resistance. Science 1996; 271:665-668

169. Hotamisligil GS, Murray DL, Choy LN, Spiegelman BM. Tumor necrosis factor alpha inhibits signaling from the insulin receptor. Proc Natl Acad Sci U S A 1994; 91:4854-4858

170. Laurencikiene J, van Harmelen V, Arvidsson Nordstrom E, Dicker A, Blomqvist L, Naslund E, Langin D, Arner P, Ryden M. NF-kappaB is important for TNF-alpha-induced lipolysis in human adipocytes. J Lipid Res 2007; 48:1069-1077

171. Yang X, Zhang X, Heckmann BL, Lu X, Liu J. Relative contribution of adipose triglyceride lipase and hormone-sensitive lipase to tumor necrosis factor-alpha (TNF-alpha)-induced lipolysis in adipocytes. J Biol Chem 2011; 286:40477-40485

172. Steinberg GR, Michell BJ, van Denderen BJ, Watt MJ, Carey AL, Fam BC, Andrikopoulos S, Proietto J, Gorgun CZ, Carling D, Hotamisligil GS, Febbraio MA, Kay TW, Kemp BE. Tumor necrosis factor alpha-induced skeletal muscle insulin resistance involves suppression of AMP-kinase signaling. Cell Metab 2006; 4:465-474

173. Wascher TC, Lindeman JH, Sourij H, Kooistra T, Pacini G, Roden M. Chronic TNF-alpha neutralization does not improve insulin resistance or endothelial function in "healthy" men with metabolic syndrome. Mol Med 2011; 17:189-193

174. Dominguez H, Storgaard H, Rask-Madsen C, Steffen Hermann T, Ihlemann N, Baunbjerg Nielsen D, Spohr C, Kober L, Vaag A, Torp-Pedersen C. Metabolic and vascular effects of tumor necrosis factor-alpha blockade with etanercept in obese patients with type 2 diabetes. J Vasc Res 2005; 42:517-525

175. Bernstein LE, Berry J, Kim S, Canavan B, Grinspoon SK. Effects of etanercept in patients with the metabolic syndrome. Arch Intern Med 2006; 166:902-908

176. Jager J, Gremeaux T, Cormont M, Le Marchand-Brustel Y, Tanti JF. Interleukin-1beta-induced insulin resistance in adipocytes through down-regulation of insulin receptor substrate-1 expression. Endocrinology 2007; 148:241-251

177. Wen H, Gris D, Lei Y, Jha S, Zhang L, Huang MT, Brickey WJ, Ting JP. Fatty acid-induced NLRP3-ASC inflammasome activation interferes with insulin signaling. Nat Immunol 2011; 12:408-415

178. Stienstra R, Joosten LA, Koenen T, van Tits B, van Diepen JA, van den Berg SA, Rensen PC, Voshol PJ, Fantuzzi G, Hijmans A, Kersten S, Muller M, van den Berg WB, van Rooijen N, Wabitsch M, Kullberg BJ, van der Meer JW, Kanneganti T, Tack CJ, Netea MG. The

inflammasome-mediated caspase-1 activation controls adipocyte differentiation and insulin sensitivity. Cell Metab 2010; 12:593-605

179. Bastard JP, Jardel C, Bruckert E, Blondy P, Capeau J, Laville M, Vidal H, Hainque B. Elevated levels of interleukin 6 are reduced in serum and subcutaneous adipose tissue of obese women after weight loss. J Clin Endocrinol Metab 2000; 85:3338-3342
180. Kim HJ, Higashimori T, Park SY, Choi H, Dong J, Kim YJ, Noh HL, Cho YR, Cline G, Kim YB, Kim JK. Differential effects of interleukin-6 and -10 on skeletal muscle and liver insulin action in vivo. Diabetes 2004; 53:1060-1067

181. Di Gregorio GB, Hensley L, Lu T, Ranganathan G, Kern PA. Lipid and carbohydrate metabolism in mice with a targeted mutation in the IL-6 gene: absence of development of age-related obesity. Am J Physiol Endocrinol Metab 2004; 287:E182-187

182. Marette A, Dimitrakoudis D, Shi Q, Rodgers CD, Klip A, Vranic M. Glucose rapidly decreases plasma membrane GLUT4 content in rat skeletal muscle. Endocrine 1999; 10:13-18

183. Kainulainen H, Komulainen J, Joost HG, Vihko V. Dissociation of the effects of training on oxidative metabolism, glucose utilisation and GLUT4 levels in skeletal muscle of streptozotocin-diabetic rats. Pflugers Arch 1994; 427:444-449

184. Andersen PH, Vestergaard H, Lund S, Vedel P, Junker S, Kahn BB, Pedersen O. The effect of intensive insulin therapy on the insulin-regulatable glucose transporter (GLUT4) expression in skeletal muscle in type 1 diabetes. Diabet Med 1993; 10:699-706

185. Ekladous D, Mehdi MZ, Costa M, Srivastava AK, Chiasson JL, Coderre L. Tissue- and fibre-specific modifications of insulin-signalling molecules in cardiac and skeletal muscle of diabetic rats. Clin Exp Pharmacol Physiol 2008; 35:971-978

186. Bahr I, Bazwinsky-Wutschke I, Wolgast S, Hofmann K, Streck S, Muhlbauer E, Wedekind D, Peschke E. GLUT4 in the endocrine pancreas--indicating an impact in pancreatic islet cell physiology? Horm Metab Res 2012; 44:442-450

187. Kelleher AR, Fairchild TJ, Keslacy S. STZ-induced skeletal muscle atrophy is associated with increased p65 content and downregulation of insulin pathway without NF-kappaB canonical cascade activation. Acta Diabetol 2010; 47:315-323

188. Foukas LC, Withers DJ. Phosphoinositide signalling pathways in metabolic regulation. Curr Top Microbiol Immunol 2010; 346:115-141

189. Folli F, Saad MJ, Backer JM, Kahn CR. Regulation of phosphatidylinositol 3-kinase activity in liver and muscle of animal models of insulin-resistant and insulin-deficient diabetes mellitus. J Clin Invest 1993; 92:1787-1794

190. Norquay LD, D'Aquino KE, Opare-Addo LM, Kuznetsova A, Haas M, Bluestone JA, White MF. Insulin receptor substrate-2 in beta-cells decreases diabetes in nonobese diabetic mice. Endocrinology 2009; 150:4531-4540

191. Lavin DP, White MF, Brazil DP. IRS proteins and diabetic complications. Diabetologia 2016;

192. Buren J, Liu HX, Jensen J, Eriksson JW. Dexamethasone impairs insulin signalling and glucose transport by depletion of insulin receptor substrate-1, phosphatidylinositol 3-kinase and protein kinase B in primary cultured rat adipocytes. Eur J Endocrinol 2002; 146:419-429

193. Withers DJ, Burks DJ, Towery HH, Altamuro SL, Flint CL, White MF. Irs-2 coordinates Igf-1 receptor-mediated beta-cell development and peripheral insulin signalling. Nat Genet 1999; 23:32-40

194. Araki E, Lipes MA, Patti ME, Bruning JC, Haag B, 3rd, Johnson RS, Kahn CR. Alternative pathway of insulin signalling in mice with targeted disruption of the IRS-1 gene. Nature 1994; 372:186-190

195. Kim JK, Zisman A, Fillmore JJ, Peroni OD, Kotani K, Perret P, Zong H, Dong J, Kahn CR, Kahn BB, Shulman GI. Glucose toxicity and the development of diabetes in mice with muscle-specific inactivation of GLUT4. J Clin Invest 2001; 108:153-160

196. Lechleitner M, Hoppichler F. Insulin therapy. Wien Med Wochenschr 2011; 161:300-304
197. Woo VC. New Insulins and New Aspects in Insulin Delivery. Can J Diabetes 2015; 39:335-343

198. Bruni A, Gala-Lopez B, Pepper AR, Abualhassan NS, Shapiro AJ. Islet cell transplantation for the treatment of type 1 diabetes: recent advances and future challenges. Diabetes Metab Syndr Obes 2014; 7:211-223

199. Kurrer MO, Pakala SV, Hanson HL, Katz JD. Beta cell apoptosis in T cell-mediated autoimmune diabetes. Proc Natl Acad Sci U S A 1997; 94:213-218

200. Foulis AK, McGill M, Farquharson MA. Insulitis in type 1 (insulin-dependent) diabetes mellitus in man--macrophages, lymphocytes, and interferon-gamma containing cells. J Pathol 1991; 165:97-103

201. Qin H, Trudeau JD, Reid GS, Lee IF, Dutz JP, Santamaria P, Verchere CB, Tan R. Progression of spontaneous autoimmune diabetes is associated with a switch in the killing mechanism used by autoreactive CTL. Int Immunol 2004; 16:1657-1662

202. McKenzie MD, Dudek NL, Mariana L, Chong MM, Trapani JA, Kay TW, Thomas HE. Perforin and Fas induced by IFNgamma and TNFalpha mediate beta cell death by OT-I CTL. Int Immunol 2006; 18:837-846

203. Kaminitz A, Stein J, Yaniv I, Askenasy N. The vicious cycle of apoptotic beta-cell death in type 1 diabetes. Immunol Cell Biol 2007; 85:582-589

204. Gurgul-Convey E, Mehmeti I, Lortz S, Lenzen S. Cytokine toxicity in insulin-producing cells is mediated by nitro-oxidative stress-induced hydroxyl radical formation in mitochondria. J Mol Med (Berl) 2011; 89:785-798

205. Dor Y, Brown J, Martinez OI, Melton DA. Adult pancreatic beta-cells are formed by self-duplication rather than stem-cell differentiation. Nature 2004; 429:41-46

206. Brennand K, Huangfu D, Melton D. All beta cells contribute equally to islet growth and maintenance. PLoS Biol 2007; 5:e163

207. Teta M, Rankin MM, Long SY, Stein GM, Kushner JA. Growth and regeneration of adult beta cells does not involve specialized progenitors. Dev Cell 2007; 12:817-826

208. Georgia S, Bhushan A. Beta cell replication is the primary mechanism for maintaining postnatal beta cell mass. J Clin Invest 2004; 114:963-968

209. Peshavaria M, Larmie BL, Lausier J, Satish B, Habibovic A, Roskens V, Larock K, Everill B, Leahy JL, Jetton TL. Regulation of pancreatic beta-cell regeneration in the normoglycemic 60% partial-pancreatectomy mouse. Diabetes 2006; 55:3289-3298

210. Bonner-Weir S, Baxter LA, Schuppin GT, Smith FE. A second pathway for regeneration of adult exocrine and endocrine pancreas. A possible recapitulation of embryonic development. Diabetes 1993; 42:1715-1720

211. Brockenbrough JS, Weir GC, Bonner-Weir S. Discordance of exocrine and endocrine growth after 90% pancreatectomy in rats. Diabetes 1988; 37:232-236

212. Jetton TL, Lausier J, LaRock K, Trotman WE, Larmie B, Habibovic A, Peshavaria M, Leahy JL. Mechanisms of compensatory beta-cell growth in insulin-resistant rats: roles of Akt kinase. Diabetes 2005; 54:2294-2304

213. Li WC, Rukstalis JM, Nishimura W, Tchipashvili V, Habener JF, Sharma A, Bonner-Weir S. Activation of pancreatic-duct-derived progenitor cells during pancreas regeneration in adult rats. J Cell Sci 2010; 123:2792-2802

214. Ackermann Misfeldt A, Costa RH, Gannon M. Beta-cell proliferation, but not neogenesis, following 60% partial pancreatectomy is impaired in the absence of FoxM1. Diabetes 2008; 57:3069-3077

215. Collombat P, Xu X, Ravassard P, Sosa-Pineda B, Dussaud S, Billestrup N, Madsen OD, Serup P, Heimberg H, Mansouri A. The ectopic expression of Pax4 in the mouse pancreas converts progenitor cells into alpha and subsequently beta cells. Cell 2009; 138:449-462

216. Criscimanna A, Speicher JA, Houshmand G, Shiota C, Prasadan K, Ji B, Logsdon CD, Gittes GK, Esni F. Duct cells contribute to regeneration of endocrine and acinar cells following pancreatic damage in adult mice. Gastroenterology 2011; 141:1451-1462, 1462 e1451-1456

217. Nakamura K, Minami K, Tamura K, Iemoto K, Miki T, Seino S. Pancreatic beta-cells are generated by neogenesis from non-beta-cells after birth. Biomed Res 2011; 32:167-174

218. Wang RN, Kloppel G, Bouwens L. Duct- to islet-cell differentiation and islet growth in the pancreas of duct-ligated adult rats. Diabetologia 1995; 38:1405-1411

219. Xu X, D'Hoker J, Stange G, Bonne S, De Leu N, Xiao X, Van de Casteele M, Mellitzer G, Ling Z, Pipeleers D, Bouwens L, Scharfmann R, Gradwohl G, Heimberg H. Beta cells can be generated from endogenous progenitors in injured adult mouse pancreas. Cell 2008; 132:197-207

220. Yatoh S, Dodge R, Akashi T, Omer A, Sharma A, Weir GC, Bonner-Weir S. Differentiation of affinity-purified human pancreatic duct cells to beta-cells. Diabetes 2007; 56:1802-1809

221. Lee YC, Nielsen JH. Regulation of beta cell replication. Mol Cell Endocrinol 2009; 297:18-27

222. Gunasekaran U, Hudgens CW, Wright BT, Maulis MF, Gannon M. Differential regulation of embryonic and adult beta cell replication. Cell Cycle 2012; 11:2431-2442

223. Bonner-Weir S, Guo L, Li WC, Ouziel-Yahalom L, Lysy PA, Weir GC, Sharma A. Islet neogenesis: a possible pathway for beta-cell replenishment. Rev Diabet Stud 2012; 9:407-416

224. Teta M, Long SY, Wartschow LM, Rankin MM, Kushner JA. Very slow turnover of beta-cells in aged adult mice. Diabetes 2005; 54:2557-2567

225. Kushner JA. The role of aging upon beta cell turnover. J Clin Invest 2013; 123:990-995

226. Scaglia L, Cahill CJ, Finegood DT, Bonner-Weir S. Apoptosis participates in the remodeling of the endocrine pancreas in the neonatal rat. Endocrinology 1997; 138:1736-1741

227. Meier JJ, Butler AE, Saisho Y, Monchamp T, Galasso R, Bhushan A, Rizza RA, Butler PC. Beta-cell replication is the primary mechanism subserving the postnatal expansion of beta-cell mass in humans. Diabetes 2008; 57:1584-1594

228. Brennand K, Melton D. Slow and steady is the key to beta-cell replication. J Cell Mol Med 2009; 13:472-487

229. Desgraz R, Herrera PL. Pancreatic neurogenin 3-expressing cells are unipotent islet precursors. Development 2009; 136:3567-3574

230. Salpeter SJ, Klein AM, Huangfu D, Grimsby J, Dor Y. Glucose and aging control the quiescence period that follows pancreatic beta cell replication. Development 2010; 137:3205-3213

231. Nir T, Melton DA, Dor Y. Recovery from diabetes in mice by beta cell regeneration. J Clin Invest 2007; 117:2553-2561

232. Cano DA, Rulifson IC, Heiser PW, Swigart LB, Pelengaris S, German M, Evan GI, Bluestone JA, Hebrok M. Regulated beta-cell regeneration in the adult mouse pancreas. Diabetes 2008; 57:958-966

233. Kulkarni RN, Jhala US, Winnay JN, Krajewski S, Montminy M, Kahn CR. PDX-1 haploinsufficiency limits the compensatory islet hyperplasia that occurs in response to insulin resistance. J Clin Invest 2004; 114:828-836

234. Bonner-Weir S, Toschi E, Inada A, Reitz P, Fonseca SY, Aye T, Sharma A. The pancreatic ductal epithelium serves as a potential pool of progenitor cells. Pediatr Diabetes 2004; 5 Suppl 2:16-22

235. Inada A, Nienaber C, Katsuta H, Fujitani Y, Levine J, Morita R, Sharma A, Bonner-Weir S. Carbonic anhydrase II-positive pancreatic cells are progenitors for both endocrine and exocrine pancreas after birth. Proc Natl Acad Sci U S A 2008; 105:19915-19919

236. Bouwens L, Wang RN, De Blay E, Pipeleers DG, Kloppel G. Cytokeratins as markers of ductal cell differentiation and islet neogenesis in the neonatal rat pancreas. Diabetes 1994; 43:1279-1283

237. Chintinne M, Stange G, Denys B, In 't Veld P, Hellemans K, Pipeleers-Marichal M, Ling Z, Pipeleers D. Contribution of postnatally formed small beta cell aggregates to functional beta cell mass in adult rat pancreas. Diabetologia 2010; 53:2380-2388

238. Furuyama K, Kawaguchi Y, Akiyama H, Horiguchi M, Kodama S, Kuhara T, Hosokawa S, Elbahrawy A, Soeda T, Koizumi M, Masui T, Kawaguchi M, Takaori K, Doi R, Nishi E, Kakinoki R, Deng JM, Behringer RR, Nakamura T, Uemoto S. Continuous cell supply from a Sox9-expressing progenitor zone in adult liver, exocrine pancreas and intestine. Nat Genet 2011; 43:34-41

239. Solar M, Cardalda C, Houbracken I, Martin M, Maestro MA, De Medts N, Xu X, Grau V, Heimberg H, Bouwens L, Ferrer J. Pancreatic exocrine duct cells give rise to insulin-producing beta cells during embryogenesis but not after birth. Dev Cell 2009; 17:849-860

240. Menge BA, Tannapfel A, Belyaev O, Drescher R, Muller C, Uhl W, Schmidt WE, Meier JJ. Partial pancreatectomy in adult humans does not provoke beta-cell regeneration. Diabetes 2008; 57:142-149

241. Kopinke D, Murtaugh LC. Exocrine-to-endocrine differentiation is detectable only prior to birth in the uninjured mouse pancreas. BMC Dev Biol 2010; 10:38

242. Rankin MM, Wilbur CJ, Rak K, Shields EJ, Granger A, Kushner JA. beta-Cells are not generated in pancreatic duct ligation-induced injury in adult mice. Diabetes 2013; 62:1634-1645

243. Cavelti-Weder C, Shtessel M, Reuss JE, Jermendy A, Yamada T, Caballero F, Bonner-Weir S, Weir GC. Pancreatic duct ligation after almost complete beta-cell loss: exocrine regeneration but no evidence of beta-cell regeneration. Endocrinology 2013; 154:4493-4502

244. Xiao X, Chen Z, Shiota C, Prasadan K, Guo P, El-Gohary Y, Paredes J, Welsh C, Wiersch J, Gittes GK. No evidence for beta cell neogenesis in murine adult pancreas. J Clin Invest 2013; 123:2207-2217

245. Desai BM, Oliver-Krasinski J, De Leon DD, Farzad C, Hong N, Leach SD, Stoffers DA. Preexisting pancreatic acinar cells contribute to acinar cell, but not islet beta cell, regeneration. J Clin Invest 2007; 117:971-977

246. Bashamboo A, Taylor AH, Samuel K, Panthier JJ, Whetton AD, Forrester LM. The survival of differentiating embryonic stem cells is dependent on the SCF-KIT pathway. J Cell Sci 2006; 119:3039-3046

247. Li J, Quirt J, Do HQ, Lyte K, Fellows F, Goodyer CG, Wang R. Expression of c-Kit receptor tyrosine kinase and effect on beta-cell development in the human fetal pancreas. Am J Physiol Endocrinol Metab 2007; 293:E475-483

248. Feng ZC, Li J, Turco BA, Riopel M, Yee SP, Wang R. Critical role of c-Kit in beta cell function: increased insulin secretion and protection against diabetes in a mouse model. Diabetologia 2012; 55:2214-2225

249. Tiemann K, Panienka R, Kloppel G. Expression of transcription factors and precursor cell markers during regeneration of beta cells in pancreata of rats treated with streptozotocin. Virchows Arch 2007; 450:261-266

250. Peters K, Panienka R, Li J, Kloppel G, Wang R. Expression of stem cell markers and transcription factors during the remodeling of the rat pancreas after duct ligation. Virchows Arch 2005; 446:56-63

251. Gong J, Zhang G, Tian F, Wang Y. Islet-derived stem cells from adult rats participate in the repair of islet damage. J Mol Histol 2012; 43:745-750

252. Hess D, Li L, Martin M, Sakano S, Hill D, Strutt B, Thyssen S, Gray DA, Bhatia M. Bone marrow-derived stem cells initiate pancreatic regeneration. Nat Biotechnol 2003; 21:763-770

253. Samuelson L. WN, Gerber DA.,. Endodermal progenitor cells isolated from mouse pancreas. Stem Cell Discovery 2011; Vol.1, :44-53

254. Rovira M, Scott SG, Liss AS, Jensen J, Thayer SP, Leach SD. Isolation and characterization of centroacinar/terminal ductal progenitor cells in adult mouse pancreas. Proc Natl Acad Sci U S A 2010; 107:75-80

255. Gopurappilly R, Bhat V, Bhonde R. Pancreatic tissue resident mesenchymal stromal cell (MSC)-like cells as a source of in vitro islet neogenesis. J Cell Biochem 2013; 114:2240-2247

256. Huang Y, Kucia M, Hussain LR, Wen Y, Xu H, Yan J, Ratajczak MZ, Ildstad ST. Bone marrow transplantation temporarily improves pancreatic function in streptozotocin-induced diabetes: potential involvement of very small embryonic-like cells. Transplantation 2010; 89:677-685

257. Abouzaripour M, Ragerdi Kashani I, Pasbakhsh P, Atlasy N. Intravenous transplantation of very small embryonic like stem cells in treatment of diabetes mellitus. Avicenna J Med Biotechnol 2015; 7:22-31

258. Bhartiya D, Mundekar A, Mahale V, Patel H. Very small embryonic-like stem cells are involved in regeneration of mouse pancreas post-pancreatectomy. Stem Cell Res Ther 2014; 5:106

259. Bhartiya D, Patel H. Very small embryonic-like stem cells are involved in pancreatic regeneration and their dysfunction with age may lead to diabetes and cancer. Stem Cell Res Ther 2015; 6:96

260. Ito CY, Li CY, Bernstein A, Dick JE, Stanford WL. Hematopoietic stem cell and progenitor defects in Sca-1/Ly-6A-null mice. Blood 2003; 101:517-523

261. Tong Z, Liu W. IgG-positive cells surround pancreatic ducts and form multiple layers after streptozotocin treatment. Autoimmunity 2013; 46:369-374

262. Khoo CP, Valorani MG, Brittan M, Alison MR, Warnes G, Johansson U, Hawa M, Pozzilli P. Characterization of endothelial progenitor cells in the NOD mouse as a source for cell therapies. Diabetes Metab Res Rev 2009; 25:89-93

263. Liu F, Yao Z, Jiao Q, Cao L, Feng H, Yao S, Li Y, Lu P. Inducing Specific Immune Tolerance to Prevent Type 1 Diabetes in NOD Mice. Pancreas 2016; 45:882-888

264. Liu J, Walp ER, May CL. Elevation of transcription factor Islet-1 levels in vivo increases beta-cell function but not beta-cell mass. Islets 2012; 4:199-206

265. Guo T, Wang W, Zhang H, Liu Y, Chen P, Ma K, Zhou C. ISL1 promotes pancreatic islet cell proliferation. PLoS One 2011; 6:e22387

266. Hunter CS, Dixit S, Cohen T, Ediger B, Wilcox C, Ferreira M, Westphal H, Stein R, May CL. Islet alpha-, beta-, and delta-cell development is controlled by the Ldb1 coregulator, acting primarily with the islet-1 transcription factor. Diabetes 2013; 62:875-886

267. Du A, Hunter CS, Murray J, Noble D, Cai CL, Evans SM, Stein R, May CL. Islet-1 is required for the maturation, proliferation, and survival of the endocrine pancreas. Diabetes 2009; 58:2059-2069

268. Ediger BN, Du A, Liu J, Hunter CS, Walp ER, Schug J, Kaestner KH, Stein R, Stoffers DA, May CL. Islet-1 Is essential for pancreatic beta-cell function. Diabetes 2014; 63:4206-4217

269. Ahlgren U, Pfaff SL, Jessell TM, Edlund T, Edlund H. Independent requirement for ISL1 in formation of pancreatic mesenchyme and islet cells. Nature 1997; 385:257-260

270. Figeac F, Uzan B, Faro M, Chelali N, Portha B, Movassat J. Neonatal growth and regeneration of beta-cells are regulated by the Wnt/beta-catenin signaling in normal and diabetic rats. Am J Physiol Endocrinol Metab 2010; 298:E245-256

271. Murtaugh LC, Law AC, Dor Y, Melton DA. Beta-catenin is essential for pancreatic acinar but not islet development. Development 2005; 132:4663-4674

272. Wang QM, Zhang Y, Yang KM, Zhou HY, Yang HJ. Wnt/beta-catenin signaling pathway is active in pancreatic development of rat embryo. World J Gastroenterol 2006; 12:2615-2619

273. Rulifson IC, Karnik SK, Heiser PW, ten Berge D, Chen H, Gu X, Taketo MM, Nusse R, Hebrok M, Kim SK. Wnt signaling regulates pancreatic beta cell proliferation. Proc Natl Acad Sci U S A 2007; 104:6247-6252

274. Wells JM, Esni F, Boivin GP, Aronow BJ, Stuart W, Combs C, Sklenka A, Leach SD, Lowy AM. Wnt/beta-catenin signaling is required for development of the exocrine pancreas. BMC Dev Biol 2007; 7:4

275. Heiser PW, Lau J, Taketo MM, Herrera PL, Hebrok M. Stabilization of beta-catenin impacts pancreas growth. Development 2006; 133:2023-2032

276. Niwa H, Miyazaki J, Smith AG. Quantitative expression of Oct-3/4 defines differentiation, dedifferentiation or self-renewal of ES cells. Nat Genet 2000; 24:372-376

277. White MG, Al-Turaifi HR, Holliman GN, Aldibbiat A, Mahmoud A, Shaw JA. Pluripotency-associated stem cell marker expression in proliferative cell cultures derived from adult human pancreas. J Endocrinol 2011; 211:169-176

278. Zhao M, Amiel SA, Christie MR, Muiesan P, Srinivasan P, Littlejohn W, Rela M, Arno M, Heaton N, Huang GC. Evidence for the presence of stem cell-like progenitor cells in human adult pancreas. J Endocrinol 2007; 195:407-414

279. Chang CM, Kao CL, Chang YL, Yang MJ, Chen YC, Sung BL, Tsai TH, Chao KC, Chiou SH, Ku HH. Placenta-derived multipotent stem cells induced to differentiate into insulin-positive cells. Biochem Biophys Res Commun 2007; 357:414-420

280. Chiou SH, Chen SJ, Chang YL, Chen YC, Li HY, Chen DT, Wang HH, Chang CM, Chen YJ, Ku HH. MafA promotes the reprogramming of placenta-derived multipotent stem cells into pancreatic islets-like and insulin+ cells. J Cell Mol Med 2011; 15:612-624

281. Goode DK, Elgar G. The PAX258 gene subfamily: a comparative perspective. Dev Dyn 2009; 238:2951-2974

282. St-Onge L, Sosa-Pineda B, Chowdhury K, Mansouri A, Gruss P. Pax6 is required for differentiation of glucagon-producing alpha-cells in mouse pancreas. Nature 1997; 387:406-409

283. Sosa-Pineda B, Chowdhury K, Torres M, Oliver G, Gruss P. The Pax4 gene is essential for differentiation of insulin-producing beta cells in the mammalian pancreas. Nature 1997; 386:399-402

284. Zaiko M, Estreicher A, Ritz-Laser B, Herrera P, Favor J, Meda P, Philippe J. Pax2 mutant mice display increased number and size of islets of Langerhans but no change in insulin and glucagon content. Eur J Endocrinol 2004; 150:389-395

285. Flock G, Drucker DJ. Pax-2 activates the proglucagon gene promoter but is not essential for proglucagon gene expression or development of proglucagon-producing cell lineages in the murine pancreas or intestine. Mol Endocrinol 2002; 16:2349-2359

286. Ritz-Laser B, Estreicher A, Gauthier B, Philippe J. The paired homeodomain transcription factor Pax-2 is expressed in the endocrine pancreas and transactivates the glucagon gene promoter. J Biol Chem 2000; 275:32708-32715

287. Rudnick A, Ling TY, Odagiri H, Rutter WJ, German MS. Pancreatic beta cells express a diverse set of homeobox genes. Proc Natl Acad Sci U S A 1994; 91:12203-12207

288. Oster A, Jensen J, Serup P, Galante P, Madsen OD, Larsson LI. Rat endocrine pancreatic development in relation to two homeobox gene products (Pdx-1 and Nkx 6.1). J Histochem Cytochem 1998; 46:707-715

289. Vishwakarma SK, Rahamathulla S, Bardia A, Tiwari SK, Srinivas G, Raj A, Tripura C, Sandhya A, Habeeb MA, Khan AA, Pande G, Reddy KP, Reddy PY. In vitro quantitative and relative gene expression analysis of pancreatic transcription factors Pdx-1, Ngn-3, Isl-1, Pax-4, Pax-6 and Nkx-6.1 in trans-differentiated human hepatic progenitors. J Diabetes Investig 2014; 5:492-500

290. Sander M, Sussel L, Conners J, Scheel D, Kalamaras J, Dela Cruz F, Schwitzgebel V, Hayes-Jordan A, German M. Homeobox gene Nkx6.1 lies downstream of Nkx2.2 in the major pathway of beta-cell formation in the pancreas. Development 2000; 127:5533-5540

291. Jensen J, Serup P, Karlsen C, Nielsen TF, Madsen OD. mRNA profiling of rat islet tumors reveals nkx 6.1 as a beta-cell-specific homeodomain transcription factor. J Biol Chem 1996; 271:18749-18758

292. Narushima M, Kobayashi N, Okitsu T, Tanaka Y, Li SA, Chen Y, Miki A, Tanaka K, Nakaji S, Takei K, Gutierrez AS, Rivas-Carrillo JD, Navarro-Alvarez N, Jun HS, Westerman KA, Noguchi H, Lakey JR, Leboulch P, Tanaka N, Yoon JW. A human beta-cell line for transplantation therapy to control type 1 diabetes. Nat Biotechnol 2005; 23:1274-1282

293. Schisler JC, Jensen PB, Taylor DG, Becker TC, Knop FK, Takekawa S, German M, Weir GC, Lu D, Mirmira RG, Newgard CB. The Nkx6.1 homeodomain transcription factor suppresses glucagon expression and regulates glucose-stimulated insulin secretion in islet beta cells. Proc Natl Acad Sci U S A 2005; 102:7297-7302

294. Henseleit KD, Nelson SB, Kuhlbrodt K, Hennings JC, Ericson J, Sander M. NKX6 transcription factor activity is required for alpha- and beta-cell development in the pancreas. Development 2005; 132:3139-3149

295. Taylor BL, Benthuysen J, Sander M. Postnatal beta-cell proliferation and mass expansion is dependent on the transcription factor Nkx6.1. Diabetes 2015; 64:897-903

296. Nelson SB, Schaffer AE, Sander M. The transcription factors Nkx6.1 and Nkx6.2 possess equivalent activities in promoting beta-cell fate specification in Pdx1+ pancreatic progenitor cells. Development 2007; 134:2491-2500

297. Gauthier BR, Gosmain Y, Mamin A, Philippe J. The beta-cell specific transcription factor Nkx6.1 inhibits glucagon gene transcription by interfering with Pax6. Biochem J 2007; 403:593-601

298. Guillam MT, Dupraz P, Thorens B. Glucose uptake, utilization, and signaling in GLUT2-null islets. Diabetes 2000; 49:1485-1491

299. Thorens B. GLUT2, glucose sensing and glucose homeostasis. Diabetologia 2015; 58:221-232

300. Navarro-Tableros V, Fiordelisio T, Hernandez-Cruz A, Hiriart M. Physiological development of insulin secretion, calcium channels, and GLUT2 expression of pancreatic rat beta-cells. Am J Physiol Endocrinol Metab 2007; 292:E1018-1029

301. Thorens B, Guillam MT, Beermann F, Burcelin R, Jaquet M. Transgenic reexpression of GLUT1 or GLUT2 in pancreatic beta cells rescues GLUT2-null mice from early death and restores normal glucose-stimulated insulin secretion. J Biol Chem 2000; 275:23751-23758

302. Guillam MT, Hummler E, Schaerer E, Yeh JI, Birnbaum MJ, Beermann F, Schmidt A, Deriaz N, Thorens B. Early diabetes and abnormal postnatal pancreatic islet development in mice lacking Glut-2. Nat Genet 1997; 17:327-330

303. Valera A, Solanes G, Fernandez-Alvarez J, Pujol A, Ferrer J, Asins G, Gomis R, Bosch F. Expression of GLUT-2 antisense RNA in beta cells of transgenic mice leads to diabetes. J Biol Chem 1994; 269:28543-28546

304. Orci L, Ravazzola M, Baetens D, Inman L, Amherdt M, Peterson RG, Newgard CB, Johnson JH, Unger RH. Evidence that down-regulation of beta-cell glucose transporters in non-insulin-dependent diabetes may be the cause of diabetic hyperglycemia. Proc Natl Acad Sci U S A 1990; 87:9953-9957

305. Jorns A, Klempnauer J, Tiedge M, Lenzen S. Recovery of pancreatic beta cells in response to long-term normoglycemia after pancreas or islet transplantation in severely streptozotocin diabetic adult rats. Pancreas 2001; 23:186-196

306. Jorns A, Tiedge M, Sickel E, Lenzen S. Loss of GLUT2 glucose transporter expression in pancreatic beta cells from diabetic Chinese hamsters. Virchows Arch 1996; 428:177-185

307. Burkhardt BR, Parker MJ, Zhang YC, Song S, Wasserfall CH, Atkinson MA. Glucose transporter-2 (GLUT2) promoter mediated transgenic insulin production reduces hyperglycemia in diabetic mice. FEBS Lett 2005; 579:5759-5764

308. Mishra M, Ndisang JF. A critical and comprehensive insight on heme oxygenase and related products including carbon monoxide, bilirubin, biliverdin and ferritin in type-1 and type-2 diabetes. Curr Pharm Des 2014; 20:1370-1391

309. Hayashi S, Omata Y, Sakamoto H, Higashimoto Y, Hara T, Sagara Y, Noguchi M. Characterization of rat heme oxygenase-3 gene. Implication of processed pseudogenes derived from heme oxygenase-2 gene. Gene 2004; 336:241-250

310. Maines MD, Trakshel GM, Kutty RK. Characterization of two constitutive forms of rat liver microsomal heme oxygenase. Only one molecular species of the enzyme is inducible. J Biol Chem 1986; 261:411-419

311. Trakshel GM, Kutty RK, Maines MD. Purification and characterization of the major constitutive form of testicular heme oxygenase. The noninducible isoform. J Biol Chem 1986; 261:11131-11137

312. Cruse I, Maines MD. Evidence suggesting that the two forms of heme oxygenase are products of different genes. J Biol Chem 1988; 263:3348-3353

313. Lavrovsky Y, Schwartzman ML, Levere RD, Kappas A, Abraham NG. Identification of binding sites for transcription factors NF-kappa B and AP-2 in the promoter region of the human heme oxygenase 1 gene. Proc Natl Acad Sci U S A 1994; 91:5987-5991

314. Mitani K, Fujita H, Kappas A, Sassa S. Heme oxygenase is a positive acute-phase reactant in human Hep3B hepatoma cells. Blood 1992; 79:1255-1259

315. Alam J, Den Z. Distal AP-1 binding sites mediate basal level enhancement and TPA induction of the mouse heme oxygenase-1 gene. J Biol Chem 1992; 267:21894-21900

316. Maines MD, Eke BC, Zhao X. Corticosterone promotes increased heme oxygenase-2 protein and transcript expression in the newborn rat brain. Brain Res 1996; 722:83-94

317. Exner M, Minar E, Wagner O, Schillinger M. The role of heme oxygenase-1 promoter polymorphisms in human disease. Free Radic Biol Med 2004; 37:1097-1104

318. Bao W, Song F, Li X, Rong S, Yang W, Wang D, Xu J, Fu J, Zhao Y, Liu L. Association between heme oxygenase-1 gene promoter polymorphisms and type 2 diabetes mellitus: a HuGE review and meta-analysis. Am J Epidemiol 2010; 172:631-636

319. Arredondo M, Jorquera D, Carrasco E, Albala C, Hertrampf E. Microsatellite polymorphism in the heme oxygenase-1 gene promoter is associated with iron status in persons with type 2 diabetes mellitus. Am J Clin Nutr 2007; 86:1347-1353

320. Ndisang JF. Synergistic Interaction Between Heme Oxygenase (HO) and Nuclear-Factor E2-Related Factor-2 (Nrf2) against Oxidative Stress in Cardiovascular Related Diseases. Curr Pharm Des 2017; 23:1465-1470

321. Srisook K, Kim C, Cha YN. Molecular mechanisms involved in enhancing HO-1 expression: de-repression by heme and activation by Nrf2, the "one-two" punch. Antioxid Redox Signal 2005; 7:1674-1687

322. Soares MA, Cohen OD, Low YC, Sartor RA, Ellison T, Anil U, Anzai L, Chang JB, Saadeh PB, Rabbani PS, Ceradini DJ. Restoration of Nrf2 Signaling Normalizes the Regenerative Niche. Diabetes 2016; 65:633-646

323. Long M, Rojo de la Vega M, Wen Q, Bharara M, Jiang T, Zhang R, Zhou S, Wong PK, Wondrak GT, Zheng H, Zhang DD. An Essential Role of NRF2 in Diabetic Wound Healing. Diabetes 2016; 65:780-793

324. Zhaleh F, Amiri F, Mohammadzadeh-Vardin M, Bahadori M, Harati MD, Roudkenar MH, Saki S. Nuclear factor erythroid-2 related factor 2 overexpressed mesenchymal stem cells transplantation, improves renal function, decreases injuries markers and increases repair markers in glycerol-induced Acute kidney injury rats. Iran J Basic Med Sci 2016; 19:323-329

325. Shelar SB, Narasimhan M, Shanmugam G, Litovsky SH, Gounder SS, Karan G, Arulvasu C, Kensler TW, Hoidal JR, Darley-Usmar VM, Rajasekaran NS. Disruption of nuclear factor (erythroid-derived-2)-like 2 antioxidant signaling: a mechanism for impaired activation of stem cells and delayed regeneration of skeletal muscle. FASEB J 2016; 30:1865-1879

326. Dayoub R, Vogel A, Schuett J, Lupke M, Spieker SM, Kettern N, Hildt E, Melter M, Weiss TS. Nrf2 activates augmenter of liver regeneration (ALR) via antioxidant response element and links oxidative stress to liver regeneration. Mol Med 2013; 19:237-244

327. Uruno A, Furusawa Y, Yagishita Y, Fukutomi T, Muramatsu H, Negishi T, Sugawara A, Kensler TW, Yamamoto M. The Keap1-Nrf2 system prevents onset of diabetes mellitus. Mol Cell Biol 2013; 33:2996-3010

328. Yagishita Y, Fukutomi T, Sugawara A, Kawamura H, Takahashi T, Pi J, Uruno A, Yamamoto M. Nrf2 protects pancreatic beta-cells from oxidative and nitrosative stress in diabetic model mice. Diabetes 2014; 63:605-618

329. Masuda Y, Vaziri ND, Li S, Le A, Hajighasemi-Ossareh M, Robles L, Foster CE, Stamos MJ, Al-Abodullah I, Ricordi C, Ichii H. The effect of Nrf2 pathway activation on human pancreatic islet cells. PLoS One 2015; 10:e0131012

330. Lee S, Hur EG, Ryoo IG, Jung KA, Kwak J, Kwak MK. Involvement of the Nrf2-proteasome pathway in the endoplasmic reticulum stress response in pancreatic beta-cells. Toxicol Appl Pharmacol 2012; 264:431-438

331. Aleksunes LM, Reisman SA, Yeager RL, Goedken MJ, Klaassen CD. Nuclear factor erythroid 2-related factor 2 deletion impairs glucose tolerance and exacerbates hyperglycemia in type 1 diabetic mice. J Pharmacol Exp Ther 2010; 333:140-151

332. Uruno A, Yagishita Y, Katsuoka F, Kitajima Y, Nunomiya A, Nagatomi R, Pi J, Biswal SS, Yamamoto M. Nrf2-Mediated Regulation of Skeletal Muscle Glycogen Metabolism. Mol Cell Biol 2016; 36:1655-1672

333. Biswas C, Shah N, Muthu M, La P, Fernando AP, Sengupta S, Yang G, Dennery PA. Nuclear heme oxygenase-1 (HO-1) modulates subcellular distribution and activation of Nrf2, impacting metabolic and anti-oxidant defenses. J Biol Chem 2014; 289:26882-26894

334. Kim KM, Pae HO, Zheng M, Park R, Kim YM, Chung HT. Carbon monoxide induces heme oxygenase-1 via activation of protein kinase R-like endoplasmic reticulum kinase and inhibits endothelial cell apoptosis triggered by endoplasmic reticulum stress. Circ Res 2007; 101:919-927

335. Yeh PY, Li CY, Hsieh CW, Yang YC, Yang PM, Wung BS. CO-releasing molecules and increased heme oxygenase-1 induce protein S-glutathionylation to modulate NF-kappaB activity in endothelial cells. Free Radic Biol Med 2014; 70:1-13

336. MacGarvey NC, Suliman HB, Bartz RR, Fu P, Withers CM, Welty-Wolf KE, Piantadosi CA. Activation of mitochondrial biogenesis by heme oxygenase-1-mediated NF-E2-related factor-2 induction rescues mice from lethal Staphylococcus aureus sepsis. Am J Respir Crit Care Med 2012; 185:851-861

337. Detsika MG, Duann P, Lianos EA. HO-1 expression control in the rat glomerulus. Biochem Biophys Res Commun 2015; 460:786-792

338. Chi X, Guo N, Yao W, Jin Y, Gao W, Cai J, Hei Z. Induction of heme oxygenase-1 by hemin protects lung against orthotopic autologous liver transplantation-induced acute lung injury in rats. J Transl Med 2016; 14:35

339. Feng XE, Liang TG, Gao J, Kong P, Ge R, Li QS. Heme Oxygenase-1, a Key Enzyme for the Cytoprotective Actions of Halophenols by Upregulating Nrf2 Expression via Activating Erk1/2 and PI3K/Akt in EA.hy926 Cells. Oxid Med Cell Longev 2017; 2017:7028478

340. Cai C, Teng L, Vu D, He JQ, Guo Y, Li Q, Tang XL, Rokosh G, Bhatnagar A, Bolli R. The heme oxygenase 1 inducer (CoPP) protects human cardiac stem cells against apoptosis through activation of the extracellular signal-regulated kinase (ERK)/NRF2 signaling pathway and cytokine release. J Biol Chem 2012; 287:33720-33732

341. Ndisang JF, Jadhav A. Hemin therapy suppresses inflammation and retroperitoneal adipocyte hypertrophy to improve glucose metabolism in obese rats co-morbid with insulin-resistant type-2 diabetes. Diabetes Obes Metab 2013; 15:1029-1039

342. Haase J, Weyer U, Immig K, Kloting N, Bluher M, Eilers J, Bechmann I, Gericke M. Local proliferation of macrophages in adipose tissue during obesity-induced inflammation. Diabetologia 2014; 57:562-571

343. Shoelson SE, Herrero L, Naaz A. Obesity, inflammation, and insulin resistance. Gastroenterology 2007; 132:2169-2180

344. Valko M, Leibfritz D, Moncol J, Cronin MT, Mazur M, Telser J. Free radicals and antioxidants in normal physiological functions and human disease. Int J Biochem Cell Biol 2007; 39:44-84

345. Padgett LE, Broniowska KA, Hansen PA, Corbett JA, Tse HM. The role of reactive oxygen species and proinflammatory cytokines in type 1 diabetes pathogenesis. Ann N Y Acad Sci 2013; 1281:16-35

346. Jadhav A, Torlakovic E, Ndisang JF. Interaction among heme oxygenase, nuclear factor-kappaB, and transcription activating factors in cardiac hypertrophy in hypertension. Hypertension 2008; 52:910-917

347. Abumiya T, Masuda J, Kawai J, Suzuki T, Ogata J. Heterogeneity in the appearance and distribution of macrophage subsets and their possible involvement in hypertensive vascular lesions in rats. Lab Invest 1996; 75:125-136

348. Silva KC, Pinto CC, Biswas SK, de Faria JB, de Faria JM. Hypertension increases retinal inflammation in experimental diabetes: a possible mechanism for aggravation of diabetic retinopathy by hypertension. Curr Eye Res 2007; 32:533-541

349. Cohen RE, Talarico G, Noble B. Phenotypic characterization of mononuclear inflammatory cells in salivary glands of bio-breeding rats. Arch Oral Biol 1997; 42:649-655

350. Schuyler CA, Ta NN, Li Y, Lopes-Virella MF, Huang Y. Insulin treatment attenuates diabetes-increased atherosclerotic intimal lesions and matrix metalloproteinase 9 expression in apolipoprotein E-deficient mice. J Endocrinol 2011; 210:37-46

351. Ishida-Oku M, Iwase M, Sugitani A, Masutani K, Kitada H, Tanaka M, Iida M. A case of recurrent type 1 diabetes mellitus with insulitis of transplanted pancreas in simultaneous pancreas-kidney transplantation from cardiac death donor. Diabetologia 2010; 53:341-345

352. Aki K, Shimizu A, Masuda Y, Kuwahara N, Arai T, Ishikawa A, Fujita E, Mii A, Natori Y, Fukunaga Y, Fukuda Y. ANG II receptor blockade enhances anti-inflammatory macrophages in anti-glomerular basement membrane glomerulonephritis. Am J Physiol Renal Physiol 2010; 298:F870-882

353. Heusinkveld M, de Vos van Steenwijk PJ, Goedemans R, Ramwadhdoebe TH, Gorter A, Welters MJ, van Hall T, van der Burg SH. M2 macrophages induced by prostaglandin E2 and IL-6 from cervical carcinoma are switched to activated M1 macrophages by CD4+ Th1 cells. J Immunol 2011; 187:1157-1165

354. Anzai A, Anzai T, Nagai S, Maekawa Y, Naito K, Kaneko H, Sugano Y, Takahashi T, Abe H, Mochizuki S, Sano M, Yoshikawa T, Okada Y, Koyasu S, Ogawa S, Fukuda K. Regulatory role of dendritic cells in postinfarction healing and left ventricular remodeling. Circulation 2012; 125:1234-1245

355. El Hadri K, Mahmood DF, Couchie D, Jguirim-Souissi I, Genze F, Diderot V, Syrovets T, Lunov O, Simmet T, Rouis M. Thioredoxin-1 promotes anti-inflammatory macrophages of the M2 phenotype and antagonizes atherosclerosis. Arterioscler Thromb Vasc Biol 2012; 32:1445-1452

356. Fukunaga M, Yura T, Badr KF. Stimulatory effect of 8-Epi-PGF2 alpha, an F2-isoprostane, on endothelin-1 release. J Cardiovasc Pharmacol 1995; 26 Suppl 3:S51-52

357. Paine A, Eiz-Vesper B, Blasczyk R, Immenschuh S. Signaling to heme oxygenase-1 and its anti-inflammatory therapeutic potential. Biochem Pharmacol 2010; 80:1895-1903

358. Bhakkiyalakshmi E, Sireesh D, Rajaguru P, Paulmurugan R, Ramkumar KM. The emerging role of redox-sensitive Nrf2-Keap1 pathway in diabetes. Pharmacol Res 2015; 91:104-114

359. Ndisang JF, Lane N, Jadhav A. The heme oxygenase system abates hyperglycemia in Zucker diabetic fatty rats by potentiating insulin-sensitizing pathways. Endocrinology 2009; 150:2098-2108

360. Henningsson R, Alm P, Ekstrom P, Lundquist I. Heme oxygenase and carbon monoxide: regulatory roles in islet hormone release: a biochemical, immunohistochemical, and confocal microscopic study. Diabetes 1999; 48:66-76

361. Henningsson R, Alm P, Lundquist I. Occurrence and putative hormone regulatory function of a constitutive heme oxygenase in rat pancreatic islets. Am J Physiol 1997; 273:C703-709

362. Lundquist I, Alm P, Salehi A, Henningsson R, Grapengiesser E, Hellman B. Carbon monoxide stimulates insulin release and propagates Ca2+ signals between pancreatic beta-cells. Am J Physiol Endocrinol Metab 2003; 285:E1055-1063

363. Ndisang JF, Zhao W, Wang R. Selective regulation of blood pressure by heme oxygenase-1 in hypertension. Hypertension 2002; 40:315-321

364. Ndisang JF, Wang R. Age-related alterations in soluble guanylyl cyclase and cGMP pathway in spontaneously hypertensive rats. J Hypertens 2003; 21:1117-1124

365. Muiesan ML, Salvetti M, Monteduro C, Bonzi B, Paini A, Viola S, Poisa P, Rizzoni D, Castellano M, Agabiti-Rosei E. Left ventricular concentric geometry during treatment adversely affects cardiovascular prognosis in hypertensive patients. Hypertension 2004; 43:731-738

366. Liu J, Fox CS, Hickson DA, May WL, Ding J, Carr JJ, Taylor HA. Pericardial fat and echocardiographic measures of cardiac abnormalities: the Jackson Heart Study. Diabetes Care 2011; 34:341-346

367. Jadhav A, Ndisang JF. Treatment with heme arginate alleviates adipose tissue inflammation and improves insulin sensitivity and glucose metabolism in a rat model of Human primary aldosteronism. Free Radic Biol Med 2012; 53:2277-2286

368. Li P, Wang D, Lucas J, Oparil S, Xing D, Cao X, Novak L, Renfrow MB, Chen YF. Atrial natriuretic peptide inhibits transforming growth factor beta-induced Smad signaling and myofibroblast transformation in mouse cardiac fibroblasts. Circ Res 2008; 102:185-192

369. Ren J, Yang M, Qi G, Zheng J, Jia L, Cheng J, Tian C, Li H, Lin X, Du J. Proinflammatory protein CARD9 is essential for infiltration of monocytic fibroblast precursors and cardiac fibrosis caused by Angiotensin II infusion. Am J Hypertens 2011; 24:701-707

370. Gupte RS, Floyd BC, Kozicky M, George S, Ungvari ZI, Neito V, Wolin MS, Gupte SA. Synergistic activation of glucose-6-phosphate dehydrogenase and NAD(P)H oxidase by Src kinase elevates superoxide in type 2 diabetic, Zucker fa/fa, rat liver. Free Radic Biol Med 2009; 47:219-228

371. Yang YY, Tsai TH, Huang YT, Lee TY, Chan CC, Lee KC, Lin HC. Hepatic endothelin-1 and endocannabinoids-dependent effects of hyperleptinemia in nonalcoholic steatohepatitis-cirrhotic rats. Hepatology 2012; 55:1540-1550

372. Okamoto T, Park CH, Noh JS, Toriizuka K, Sei Y, Park JC, Yokozawa T. Hepato-/reno-protective activity of Chinese prescription Kangen-karyu through inhibition of AGE formation and fibrosis-related protein expression in type 2 diabetes. J Pharm Pharmacol 2011; 63:952-959

373. Flisiak R, Pytel-Krolczuk B, Prokopowicz D. Circulating transforming growth factor beta(1) as an indicator of hepatic function impairment in liver cirrhosis. Cytokine 2000; 12:677-681

374. Kleiner DE, Brunt EM, Van Natta M, Behling C, Contos MJ, Cummings OW, Ferrell LD, Liu YC, Torbenson MS, Unalp-Arida A, Yeh M, McCullough AJ, Sanyal AJ, Nonalcoholic Steatohepatitis Clinical Research N. Design and validation of a histological scoring system for nonalcoholic fatty liver disease. Hepatology 2005; 41:1313-1321

375. Hayashi H, Sakai T. Animal models for the study of liver fibrosis: new insights from knockout mouse models. Am J Physiol Gastrointest Liver Physiol 2011; 300:G729-738

376. Finer G, Schnaper HW, Kanwar YS, Liang X, Lin HY, Hayashida T. Divergent roles of Smad3 and PI3-kinase in murine adriamycin nephropathy indicate distinct mechanisms of proteinuria and fibrogenesis. Kidney Int 2012; 82:525-536

377. Lackner C. Hepatocellular ballooning in nonalcoholic steatohepatitis: the pathologist's perspective. Expert Rev Gastroenterol Hepatol 2011; 5:223-231

378. Machado MV, Cortez-Pinto H. Cell death and nonalcoholic steatohepatitis: where is ballooning relevant? Expert Rev Gastroenterol Hepatol 2011; 5:213-222

379. Lamacchia O, Nicastro V, Camarchio D, Valente U, Grisorio R, Gesualdo L, Cignarelli M. Para- and perirenal fat thickness is an independent predictor of chronic kidney disease, increased renal resistance index and hyperuricaemia in type-2 diabetic patients. Nephrol Dial Transplant 2011; 26:892-898

380. Hamdy O, Porramatikul S, Al-Ozairi E. Metabolic obesity: the paradox between visceral and subcutaneous fat. Curr Diabetes Rev 2006; 2:367-373

381. Postorino M, Marino C, Tripepi G, Zoccali C, Group CW. Abdominal obesity and all-cause and cardiovascular mortality in end-stage renal disease. J Am Coll Cardiol 2009; 53:1265-1272

382. Wang Y, Wang DH. Protective effect of TRPV1 against renal fibrosis via inhibition of TGF-beta/Smad signaling in DOCA-salt hypertension. Mol Med 2011; 17:1204-1212

383. Jim B, Ghanta M, Qipo A, Fan Y, Chuang PY, Cohen HW, Abadi M, Thomas DB, He JC. Dysregulated nephrin in diabetic nephropathy of type 2 diabetes: a cross sectional study. PLoS One 2012; 7:e36041

384. Marshall SM. The podocyte: a potential therapeutic target in diabetic nephropathy? Curr Pharm Des 2007; 13:2713-2720

385. Menne J, Meier M, Park JK, Boehne M, Kirsch T, Lindschau C, Ociepka R, Leitges M, Rinta-Valkama J, Holthofer H, Haller H. Nephrin loss in experimental diabetic nephropathy is prevented by deletion of protein kinase C alpha signaling in-vivo. Kidney Int 2006; 70:1456-1462

386. Satchell SC, Tooke JE. What is the mechanism of microalbuminuria in diabetes: a role for the glomerular endothelium? Diabetologia 2008; 51:714-725

387. Mosen H, Salehi A, Alm P, Henningsson R, Jimenez-Feltstrom J, Ostenson CG, Efendic S, Lundquist I. Defective glucose-stimulated insulin release in the diabetic Goto-Kakizaki (GK) rat coincides with reduced activity of the islet carbon monoxide signaling pathway. Endocrinology 2005; 146:1553-1558

388. Li M, Kim DH, Tsenovoy PL, Peterson SJ, Rezzani R, Rodella LF, Aronow WS, Ikehara S, Abraham NG. Treatment of obese diabetic mice with a heme oxygenase inducer reduces visceral and subcutaneous adiposity, increases adiponectin levels, and improves insulin sensitivity and glucose tolerance. Diabetes 2008; 57:1526-1535

389. Peterson SJ, Drummond G, Kim DH, Li M, Kruger AL, Ikehara S, Abraham NG. L-4F treatment reduces adiposity, increases adiponectin levels, and improves insulin sensitivity in obese mice. J Lipid Res 2008; 49:1658-1669